Microbial Oxidation of Dodecane and Tridecane into α,ω-Dicarboxylic Acids using Recombinant *Yarrowia lipolytica*

Danie Diedericks

Half-thesis submitted for the fulfilment of the academic requirements for the degree of Masters of Science in Engineering in the Department of Chemical Engineering

University of Cape Town

2007

Declaration on Plagiarism

I know the meaning of plagiarism and declare that all the work in the document, save for that which is properly acknowledged, is my own.

Signed by candidate

Danie Diedericks
2 October 2007

Abstract

α,ω-Dicarboxylic acids are reactive intermediates, widely used as raw materials to synthesise products such as perfumes, hot-melting adhesives, engineering plastics and high quality lubricants. These acids can be obtained via chemical or biological routes by using various feedstocks such as linear alkanes. Linear alkanes are chemically inert; hence, the production of reactive products requires complex and sophisticated reactions catalysed by either catalysts or enzymes. However, simultaneous by-product formation on chemical synthesis increases production cost and limits commercial availability, preventing their widespread application. Biological routes alternatively, selectively transform linear alkanes into fatty and α,ω-dicarboxylic acids. Linear alkanes, due to their relative abundance and increased availability, following the expansion of gas-to-liquid fuels technology, are viewed as prospective feedstocks for the microbial production of α,ω-dicarboxylic acids .

The commercialisation of the biological conversion of linear alkanes is constrained by the low turnover frequency of the cytochrome P450 hydroxylase complex responsible for catalysing the first and rate limiting step of the monoterminal and diterminal pathways. Low product yields may be caused by the further catabolism of α,ω-dicarboxylic acids, through the β-oxidation pathway into energy, carbon dioxide and water. To prevent this, metabolic engineering techniques can be applied to prevent β-oxidation by disrupting the genes encoding the enzyme catalysing the first step in the β-oxidation pathway. The specific productivity of bioconversion can then be increased further by over-expressing the genes encoding the cytochrome P450 hydroxylase complex. Recombinant *Yarrowia lipolytica* strains TVN 497, TVN 499, TVN 501 and TVN 502 were developed in such a manner by the collaborating research group at the University of the Free State and made available for this research.

Apart from metabolic engineering techniques, the production of α,ω-dicarboxylic acids can be further increased by optimising the operating conditions of the hydrocarbon-based bioprocess with the aid of a suitable kinetic model. The aim of this research was to characterise the above metabolically engineered strains of *Y. lipolytica* in terms of their growth and ability to produce α,ω-dicarboxylic acids and to develop a suitable basic kinetic model for *Y. lipolytica* TVN 497 under glucose and alkane limiting conditions. Factors affecting growth and biotransformation were also evaluated.

Following the collection of appropriate kinetic data for the growth of *Y. lipolytica* and its subsequent conversion of alkanes into α,ω-dicarboxylic acids an unstructured basic kinetic model, based on the Monod and Luedeking-Piret relationships, was developed for growth and biotransformation, respectively. The Monod based model predicted biomass production and glucose utilisation in a semi-defined medium adequately. The maximum specific growth rate (μ_m), the saturation constant (K_s) and the yield coefficient at initial glucose concentrations of 5 $g.l^{-1}$, 13 $g.l^{-1}$ and 42 $g.l^{-1}$ were calculated as 0.18 h^{-1}, 0.19 h^{-1} and 0.20 h^{-1}, 0.37 $g.l^{-1}$, 0.50 $g.l^{-1}$ and 0.10 $g.l^{-1}$ and 0.67 $g.g^{-1}$, 0.46 $g.g^{-1}$ and 0.29 $g.g^{-1}$, respectively.

The Monond equation was modified and extended into the Andrews model which takes cognisance of the effect of substrate inhibition. The specific growth rate of *Y. lipolytica* TVN 497 initially increased with an increase in initial glucose concentration to reach a maximum value of 34 h^{-1} at an initial glucose concentration of 20 $g.l^{-1}$ after which the specific growth rate decreased with an increase in initial glucose concentration due to substrate inhibition. The Andrews based model predicted this effect of substrate inhibition adequately.

The Luedeking-Piret based model for biotransformation of alkane was able to predict the production of α,ω-dicarboxylic acids and the utilisation of the corresponding alkanes adequately up to the point of alkane depletion. The values of the kinetic parameters were estimated for three different initial

alkane concentrations i.e. 1%, 1.5% and 3% (v/v). The corresponding values of β (specific production rate) were calculated as $8.4x10^{-4}$ h^{-1}, $6.8 x10^{-4}$ h^{-1} and $9.0 x10^{-4}$ h^{-1} for dodecanedioic acid production and $6.2 x10^{-4}$ h^{-1}, $5.3 x10^{-4}$ h^{-1} and $5.9 x10^{-4}$ h^{-1} for tridecanedioic acid production whilst the values of Y (yield coefficient) were calculated as 0.22 $g.g^{-1}$, 0.24 $g.g^{-1}$ and 0.24 $g.g^{-1}$ for dodecanedioic acid from dodecane and 0.26 $g.g^{-1}$, 0.34 $g.g^{-1}$ and 0.39 $g.g^{-1}$ for tridecanedioic acid from tridecane, respectively. A limitation of the Luedeking-Piret relationship, on which the simplified kinetic model was based however, caused the model to incorrectly continue predicting product formation even in the absence of the corresponding substrate.

This limitation was accounted for by modifying the Luedeking-Piret equation to take cognisance of substrate limitation. This modified model, when applied to the experiment conducted at an initial alkane concentration of 1% (v/v), adequately predicted biotransformation but was unable to account for the formation of α,ω-dicarboxylic acids which originated from the apparent ability of the strains to store alkanes intracellularly. The specific production rate of dodecanedioic acid and tridecanedioic acid was calculated as $1.42x10^{-4}$ h^{-1} and $8.95x10^{-4}$ h^{-1}, respectively whilst the yield coefficient of dodecanedioic acid from dodecane and tridecanedioic acid from tridecane was calculated as 0.25 $g.g^{-1}$ and 0.35 $g.g^{-1}$, respectively. Correspondingly, the saturation constant of dodecane and tridecane was calculated as 1.00 $g.l^{-1}$ and 0.26 $g.l^{-1}$, respectively.

To assess the ability of *Y. lipolytica* strains TVN 497, TVN 499, TVN 501 and TVN 502 to produce α,ω-dicarboxylic acids, shake flask experiments were carried out in a complex medium during which an alkane cut comprising dodecane and tridecane were added to each culture medium 48 h after inoculation. The results of these experiments indicated that during a 104 h biotransformation period, strains TVN 497, TVN 499, TVN 501 and TVN 502 were able to produce 0.68 ± 0.16 $g.l^{-1}$, 1.29 ± 0.06 $g.l^{-1}$, 1.11 ± 0.20 $g.l^{-1}$ and 0.65 ± 0.02 $g.l^{-1}$ dodecanedioic acid and 0.63 ± 0.01 $g.l^{-1}$, 1.29 ± 0.07 $g.l^{-1}$, 1.37 ± 0.09 $g.l^{-1}$ and 0.56 ± 0.01 $g.l^{-1}$ tridecanedioic acid, respectively. Although *Y. lipolytica* TVN 497 was not superior in its ability to produce

α,ω-dicarboxylic acids, this particular strain was chosen for further research in order to be coherent with the research conducted by the collaborating research group.

Factors affecting growth and biotransformation include medium pH, alkane concentration and more specifically time of alkane addition. When alkane was added to the culture medium during the early exponential phase, microbial growth experienced an adaptation phase of approximately 2 h, a phenomenon which may be attributed to the time required by the cells to adapt themselves to their new lipophilic environment and the diversion of energy to synthesise the P450s required for alkane oxidation. Another factor of importance was the ability of *Y. lipolytica* to produce α,ω-dicarboxylic acids during the growth phase. This has great industrial implications since, being a bulk product, the continuous production of α,ω-dicarboxylic acids would be advantageous.

The modified and extended model developed during this research together with the above factors which affect growth and biotransformation establish a foundation of understanding that can assist in process development and process optimisation. The model provides a basis for future refinement into a more complex kinetic model able to verify the economic viability of *Y. lipolytica* TVN 497 in a hydrocarbon-based process.

Acknowledgments

I would like to start by acknowledging Jesus Christ for his guidance and wisdom throughout my thesis.

To my supervisor, Prof. Sue Harrison and my Co-supervisors Prof. Martie Smit and Dr. Randhir, I offer my gratitude for their patience and professional guidance. Without them my MSc would not have been a success.

To each of the following individuals I wish to extend a sincere word of appreciation:

Dr. Randhir Rawatlal for helping me with the computer programming.

Dr. Rob Van Hille for his friendship and supervisory assistance in the laboratory.

Mrs. Fran Pocock, our lab manager, for whom our students problems were always her first priority.

Mrs. Sue Jobson for all the administration work.

My Chinese, Nigerian and Congolese friends for their friendship and help and support.

I would also like to acknowledge the financial support provided by c*change the DST-NRF Centre of Excellence in Catalysis, who made my research a reality.

Finally, I would like to express my deepest gratitude to my dearest wife, Mienie Diedericks, for her love, prayers, long nights and moral support. My mother for her prayers and my dad for his concern, the editing of my thesis and his presence in time of need.

Table of Contents

List of Figures

List of Tables

Nomenclature

Abbreviations

DNS	dinitrosalicylic acid	
GC	gas chromatography	
OD	optical density	
OTR	oxygen transfer rate	$[g.l^{-1}.h^{-1}]$
OUR	oxygen utilisation rate	$[g.l^{-1}.h^{-1}]$
TCA	tricarboxylic acid cycle	
UFS	University of the Free State	
YNB	yeast nitrogen base	

Roman Symbols

$K_{NH_4^+}$	saturation constant of ammonium ion	$[g.l^{-1}]$
a_{alk}	alkane to liquid interfacial area per unit volume	$[dm^{-1}]$
a_{O2}	oxygen to liquid interfacial area per unit volume	$[dm^{-1}]$
C^*_i	saturation concentration of species i in the liquid	$[g.l^{-1}]$
C_i	concentration of species i	$[g.l^{-1}]$
E_d	activation energy for cell death	$[cal.gmol^{-1}]$
E_g	activation energy for growth	$[cal.gmol^{-1}]$
F^*_i	utilisation rate of species i	$[gmol.h^{-1}]$
$F_{i,in}$	molar flow rate of species i into the system	$[gmol.h^{-1}]$
$F_{i,out}$	molar flow rate of species i out of the system	$[gmol.h^{-1}]$
H^+	hydrogen ion concentration	$[gmol.l^{-1}]$
k_{alk}	alkane transfer coefficients	$[dm.s^{-1}]$
k_d	Arrhenius constant for cell death	
K_d	specific death rate	$[h^{-1}]$
K_{dd}	saturation constant of dodecane	$[g.l^{-1}]$
k_g	Arrhenius constant for growth	
K_g	Saturation constant of glucose	$[g.l^{-1}]$
K_i	substrate growth inhibition concentration	$[g.l^{-1}]$

k_L	oxygen transfer coefficients	[$dm.s^{-1}$]
K_p	product growth inhibition concentration	[$g.l^{-1}$]
K_s	saturation constant	[$g.l^{-1}$]
K_{td}	saturation constant of dodecane	[$g.l^{-1}$]
m	maintenance constant	[h^{-1}]
N_i	transfer rate of species i	[$g.l^{-1}.h^{-1}$]
P_i	production rate of species i	[$gmol.h^{-1}$]
R	universal gas constant	[$cal.gmol^{-1}.K^{-1}$]
T	temperature	[K]
t	time	[h^{-1}]
$X_{i,in}$	mole fraction of species i in the inlet stream	
$X_{i,in}$	mole fraction of species i in the outlet stream	
Y_i	yield coefficient	[$g.g^{-1}$]

Subscripts

alk	alkane
CO_2	carbon dioxide
dda	dodecanedioic acid
dda/dd	dodecanedioic acid from dodecane
gas	air
N_2	nitrogen
NH_4^+	ammonium ion
O_2	oxygen
p	product
p/s	products from substrates
p/sg	products from glucose
s	substrate
dd	dodecane
g	glucose
td	tridecane
tda	tridecanedioic acid
tda/td	tridecanedioic acid form tridecane
X	biomass

x/s	biomass from substrates
x/sg	biomass from glucose

Greek Symbols

β'_{dda}	maximum specific production rate of dodecanedioic acid	$[h^{-1}]$
β'_{tda}	maximum specific production rate of tridecanedioic acid	$[h^{-1}]$
β_{dda}	specific production rate of dodecanedioic acid	$[h^{-1}]$
β_{tda}	specific production rate of tridecanedioic acid	$[h^{-1}]$
μ	specific growth rate	$[h^{-1}]$
μ'_i	maximum specific growth rate with species i as the rate limiting substrate	$[h^{-1}]$
μ_m	maximum specific growth rate	$[h^{-1}]$

Chapter 1

Introduction

Linear alkanes are readily available, relatively inexpensive feedstocks which are mainly used as fuels to produce energy and low value carbon dioxide (Ayala and Torres, 2004). The expansion of the gas-to-liquid fuels technology and the need to maximise resource productivity, are directing the focus of current research towards the development of methods to convert linear alkanes into higher-value products (Labinger, 2002). Linear alkanes are however, chemically inert and are therefore not easy to activate, especially in the terminal positions (Ayala and Torres, 2004). As a result, limited commercialised routes are available for the conversion of linear alkanes as a feedstock to produce higher-value and more reactive products such as alcohols, aldehydes and carboxylic acids, the annual world market of which are estimated in excess of 60 billion dollars (Boswell, 1999).

Currently, linear alkanes are transformed into higher-value products using either a chemical or biological process (Periana *et al.* 2004). The chemical processes are characterised by low yields, poor selectivity, and harsh conditions. Biological processes make use of microorganisms which are capable of catalysing these complex oxidation reactions at physiological pressures and temperatures (Ayala and Torres, 2004). Due to a high selectivity, few or no side-products are generated (Picataggio *et al.*1991). Low catalytic turnover rates and limited enzyme stability have limited the economic feasibility of applying these biological processes in industrial processes to date (Ayala and Torres, 2004).

Wild type strains of *Yarrowia lipolytica* are able to convert linear alkanes via monoterminal, diterminal and β-oxidation pathways into energy, carbon dioxide and water (Craft *et al.* 2003). However, when the β-oxidation pathway is blocked, by disrupting the *POX* genes which encode the enzyme catalysing the first step in the β-oxidation pathway, α,ω-dicarboxylic acids accumulate

and are secreted into the surrounding medium (Picataggio *et al.*1991). α,ω-Dicarboxylic acids are versatile chemical intermediates which are used as feedstocks for the preparation of various higher-value products such as perfumes, hot-melting adhesives, engineering plastics and high quality lubricants (Liu *et al.* 2004). The microbial oxidation of linear alkanes for the purpose of producing α,ω-dicarboxylic acid is the subject of this research.

Previous studies on the microbial oxidation of linear alkanes into α,ω-dicarboxylic acids, focussed on the isolation of high-yield mutants (Yi and Rehm, 1982), the application of engineered strains (Hara *et al*, 2001) and the optimisation of operating conditions (Uchio and Shiio, 1971; Uchio and Shiio, 1972b). In the majority of cases research was limited to *Candida* sp. under glucose limiting conditions. For *Yarrowia lipolytica* research to date has mainly focused on citric acid production under nitrogen limiting conditions.

Productivity of a specific strain can be further optimised by the development of an appropriate kinetic model able to predict the performance of the strain under defined operating conditions (Fredrickson *et al.* 1970). In general, a kinetic model comprises a set of hypotheses which describe the mathematical relations between measurable quantities associated with the system or process used (Ghaly and El-Taweel, 1997). Such a model may serve as a mathematical tool to isolate important parameters and to reduce the number of experiments required to design and optimise the process conditions (Deindoerfer, 1960). Currently, few or no literature exists which describe the quantitative relationship between the environmental parameters and the cell kinetics of *Yarrowia lipolytica*, under glucose and alkane limiting conditions.

A major aim of the project was therefore directed towards the development of a basic kinetic model able to predict the growth and biotransformation of *Yarrowia lipolytica* under these conditions using an unstructured modelling approach. The basic kinetic model developed during this research was extended and modified to incorporate the rate limiting effects of a second rate limiting substrate and to take cognisance of substrate inhibition. Further, the modelling approach highlighted critical areas requiring further understanding,

such as the continued production of α,ω-dicarboxylic acids on depletion of alkanes and the relative flux of alkanes to desired products in comparison to by-products.

The work commences with Chapter 2 which reviews the literature that relates to linear alkanes as a potential feedstock for the production of value-added products, biotransformation of alkanes into α,ω-dicarboxylic acids, typical growth and biotransformation conditions, process challenges and a general introduction to growth and biotransformation kinetics. Chapter 3 presents the materials and methods used in this study. A basic kinetic model to predict growth and biotransformation is developed in Chapter 4. The chapter also presents a method to quantify the kinetic parameters of the basic kinetic model proposed. Chapters 5 and 6 provide an overview of the growth and biotransformation phases, respectively. Basic kinetic data for the system studied are presented and used to estimate the kinetic parameters as well as to evaluate the predictive performance of the proposed model. Further the influence of specific operating conditions on performance is presented. Chapter 7 compares four different recombinant *Y. lipolytica* strains in terms of their ability to produce α,ω-dicarboxylic acids. Chapter 8 presents the conclusions of the research findings and makes recommendations with regards to further research.

Chapter 2

Literature Review

The study of the biotransformation of linear alkanes into α,ω-dicarboxylic acids requires the review of literature which include aspects related to the suitability of alkanes as a potential feedstock, the microbial oxidation process of linear alkane into α,ω-dicarboxylic acids, required growth and biotransformation conditions, process challenges and mathematical modelling which can assist in predicting the performance of the growth and biotransformation processes. Each of the above aspects is considered separately in this chapter.

2.1 Linear Alkanes: a Potential Feedstock for the Production of High-Value Chemicals

2.1.1 Properties of linear alkanes

Linear alkanes from natural gas and fossil fuel are amongst the world's most abundant and low-cost feedstock (Periana *et* al. 2004). Linear alkanes are naturally produced by decaying plants (van Beilen, 2003), but can also be synthesised by means of a gas-to-liquid fuels technology i.e. the Fischer–Tropsch process. Under standard conditions, linear alkanes with a carbon number of 1 to 4 are gases, 5 to 17 liquids and 18 and greater solids

Linear alkanes are comprised of a highly reduced carbon-backbone which causes linear alkanes to display very little chemical reactivity, especially in the terminal positions. This characteristic limits their direct conversion into value added chemicals such as alcohols and amines (Ayala and Torres, 2004; Labinger and Bercaw, 2002). Linear alkanes however, do react spontaneously with oxygen, under high temperature, to produce energy and low value carbon dioxide (Ayala and Torres, 2004).

2.1.2 The activation of alkanes and resultant products

The current transformation of linear alkanes into value added chemicals is limited. Use of high-temperature heterogeneous catalysis, organometallic activation and microbial oxidation is reported. High-temperature heterogeneous catalysis is typically carried out on a metal-oxo catalyst at 200-600 °C by a radical pathway (Labinger, 2004). Organometallic activation on the other hand, is a selective, low temperature process during which a homogeneous metal catalyses the hydroxylation of linear alkanes. Fundamental understanding of this catalyst design however, remains limited which prevents their industrial application (Periana *et al.* 2004).

Table 2.1 lists a few commercial technologies which are currently available for linear alkane activation, applying high-temperature heterogeneous catalysis.

Table 2.1: Current commercial technologies available for direct alkane activation applying high-temperature heterogeneous catalysis (Boswell, 1999)

Company	Transformation	Catalyst
Natural Resources	Methane into acetic acid	Rh-based
Air products	Ethane to acetonitrile	Co-zeolite
SABIC	Ethane to acetic acid	Metal oxides
EVC Technologies	Ethane to vinyl chloride	Cu-alkali metal
Symyx	Ethane to ethylene	Mo-V-Nb
Cyclar Process	Propane/butane aromatization	Ga/zeolite
Mitsubishi/BP Amoco	Propane to acrylonitrile	$VSbO/Ai_2O_3$
Mitsubishi	Propane to acrylic acid	TE-Mo-V-Nb
DuPont/BOC-Mitsubishi	Butane to Maleic anhydride	$(VO)_2P_2O_7$
UOPs OleflexProcess	Propane and isobutane to alkenes	$Pt\text{-}Al_2O_3$
ABB Lummus Catofin Process	Propane and butane to alkenes	$Cr_2O_3\text{-}Ai_2O_3$

Heterogeneous catalysis is obstructed by low catalyst activity and substrate selectivity. As an example, ethane can be oxidised into acetic acid by using a metal oxide as catalyst. Typically 10% of the ethane is converted, with a selectivity of 80%. When the temperature is increased to obtain a conversion

of 21%, the selectivity is typically reduced to 30% (Borchert *et al.* 2001). Selectivity under these conditions is therefore difficult to control since the product is more reactive than the substrate (Ayala and Torres, 2004). Currently, it is not yet known whether catalyst improvement can solve this problem (Labinger, 2004). As a consequence, direct activation of linear alkanes remains a challenge for modern catalysis (Ayala and Torres, 2004).

Microbial activation of linear alkanes offers an alternative to the conventional chemical processes. Microbial oxidation involves several metabolic pathways spanning the subcellular compartments of yeast (Smit *et al.* 2005). Microorganisms are able to catalyse complex reactions at physiological pressures and temperatures with few or no side products being produced, due to high product selectivity. To date, the industrialisation of the microbial process has been hampered by the low productivity associated with the oxidisation of linear alkanes into value added chemicals (Ayala and Torres, 2004).

Significant research has therefore been focused on developing yeast strains with a higher activity, through molecular biology approaches. Once a functional group has been introduced, the product can further be processed via the β-oxidation pathway allowing incorporation of the alkane carbon into the central carbon metabolism. Compounds which are reported to be produced by alkane utilising microorganisms include amino acids, organic acids, carbohydrates, lipids, nucleic acids, vitamins, enzymes, co-enzymes, antibiotics and biomass (Fukui and Tanaka, 1980). Alternatively, through the blocking of β-oxidation, the yeast may function as a catalyst, allowing biotransformation of the linear alkane through addition of functional groups only, with no reduction in chain length. Potential products include alcohol, mono-carboxylic acid, hydroxyl-acid and dicarboxylic acid of which the latter is most stable.

Synthesis of the α,ω-dicarboxylic acid is of specific interest because the chemical synthesis usually results in numerous by-products which reduce yield and impose extensive purification to retrieve the final product (Picataggio

et al. 1992) (Table 2.2). In this study, the key focus was therefore placed on the activation and functionalisation of alkanes for further development, hence the microbial production of organic acids, particularly aliphatic long chain α,ω-dicarboxylic acids, was the subject of this research.

Table 2.2: Chemical synthesis of α,ω-dicarboxylic acids

Product/s	Reagent/s	Catalyst/s	Product yield (%)	Reference
Pimelic Acid	ε-caprolactone Carbon-monoxide	Palladium	46.7	Murib and Katy (1989)
Suberic Acid	1,3-cyclohexanedione Ethyl bromoacetate	-	50	Stetter and Forest (1963)
Azelaic Acid	Oleic acid Hydrogen peroxide	Chlorine	72	Nakazawa *et al.* (1986)
Dodecanedioic Acid	Undecylenic acid Carbon monoxide	Triphenylpho s-phine-rhodium complex	70	Andrade *et al.* (1988)
Brassylic Acid	Erucic acid Ozone	-	72	Dufek *et al.* (1974)

2.1.3 Applications of aliphatic α,ω-dicarboxylic acids

Aliphatic α,ω-dicarboxylic acids are versatile chemical intermediates and may serve as a feedstock for the preparation of diesters, polyesters and polyamides (Craft *et al.* 2003). These derivatives find application as plasticizing agents, lubricants, heat transfer fluids, dielectric fluids, fibres, copolymers, inks and resins, surfactants, fungicides, insecticides, hot-melt coating and adhesives (Table 2.3).

The industrial importance of longer α,ω-dicarboxylic acids (C_8 upwards) was also recognised in recent years but their limited commercial availability and high price have prevented widespread growth in many of their applications (Craft. *et al.* 2003, Morgan, 1979). The current market price of long chain α,ω-dicarboxylic acids (C_8-C_{14}) ranges between US$5.00 and US$6.75 per

kg. Recently, pentadecanedioic acids and hexadecanedioic acid became commercially available at approximately US$50 per kg (Caswell, 2006).

Table 2.3: Commercially available α,ω-dicarboxylic acids and their corresponding applications

Compounds	Application
Undecanedioic Acid	Corrosion inhibitor High class lubricants Hot melt adhesives Plasticizer Polyamide resins
Dodecanedioic Acid	Corrosion inhibitor High class lubricants Hot melt adhesives Polyamide resins Macrocyclic Musk
Tridecanedioic Acid	Corrosion inhibitor High class lubricants Hot melt adhesives Macrocyclic Musk Plasticizer Polyamide resins Power coating
Tridecanedioic Acid	Hot melt adhesives Macrocyclic Musk Polyamide resins
Tetradecanedioic Acid	Corrosion inhibitors High class lubricants High class synthetic flavours Hot melt adhesives Plasticizer Polyamide resins Power coating
Pentadecanedioic Acid	Fragrance ketones Lubricant additives Plasticizers

The table contents was obtained from the Cathay Biotechnology website, http://www.cathaybiotech.com

2.1.4 Microorganisms capable of producing α,ω-dicarboxylic acids

Numerous microorganisms including, bacteria, yeast and fungi are able to grow on linear alkanes as their sole carbon and energy source (Levi *et al.*

1979). However, not all microorganisms, when cultured in a medium containing linear alkanes, excrete α,ω-dicarboxylic acids as a by-product. Table 2.4 lists microorganisms which have been identified previously as strains which produce α,ω-dicarboxylic-acids by conversion of linear alkanes.

Table 2.4: Microorganisms capable of producing α,ω-dicarboxylic acids when cultured on a medium containing linear alkanes

Strain	Reference
Candida tropicalis	Hill *et al.* (1986) Liu *et al.* (2004) Picataggio *et al.* (1992)
Candida cloacae	Uchio and Shiio, (1971) Uchio and Shiio, (1972a) Green *et al.* (2000)
Corynebacterium sp	Broadway *et al.* (1993)
Yarrowia lipolytica	Smit *et al.* (2005) Fickers *et al.* (2005)
Cryptococcus neoformans	Chan and Kou, (1997) Chan *et al.* (1991)
Pseudomonas aeruginosa	Chan and Kou, (1997) Chan *et al.* (1991)

The strains listed in Table 2.4 are able to metabolise linear alkanes through the ω-oxidation and β-oxidation pathway to yield energy, carbon dioxide and water (Craft *et al.* 2003). Several approaches are reported to enhance conversion of linear alkanes to α,ω-dicarboxylic acids and to minimise their complete oxidation to carbon dioxide and water. Through genetic manipulation, the genes encoding the enzyme catalysing the first step in the β-oxidation pathway may be disrupted. As a result, α,ω-dicarboxylic acids which are structurally similar to the substrate, accumulate and are excreted into the surrounding medium (Picataggio *et al.* 1992). In another approach, wild-type strains were treated with organic solvents or surface active agents to alter the cell membrane permeability (Chan *et al.* 1991). This allowed rapid secretion of α,ω-dicarboxylic acids into the medium, thereby avoiding further degradation inside the cell. Table 2.5 lists the different strains, different products, different product yield and the different methods applied to prevent the complete oxidation of linear alkanes.

Table 2.5: Strains, products, yields and methods applied to prevent the complete oxidation of linear alkanes

Strain	Method of Prevention	Acid Type	Yield ($g.l^{-1}$)	Reference
Candida tropicalis	ME	C_{12}, C_{13}, C_{14}	166, 152, 138	Liu *et al.* (2004)
Candida cloacae	ME	C_{10}, C_{12}, C_{14}, C_{16}	0.3, 2, 1.2, 1.2	Green *et al.* (2000)
Yarrowia lipolytica	ME	C_{12}, C_{14}	8, 0.7	Smit *et al.* (2005)
Cryptococcus neoformans	MP	C_{15}	7.5	Chan and Kuo, (1997)
Pseudomonas aeruginosa	MP	C_{15}	2.5	Chan *et al.* (1991)

ME: Metabolic Engineering (*POX* genes disrupted, P450ALK genes overexpressed), MP: Membrane Permeability

2.2 Microbial Oxidation of Linear Alkanes into α,ω-Dicarboxylic Acids

2.2.1 Microbial utilisation of linear alkanes

The initial step in alkane utilisation by yeasts is the uptake and transportation of alkanes into the yeast cells. In the cells, the alkanes are hydroxylated and oxidised via a monoterminal oxidation pathway to yield fatty acids. Fatty acids produced via this pathway, are often hydroxylated and oxidised a second time via a diterminal oxidation pathway to yield α,ω-dicarboxylic acids, structurally similar to the fatty acids. Both the fatty acids and the α,ω-dicarboxylic acids are then activated to their corresponding acetyl-CoA esters. The acetyl-CoA esters are metabolised via the β-oxidation pathway to yield acetyl-CoA and truncated (n-2) acyl-CoA molecules. Subsequently, the truncated acyl-CoA molecules are then reintroduced into the β-oxidation pathway to yield another acetyl-CoA and further truncated (n-2) acyl-CoA molecules. This process may continue until the acyl-CoA molecules are completely broken down. The acetyl-CoA molecules on the other hand, act as a feedstock to the tricarboxylic acid cycle where they are converted to sugars, vitamins and amino acids or undergo complete oxidation to carbon dioxide. The metabolic pathway is shown in Figure 2.1.

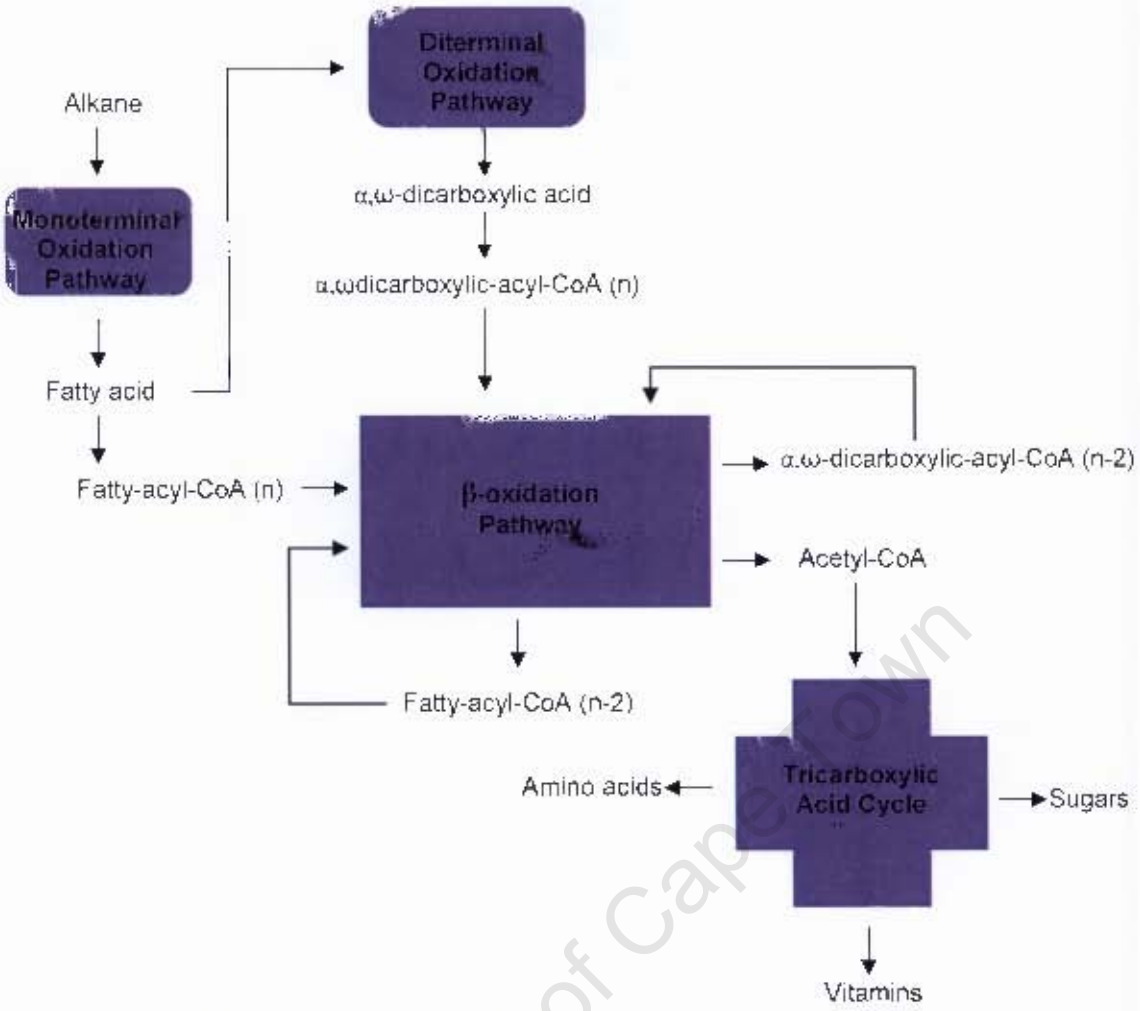

Figure 2.1: The microbial oxidation process of linear alkanes in wild-type yeast strains (Fickers et al. 2005)

2.2.2 Monoterminal and diterminal oxidation pathways

The first step in the mono-terminal oxidation of alkanes in yeast involves a terminal hydroxylation by a P450-dependent alkane monooxygenase system (Fickers *et al.* 2005) to produce alcohols. The P450-dependent alkane monooxygenase system comprises of a cytochrome P450 monooxygenase (CYP52) and an accompanying NADPH cytochrome P450 reductase (CPR). This system is responsible for catalysing the first and rate-limiting steps in both the mono-terminal and di-terminal oxidation pathways (Craft *et al.* 2003). Much research has been dedicated towards improving the specific productivity of this rate-limiting step. Currently, it is done by overexpressing the CYP52 and CPR genes which encode the rate-limiting hydroxylaseenzyme complex

(Picataggio *et al.* 1992). The effectiveness of this method is discussed in Section 2.2.4.2.

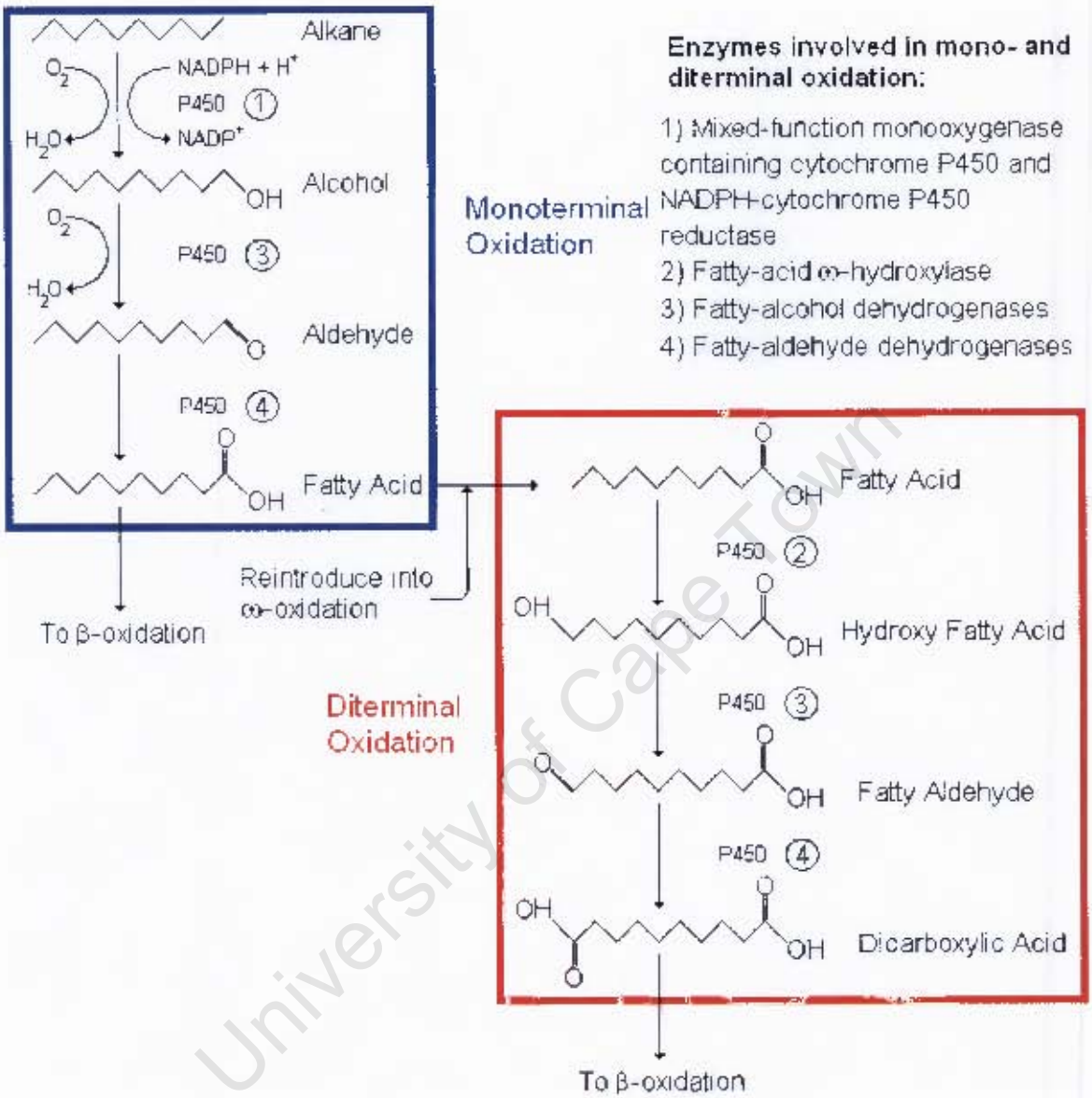

Figure 2.2: Monoterminal and diterminal oxidation pathways in yeast (Fickers *et al.* 2005)

The alcohols, produced during the initial oxidation step, are transformed to fatty acids via the monoterminal pathway which comprises of two additional oxidation steps (Figure 2.2). The two steps are catalysed by a fatty alcohol oxidase and a fatty-aldehyde dehydrogenase, respectively (Fickers *et al.* 2005). The fatty acids produced via the monoterminal oxidation pathway can either be activated to the corresponding acyl-CoA esters and metabolised via the β-oxidation pathway or oxidised via the di-terminal-oxidation pathway. The

diterminal-oxidation pathway, which applies similar oxidation steps to those of the monoterminal oxidation pathway, produces α,ω-dicarboxylic acids from the fatty acids. The P450-dependent alkane monooxygenase system however, is also able to produce α,ω-dicarboxylic acids directly from linear alkanes, since all the oxidation steps can be catalysed by it (Scheller *et al.* 1998). These α,ω-dicarboxylic acids are then activated to the corresponding acyl-CoA ester and similarly metabolised through the β-oxidation pathway. The β-oxidation pathway is discussed in more detail in Section 2.2.3.

From Figure 2.2, it is clear that α,ω-dicarboxylic acids are produced as a result of a series of oxidation steps. The intermediates produced after each oxidation step are, however, rarely detected in the media. This phenomenon is attributed to the progressive reactivity of these intermediates, causing them to exist only for a short period of time, before being converted to the next molecule. The oxidation steps in both the mono-terminal and di-terminal oxidation pathways are catalysed by the same enzyme, thereby preventing gene disruption as the route to accumulate these intermediates. Consequently, experimental results have portrayed a process whereby most of the alkanes are converted to either fatty or α,ω-dicarboxylic acids. These in turn, are metabolised via the β-oxidation pathway unless the latter is blocked.

2.2.3 β-oxidation pathway

The fatty and α,ω-dicarboxylic acids, produced during the mono-terminal and di-terminal oxidation pathways respectively, are both initially activated, through thiokinase, to their corresponding acyl-CoA esters before they are introduced to the β-oxidation pathway (Craft *et al*, 2003). The acyl-CoA esters are then degraded by the β-oxidation pathway, in four sequential steps i.e. oxidation, hydration, dehydrogenation and thiolytic cleavage, to produce acetyl-CoA and another acyl-CoA, the length of which is reduced by two carbon atoms, as shown in Figure 2.3. This cycle is repeated until the acyl-CoA esters are completely degraded. The acetyl-CoA molecules are transported to the mitochondria as an acetyl-carnitine derivative where it

undergoes complete oxidation to carbon dioxide in the citric acid cycle and used in the anabolic pathways for synthesised of intermediates (Craft *et al.* 2003). In view of the similarity between the metabolic pathways to degrade the two acyl-CoA esters which originate from fatty and α,ω-dicarboxylic acids respectively, only the degradation of fatty acids in the β-oxidation pathway, is used to illustrate the β-oxidation process in Figure 2.3.

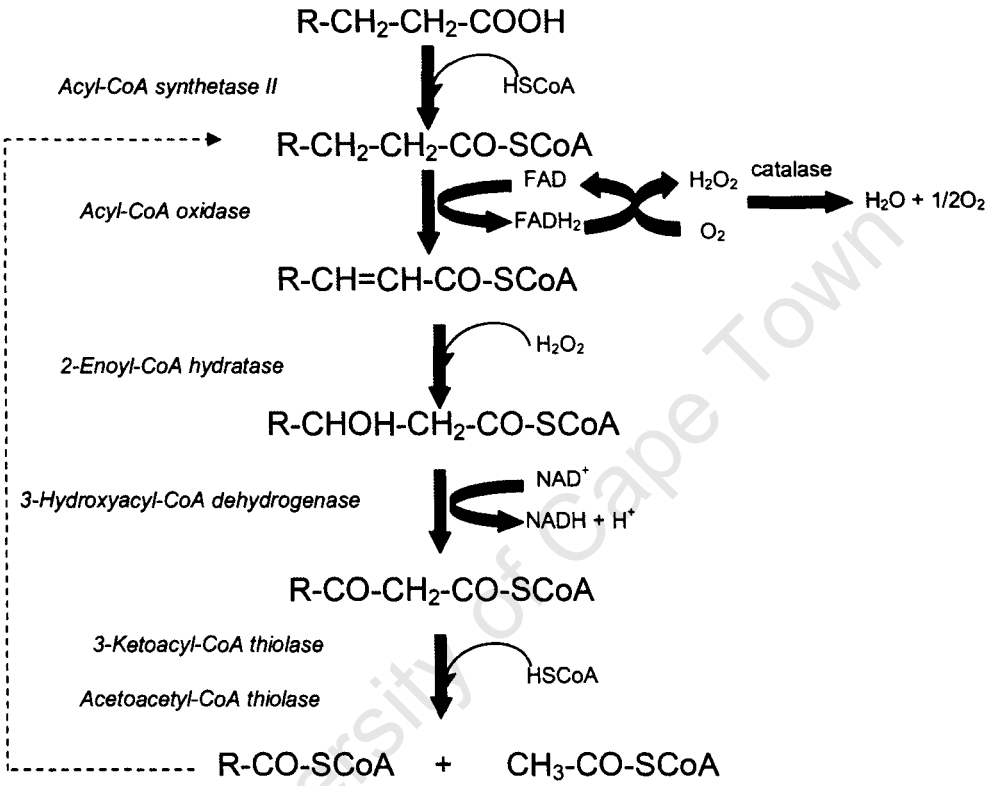

Figure 2.3: β-oxidation of fatty acids (Fickers *et al.* 2005)

When β-oxidation is prevented, α,ω-dicarboxylic acids accumulate in the media. These acids are structurally similar to the substrates from which they were produced. To date, the most effective method used to prevent β-oxidation is to block the β-oxidation pathway by disrupting the *POX* genes which encode the acyl-CoA oxidase, the enzyme catalysing the first oxidation step in the β-oxidation pathway. The effectiveness of this method and other methods are discussed in Section 2.2.4.1.

2.2.4 Metabolic engineering of yeasts to enhance α,ω-dicarboxylic acid production

Several wild-type yeast strains, listed in Table 2.4, are known for their ability to excrete α,ω-dicarboxylic acids when cultured on media containing linear alkanes. α,ω-Dicarboxylic acids produced by these strains are often shorter than their original substrate by one or more pairs of carbon atoms, with product mixtures being common. This phenomenon is attributed to the partial degradation effect of β-oxidation. As a result, a combination of poor conversion efficiency, chemical selectivity and productivity has prevented the use of wild-type yeasts in commercial processes (Picataggio et al., 1992). The various approaches which are currently being used to increase the accumulation yield and production rate of α,ω-dicarboxylic acids, respectively, are discussed in Sections 2.2.4.1 and 2.2.4.2.

2.2.4.1 Prevention of product degradation by the β-oxidation pathway

High yields of α,ω-dicarboxylic acids, structurally similar to their corresponding substrate, can be obtained by preventing fatty and α,ω-dicarboxylic acids from being metabolised via the β-oxidation pathway. This can be achieved by blocking the β-oxidation pathway by disrupting the *POX* genes, encoding the acyl-CoA oxidase, the enzyme responsible for catalysing the first step in the β-oxidation pathway (Eschenfeldt *et al.* 2003). Inactivation of this pathway, redirects the flow of fatty acids to the di-terminal-oxidation pathway. As a result, alkanes and fatty acids are converted to corresponding α,ω-dicarboxylic acids, while chain modifications associated with the β-oxidation pathway are simultaneously prevented. Picataggio *et al.* (1992) pioneered this approach by disrupting the *POX*4 and *POX*5 genes present in *C. tropicalis* ATCC 20336. The resulting metabolically engineered strain *C. tropicalis* H5342, produced 140 $g.l^{-1}$ dodecanedioic acid in 130 h. The corresponding productivity of the strain was increased by 100%.

As an alternative to metabolic engineering, high α,ω-dicarboxylic-acid-producing mutants have also been isolated by physical or chemical mutagenesis. These strains may accumulate α,ω-dicarboxylic acids shorter than the original substrate or may accumulate significant quantities of α,ω-dicarboxylic acids of similar structure to the substrate used (Mauersberger *et al.* 1996). For example, *Candida tropicalis* CGMCC 356, was derived by Liu *et al.* (2004) from strain SP-1, by treating the parent strain with ultraviolet light/radiation. *Candida tropicalis* CGMCC 356 was found to be able to produce 153 $g.l^{-1}$ tridecanedioic acids by conversion of tridecane. Examples of genetically engineered strains and mutants able to accumulate increased quantities of α,ω-dicarboxylic acid are presented in Table 2.6.

Table 2.6: Mutants and genetically engineered strains created for α,ω-dicarboxylic acid accumulation

Strain	Mutagenesis/ Metabolic Engineering Transformation	Product Yield ($g.l^{-1}$)	Product	Time (h)	Reference
C. cloacae M12	Mutagenesis (Nitrosoguanidine)	61.5	DAC_{16}	100	Uchio and Shiio (1972c)
C. tropicalis H5343	Disruption of *POX*4 and *POX*5 genes	140	DCC_{12}	155	Picataggio *et al.* (1992)
Y. lipolytica MTLY 37	Disruption of *POX*2, *POX*3, *POX*4 and *POX*5 genes	8	DCC_{12}	144	Smit *et al.* (2005)
C. tropicalis CGMCC 356[a]	Mutagenesis (Ultraviolet Light)	166	DCC_{12}	120	Liu *et al.* (2004)
		153	DCC_{13}	120	
		138	DCC_{14}	120	

2.2.4.2 Additional strain improvement to enhance α,ω-dicarboxylic acid productivity

Once the β-oxidation pathway is blocked by disrupting the *POX* genes encoding acyl-CoA oxidase responsible for catalysing the first step in the

β-oxidation pathway, the production rate of α,ω-dicarboxylic acids can be enhanced by increasing the metabolic flux through both the mono-terminal and di-terminal oxidation pathways (Craft *et al.*, 2003). This is achieved by overexpressing the CYP52 and CPR genes encoding the rate-limiting hydroxylase complex. This complex forms the enzyme which is responsible for catalysing the first and rate limiting step in both the mono-terminal and di-terminal oxidation pathways (Section 2.2.2).

The effect of inserting both these genes was clearly illustrated by Picataggio (1991; 1992). *Candida tropicalis* H5342, constructed by disrupting four *POX*4 and *POX*5 genes of the parent strain, had a tetradecanedioic acid productivity of 1.3g.l^{-1}.hr^{-1} when cultured on a medium containing methyl myristate. When this strain was used to construct *Candida tropicalis* AR40, a genetically engineered strain containing three additional CYP and two additional CPR genes, the tetradecanedioic acid productivity was enhanced to 2 g.l^{-1}.hr^{-1}. This additional metabolic improvement enhanced the productivity of strain *C. tropicalis* H5342 by 30%. The productivity of the strain however, could not be further enhanced by adding addition CPR genes. It is therefore apparent that cytochrome P450 monooxygenase catalyses the rate-limiting step in both the mo-terminal and di-terminal pathways.

β-Oxidation oxidation, however, is required for cell growth and maintenance, hence, by blocking the β-oxidation pathway the strain is negatively affected (Hara, 2001). In a study conducted by Coa *et al.* (2006) the tridecanedioic acid productivity of *C. tropicalis* W10-1 was enhanced by 21% by disrupting the gene encoding the acetyl-CoA transportation system. Without the acetyl-CoA transportation system, Acetyl-CoA, the end-product of β-oxidation, accumulates since it cannot enter the mitochondrion. The unwanted chain modifications associated with the β-oxidation pathway was therefore prevented since feedback inhibition lowers the enzymatic activity of the β-oxidation pathway.

2.3 Growth and Biotransformation Conditions

To maximise product yield, the growth and biotransformation phases are generally uncoupled through genetic manipulation to prevent product oxidation. Hence, microbial growth and maintenance require the provision of a second carbon source not metabolised through β-oxidation. The biotransformation phase commences with the addition of alkane to the culture media following microbial growth. Research reported to date suggests different optimal conditions for growth and biotransformation and considers them separately (Table 2.7). The same approach was followed during this research.

Microbial growth and biotransformation are generally affected by various factors including the medium pH, the type of carbon and nitrogen sources used for growth, alkane concentration, chain length and product concentration (Uchio and Shiio, 1971, 1972a,b&c and Vasileva-Tonkova *et al.* 1996). Uchio and Shiio (1971,1972a) evaluated the effects of different carbon and nitrogen sources on hexadecanedioic acid production using resting cells of *C. cloacae*. Product formation was enhanced by organic acids and inhibited by glucose. When sodium acetate was used as a carbon source, a maximum hexadecanedioic acid concentration of 29.3 $g.l^{-1}$ was obtained. This value reduced to 6.1 $g.l^{-1}$ when glucose was used. It was suggested that glucose suppressed the formation of enzymes responsible for catalysing the alkanes.

Similar results were obtained with different nitrogen sources. Hexadecanedioic acid production was optimised in the presence of $(NH_4)_2HPO_4$ and suppressed by all other ammonium salts tested. KNO_3 alternatively, was not suitable for either growth or biotransformation. The *XPR2* promoter which bears great historical importance in the development of heterologous production in *Y. lipolytica* is also affected by media lacking preferred carbon and nitrogen sources, and its full induction requires high levels of peptone in the culture medium (Ogrydziak *et al.* 1997). This limitation was partially eliminated by designing a hybrid promoter able to drive strong

Table 2.7: Different media and operating conditions for the microbial growth and biotransformation phases in the production of α,ω-dicarboxylic acid, reported in literature

Authors		Liu *et al.*	Picataggio *et al.*	Jiao *et al.*	Uchio and Shiio	Smit *et al.*
Year		2004	1992	2001	1972	2005
Organism		*C. tropicalis* [a] CGMCC 356	*C. tropicalis* [b] H5343	*C. tropicalis* [c] CT1-12	*C. cloacae* [d] M12	*Y. lipolytica* [e] MTLY 37
Type of Media		Complex	Complex	Semi-Defined	Semi-Defined	Complex
Agitation (rpm)		1 300	700	Not Specified	1 400	180
Aeration (vvm)		1	0.8	1	Surface Aeration	Surface Aeration
Reactor Volume (l)		5	15	3	0.3	0.13
Reactor Configuration		Semi-Batch	Semi-Batch	Batch	Batch	Batch
Temperature		30	30	30	30	25
Growth Media	**Carbon Source**	Sucrose Polypropylene Glycol CH_3CO_2Na	Glucose	Sucrose	Sucrose	Glucose
	Nitrogen Source	Corn Steep Liquor Urea	YNB Yeast Extract $(NH_4)_2SO_4$	Yeast Extract Urea $(NH_4)_2SO_4$	Ammonium Acetate $(NH_3)_2HPO_4$	Peptone Yeast Extract
	Salts	KH_2PO_4 $MgSO_4.7H_2O$ NaCl	KH_2PO_4 K_2HPO_4		KH_2PO_4 $MnSO_4.nH_2O$ $ZnSO_4.nH_2O$ $FeSO_4.7H_2O$ $MgSO_4.7H_2O$	
	Vitamins	-	-	-	Biotin	-
Growth Phase pH		6	6.5	6.5	6.5	Not Specified
Time of Alkane Addition (h) [g]		18	18	20	16-40	48
Production Phase Duration (h)		120	92	130	72	150
Diacid Production Phase pH [f]		7.2-8.2	7.8-8.3	8	7.75	8
Alkane Concentration % (v/v)		30	0.5-3.0	10	13-50	0.7-8.0
Alkane Chain Length		C_{12}-C_{13}	C_{13}	C_{13}	C_{11}-C_{18}	C_{12}, C_{14}, C_{16}
Diacid Concentration (g.l-1)		138-166	120	154	13-50	0.7-8.0

[a] *C. tropicalis* was obtained by treating *C. tropicalis* SP-1 with ultraviolet

[b] *C. tropicalis* H5343 was obtained by disrupting the *POX*4 and *POX*5 genes and overexpressing the P450alk1 and CPR genes of *C. tropicalis* ATTC 750.

[c] Heritage of *C. tropicalis* CT1-12 is unknown

[d] *C. cloacae* M12 was obtained by treating *C. cloacae* M1 with Nitrosoguanidine

[e] *Y. lipolytica* MTLY 37 was obtained by disrupting the Δ *POX*2, *POX*3, *POX*4 and *POX*5 genes of *Y. lipolytica* W29

[f] The pH of the medium in each case was changed at the time of alkane addition

[g] Alkane was added to the culture medium when the residual glucose concentration was depleted or less than 5 $g.l^{-1}$

expression in virtually any media (Madzak *et al.* 2000). Expression normally takes place at the beginning of the stationary phase which is desirable for avoiding substrate and product toxicity or inhibition. p*POT1* and p*POX2* have also been identified as strong inducible promoters available for *Y. lipolytica*. These promoters are highly inducible by fatty acids and alkanes and repressed by glucose and glycerol. Their application however, has been hampered by being not compatible with efficient heterologous production or protein purification.

From Table 2.7 it is clear that research reported to date mainly focused on *Candida* sp. as a suitable biocatalyst for α,ω-dicarboxylic acid production. As a result little information concerning α,ω-dicarboxylic acid production is available on *Y. lipolytica* as biocatalyst. Current literature on *Y. lipolytica* focuses mainly on citric acid production under nitrogen limiting conditions. Citric acid is generally considered to be produced as a secondary metabolite, produced only when microbial growth has ceased due to nitrogen depletion (Klasson *et al.* 1989). α,ω-Dicarboxylic acids alternatively are also produced as non-growth associated products, since these strains cannot use alkane as a carbon and energy source. Hence literature to date are confined to the use of batch and semi-batch bioreactors although the use of a continuous process should prove advantageous since α,ω-dicarboxylic acids are considered bulk-chemicals.

The production rate of non-growth associated products is related to the biomass and the substrate concentration. From Table 2.7 it is clear that alkane concentrations of 0.5% and 50% (v/v) are typically used for α,ω-dicarboxylic acid production, the effect thereof however, have not been established.

Moresi (1994) have evaluated the effect of biomass concentration on citric acid production. Wild-type *Y. lipolytica* ATCC 20346 was initially cultivated on semi-defined medium under nitrogen-excess conditions. When the initial glucose concentration was increased from 40 $g.l^{-1}$ to 108 $g.l^{-1}$ the biomass

concentration increased from 13.6 $g.l^{-1}$ to 30.1 $g.l^{-1}$. The yield coefficient (biomass from glucose) was unaffected by the glucose concentration whereas the specific growth was negatively affected (Section 2.4.2). The citric acid production phase was initiated by resuspending the cells into a carbon rich medium (C:N ratio typically 3500:1). The corresponding citric acid productivity increased linearly with biomass concentration from 0.292 $g.dm^{-3}.h^{-1}$ to 1.044 $g.dm^{-3}.h^{-1}$ and was unaffected by the glucose concentration. The effect of biomass concentration on α,ω-dicarboxylic acid production however, have not been established.

From Table 2.7 it is also clear that growth and biotransformation are affected by a variety of factors including the time of alkane addition, the medium pH, initial glucose concentration, alkane chain length and product concentration. These factors are addressed in subsequent sections. Since little information are available on *Y. lipolytica* under similar conditions it was assumed for this study that *Y. lipolytica* will be similarly affected by the operating conditions as would have been the case for *Candida* sp.

2.3.1 Time of alkane addition

Literature proposes that alkanes should be added to the culture medium 18 h to 48 h after inoculation, once microbial growth has reached the stationary phase (Picataggio *et al.* 1992; Smit *et al.* 2005; Jiao *et al.* 2001; Green *et al.* 2000 and Liu *et al.* 2004), but is silent as to the rationale behind this requirement. As such, the time of alkane addition has become a condition specified in the experimental protocol.

Green *et al.* (2000) proposed that glucose suppresses the oxidation of lauric acid, a mono-oxidised derivative of dodecane, into dodecanedioic acid. This was concluded after observing that the period between the addition of lauric acid and the oxidation thereof increased with an increase in initial glucose concentration. This was demonstrated by cultivating *C. cloacae* FERM-P736, a strain unable to utilise lauric acid as a carbon or energy source, in a medium

containing different initial glucose concentrations and 10 $g.l^{-1}$ lauric acid. The findings are tabulated in Table 2.8.

Table 2.8: Effect of initial glucose concentrations on dodecanedioic acid production from lauric acid (Green *et al.* 2000)

Initial Glucose Concentration ($g.l^{-1}$)	Time before Dodecanedioic Acid Production (h)
5	0
10	24
16.5	48
25	72

From the results in Table 2.8 Green *et al.* concluded that high glucose concentrations or the accumulation of stored sugars or both, repressed the activity of cytochrome P450 and its corresponding reductase. Since cytochrome P450 catalyses the first step in both the mono and diterminal oxidation pathways, alkane oxidation should also be delayed by the presence of glucose in the culture medium.

An enzymology study conducted by Gallo *et al.* (1973) supports this hypothesis. Gallo *et al.* showed that when wild-type *C. tropicalis* 101 was cultivated on a minimal medium containing tetradecane, as the sole carbon source, the cytochrome P450 and its corresponding reductase activity was 0.06 $nmol.mg^{-1}$ and 200 $nmol.min^{-1}.mg^{-1}$, respectively. When however, the strain was cultivated in a medium containing both glucose and tetradecane, the activity of the cytochrome P450 and its corresponding reductase reduced to 0.05 $nmol.mg^{-1}$ and 160 $nmol.min^{-1}.mg^{-1}$, respectively. From these results they concluded that the hydroxylase system is inducible and that glucose exerts a catabolic repression effect on its biosynthesis.

2.3.2 The role of medium pH on α,ω-dicarboxylic acid formation

Medium pH is one of the key parameters which plays a role in the accumulation of α,ω-dicarboxylic acids in the medium. After alkane addition to initiate the biotransformation phase, the medium pH is typically raised and

maintained at a constant elevated level in the range of 7.5 and 8.5 (Liu *et al.* 2004; Jiao *et al.* 2001 and Smit *et al.* 2005). Other cases are reported where the medium pH was regulated within a narrow range of 7.8-8.3 (Picataggio *et al.* 1992; Liu *et al.* 2004).

Literature is silent about the rationale behind why a change in medium pH is required at the time of alkane addition. Liu et *al.* (2004) and Lin *et al.* (2002) speculate that an elevated medium pH prevents intracellular accumulation of α,ω-dicarboxylic acid. Scheller *et al.* (1998) showed that hexadecanedioic acid competitively inhibits hexadecane binding to active site of the P450's. By lowering the intracellular accumulation of hexadecanedioic acid, process productivity can be increased by preventing product inhibition. Scheller *et al.* (1998) estimated that hexadecanedioic acid production is affected by product concentrations as low as 74 μm^3. Product inhibition is reviewed in detail in Section 2.4.2.

2.4 Process Challenges

Hydrocarbon-based bioprocesses are characterised by numerous process challenges. These challenges are mainly related to the formation of a four phase system (biomass-water-alkane-air) (Blanch and Einsele, 1973). In a four phase system, volumetric productivity depends not only on the activity of the biocatalyst, but also on mass-transfer (Clarke *et al.* 2006). Other factors including the toxic effect of substrates and products can also affect volumetric productivity (Schmid *et al.* 1998). Apart from this, the use of hydrocarbons, in the presence of air also poses a number of health and safety risks. In this section the various process challenges and potential approaches to address these are presented.

2.4.1 Mass transfer in alkane bioconversion

Mass transfer limitations in hydrocarbon-based bioprocesses, originate from oxygen and alkanes being sparingly soluble in water. As a consequence, the

rate of biomass and α,ω-dicarboxylic acid formation may become transport-controlled rather than kinetically-controlled (Gmünder *et al.* 1981; Schmid *et al.* 1998). Literature appears to be silent about the manner in which α,ω-dicarboxylic acid production is affected by oxygen and alkane limiting conditions. For this reason a parallel is drawn with the way in which single cell protein production is affected by such conditions. Although not directly related to α,ω-dicarboxylic acid production, the way in which alkanes and oxygen are transported, are principally the same.

Mass-transfer results when a concentration gradient exists between two phases. The gas to liquid and the liquid to liquid mass-transfer rates can be calculated by applying equations 2.1 and 2.2, respectively:

$$N_{O_2} = k_L a_{O_2} \left(C^*_{O_2} - C_{O_2}\right) \qquad 2.1$$

$$N_{alk} = k_{alk} a_{alk} \left(C^*_{alk} - C_{alk}\right) \qquad 2.2$$

where N_{O2} and N_{alk} are the rate of oxygen and alkane transfer ($g.l^{-1}.h^{-1}$) respectively, k_L and k_{alk} are the oxygen and alkane transfer coefficients ($l.h^{-1}$) respectively, a_{O2} and a_{alk} are the oxygen to liquid and alkane to liquid interfacial area per unit volume respectively (l^{-1}), C^*_{O2} and C^*_{alk} are the saturated dissolved oxygen and saturated dissolved alkane concentrations in the liquid phase respectively ($g.l^{-l}$) and C_{O2} and C_{alk} are the dissolved oxygen and alkane concentrations in the liquid phase ($g.l^{-1}$).

Johnson (1964) and Mimura *et al.* (1971) observed that, when using alkanes as the sole carbon and energy source, the biomass growth rate cannot be explained by assuming that only alkanes which are dissolved in the aqueous phase are accessible to the microorganism. The predicted alkane transfer rate into the liquid phase (Q_{alk}) is too low to maintain the required uptake rate of dissolved alkanes, necessary to support the growth rate observed (Goswami and Singh, 1991). From observation made by Goswami and Singh (1991), it appears as if the mass transfer to the cells also takes place as a result of

either the direct contact of the cells with larger hydrocarbon droplets or as a result of the interaction of the cells with much smaller pseudo-solubilised hydrocarbon micelles or a combination of both.

The result of alkane limiting conditions and hence of alkane transport is that it reduces the specific growth rate of the strain. Schmid *et al.* (1998) cultivated *Pseudomonas oleovorans* in a fed-batch culture which contained either *n*-octane or *n*-decane as the sole carbon source. The culture conditions were such that growth was neither limited by oxygen nor by any other water soluble substrate. The maximum specific growth rates (μ_m) on *n*-octane and *n*-decane, observed during the initial growth phase, were 0.45 h^{-1} and 0.32 h^{-1}, respectively. However, 3 h before the end of the *n*-octane experiment the specific growth rate of the strain started a gradual decline whilst biomass growth continued at a constant volumetric growth rate of 3.9 $g.l^{-1}.h^{-1}$. A similar trend was observed with the *n*-decane experiment during which biomass growth continued at a constant volumetric growth rate of 2 $g.l^{-1}.h^{-1}$ after the biomass density reached 4 $g.l^{-1}$. Schmid *et al.* (1998) conclude that the implication of these linear volumetric growth rates is that the transfer rate from the organic phase to the biomass limits the metabolic activity, under mass transfer limiting conditions.

The solubility of oxygen in water is 3 to 18 000 times greater than that of alkanes in water. As a result, the rate of oxygen transport through the aqueous phase to the microbial biomass is able to support the biomass growth rate observed (Bell, 1973). However, since hydrocarbon utilising strains tend to attach themselves to hydrocarbon droplets, it is logical to assume that oxygen dissolved in these droplets may be directly transported to the cells. Hence, the rate of biomass growth cannot be explained solely by the rate of oxygen transport into the aqueous phase as a result of the concentration gradient which exists between the aqueous and gaseous phases.

The oxygen requirements for a hydrocarbon-based and carbohydrate-based system differ significantly. This difference is due to the absence of oxygen in

the hydrocarbon backbone (Mimura *et al.* 1971a). This phenomenon was illustrated by Moo-Young and Shimizu (1971) who developed the following two stoichiometric equations for yeast growing in a hydrocarbon-based and carbohydrate-based system, respectively:

$$2CH_2 + 0.19NH_3 + 2O_2 \rightarrow CH_{1.7}O_{0.5}N_{0.19} + CO_2 + 1.5H_2O \qquad (2.3)$$

$$1.68CH_2O + 0.19NH_3 + 0.68O_2 \rightarrow CH_{1.7}O_{0.5}N_{0.19} + 0.71CO_2 + 1.14H_2O \qquad (2.4)$$

$CH_{1.7}O_{0.5}N_{0.19}$ represents the general formula for 1 gmol biomass (Moo-Young and Shimizu, 1971). From equation 2.3 and 2.4, Moo-Young and Shimizu concluded that yeasts produced from hydrocarbons require at least three times more oxygen per unit mass of cells than if produced from carbohydrates. Consequently, the metabolic oxygen requirements of strains growing in a hydrocarbon-based system have to be met entirely by transferring oxygen into the microbial culture (Clarke *et al.* 2006).

The cost of energy to supply atmospheric oxygen however, is high. The rate by means of which oxygen is transported from the gas to the liquid phase is therefore of great importance. This rate can be optimised by maximising the oxygen mass transfer coefficient, K_La, and the saturated dissolved oxygen concentration C^*_{O2} (Equation 2.1). The oxygen mass transfer coefficient can be altered by changing the concentration of the solid phase, the alkane fraction, the intensity of agitation, the aeration rate and the reactor type (Mimura *et al.* 1973). It is also affected by solutes present, especially those affecting bubble interface. The dissolved oxygen concentration is a function of the temperature and medium composition.

In a recent study conducted by Clarke *et al.* (2006), the oxygen transfer rate into an air-water-alkane system was maximised by optimising the value of K_La by altering the agitation rate, aeration rate and the alkane fraction. The influence of alkane on K_La and hence the oxygen transfer rate, was shown to be markedly dependent on the agitation rate and the alkane fraction and to a

lesser degree on the aeration rate. K_La generally increased when the agitation rate or the alkane fraction or both were increased and reached a maximum value of 0.052 s^{-1} at an agitation rate of between 1000 and 1200 rpm, an aeration rate of 1.125 vvm and an alkane concentration of 5 to 10% (v/v). The dependence of oxygen concentration on gas liquid mass transport can also be reduced through its chemical provision e.g. by the addition of moderate amounts of H_2O_2 to the culture media. H_2O_2 can be converted to water and oxygen (Sriram *et al.* 1998), immediately available for consumption (Jiao *et al.* 2001).

The result of limitation in oxygen supply during batch growth of microorganism is reduction in the yield and growth rate of biomass. Preusting *et al.* (1993) evaluated the effect of oxygen limitation on biomass yield. *Pseudomonas oleovorans* was grown in a batch culture using *n*-octane as the sole carbon substrate. When cell growth ceased due to oxygen limiting conditions, the cell density was 27 $g.l^{-1}$. By lowering the growth temperature from 30 °C to 18 °C the demand for oxygen decreased. As a result, the biomass continued to grow to reach a final cell density of 35 $g.l^{-1}$.

The effect of oxygen limitation on the specific growth rate of *Candida tropicalis,* cultivated on *n*-hecadecane as a sole carbon source, was clearly illustrated by Gmünder *et al.* (1981). When the partial pressure of oxygen was set between 4 and 20 kPa, *C. tropicalis* grew at a maximum specific growth rate of 0.28 h^{-1}. However, when the partial pressure of oxygen was reduced to 2 kPa, the specific growth rate initially reached 0.27 h^{-1} at low biomass concentrations after which it decreased to 0.09 h^{-1} when the oxygen requirement, proportional to the product or specific growth rate and biomass concentration, exceeded the supply rate.

Oxygen supply is required in the biotransformation phase of the α,ω-dicarboxylic acids production process as well as the growth phase, as indicated in Equation 2.5:

$$H_3C-(CH_2)_n-CH_3+3O_2 \rightarrow HO_2C-(CH_2)_n-CO_2H+2H_2O \qquad (2.5)$$

Specific discussions of oxygen provision for α,ω-dicarboxylic acid production do not appear in literature.

2.4.2 Inhibition of growth and biotransformation

Microbial growth and product formation could become inhibited if cells are exposed to high substrate - or product concentrations or both (Wayman and Tseng, 1976). Glucose, a carbon substrate commonly used for microbial growth, inhibits growth of *Saccharomyces cerevisiae* at concentrations which vary typically between 150 $g.l^{-1}$ and 200 $g.l^{-1}$, with complete inhibition at 40% (w/v) (Casey and Ingledew, 1986; Holcberg and Margalith, 1981). This inhibition is the result of high osmotic pressures and low water activity, the onset of which is caused by high substrate concentrations, leading to the inhibition of the enzymes in the fermentative pathway (Casey and Ingledew, 1986; Stewart *et al.* 1984). This is often mistaken for the catabolite repression of the oxidative pathways, known as the Crabtree effect and relevant to alcoholic fermentation (Maiorella, 1985).

Although substrate inhibition has been well documented for *S. cerevisiae*, literature on the inhibition effect of glucose on *Y. lipolytica* is limited. Moresi (1994) showed that the specific growth rate of a wild-type *Y. lipolytica* strain on a semi-defined medium in a batch bioreactor initially increases with increasing initial glucose concentration in the medium, until such time that a maximum specific growth rate of 0.36 h^{-1} is reached at an initial glucose concentration of 61.7 $g.l^{-1}$. These results, tabulated in Table 2.9, clearly show that once the maximum specific growth rate has been reached, any further increase in the initial glucose concentration resulted in a decrease in the specific growth rate. This clear demonstration of substrate inhibition was not identified as such by the author.

Table 2.9: Specific growth rates of a wild-type *Yarrowia lipolytica* strain at different initial glucose concentrations (Moresi, 1994)

Initial Glucose Concentration ($g.l^{-1}$)	42.8	46.9	61.7	81.0	108
Maximum Specific Growth Rate (h^{-1})	0.30	0.34	0.38	0.20	0.16

Linear alkanes comprised of 8 or less carbon atoms are generally considered to be toxic to both alkane-utilising and non-alkane-utilising yeasts. These toxins inhibit both the growth and respiration of the yeasts (Gill and Ratledge, 1972). In a study conducted by Cameotra and Sindh (1990), the specific growth rate and final biomass concentration of *Pseudomonas* PG-1, were affected by the concentration of hexane in the medium. When the hexane concentration in the medium was increased from 0.06 to 0.24% (v/v) the specific growth rate and the final biomass concentration increased from 0.104 to 0.214 h^{-1} and from 0.21 and 1.15 $g.l^{-1}$, respectively. However, after reaching a maximum, the specific growth rate and the final biomass concentration decreased with a further increased in hexane concentration. Cameotra and Sindh attributed the decline to the volatility of the alkanes.

The toxicity of linear alkanes towards yeasts is related to their solubility in the aqueous phase (Gill and Ratledge, 1972). Foster (1962) showed that inhibition incured by linear alkanes increases with an increase in solubility. The reason for the toxicity of short carbon alkanes is unclear; however, both altered surface tension (Cowles, 1938) and the denaturation of the microsomal electron carrier system (Gilewicz *et al.* 1978) have been suggested. The toxicity of short linear alkanes can however, be reduced by their preferential solubility in a non-metabolised immiscible long-chain hydrocarbon solvent (Gill and Ratledge, 1972, Schmid *et al.* 1998, Green *et al.* 2000). This causes the inhibitory symptoms to decline once the concentration of the toxic linear alkanes in the aqueous phase is reduced (Schmid *et al.* 1998).

Product inhibition, on the other hand, has been identified as a potential obstacle to α,ω-dicarboxylic acid production. Scheller *et al.* (1998) identified this inhibition by showing that hexadecanedioic acid competitively inhibits hexadecane binding. The system used by Scheller *et al.* (1998) to illustrate this principle was comprised of purified recombinant cytochrome P450 52A3 and corresponding NADPH-cytochrome P450 reductase from *Candida maltosa*, reconstructed into an active enzyme system of *Saccharomyces cerevisiae*. The type of inhibition was identified and the degree thereof measured, by means of substrate difference spectrophotometry in the presence of 0.13, 0.25 and 0.50 mM hexadecanedioic acid. A double-reciprocal plot of the change in absorbance as a function of the hexadecane concentration was then used to identify the type of inhibition as competitive inhibition and to estimate the product inhibition constant (K_p) as 74 μM, a clear indication of product inhibition.

A similar finding was documented by Chan *et al.* (1997) with a wild-type strain of *Pseudomonas aeruginosa* in a medium containing pentadecane, cultivated in a batch type bioreactor. Chan and co-workers observed that the conversion of pentadecane into pentadecanedioic acid ceased when a pentadecanedioic acid concentration of 0.6 $g.l^{-1}$ were reached approximately 250 h after alkane addition. The final acid concentration correlates with 0.3 g of pentadecanedioic acid. In contrast, the same experiment conducted with immobilised cells in a continuous process made it possible to prevent product inhibition by controlling the product concentration at 0.2 $g.l^{-1}$. By preventing product inhibition *Pseudomonas aeruginosa* was able to produce up to 1.3 g of pentadecanedioic acid in 250 h.

2.4.3 Health and safety risks associated with hydrocarbon-based bioprocesses

The health and safety risks of linear alkane require the implementation of numerous safety measures, due to the highly flammable nature of these substances. Gaseous alkanes are extremely flammable with flash points

varying between -221 °C and -60 °C. Liquid alkanes are also highly flammable. Their explosion risk decreases with an increase in carbon number (Table 2.10).

Table 2.10: Health and safety risks involved in the use of gaseous and liquid linear alkanes [a]

Compound Name	State	Toxicology	Flash point (°C)	Explosion limits (%) [b]
Methane	gas	Asphyxiant	-221	5 -15
Ethane	gas	Asphyxiant	-172	3 - 12.5
Propane	gas	Asphyxiant	-104	2.4 - 9.5
Butane	gas	Eye irritant	-60	1.8 - 8.4
Pentane	liquid	Irritant	- 49	1.4 - 8.3
Hexane	liquid	Impaired fertility	-23	1.2 - 7.7
Heptane	liquid	May cause dermatitis	-1	1.1 - 7
Octane	liquid	Respiratory and eye irritant	15	0.96 - 6.5
Nonane	liquid	Respiratory and eye irritant	31	0.87 - 2.9
Decane	liquid	Respiratory and eye irritant	46	0.8 - 2.6
Nonadecane	liquid	-	168	-
Dodecane	liquid	Respiratory and eye irritant	71	0.6>
Tridecane	liquid	Respiratory and eye irritant	102	-
Tetradecane	liquid	Respiratory and eye irritant	99	0.5>
Pentadecane	liquid	Respiratory and eye irritant	132	0.45 - 6.5
Hexadecane	liquid	Not hazardous	135	-
Heptadecane	liquid	Not hazardous	148	-

[a] The table contents was obtained from MSDS on the internet (http://ptcl.chem.ox.ac.uk/msds)

[b] Explosion Limits are the upper and lower limits of percentage composition of a combustible gas mixed with other gases or air within which the mixture explodes when ignited.

A further hazard of hydrocarbon-based bioprocesses results from the need to sparg air continuously through the microbial system to prevent oxygen limiting conditions. Safety precautions proposed by Schmid *et al.* (1998) include the use of closed chemical hoods, the earthing of electrical equipment and the avoidance of open flames. When working with low flash point alkanes (C_1-C_8),

it is required to dilute the alkane vapour and to cool the exhaust gas to prevent an explosion.

2.5 Modelling Growth and Biotransformation Kinetics

A microbial kinetic model is a set of hypotheses concerning the mathematical relations between measured or measurable quantities associated with the system or process used. It can also be used as a tool to isolate important parameters which can lead to process optimisation. A mathematical model may be simple or complex, depending on the system or process to be modelled and the degree to which the mechanistic approach is used. Unstructed mathematical modelling typically starts with the simplest model, which is modified and extended until it leads to an adequate process kinetic model.

2.5.1 Basic assumptions

Microbial growth can be described using either a structured or unstructured model. Structured models include the effect of cell physiology and metabolism by taking into account the changes in physiology and differentiation of the cell during the course of the experiment and the detailed metabolic reactions. Unstructured growth models, on the other hand, gather all cellular physiology information into a single biomass term so that no explicit structural information is required or used. The structured models are the most realistic, but are computationally complex. Further, detailed physiological and metabolic information is required for their development, a factor which prevents their application on less characterised systems such as *Yarrowia*. The unstructured model gives the most fundamental observation concerning microbial processes and can therefore be considered as a good approximation when the cell composition is time independent or when the substrate concentration is high (Moser, 1985).

An unstructured kinetic model is either segregated or nonsegregated. The unstructured segregated model treats each cell individually with the assumption that the cells might differ from each other. The unstructured nonsegregated model assumes that the entire culture is homogeneous. Since microbial growth is characterised by an exponential growth phase characterised by balance growth, segregation can be neglected since the average composition of single cells remain approximately constant.

2.5.2 Unstructured nonsegregated model for growth

Typical microbial growth is an exponential function of time. The equation describing the rate of microbial growth characterised by the specific growth rate was defined by Malthus in 1798 (Bailey and Ollis, 1986):

$$\frac{dC_x}{dt} = \mu C_x \tag{2.6}$$

where C_x is the biomass concentration ($g.l^{-1}$), μ the specific growth rate (h^{-1}), and μC_X, the term describing the rate at which biomass is produced. Similarly, substrate utilisation can be described as a function of biomass formation through the biomass yield coefficient (Shuler and Kargi, 2002):

$$\frac{dC_S}{dt} = -\left(1/Y_{X/S}\right)\cdot\left(\frac{dC_X}{dt}\right) \tag{2.7}$$

where C_s is the substrate concentration ($g.l^{-1}$), $Y_{x/s}$ the yield coefficient ($g.g^{-1}$) and $\left(1/Y_{X/S}\right)\cdot\left(dC_X/dt\right)$, the term describing the rate at which substrate is consumed for microbial growth. Equations 2.6 and 2.7 neglect cell death and assume all substrate consumed is converted to biomass. These can be extended to include cell death and cell maintenance:

$$\frac{dC_x}{dt} = \mu C_x - k_d C_x \tag{2.8}$$

$$\frac{dC_S}{dt} = -(1/Y_{X/S}) \cdot \mu C_x + mC_x \quad (2.9)$$

where k_d represents the specific cell death rate (h^{-1}) and m the maintenance constant (h^{-1}).

2.5.2.1 Calculating the specific growth rate

The specific growth rate is a measure of the rate of growth or multiplication of an organism, as follows:

$$\mu = \frac{dC_x/dt}{C_x} \quad (2.10)$$

The mathematical model relates the specific growth rate to the chemical and physical factors influencing it. In general the physical factors e.g. temperature and pH, are maintained at a constant and optimal value throughout the growth phase. Under these conditions, the specific growth rate may vary as a function of a single rate limiting substrate. However, when the effects of the physical factors are considered, μ can be calculated using (Birol *et al.*, 2002):

$$\mu = \mu_m \left[\frac{C_s}{K_s + C_s}\right] \cdot \left[\left[k_g \exp\left(-\frac{E_g}{RT}\right)\right] - \left[K_d \exp\left(-\frac{E_d}{RT}\right)\right]\right] \cdot \left[\frac{1}{1 + K_1/[H^+] + [H^+]/K_2}\right] \quad (2.11)$$

where μ_m is the maximum specific growth rate (h^{-1}), C_s the concentration of rate limiting substrates ($g.l^{-1}$), K_s the saturated constant of the rate limiting substrates ($g.l^{-1}$), K_1 and K_2 constants ($gmol.l^{-1}$), H^+ the hydrogen ion concentration ($gmol.l^{-1}$), k_g the Arrhenius constant for growth, E_g the activation energy for growth ($cal.gmol^{-1}$), R the universal gas constant ($cal.gmol^{-1}.K^{-1}$), T the temperature (K), K_d the Arrhenius constant for cell death and E_d the activation energy for cell death ($cal.gmol^{-1}$).

The first term (in brackets) of Equation 2.11 represents the effect of the rate limiting substrate. The second term represents the influence of temperature, in the form of Arrhenius type kinetics (Shuler and Kargi, 2002), and the third the inhibition effect of the medium pH ($[H^+]$). The dependence of cell activity on medium pH is much more complex but Nielsen and Villadsen (1994) showed that the relationship provided by Equation 2.11 adequately fits many microorganisms.

When the physical parameters remain constant Equation 2.11 reduces to:

$$\mu = \frac{\mu_m C_s}{K_s + C_s} \tag{2.12}$$

Equation 2.12 was developed by Monod in 1947. Monod made the following assumptions when developing the model:

- the specific growth rate is limited by a single rate limiting substrate,
- the specific growth rate assumes the form of saturation kinetics
- the consumption rate of the limiting substrate is proportional to the specific growth rate. Figure 2.4 illustrates the relationship between the specific growth rate and the substrate concentration.

Other related forms of specific growth rate dependence have been proposed which in particular instances give a better fit to experimental data than the Monod expression (Bailey and Ollis, 1986).

Tessier $$\mu = \mu_m\left(1 - e^{-C_S/K_S}\right) \tag{2.13}$$

Moser $$\mu = \mu_m\left(1 + K_S C_S^{-\lambda}\right)^{-1} \tag{2.14}$$

Contois $$\mu = \mu_m \frac{C_S}{BC_X + C_S} \tag{2.15}$$

The models develop by Tessier and Moser are a modification of the Monod expression. When the value of C_s/K_s is small and λ is one, the Tessier and Moser expression reduce back to the Monod expression. The use of the Tessier and Moser model in many instances is hampered by the level of complexity by which an algebraic solution is reached. The Contois equation on the other hand includes a saturation constant BC_x, equivalent to K_s and proportional to cell concentration. This describes substrate-limiting growth at high cell densities. This expression is often used to describe growth of filamentous microorganisms where high biomass concentrations inhibit microbial growth.

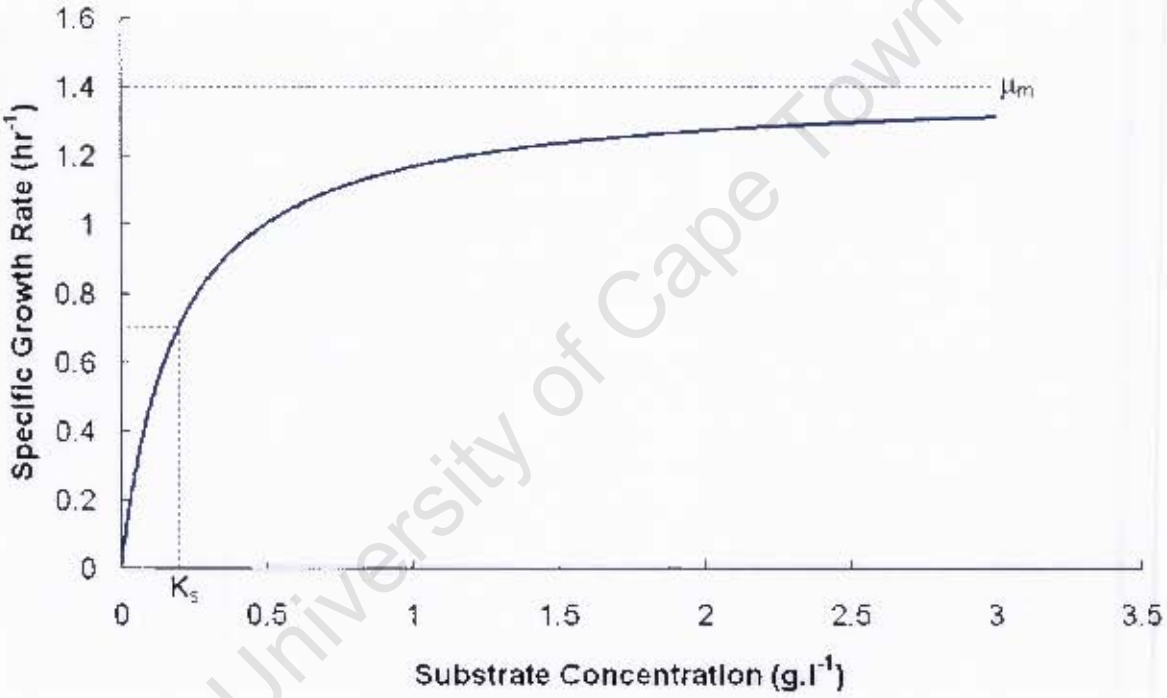

Figure 2.4: Representation of the specific growth rate following Monod kinetics as a function of glucose concentration

Although the Monod expression is a great oversimplification, it has found widespread application in relating population density and limiting nutrient concentration in the continuous culture of unicellular microorganisms in continuous and batch experiments. Consequently, the Monod expression and its modification, which will be discussed in the following section, are generally applied. However, it is important to note that the Monod expression can not account for a lag phase, can not describe the sequential uptake of substrate,

can only describe substrate-limited growth when growth is slow and the population density is low and can only described biomass growth when the rate of biomass production is hyperbolic with respect to the concentration of the rate limiting substrate (Deindoerfer, 1960).

2.5.2.2 Modification to the Monod equation

The Monod equation may fail to predict experimental data at moderate to high substrate or product concentrations or both. The incapability of the Monod equation to predict growth at these moderate to high concentrations is attributed to the inhibitory mechanisms known as substrate and product inhibition. When a strain is affected by substrate inhibition, the specific growth rate of the strain initially increases with an increase in substrate concentration but reaches a maximum whereafter the specific growth rate decreases with a further increase in substrate concentration until it eventually ceases. A similar trend is observed for a strain affected by product inhibition. Beyond a certain threshold value the specific growth rate of a strain will also decrease until it ceases at a certain product concentration.

Several mathematical models have been proposed for quantifying the inhibitory effect of substrate and product inhibition on growth. These models were generally adapted from enzyme inhibition kinetic studies (Shuler and Kargi, 2002):

$$\mu = \frac{\mu_m}{\left(1+\frac{K_s}{C_s}\right)\left(1+\frac{C_s}{K_i}\right)} \qquad (2.16)$$

$$\mu = \frac{\mu_m C_s}{K_s\left(1+\frac{C_s}{k_i}\right)+C_s} \qquad (2.17)$$

$$\mu = \frac{\mu_m}{\left(1+\frac{K_s}{C_s}\right)\left(1+\frac{C_p}{K_p}\right)} \tag{2.18}$$

$$\mu = \frac{\mu_m C_s}{K_s\left(1+\frac{C_p}{K_p}\right)C_s} \tag{2.19}$$

where k_i is the substrate growth inhibition concentration ($g.l^{-1}$), C_p the product concentration ($g.l^{-1}$) and K_p the product growth inhibition concentration ($g.l^{-1}$). Equations 2.16 and 2.17 represent non-competitive and competitive substrate inhibition, respectively, whereas Equations 2.18 and 2.19 represent non-competitive and competitive product inhibition, respectively. It should however be noted that whereas these forms of equations can be derived directly from mechanism for enzyme reactions, the compounded nature of the growth equation does not permit the same mechanistic interpretation. Hence the values of the kinetic parameters can only be obtained form experimental data.

As mentioned in Section 2.5.2.1, simple Monod kinetics accounts for a single rate-limiting substrate only. Industrial fermentations however, utilise media that are balanced with multiple substitutable substrates including complex carbon and nitrogen sources. To incorporate the effect of a second rate limiting substrate the Monod equation can be extended and modified to (Volesky and Votruba, 1992):

$$\mu = \mu_m \frac{C_{s1}}{K_1 + C_{s1}} \cdot \frac{C_{s2}}{K_2 + C_{s2}} \tag{2.20}$$

$$\mu = \mu_1 \frac{C_{s1}}{K_1 + C_{s1}} + \mu_2 \frac{C_{s2}}{K_2 + C_{s2}} \tag{2.21}$$

where μ_1 and μ_2 represent the maximum specific growth rates of two different rate limiting substrates, C_{s1} and C_{s2} the concentrations of two different rate limiting substrates and K_1 and K_2 the saturation constant of two different rate limiting substrates ($g.l^{-1}$).

Equation 2.20 applies to situations where two substrates simultaneously act as the rate-limiting substrate. The equation also implies that growth ceases when both substrates are depleted. A more common occurrence in industry is however, the sequential uptake of more than one rate-limiting substrate which normally results in diauxic growth. Equation 2.21 presents a simplification of the model, normally used to predict this type of growth. When substitutable substrates e.g. s_1 and s_2, are used, the substrate (s_1) supporting the highest specific growth rate is utilised first. During this period microbial growth is described by the first term in Equation 2.21. After depleting the preferential rate-limiting substrate, the specific growth will be described by the second term in Equation 2.21 in which s_2 acts as the rate-limiting substrate.

2.5.2.3 Unstructured nonsegregated model for product formation

Microbial product formation is generally considered to be related directly or indirectly to microbial growth, hence they are classified as either growth-associated, non growth-associated or mixed growth-associated products. Growth-associated products are produced simultaneously with microbial growth at a rate which is proportional to the specific growth rate of the strain. Typically these products are a by-product of the central carbon metabolism. Non growth-associated products are only produced once microbial growth has reached the stationary phase. In such a case the production rate of product is proportional to cell concentration rather than the specific growth rate of the strains. Finally, mixed growth-associated product formation takes place during both the growth and the stationary phase. Currently, the most commonly used kinetic model to predict product formation is the Luedeking-Piret model (Bailey and Ollis, 1986):

$$\frac{dC_p}{dt} = \alpha\mu C_x + \beta C_x \qquad (2.22)$$

where C_p represents product concentration ($g.l^{-1}$), α and β are proportionality constants defined as the specific product formation rate of the growth associated and biomass associated product formation, respectively. It should be noted that when β equals zero, Equation 2.22 reduces to an expression describing the formation of growth-associated products. Similarly, when α equals zero the model only predicts the formation of non-growth associated products.

A similar equation to the Luedeking-Piret model can be used to describe the utilisation of the corresponding substrate for product formation (Fredrickson *et al.* 1970):

$$\frac{dC_s}{dt} = \frac{1}{Y_{p/s}} \cdot [\alpha\mu C_x + \beta C_x] \qquad (2.23)$$

where C_s is the corresponding substrate concentration ($g.l^{-1}$), $Y_{p/s}$ is a yield coefficient ($g.g^{-1}$). Both Equations 2.22 and 2.23 are however limited, since they predict product formation even in the absence of substrate. This limitation can however be overcome by adding to the Luedeking-Piret equation a substrate limitation term, as described by Fredrickson *et al.* (1970):

$$\frac{dC_p}{dt} = \alpha\mu C_x + \beta \cdot \left(\frac{C_s}{K_s + C_S}\right) \cdot C_x \qquad (2.24)$$

$$\frac{dC_s}{dt} = \frac{1}{Y_{p/s}} \cdot \left[\alpha\mu C_x + \beta \cdot \left(\frac{C_s}{K_s + C_s}\right) \cdot C_x\right] \qquad (2.25)$$

where K_s is a saturation constant ($g.l^{-1}$).

2.6 Conclusions

The microbial oxidation of linear alkanes into higher value chemicals offers an alternative to chemical processes but a combination of low catalyst turnover rates and limited stability have prevented the widespread use thereof in commercial processes to date.

Growth and biotransformation conditions which influence microbial growth and α,ω-dicarboxylic acid formation include temperature, pH, the type of carbon and nitrogen sources used for growth, alkane concentration, alkane chain length, time of alkane addition, product concentration and the effect of substrate inhibition. Literature on these specific conditions, however, is mostly confined to *Candida* sp. and deals only to a limited degree with *Y. lipolytica*. *Yarrowia lipolytica* has been identified as being able to excrete α,ω-dicarboxylic acids from linear alkanes. Further, it is becoming increasingly interesting as a generic fungal host system. Hence, the overall objective of this dissertation aims to investigate the potential of genetically manipulated strains of *Y.lipolytica* for dicarboxylic acid formation as a form of alkane activation.

It is recognised that the development of an appropriate kinetic model able to predict the performance in terms of growth and biotransformation under defined operating conditions can be used to assist to enhance productivity. No such model is reported for microbial alkane oxidation using *Yarrowia*. Further, little literature exists describing the quantitative relationship between the environmental parameters and the growth and oxidation kinetics of *Yarrowia lipolytica* under glucose and alkane limiting conditions. A specific objective of this thesis is to provide such a model using a standard unstructured modelling approach.

Following review of the literature, this dissertation focuses on the potential for *Y. lipolytca* to catalyse activation of linear alkanes through their conversion to dicarboxylic acids. In addition to addressing the above objectives, the following research questions were formulated:

- Will the ability of *Y. lipolytica* TVN 497 to produce α,ω-dicarboxylic acid be influenced by the presence of residual glucose in the biotransformation phase?
- Will the specific growth rate of *Y. lipolytica* TVN 497 be affected by substrate (glucose) inhibition?
- How is the α,ω-dicarboxylic acid productivity of *Y. lipolytica* TVN 497 influenced by the alkane concentration and the pH of the production phase?
- Can a simplified unstructured kinetic model be developed for *Y. lipolytica* TVN 497 to adequately predict growth and biotransformation?
- Do *Y. lipolytica* strains TVN 497, TVN 499, TVN 501 and TVN 502, which are formed using similar insertion and deletion mutations, produce α,ω-dicarboxylic acid in similar quantities and are these adequate for industrial applications?

Chapter 3

Materials and Methods

3.1 Microorganisms

During this research, four recombinant strains of *Yarrowia lipolytica*, described in Table 3.1, were used. These strains were obtained from the collaborating laboratory of Prof. Martie Smit at the Department of Microbial, Biochemical and Food Biotechnology of the University of the Free State (UFS), South Africa. The recombinant strains differ from the parent strain (*Y. lipolytica* W29) as they are unable to utilise alkanes as a sole source of carbon and energy. This results from disruption of the genes encoding acyl-CoA oxidase the enzyme which catalyses the first reaction in the β-oxidation pathway. Consequently, all recombinant strains were able to produce and excrete α,ω-dicarboxylic acids structurally similar to the substrate. To increase the specific productivity of all recombinant *Y. lipolytica* strains, overexpression of the genes which encode the cytochrome P450 monooxygenase (the enzymes which catalyse the first and rate-limiting step in the ω-oxidation pathway) had been engineered into these strains.

Table 3.1: Yeast strains utilised in this study.

		Additional *CYP* genes added			
Yeast	Strain Number	*CYP* Gene Cloned	Source	Hydroxylase Activation	β-oxidation
Y. lipolytica	TVN 497[1] TVN 499[1] TVN 501[1] TVN 502[1]	*CYP*557A1 (Multiple copies)	*Rhodorula retinophila*	Native & cloned alkane / fatty acid hydroxylase	Disrupted

[1]Strains were constructed by Professor M.S. Smit in the laboratory of Dr. J.-M Nicaud at the Laborotoire de Microbiologie et Génétique Moléculaire, INRA CNRS INAP-G, UMR2585, Centre de Biotechnologie Argo-Industrielle, 78850 Thiverval-Grignon, France

3.2 Growth and Preservation Media

During this research, three types of growth media were used. Two media represented complex media of which the defined chemical composition was

unknown whilst the third was semi-defined. The complex media were adapted from growth media formulations developed by the collaborating research group (UFS) and by Picataggio *et al.* (1992). The Picataggio medium was modified by replacing the Yeast Nitrogen Base (YNB) with peptone (an inexpensive nitrogen source), based on findings of Williams (2005). Williams showed that while a small (0.083 $g.l^{-1}.hr^{-1}$) decrease in the overall biomass productivity was observed, the productivity of α,ω-dicarboxylic acids remained unchanged when the YNB nitrogen source in the Picataggio media is replaced with Peptone. As a result, the production costs of α,ω-dicarboxylic acids can be reduced by using peptone as the nitrogen source. Tables 3.2 and 3.3 list the compositions of the resulting complex media used.

Table 3.2 Composition of medium developed by the UFS

Component	Composition (g/l)
Yeast Extract	10
Peptone	10
Glucose	10-60

Table 3.3 Composition of the modified Picataggio medium (Williams, 2005)

Component	Composition (g/l)
Yeast Extract	8
Peptone	4.8
Glucose	38
Ammonium Sulphate	1.5
Potassium Dihydrogen Phosphate	0.5
Potassium Phosphate Dibasic	0.5

Preliminary shake flaks experiments were conducted on the UFS medium. These experiments was performed to evaluated the ability of strains TVN 497, TVN 499, TVN 501 and TVN 502 to produce biomass and α,ω-dicarboxylic acids. The modified Picataggio medium assisted in the development of

preliminary kinetic data and was applied to investigate the effect of initial glucose and alkane concentration on α,ω-dicarboxylic acid production.

Table 3.4 Composition of medium developed by Antonucci *et al.* (2001)

Component	Composition (g/l)
Yeast Extract	1
Glucose	5-42
Ammonium nitrate	3.5
Potassium dihydrogen phosphate	1
Ferrous sulphate heptahydrate	0.1
Magnesium sulphate heptahydrate	0.25
Manganese sulphate monohydrate	0.015

Table 3.5 Composition of stock culture media YPD4

Component	Composition (g/l)
Yeast Extract	10
Peptone	10
Glucose	40

The semi-defined medium (Table 3.4) was adopted from the research of Antonucci *et al.* (2001) on citric acid production using a wild-type *Y. lipolytica* strain. The semi-defined medium facilitated development of more rigorous kinetic data and understanding of nitrogen utilisation. To maintain the stock cultures, the strains were plated on an YPD4 agar plate (Table 3.5), incubated at 30 °C for 3 days and stored at 4 °C. The stock cultures were re-plated every six weeks.

3.3 Non-Growth Substrate

All biotransformation studies were conducted with a C_{12}–C_{13} alkane cut obtained from Sasol Ltd. A gas chromatograph (GC) analysis was conducted on this alkane cut to determine the composition thereof and to highlight any possible impurities. The result obtained confirmed a composition comprising

mainly dodecane and tridecane as indicated in Figure 3.1. The concentration of both compounds in the mixture was established as 50% (v/v). This was done by dividing the area under the dodecane and tridecane peak by the area under the sebacic acid methyl ester peak (added internal standard), and applying the results to the standard curve in Appendix A4. In all cases, sebacic acid was used as the standard of reference. The visible noise on the GC baseline at retention times of 3 min, 4 min and 7.5 min is attributed to unknown impurities present in the alkane mixture.

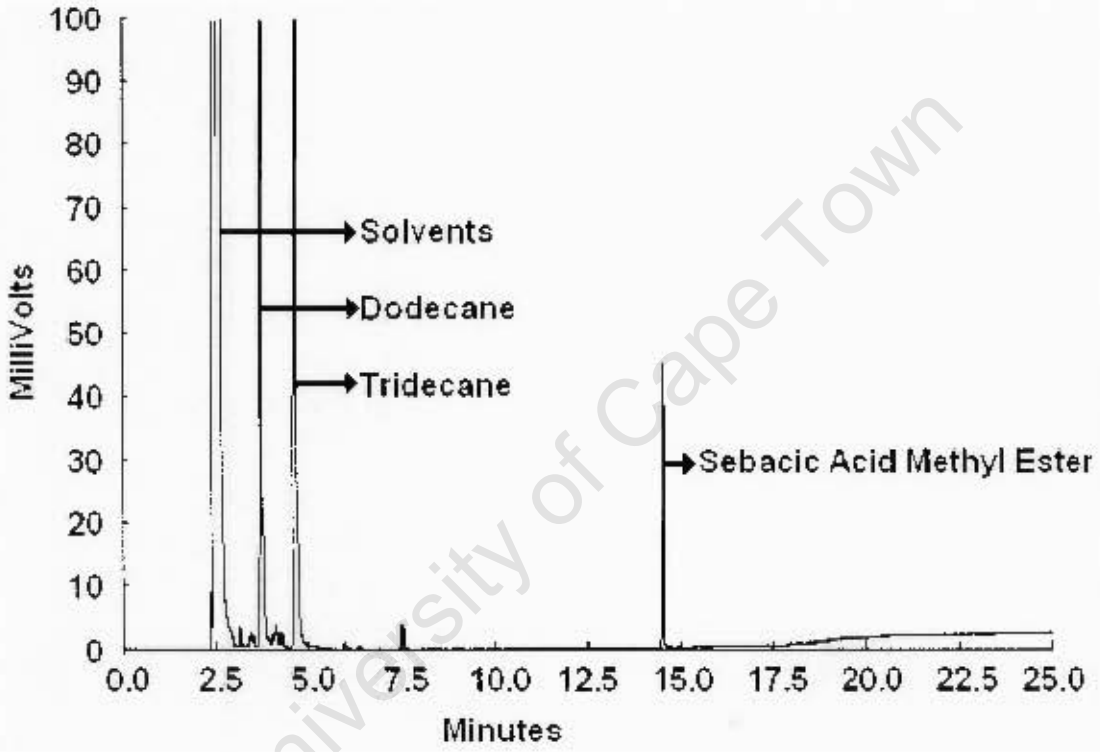

Figure 3.1: A gas chromatograph of the alkane cut obtained from Sasol Ltd.

3.4 Equipment

3.4.1 Braun BIOSTAT C bioreactor

The Braun BIOSTAT C bioreactor has a total internal volume of 15 litres with a working volume of 10 litres. It is equipped with three, six-blade Rushton impellers in combination with four baffles to ensure efficient mixing. The three impellers were installed at an equidistant, spacing of one impeller diameter from each other with a spacing of 4 cm between the lowest impeller and

bottom of reactor. Aeration was provided by sparging compressed air through a ring sparger, situated below the bottom turbine. The in and outlet gas streams were filter-sterilised using a microporous filter with a 0.22 µm pore size. Temperature was controlled by circulating either warm or cold water through the jacket of the vessel. Dissolved oxygen was measured by a polarographic dissolved oxygen probe (Mettler Toledo InPro 6900) fitted with a Teflon membrane. The pH of the medium was measured with the aid of a pressurised gel-filled pH probe (Mettler Toledo 405-DPAS-SC-K8S) and automatically maintained at set points by the addition of 8 Molar NaOH and 5 Molar H_2SO_4.

3.5 Methodology

3.5.1 Sterilisation and filtration

The YNB solutions and alkanes were sterilised using a Millex vent filter measuring 50 mm in diameter with a maximum pore size of 0.2 µm. The mineral salt media were heat-sterilised at 121 °C for 20 minutes in the reactor vessel. To prevent the Maillard reaction, glucose was autoclaved separately in solution and combined with the mineral salts aseptically at room temperature.

3.5.2 Growth conditions

In order to facilitate comparison with literature data, the same growth conditions stipulated by the authors who formulated the UFS, Picataggio and Antonucci media were used. Consequently, the growth conditions applied were associated with the type of medium used.

For the UFS medium, shake flask experiments were performed in a 28 °C room on a rotary shaker at 180 rpm. The experiments were conducted in 500 ml Erlenmeyer flasks containing one tenth broth (50 ml) to provide sufficient aeration. The broth in each case was buffered to pH 7.8 by adding 82.5 mg of K_2HPO_4 and 3.6 mg of KH_2PO_4 to the culture media.

For the modified Picataggio medium, the culture was grown aerobically in the Braun BIOSTAT C bioreactor at a medium pH of 6 and a temperature of 30 °C. Agitation took place at 700 rpm with an aeration rate of 0.8 vvm. In the case of the Antonucci medium, the bioreactor conditions were set at pH 5 and a temperature of 30 °C. Mixing was effected at 900 rpm and an aeration rate of 0.6 vvm.

3.5.3 Biotransformation conditions

When biotransformation took place in the 500 ml Erlenmeyer flasks, the growth and biotransformation conditions were identical (Section 3.5.2). When biotransformation took place in the Braun BIOSTAT C bioreactor, the medium pH was adjusted and maintained at pH 7.8 using 8 Molar NaOH and 5 Molar H_2SO_4. No further modification to operating conditions was made (Section 3.5.2).

3.5.4 Inoculum

Defined inoculum development is required to ensure culture history does not influence experiment. To ensure a dense suspension of biomass, to minimise the lag phase, the inoculum volume is typically 1 to 20% (v/v) of the working volume of the bioreactor (Bailey and Ollis, 1986). The inoculum preparation procedure is therefore a stepwise process during which the volume of the inoculum is increased.

The shake flask experiments were performed in 500 ml Erlenmeyer flasks, containing 45 ml of UFS media. A single inoculum preparation step was used as inter-experiment variation was accounted for through appropriate control flasks. The inoculum was prepared by aseptically transferring a loop of yeast from an YPD agar plate to a 500 ml Erlenmeyer flask which contained 45 ml of UFS media. The pre-culture was cultivated for 48 hours at 29 °C on a rotary shaker at 180 rpm. The shake flask experiments were inoculated by aseptically transferring 5 ml of the pre-culture to each flask.

A three-step inoculation procedure was used to inoculate the working volume of 10 l used in the Braun BIOSTAT C bioreactor. The pre-inocula were prepared in five 250 ml Erlenmeyer flasks, each containing 20 ml of either Picataggio or Antonucci media. After inoculation, the pre-cultures were cultivated for 48 h at 28 °C on a rotary shaker at 180 rpm. The pre-cultures were transferred aseptically to a second set of five 2000 ml Erlenmeyer flasks, each containing a 180 ml of either the Picataggio or Antonucci media. This second set of inocula was cultivated in the same way for 30 h. After cultivation the final inocula (totalling 900 ml) were aseptically transferred to a one litre inoculum flask. The final inoculum was aseptically inoculated into 9 l of either the Picataggio or Antonucci media in the Braun BIOSTAT C bioreactor.

3.6 Analysis

3.6.1 Dry weight measurements for biomass determination

Dry biomass concentration was measured gravimetrically. Method modification over the standard approach was required to ensure removal of the residual alkane and α,ω-dicarboxylic acids from the culture media. To perform the analyses, cellulose nitrate membrane filters (0.45 µm) were dried in an oven at 80 °C for 48hrs before and after filtration. After drying they were cooled in a desiccator before being weight to 4 decimal places. The difference in filter weight before and after filtration was attributed to biomass collected by filtration of a fixed volume sample.

These samples were prepared by transferring well mixed culture samples (4 ml) to 30 ml test tubes and adding a 5 Molar NaOH solution (500 µl) to promote the dissociation of α,ω-dicarboxylic acids, thereby increasing their solubility. After the addition of NaOH, 2 ml of cyclohexane was added to the culture media to create a secondary organic phase to promote the removal of alkanes from the culture media. The mixture was vortexed for 5 min before being poured onto a pre-weighed cellulose nitrate membrane filter paper. The filter cakes were washed twice, first with a mixture of distilled water (4 ml),

cyclohexane (2 ml) and 5 M NaOH (400 µl) and secondly with 26 ml of distilled water. It was assumed that the initial dissociation and solvent-solvent extraction step together with the washing of the filter cakes were sufficient enough to remove all the residual α,ω-dicarboxylic acids and alkanes from the biomass fraction collected by filtration. The filter paper and biomass were then dried and weighed as before. A maximum standard deviation of 5% was calculated for a set of samples containing a biomass concentration ranging from 1.7 to 12.1g.l^{-1}. The calculations are shown in Appendix A5.

3.6.2 Turbidimetric measurements for biomass determination

Turbidimetric measurements were used as an alternative measure of biomass concentration. When sampling before alkane addition, 500 µl culture samples were transferred to 1.5 ml Eppendorf tubes and diluted accordantly. When sampling after alkane addition, 500 µl culture samples were treated with 200 µl cyclohexane and 100 µl 5 Molar NaOH solution. Cyclohexane was used to dissolve residual alkane and NaOH solution was used to promote the dissociation of the α,ω-dicarboxylic acids in the aqueous phase. The samples were vortexed for 5 min and then centrifuged for 10 min at 60 000 m.s^{-1}. The pellets were re-suspended in 500 µl saline solution (0.9% NaCl). Before measuring optical density, the samples were vortexed and diluted accordantly.

The absorbance of both samples was measured at a wavelength of 620 nm by transferring 200 µl samples into a Labsystem iEMS microtitre plate reader MF (Thermo BioAnylysis Company, Helsinki Finland). Both samples were diluted by a recorded factor until the absorbance reading was below 0.6. Hence the culture absorbance was calculated as the product of absorbance and dilution factor.

3.6.3 Reducing sugars assay

In the present study a simple and quantitative colorimetric method, for reducing sugars, modified from that developed by Miller (1959), was used to estimate the concentration of glucose in the culture media. The principle of the assay is based on the conversion of dinitrosalicylic acid to form a red to brownish colour. This develops when the aldehyde group present in glucose is oxidised to yield a carboxyl group. Beer's law was obeyed when the glucose concentration ranged between 0.08 to 0.53 $g.l^{-1}$. The standard deviation at these detection limits was calculated as 0.01 $g.l^{-1}$ and 0.02 $g.l^{-1}$, respectively. The calculations are shown in Appendix A1.

The above method is convenient and relatively inexpensive to obtain the concentration of reducing sugars. It must be recognised that measurements are influenced by a variety of salts, resulting in either an over- or underestimation of the true reducing sugar concentration in the sample (Sinegani and Emtiazi, 2006). Since a variety of salts including K_2HPO_4 and KH_2PO_4, were used as part of the media formulation, a certain extent of interference was expected. Due to the small quantities of salt used however, the extent of the interference was assumed to be insignificant.

Table 3.6: Composition of medium DNS reagent

Component	Concentration ($g.l^{-1}$)
Dinitrosalicylic Acid	10
Phenol	2
Sodium sulphite	0.5
Sodium hydroxide	10

To perform the analysis, culture supernatants were diluted to obtain a glucose concentration within the detection limits. Three millilitres of diluted supernatants were mixed with 3 ml of DNS reagent (Table 3.6) in lightly capped test tubes. The mixtures were heated for 10 minutes at 90 °C in a waterbath. After heating, 1 ml potassium sodium tartrate (40% (w/v)) solution

was pipetted into each mixture which was cooled to room temperature in a waterbath. Absorbance of 575 nm was read in the Labsystem iEMS microtitre plate reader MF (Thermo BioAnalysis Company, Helsinki Finland). The concentration of glucose in the culture supernatant was calculated from the correlation curve available in the Appendix A1.

3.6.4 Ammonium ion assay

The ammonium ion concentration in this research was estimated using the phenol-hypochlorite reaction developed by Weatherburn (1967). It is a simple colorimetric method with a detection limit ranging from 0 $mmol.l^{-1}$ to 0.52 $mmol.l^{-1}$. The standard deviation at these detection limits was calculated as less than 0.05 $mmol.l^{-1}$. The calculations are shown in Appendix A2. The principle of the assay is based on the formation of an intensely blue compound, indophenol, by the reaction of ammonia, hypochlorite, and phenol catalysed by sodium nitropruside (Russell, 1944). The colour production by this reaction is influenced by the copper, magnesium and calcium ions which tend to inhibit colour development (Russell, 1944). This method could not be used to estimate the total nitrogen content of the biological fluids and was specifically used to obtain the residual ammonium ion concentration in the culture media.

To perform the analysis, culture supernatant were diluted to obtain an ammonium ion concentration within the detection limits. In 1.5 ml Eppendorf tubes, 100 µl of diluted culture samples were mixed with 550 µl each of reagent A and reagent B (Tables 3.7 and 3.8). The samples were vortexed for 1 min before being placed in the dark for approximately 30 min. Once the colour intensity stabilised, 200 µl samples were pipetted into a Labsystem iEMS microtitre plate reader MF (Thermo BioAnalysis Company, Helsinki Finland) where absorbance was measured at 625 nm. The concentration of the ammonium ion in the culture supernatant was calculated using the calibration curve available in the Appendix A2.

Table 3.7: Composition of reagent A, used in the ammonium ion assay (Weatherburn, 1967)

Component	Concentration ($g.l^{-1}$)
Phenol	10
Sodium Nitroprusside	0.05

Table 3.8: Composition of reagent B, used in the ammonium ion assay (Weatherburn, 1967)

Component	Concentration ($g.l^{-1}$)
Sodium Hydroxide	5
Sodium Hydrochlorite	0.0084

3.6.5 Extraction and Analysis of Alkanes and α,ω-Dicarboxylic Acids from Culture

A multistep method was used to quantify the alkanes and α,ω-dicarboxylic acids in the culture media. The method used was adopted and refined from Green *et al.* (2000) and Uchio and Shiio (1972a) by the collaborating research group of Prof. Martie Smit (UFS). A 500 µl aliquot of culture media was transferred into 1.5 ml Eppendorf tubes. The α,ω-dicarboxylic acids in each case was solubilised by lowering the pKa value of the samples by adding 50 µl of a 5 Molar HCl solution to each of the samples. The solubilised α,ω-dicarboxylic acids and the residual alkanes were extracted into the organic phase using 600 µl of tertiary butyl methyl ether solution, containing 0.2% (w/v) suberic acid as an internal standard. The bilayer liquid samples were vortexed for 5 min, then centrifuged for 10 min at 60 000 $m.s^{-2}$. The supernatant of each sample was extracted and stored at -20 °C until analysed.

The alkane and α,ω-dicarboxylic acid content of the organic phase were analysed by gas chromatography (GC) following methylation. Trimethylsulphonium hydroxide (TMSH, 50µl) was added to 50 µl organic fraction from sample (supernatant) and vortexed for 5 min. After methylation,

a 1.5 µl aliquot of each sample was injected into the GC, operated at conditions tabulated in Table 3.9. The multipoint internal standard method was used to quantify the individual components (alkanes and α,ω-dicarboxylic acids) to avoid the uncertainties introduced by sample injection. The unknown concentration of the individual components in the culture media was estimated using standard curves available in Appendixes A3 and A4.

Table 3.9: GC conditions (Williams, 2005)

Entity	Value
Column	BP 20 Macro bore 30 m x 0.32 µm x 0.25 µm
Head Pressure	9.1 psi
Split	5:1
Carrier Gas	N_2 30 ml.min^{-1}
Detector	FID 300 °C
Oven	120 °C held for 5 min Increase 10 °C.min^{-1} to 220 °C Held for 7 min

3.7 Carbon and Oxygen Balance

A steady state mass balance approach was used to calculate the rate of oxygen utilisation and carbon dioxide production during microbial growth and product formation (Shuler and Kargi, 2002). The chemical composition and flow-rate of the inlet and outlet gas streams to and from the Braun BIOSTAT C bioreactor were measured using an off-gas analyser (Hartmann and Brown, Advance Optima) and a single stage flowmeter, respectively. The molar flow rate of oxygen at the inlet gas stream was calculated using Equation 3.1:

$$F_{O_2,in} = \left(F_{Gas,in} - F_{Gas,in}X_{CO_2,in} - F_{Gas,in}X_{Argon}\right)\cdot \Omega_{in} \qquad (3.1)$$

with

$$\Omega_{in} = \frac{F_{O_2,in}}{F_{O_2,in} + F_{N_2,in}} \qquad (3.2)$$

where $F_{O2,in}$ and $F_{gas,in}$ are the molar flow-rate of oxygen and air into the system (gmol.h^{-1}), respectively and $X_{CO2,in}$ and X_{Argon} the carbon dioxide and argon mole fraction in the inlet air stream, respectively.

$F_{Gas,in}$ was obtained by applying the ideal gas law using the inlet volumetric flow rate, $X_{CO2,in}$ and Ω_{in} the off-gas analyser and X_{Argon} as 0.934% from literature (Himmelblau, 1996). Since the strains used during this research could not fix nitrogen, nitrogen was used as a tie substance i.e. $F_{N2,in}=F_{N2,out}$. Consequently, the molar flow rate of oxygen at the outlet gas stream was back calculated using Equation 3.3:

$$\Omega_{out} = \frac{F_{O_2,out}}{F_{O_2,out} + F_{N_2,out}} \tag{3.3}$$

with

$$F_{N2,out} = F_{N_2,in} = \left(F_{Gas,in} - F_{Gas,in}X_{CO_2,in} - F_{Gas,in}X_{Argon}\right)\cdot \Omega^{*}_{in} \tag{3.4}$$

and

$$\Omega^{*}_{in} = 1 - \Omega_{in} \tag{3.5}$$

where $F_{O2,out}$ and $F_{N2,out}$, are the molar flow-rate of oxygen and nitrogen out of the system (gmol.h^{-1}), respectively, and $F_{N2,in}$ the molar nitrogen flow-rate into the system, (gmol.h^{-1}). The oxygen utilisation rate was calculated as:

$$F^{*}_{O_2} = F_{O_2,in} - F_{O_2,out} \tag{3.6}$$

and the rate of carbon dioxide production was calculated by:

$$P_{CO_2} = \left(F_{Gas,out}X_{CO2,out} - F_{Gas,in}X_{CO2,in}\right) \tag{3.7}$$

where $X_{CO2,out}$ represents the molar carbon dioxide fraction in the outlet air stream. $F_{Gas,out}$ was obtained by applying the ideal gas law using the outlet volumetric flow. The total amounts of oxygen used and carbon dioxide produced were calculated using an appropriate numerical integration method.

The carbon balance was evaluated by assuming glucose to be the only carbon source for growth. The biomass composition was estimated as $C_5H_7NO_2$ which is specific for *Yarrowia lipolytica* (Papanikolaou *et al.* 2002).

3.8 Experimental Approach

To develop kinetic data for growth, six experiments were conducted with *Y. lipolytica* TVN 497 using the modified Picataggio complex medium and the Antonucci semi-defined medium in the Braun BIOSTAT C bioreactor. Basic kinetic data was developed by conducting two base case experiments in the modified Picataggio medium at an initial glucose concentration of 40 $g.l^{-1}$. To develop more rigorous kinetic data and to evaluate the effect of glucose concentration on the kinetic parameters, four experiments were conducted in the Antonucci medium at initial glucose concentrations of 5 $g.l^{-1}$, 13 $g.l^{-1}$, 42 $g.l^{-1}$ and 51 $g.l^{-1}$.

The effect of substrate inhibition was evaluated by conducting five shake flask experiments with strain *Y. lipolytica* TVN 497 in the UFS medium at initial glucose concentrations of 10 $g.l^{-1}$, 20 $g.l^{-1}$, 30 $g.l^{-1}$, 40 $g.l^{-1}$ and 60 $g.l^{-1}$.

The potential for alkane activation was determined through the addition of a C_{12} – C_{13} alkane cut to the Yarrowia culture in late exponential or early stationary phase with subsequent monitoring of its bioconversion to dicarboxylic acids. Further experiments conducted focused on the five research questions discussed in Section 2.6. The effect of alkane on biotransformation was evaluated by conducting four experiments in the modified Picataggio complex medium using the Braun BIOSTAT C bioreactor. During two of the experiment 1% and 3% (v/v) alkane was added to the

culture media 18 h after inoculation. In both experiments, the pH of the production phase was elevated and maintained at pH 7.8. The other two experiments served as reference with alkane being added to one of the experiments 48 h after inoculation whilst the pH of the production phase for the other was maintained at pH 6.0. The same experiments were used to evaluate the effect alkane concentration, medium pH, time of alkane addition on biomass production and to develop a basic kinetic model for biotransformation.

The ability of *Y. lipolytica* strains i.e. TVN 497, TVN 499, TVN 501 and TVN 502 to produce biomass and α,ω-dicarboxylic acids and their relative performance was evaluated by conducting duplicate shake flask experiments in the UFS medium. An alkane cut (3% (v/v)) comprising equal volume dodecane and tridecane was added to each culture medium 48 h after inoculation.

Chapter 4

Developing of a Mathematical Model

An unstructured kinetic model, consisting of 10 non-linear differential equations and 8 kinetic parameters, was developed to predict the quantitative performance of *Y. lipolytica* TVN 497 in a complex and semi-defined medium. The model quantitatively predicts the ability of strain TVN 497 to produce biomass, utilise glucose, oxidise alkanes and produce α,ω-dicarboxylic acids. The kinetic parameters of the model are quantified by applying a two step approach discussed in Section 4.3. The two step approach is comprised of a graphical as well as a computer based iterative process by means of which the kinetic parameters of the model are first estimated and then calculated.

4.1 Developing of an Unstructured Kinetic Model to Predict Growth and Glucose Utilisation

Biomass production was approximated with the Malthus equation (Shuler and Kargi, 1992) in which the rate of biomass production is first order with respect to biomass concentration. The Malthus equation is expressed mathematically as:

$$\frac{dC_x}{dt} = \mu C_x \qquad (4.1)$$

where μ is the specific growth rate (h^{-1}) and C_X the biomass concentration ($g.l^{-1}$). The Malthus equation can be applied to situations where microbial growth is exponential ($d\mu/dt=0$ where $\mu>0$) and where the rate of cell death rate is negligible. The specific growth rate however, varies during growth and is influenced by a variety of physical and chemical factors reviewed in Section 2.5.2.1. During this research, the physical factors (temperature and pH) were maintained at a constant value or were regulated within a narrow margin. Consequently, it was assumed that the specific

growth rate was only influenced by the presence of substrates and products and their concentration. As a first assumption it was assumed that the specific growth rate was only a function of the availability of a single limiting substrate, glucose. Hence, the Monod equation was applied to quantify μ:

$$\mu = \frac{\mu_m C_{sg}}{K_s + C_{sg}} \tag{4.2}$$

where μ_m is the maximum specific growth rate (h^{-1}), K_S is the saturation constant ($g.l^{-1}$) and C_{sg} the glucose concentration ($g.l^{-1}$).

In some cases, an increase in substrate concentration beyond a critical value results in a decrease in specific growth rate. This phenomenon is known as substrate inhibition and requires modification of the Monod equation. Since the growth rate of wild-type *Y. lipolytica* is affected by high glucose concentrations (Moresi, 1994), the Monod equation was modified to incorporate the effect of substrate inhibition. The modified Monod equation, also known as the Andrews model (Andrews, 1968), can be expressed as:

$$\mu = \frac{\mu_m}{K_s + C_{sg} + C_{sg}^2/K_i} \tag{4.3}$$

where K_i is the inhibition constant ($g.l^{-1}$) and numerically equates the highest concentration of inhibitor at which the specific growth rate is equal to one-half of the maximum specific growth rate in the absence of inhibition. The appropriateness of both expressions (Monod and Andrews) in conjunction with the Malthus equation was evaluated during this research. The Monod and Andrews models when combined with the Malthus equation are expressed mathematically as:

$$\frac{dC_x}{dt} = \mu_m \frac{C_{sg}}{K_s + C_{sg}} C_x \tag{4.4}$$

$$\frac{dC_x}{dt} = \mu_m \frac{1}{K_s + C_{sg} + C_{sg}^2/K_i} C_x \qquad (4.5)$$

where Equations 4.4 and 4.5 originate from the Monod and Andrews equation, respectively.

When performing a mass balance on the restricted rate limiting substrate, glucose in batch culture, the following equation applies:

$$-\frac{dC_{sg}}{dt} = \frac{1}{Y_{x/sg}} \cdot \frac{dC_x}{dt} + m \cdot C_x + \frac{1}{Y_{p/sg}} \cdot \frac{dC_p}{dt} \qquad (4.6)$$

where C_{sg} is the glucose concentration ($g.l^{-1}$), $Y_{x/sg}$ and $Y_{p/sg}$ are yield coefficients ($g.g^{-1}$) for biomass and products from glucose, respectively, m a maintenance term (h^{-1}) and C_p the concentration of a product or products ($g.l^{-1}$) other than biomass. In the present study it was assumed, based on material balance data, that the amount of glucose used for maintenance was negligible and that biomass and corresponding carbon dioxide was produced from glucose alone. As a result Equation 4.6 reduces to:

$$-\frac{dC_{sg}}{dt} = \frac{1}{Y_{x/sg}} \cdot \frac{dC_x}{dt} \qquad (4.7)$$

where Equation 4.7 relates the utilisation rate of glucose directly to the production rate of biomass.

4.2 Developing of an Unstructured Kinetic Model to Predict the Production of α,ω-Dicarboxylic Acids and the Oxidation of Alkanes

In the experimental system studied, the extracellular products, α,ω-dicarboxylic acids, were produced by biotransformation of alkanes. Here it was assumed and confirmed experimentally, that the intermediates alcohol,

aldehyde, monocarboxylic acids and hydroxyacids did not accumulate. The rate of α,ω-dicarboxylic acid production was modelled using the Luedeking–Piret model, generally applied to predict the production of growth associated, non-growth associated and mixed-growth associated products:

$$\frac{dC_p}{dt} = \alpha\frac{dC_x}{dt} + \beta C_x \qquad (4.8)$$

where α and β are constants of proportionality. The first term in Equation 4.8 represents the production of growth-associated products and the second, the production of non-growth associated products. α,ω-Dicarboxylic acids were produced as non-growth associated products during this research owing to the addition of alkanes following microbial growth. Consequently, the appropriate model can be reduced to:

$$\frac{C_{dda}}{dt} = \beta_{dda} C_x \qquad (4.9)$$

and

$$\frac{C_{tda}}{dt} = \beta_{tda} C_x \qquad (4.10)$$

where C_{dda} and C_{tda} represent the concentration of dodecanedioic acid and tridecanedioic acid in the medium ($g.l^{-1}$), respectively. A shortcoming of the Luedeking-Piret model is its prediction of product formation even in the absence of a substrate.

To account for the substrates from which the corresponding α,ω-dicarboxylic acids were produced, a mass balance was performed on both alkanes (dodecane and tridecane). The following two expressions predict the oxidation of dodecane and tridecane where the complete blocking of β-oxidation prevents its use in further metabolic pathways:

$$-\frac{dC_{sdd}}{dt} = \left(\frac{1}{Y_{dda/dd}}\right) \cdot (\beta_{dda} C_x) \qquad (4.11)$$

and

$$-\frac{dC_{s/d}}{dt} = \left(\frac{1}{Y_{tda/td}}\right) \cdot (\beta_{tda} C_x) \qquad (4.12)$$

C_{sdd} and C_{std} represent the dodecane and tridecane concentration in the medium ($g.l^{-1}$) respectively. $Y_{dda/dd}$ and $Y_{tda/td}$ are yield coefficients of dodecanedioic acid from dodecane and tridecanedioic acid from tridecane ($g.g^{-1}$), respectively.

4.3 Kinetic Parameter Quantification

The kinetic parameters of the model are quantified using a two step approach. Since the model is non-linear with multiple kinetic parameters, the optimisation of the set of parameters depends significantly on the initial estimations of the parameter values. For this reason a two step approach, comprising a graphical and a computer based iterative process, was developed to quantify the values of the kinetic parameters.

4.3.1 Graphical approach

Initial estimates of kinetic parameters μ_m, β, $Y_{x/sg}$, $Y_{dda/dd}$ and $Y_{tda/td}$ were made by graphical analysis of the experimental data. The initial approximation of μ_m was obtained by estimating the slope of the tangent drawn to the linear portion of the sigmoid curve which is fitted to the data representing the natural logarithm of the cell concentration against time, according to Equation 4.13 obtained on integration of the Malthus equation.

$$\ln(C_x) = \mu_m t + \ln(C_{xo}) \qquad (4.13)$$

where t represents the time (h) and C_{xo} the biomass concentration ($g.l^{-1}$) at the point where growth starts it's exponential increase.

The value of β represents the specific production rate of a non-growth associated product, which is related to the biomass concentration as follows:

$$\beta = \frac{dC_p/dt}{C_x} \tag{4.14}$$

An average value of β was used as first estimate. The yield coefficients $Y_{x/sg}$, $Y_{dda/dd}$ and $Y_{tda/td}$ were estimated from the slope of the linear regression model fitted to the experimental data representing product produced as a function of substrate used.

4.3.2 Computer based iterative process

To quantify the kinetic parameters, a computer based iterative process (Figure 4.1), which accommodates the above differential equations, was developed in Matlab R12. The process involves an initial integration step, during which the differential equations of the model together with the initial kinetic parameters, estimated with the graphical approach, were numerically integrated with the aid of the Runga-Kutta method. The integrated values obtained were compared with the experimental data after which, depending on the error, new values of the kinetic parameters were calculated, using the Nelder-Mead non-linear least squares method. This process continued until the sum of squared errors between the predicted and experimental values were minimised or less than $1x10^{-8}$.

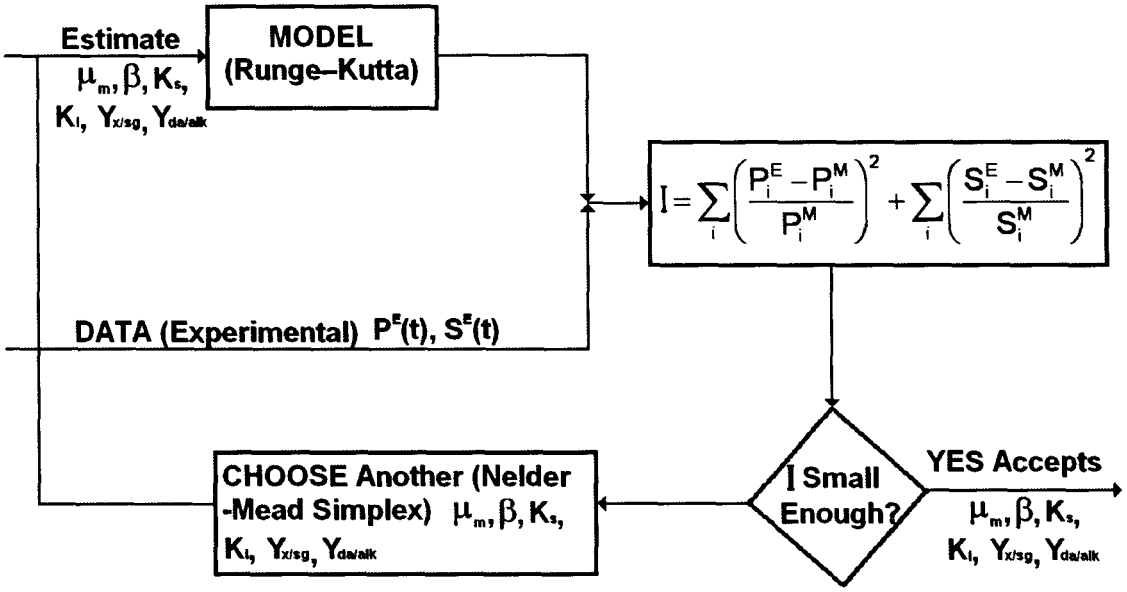

Figure 4.1: Algorithm used to estimate the kinetic parameters of the model

4.4 Conclusion

In this chapter an unstructured kinetic model was developed for growth based on the Monod equation. The following assumptions were made in the development of the model:

- the specific growth rate was limited by a single rate-limiting substrate,
- the consumption rate of the limiting substrate was proportional to the specific growth rate,
- the rate of cell death was considered insignificant throughout the growth and stationary phase,
- utilisation of the growth-limiting substrate was mainly used for biomass production and an insignificant amount of substrate was used for cell maintenance and the production of products other than biomass and
- substrate inhibition was not considered

The above model was modified and extended using the Andrews model to take cognisance of substrate inhibition.

A similar model was developed for biotransformation based on the Luedeking–Piret model. The following assumptions were made in the development of the model:

- α,ω-dicarboxylic acids were produced as non-growth associated products
- the production rate of α,ω-dicarboxylic acids was function of the biomass concentration only and
- no other products other than α,ω-dicarboxylic acids acid were produced during biotransformation

The kinetic parameters of the above models were quantified by making use of a two step approach comprising a graphical approach supported by a computer based iterative process developed in MATLAB.

Chapter 5

Results and Discussion I

Growth of *Yarrowia lipolytica* TVN 497 in a Complex versus a Semi-Defined Medium

5.1 Characterisation of the Microbial Growth Phase

During the first phase of the research, the growth of a recombinant *Yarrowia lipolytica* strain TVN 497 was investigated. The experiments were carried out in a batch Braun BIOSTAT C bioreactor. Both a complex and a semi-defined medium were used, as detailed in Section 3.5.2. A total of 8 experiments were conducted. Three experiments studied growth in the complex medium and the remaining five experiments used the semi-defined medium. The base case experiment on complex-medium under standard conditions was repeated to confirm reproducibility of the experiments. The third experiment investigated the effect of growth on ammonium ion utilisation. Experiments conducted with the semi-defined medium were performed at four different initial glucose concentrations. These experiments were used to evaluate the effect of the initial glucose concentration on growth as well as a change in limiting substrate from carbon to nitrogen.

Growth was investigated in terms of glucose, oxygen and ammonium ion utilisation as well as carbon dioxide and biomass production. To accomplish this, data were collected on biomass, glucose and ammonium ion concentration in the liquid phase and carbon dioxide and oxygen concentrations in the gas phase as a function of time.

5.1.1 Growth on the complex modified Picataggio medium: a base case

In the base case experiment on complex medium, the growth of *Y. lipolytica* TVN 497 was evaluated on the modified Picataggio medium. The initial

glucose concentration, pH, temperature, aeration rate and agitation speed were set at 40 g.l^{-1}, pH 6.0, 30 °C, 0.8 vvm and 700 rpm, respectively. A 10% (v/v) inoculum (Section 3.5.4) was used.

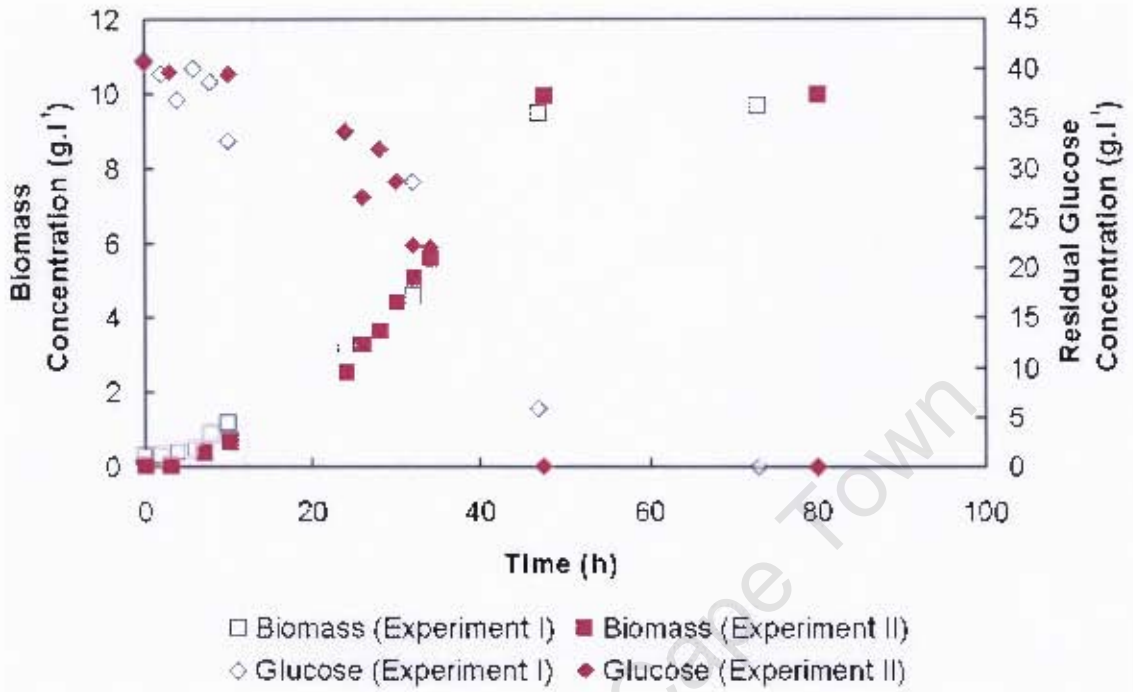

Figure 5.1: Biomass production and glucose utilisation on growth of *Y. lipolytica* TVN 497 in the complex Picataggio medium. Experiments were carried out in duplicate with strain TVN 497 in the Braun BIOSTAT C bioreactor using the modified Picataggio medium. The initial glucose concentration, pH, temperature, aeration rate and agitation speed of the medium were set at 40 g.l^{-1}, pH 6.0, 30 °C, 0.8 vvm and 700 rpm, respectively. A 10% (v/v) inoculum was used.

The biomass and residual glucose concentrations of the repeat experiment under standard conditions are given as a function of time in Figure 5.1. Neither experiment exhibited a lag phase, growth commenced instantaneously and continued exponentially until biomass concentrations of 9.4 g.l^{-1} and 9.9 g.l^{-1} were reached, approximately 48 h after inoculation. Following the exponential growth phase, the biomass density of both experiments remained constant. Reproducibility was confirmed by comparing the coefficient of variance between the biomass concentrations as a function of time. A maximum standard deviation of 0.19 g.l^{-1} at an average biomass concentration of 0.13 g.l^{-1} and a minimum standard deviation of 0.20 g.l^{-1} at an average biomass concentration of 9.80 g.l^{-1} were obtained.

The utilisation of glucose followed an inverse trend to the biomass production. The initial glucose concentration in both experiments was approximately 40 $g.l^{-1}$. After inoculation, the glucose concentration decreased exponentially until microbial growth reached the stationary phase, 48 h after inoculation. In experiment II the glucose concentration was depleted within 48 h. In experiment I, glucose depletion was predicted to occur between 52 h and 56 h. By comparing the coefficient of variance between experiments, reproducibility was confirmed by a maximum standard deviation of 6.58 $g.l^{-1}$ at an average glucose concentration of 40.90 $g.l^{-1}$ and a minimum standard deviation of 0.12 $g.l^{-1}$ at an average glucose concentration of 33.79 $g.l^{-1}$.

The depletion of the inorganic nitrogen source in the form of the ammonium ion was quantified in the third experiment. Experiment III was conducted under identical conditions as experiments I and II except that a higher biomass concentration was achieved on inoculation. As a result, the biomass profile of experiment III lies above those of experiments I and II as shown in Figure 5.2. The initial biomass densities on inoculation of experiments I, II and III were 0.2 $g.l^{-1}$, 0.2 $g.l^{-1}$ and 0.8 $g.l^{-1}$, respectively. However, the specific growth rate and overall biomass yield were similar for all experiments (Section 5.2).

Biomass, residual glucose and ammonium ion concentrations for Experiment III are given as a function of time in Figure 5.2. The initial glucose and ammonium ion concentrations of 40 $g.l^{-1}$ and 24 $g.l^{-1}$ respectively, reduced with an increase in biomass concentration. Depletion of the ammonium ion occurred 25 h after inoculation. At this point the glucose and biomass concentrations were 25 $g.l^{-1}$ and 5.7 $g.l^{-1}$, respectively. Since production of biomass continued, following ammonium ion depletion, it is apparent that biomass growth was not limited by the ammonium ion concentration, suggesting that a second nitrogen source was being utilised (proteins present in the complex medium). This is confirmed in Section 5.2 where it is shown that two distinct specific growth rates existed during growth, suggesting the

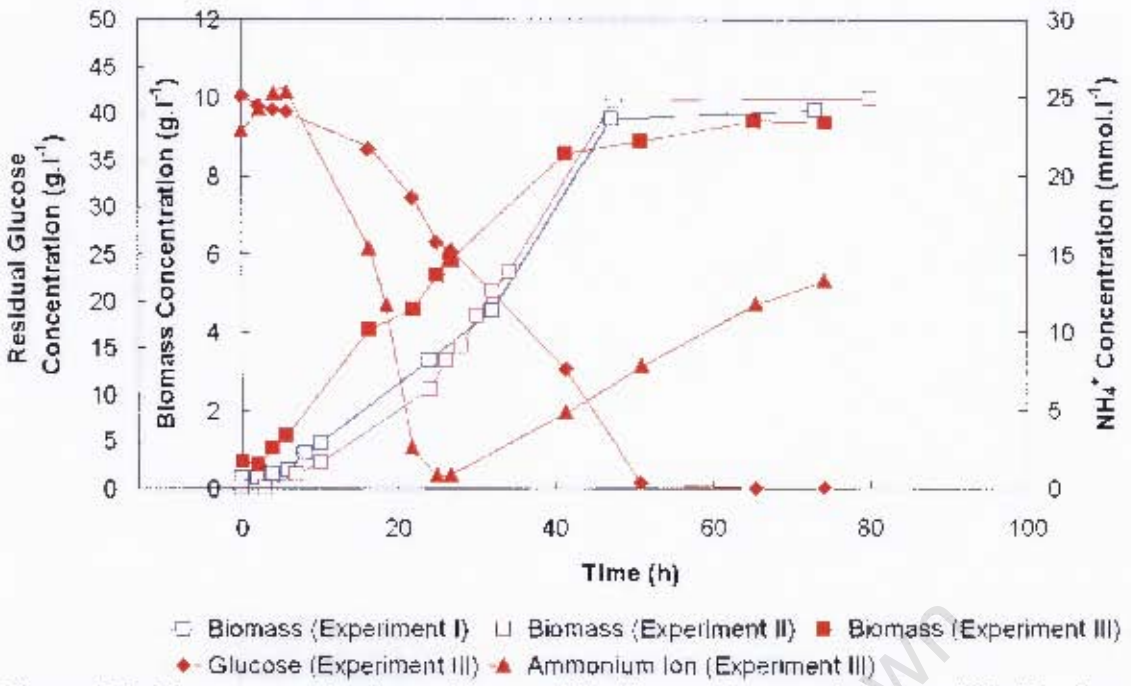

Figure 5.2: Biomass production, glucose utilisation and ammonium ion utilisation in a complex medium. Strain TVN 497 was cultured in the Braun BIOSTAT C bioreactor using the modified Picataggio medium. The initial glucose concentration, pH, temperature, aeration rate and agitation speed of the medium were set at 40 $g.l^{-1}$, pH 6.0 30 °C, 0.8 vvm and 700 rpm, respectively. A 10% (v/v) inoculum was used.

subsequent utilisation of substitutable nitrogen sources. However, the proteins (containing complex nitrogen) may also be utilised simultaneously with ammonium ions as an alternative nitrogen source during growth.

The glucose concentration decreased further with an increase in biomass concentration until its depletion 51 hrs after inoculation. During this time the ammonium ion concentration increased after the apparent depletion, 25 h after inoculation.. After glucose depletion the rate of biomass production decreased significantly where after it continues to increase gradually to reach a final value of 9.2 $g.l^{-1}$, 64 h after inoculation. Within an acceptable margin of experimental error (standard deviation of 0.40 $g.l^{-1}$), it was assumed that growth ceased when the glucose was depleted, suggesting glucose acted as the stoichiometric limiting substrate.

In Figure 5.3, the carbon dioxide production rate and oxygen utilisation rate are presented as a function of time and compared with biomass formation. No

initial lag phase was observed for carbon dioxide production, oxygen utilisation or biomass formation. Both rates increased exponentially. Maximum production and utilisation rates of 186 mmol.h^{-1} and 212 mmol.h^{-1}, respectively, were observed towards the end of the exponential growth phase, 48 h after inoculation. On glucose depletion both rates decreased rapidly. This marked the beginning of the stationary phase during which both the carbon dioxide production rate and oxygen utilisation rate varied between 20 mmol.h^{-1} and 40 mmol.h^{-1}.

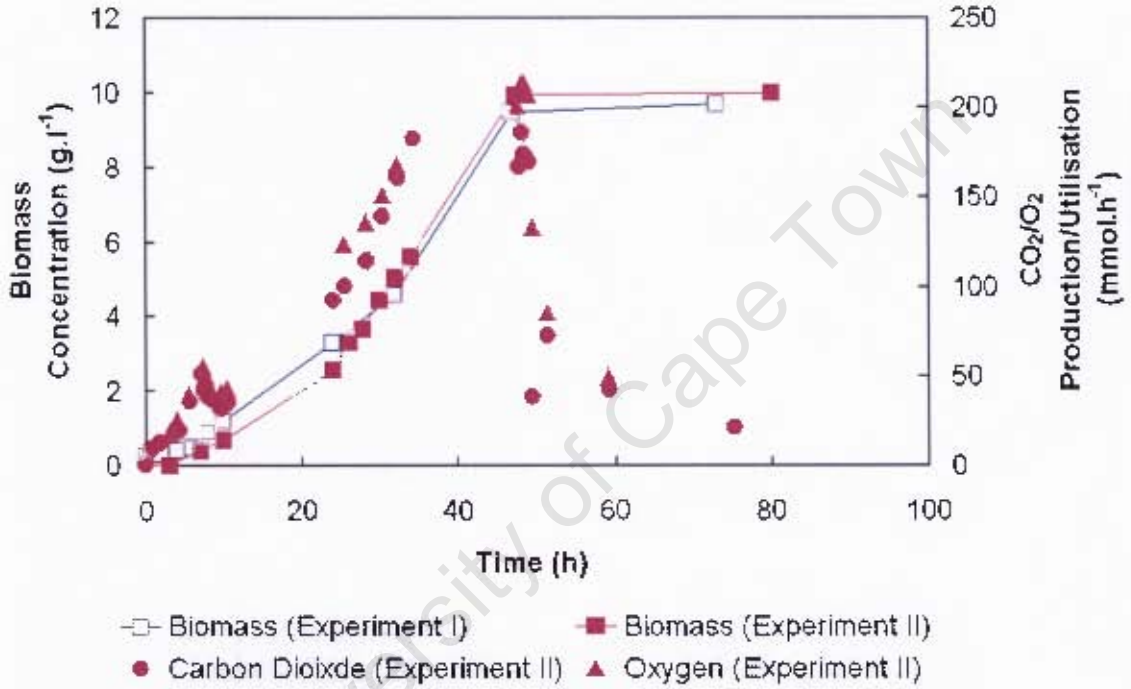

Figure 5.3: Carbon dioxide production and oxygen utilisation during growth. Strain TVN 497 was cultured in the Braun BIOSTAT C bioreactor using the modified Picataggio medium. The initial glucose concentration, pH, temperature, aeration rate and agitation speed of the medium were set at 40 g.l^{-1}, pH 6.0, 30 °C, 0.8 vvm and 700 rpm, respectively. A 10% (v/v) inoculum was used.

For experiment II, mass conservation was validated by performing carbon and oxygen balances over the bioreactor. It was assumed that under glucose limiting conditions, no extracellular products other than biomass, water and carbon dioxide were produced from glucose, which acted as the sole carbon and energy source. The following stoichiometric equations were used to describe the relationships between substrate utilisation and product formation:

$$4C_6H_{12}O_6 + 4NH_4^+ + 5O_2 \rightarrow 4C_5H_7NO_2 + 18H_2O + 4CO_2 \quad (5.1)$$

$$C_6H_{12}O_6 + 6O_2 \rightarrow 6H_2O + 6CO_2 \quad (5.2)$$

where Equations 5.1 and 5.2 represent cell growth and cell maintenance, respectively. During the exponential growth phase both reactions occurred. At the onset of the stationary phase, growth ceased and glucose was used solely for maintenance (Equation 5.2). Since water was in excess, the amount of water produced could not be quantified experimentally. Hence the stoichiometric relationships in Equations 5.1 and 5.2, based on the amount of carbon dioxide produced, were used to determine the quantity of water produced. The results of these balances are given in Table 5.1.

Table 5.1: Carbon and oxygen balance conducted across base case experiment II

		Carbon Balance		Oxygen Balance	
Phase	**Substrates**	**In (gmol C)**	**Out (gmol C)**	**In (gmol O)**	**Out (gmol O)**
Growth (0-48 h)	Glucose	12.5	0	12.5	0
	Biomass	negl.	4.4	negl.	1.8
	Carbon Dioxide	0.49	5.3	1	10.6
	Water (Calculated Stoichiometrically)	-	-	-	4
	Oxygen from Air	-	-	237.2	226.3
Stationary (48-120 h)	Glucose	-	-	-	-
	Biomass	-	-	-	-
	Carbon Dioxide	0.7	3.2	1.5	6.5
	Water (Calculated Stoichiometrically)	-	-	-	2.5
	Oxygen from Air	-	-	710.5	700.5
		Overall Balance			
		13.7	12.9	962.7	952.2
		Error: 6%		Error: 1%	

From Table 5.1, the error of mass balance closure on oxygen of 1% is insignificant. Further the error in mass balance closure on carbon of 6% is reasonable, based on the experimental error associated with the assay techniques used (coefficient of variance of 12.5% and 5 % for glucose and

biomass respectively). The complex carbon present in the peptone (19% (w/w)) and yeast extract (32% (w/w)) (Williams, 2005) however, aggravates the carbon closing error (23%), thereby weakening the assumption made in development of the kinetic model that no products other than biomass are produced from carbon.

5.1.2 Growth in a semi-defined medium

The effects of different initial glucose concentrations and a shift in the limiting substrate from carbon to nitrogen on the growth of *Y. lipolytica* TVN 497 were evaluated in the Antonucci semi-defined medium. This was accomplished by increasing the initial glucose concentration i.e. 5 $g.l^{-1}$, 13 $g.l^{-1}$, 42 $g.l^{-1}$, 51 $g.l^{-1}$, until the growth of *Y. lipolytica* TVN 497 was limited by the ammonium ion concentration. The pH, temperature, aeration rate and agitation speed were set at pH 5.0, 30 ^{o}C, 0.6 vvm and 900 rpm, respectively. A 10% (v/v) inoculum was used, prepared in accordance with the method described in Section 3.5.4.

The effect of initial glucose concentration on biomass production, glucose and ammonium ion utilisation is shown in Figures 5.4 and 5.5. The onset of biomass production, glucose and ammonium ion utilisation in experiments conducted at initial glucose concentrations of 5 $g.l^{-1}$, 13 $g.l^{-1}$, 42 $g.l^{-1}$ and 51 $g.l^{-1}$ was delayed by an initial lag phase with durations of approximately 22 h, 22 h, 32 h and 22 h, respectively. Hereafter, the corresponding biomass concentrations increased exponentially to reach final biomass concentrations of 3.7 $g.l^{-1}$, 5.2 $g.l^{-1}$, 12.7 $g.l^{-1}$ and 20.0 $g.l^{-1}$, approximately 47 h, 56 h, 53 h and 62 h after inoculation, respectively.

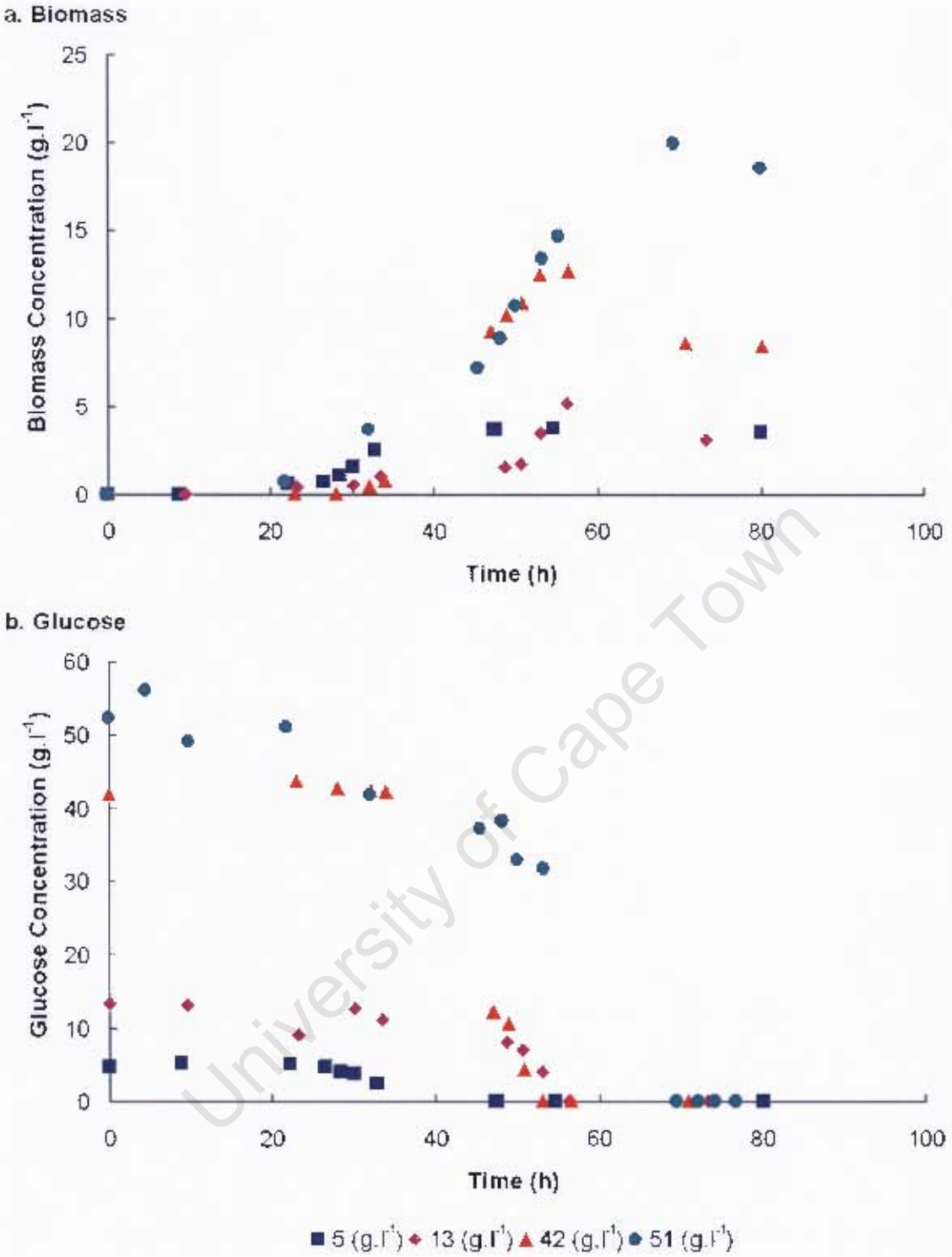

Figure 5.4: (a) Biomass production and (b) glucose utilisation in a semi-defined medium. Strain TVN 497 was cultivated in the Antonucci medium at four different initial glucose concentrations i.e. 5 $g.l^{-1}$, 13 $g.l^{-1}$, 42 $g.l^{-1}$, 51 $g.l^{-1}$, using the Braun BIOSTAT C bioreactor. The pH temperature, aeration rate and agitation speed of the medium were set at pH 5.0, 30 °C, 0.6 vvm and 900 rpm, respectively. A 10% (v/v) inoculum was used.

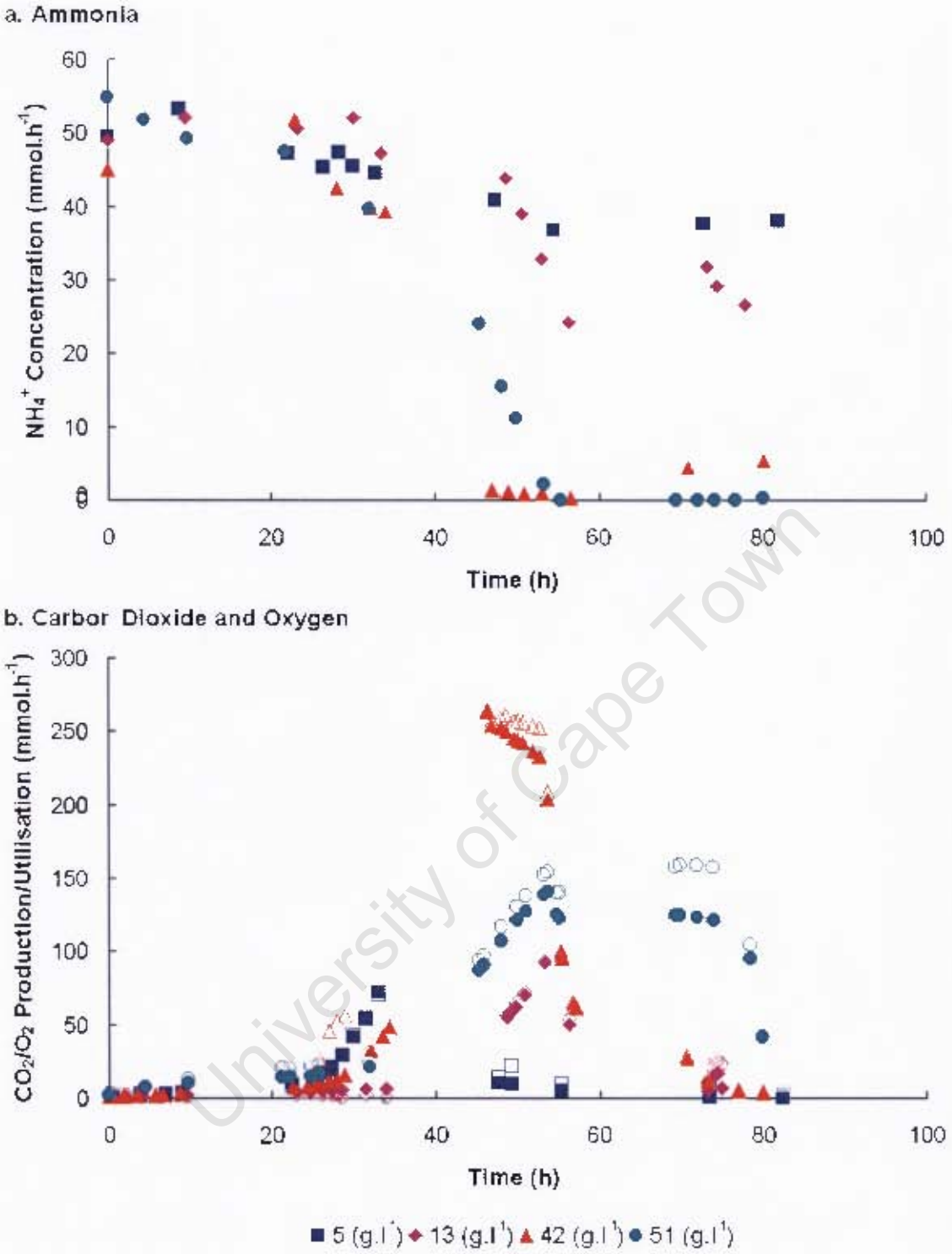

Figure 5.5: (a) Carbon dioxide production, oxygen utilisation (open symbol: oxygen, close symbol: carbon dioxide) and (b) ammonium ion utilisation in a semi-defined medium. Strain TVN 497 was cultivated in the Antonucci medium at four different initial glucose concentrations i.e. 5 g.l^{-1}, 13 g.l^{-1}, 42 g.l^{-1}, 51 g.l^{-1}, using the Braun BIOSTAT C bioreactor. The pH, temperature, aeration rate and agitation speed of the medium were set at pH 5.0, 30 °C, 0.6 vvm and 900 rpm, respectively. A 10% (v/v) inoculum was used.

In each case, glucose and ammonium ion utilisation followed an inverse trend to biomass production. The residual ammonium ion was however, not depleted in experiments conducted at initial glucose concentrations of 5 g.l^{-1} and 13 g.l^{-1}. Microbial growth ceased at the time of glucose depletion when the corresponding residual ammonium ion concentration was 37 ± 0.6 mmol.l^{-1} and 28 ± 4.6 mmol.l^{-1}. These results suggest that glucose has acted as the growth limiting substrate.

When experiments were conducted at initial glucose concentrations of 42 g.l^{-1} and 51 g.l^{-1} the ammonium ion concentration decreased to depletion approximately 46 h and 55 h after inoculation, respectively. The corresponding glucose concentrations on depletion were 10 g.l^{-1} and 29 g.l^{-1}, respectively. It was however, proposed that nitrogen did not act as the growth limiting substrate in the experiment conducted at an initial glucose concentration of 42 g.l^{-1}. Biomass production continued until the residual

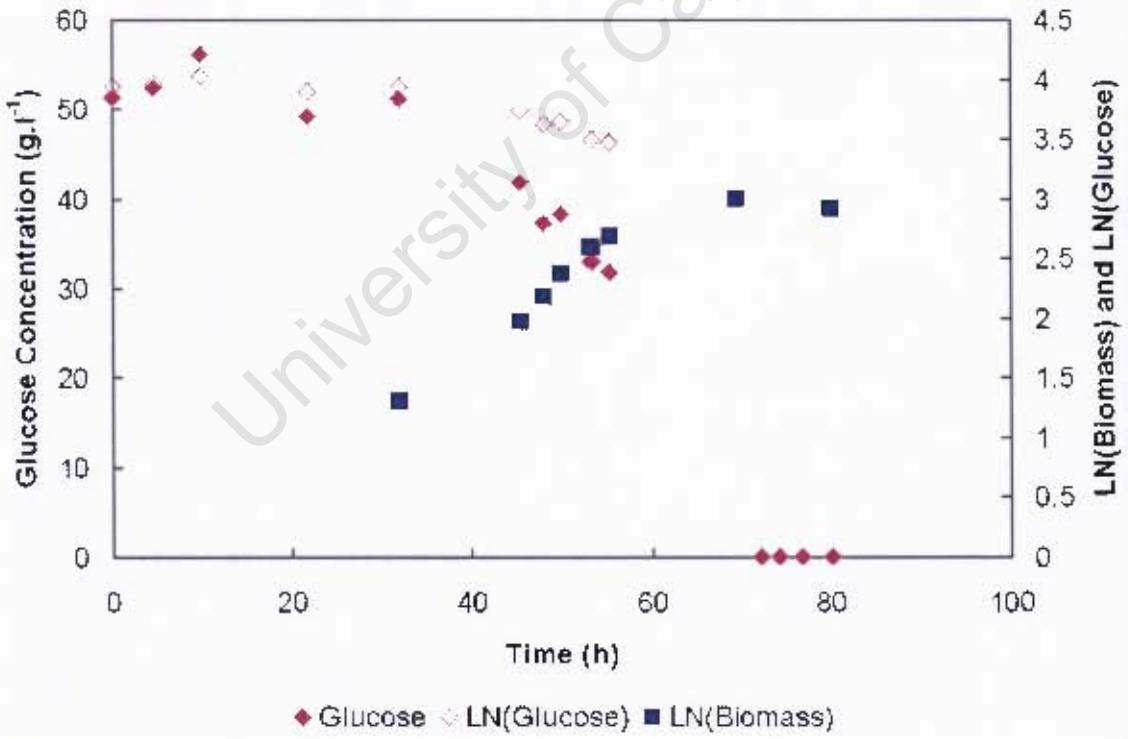

Figure 5.6: Microbial growth and glucose utilisation at an initial glucose concentration of 51 g.l^{-1}. Strain TVN 497 was cultured in the Braun BIOSTAT C bioreactor using the Antonucci semi-defined medium. The pH, temperature, aeration rate and agitation speed of the medium were set at pH 6.0, 30 °C, 0.8 vvm and 700 rpm, respectively. A 10% (v/v) inoculum was used.

glucose was consumed, approximately 4 h after ammonium ion depletion. For the experiment conducted at an initial glucose concentration of 51 $g.l^{-1}$, the experimental results were less conclusive. However, from Figure 5.6 it was proposed that since the rate of glucose utilisation did not change when biomass production reached the late exponential phase, nitrogen may have acted as the growth limiting substrate.

The carbon dioxide production and the oxygen utilisation rates in Figure 5.5 display a corresponding lag phase observed previously for biomass production, glucose and ammonium ion utilisation. Hereafter, both rates in the experiments conducted at initial glucose concentrations of 5 $g.l^{-1}$, 13 $g.l^{-1}$ and 42 $g.l^{-1}$ increased exponentially until maximum production rates of 72 $mmol.h^{-1}$, 92 $mmol.h^{-1}$ and 263 $mmol.h^{-1}$ and maximum utilisation rates of 70 $mmol.h^{-1}$, 93 $mmol.h^{-1}$ and 264 $mmol.h^{-1}$ were reached, approximately 34 h, 56 h and 46 h after inoculation, respectively. After reaching a maximum, both rates decrease to lower values thereby announcing the onset of the stationary phase.

In the experiment conducted at an initial glucose concentration of 51 $g.l^{-1}$, a maximum production and utilisation rate of 123 ± 1 $mmol.h^{-1}$ and 152 ± 8 $mmol.h^{-1}$, respectively, were reached at the time of ammonium ion depletion. Theses rates were significantly lower (50%) than the rates observed for the experiment conducted at an initial glucose concentration of 42 $g.l^{-1}$, suggesting a change in growth limiting substrate (carbon to nitrogen). The rates were maintained until the apparent intracellular glucose was depleted approximately 82 h after inoculation. This phenomenon was previously observed by Briffaud and Engasser (1979) for wild-type *Y. lipolytica* D 1805 under nitrogen limiting conditions.

The goodness of data was evaluated by performing carbon and oxygen mass balances on experiments conducted at initial glucose concentrations of 13 $g.l^{-1}$, 42 $g.l^{-1}$ and 51 $g.l^{-1}$. The formation of extracellular products was assumed to be negligible in all cases. The stoichiometric equations, described in Section 5.1.1, were used to quantify the amount of water produced.

Table 5.2: Carbon and oxygen material balances conducted on the semi-defend medium with an initial glucose concentration of 13 $g.l^{-1}$, 42 $g.l^{-1}$ and 52 $g.l^{-1}$

		13 $g.l^{-1}$				42 $g.l^{-1}$				52 $g.l^{-1}$			
		Carbon		Oxygen		Carbon		Oxygen		Carbon		Oxygen	
Phase	**Substrate**	**In**	**Out**	**In**	**Out**	**In**	**Out**	**In**	**Out**	**In**	**Out**	**In**	**Out**
Growth	Glucose	3.3	-	3.3	-	10.7	-	10.7	-	13.9	2.6	13.9	2.6
	Biomass	-	2.1	-	0.8	-	5.6	-	2.2	-	8.8	-	3.5
	Carbon Dioxide	0.3	1.4	0.7	2.9	0.3	4.7	0.7	9.3	0.4	4.5	0.8	9
	Water (Calculated Stoichiometrically)	-	-	-	1.9	-	-	-	5	-	-	-	7.9
	Oxygen from Air	-	-	334.1	332.1	-	-	336.3	327.2	-	-	415.2	424.7
Stationary	Glucose	-	-	-	-	-	-	-	-	2.6	-	2.6	-
	Biomass	-	-	-	-	-	-	-	-	-	-	-	-
	Carbon Dioxide	0.1	0.6	0.2	1.2	0.5	1.7	1	3.4	0.3	2	0.5	4.1
	Water (Calculated Stoichiometrically)	-	-	-	0.5	-	-	-	1.2	-	-	-	1.8
	Oxygen from Air	-	-	110.7	109.5	-	-	516.1	513.9	-	-	281.8	277.9
						Overall Balance							
	Total (gmol)	**3.8**	**4.1**	**449**	**448.8**	**11.5**	**12**	**864.8**	**862.3**	**17.1**	**17.9**	**714.8**	**731.5**
		Error: 8%		**Error: 0.04%**		**Error: 4%**		**Error: 0.29%**		**Error: 5%**		**Error: 2%**	

From Table 5.2, the error in the closure of the oxygen material balance was insignificant at 0.04% to 2.00%. In comparison, the errors in closing of the mass balance on carbon in experiments conducted with initial glucose concentrations of 13 $g.l^{-1}$, 42 $g.l^{-1}$ and 51 $g.l^{-1}$ were 8%, 4% and 5%, respectively. These errors are consistent with the errors associated with the assay for glucose and biomass (Section 5.1.1). However, when the carbon in yeast extract (32% (w/w)) (Williams, 2005) is taking into consideration the carbon closing balancing error of all three experiments become less than 3%. It is therefore proposed that negligible amounts of products, other than the ones mentioned above, were produced thereby confirming the assumption made in development of the kinetic model in Section 4.2.

5.2 Quantifying the Preliminary Growth Kinetic Parameters of *Yarrowia lipolytica* TVN 497 in both a Complex and a Semi-Defined Medium for the Modeling of the Growth Phase

To model the production of biomass and utilisation of glucose in both a complex and a semi-defined medium, the following simplified kinetic models, described in Section 4.1, were used:

$$\frac{dC_x}{dt} = \frac{\mu_m C_{sg}}{K_s + C_{sg}} C_x \tag{5.3}$$

$$\frac{dC_{sg}}{dt} = \frac{1}{Y_{x/sg}} \left(\frac{dC_x}{dt} \right) \tag{5.4}$$

where C_x represents the biomass concentration ($g.l^{-1}$), μ_m is the maximum specific growth rate (h^{-1}), C_{sg} the concentration of glucose ($g.l^{-1}$), K_s the saturation constant ($g.l^{-1}$) and $Y_{x/sg}$ a yield coefficient ($g.g^{-1}$).

Since these models are non-linear equations with multiple kinetic parameters i.e. μ_m, K_s and $Y_{x/sg}$, the optimisation of the kinetic parameters depend

significantly on the estimation of their initial values. By applying the graphical approach developed in Section 4.3.1, initial values were estimated for kinetic parameter μ_m and $Y_{x/sg}$ for both the complex medium base case experiments and the semi-defined medium experiments at three initial glucose concentrations where glucose acted as the limiting substrate (Section 5.1.2). The graphical approach for the base case experiment and the semi-defined medium experiment using an initial glucose concentration of 5 $g.l^{-1}$ are shown in Figures 5.7 and 5.8, respectively. Analysis of the experiments at initial glucose concentrations of 13 $g.l^{-1}$ and 42 $g.l^{-1}$ are included in Appendix D1. The estimated values of the kinetic parameters for the complex medium and semi-defined medium are tabulated in Table 5.3.

Table 5.3: Graphical estimations of the growth kinetic parameters for both the complex and semi-defined medium experiments

Medium	Initial glucose Concentration ($g.l^{-1}$)	Graphical Estimations of Kinetic Parameters		
		$Y_{x/s}$ ($g.g^{-1}$)	μ_m (h^{-1})	K_s ($g.l^{-1}$)
Complex		0.26	0.19 (μ_1) 0.06 (μ_2)	35.48*
Semi-Defined	5	0.63	0.20	1.10
	13	0.37	0.19	0.98
	42	0.29	0.20	2.42

* μ_2 predicted a scientifically meaningless value for K_s

From Table 5.3 it is clear that an apparent inverse relationship exists between the overall yield coefficients and initial glucose concentrations estimated for *Y. lipolytica* TVN 497 in the semi-defined medium experiments. This relationship may be attributed to the yeast's ability to degrade glucose via different metabolic pathways. In the presence of excess glucose, the substrate may be deflected to non-core roles, challenging the assumption of negligible maintenance energy and extracellular products (Section 4.1).

Table 5.3 also displays two distinct specific growth rates for *Y. lipolytica* TVN 497 in a complex medium. Discrete regions characterised by different growth rate may result from diauxic growth which occurs when more than one

a. Yield Coefficient

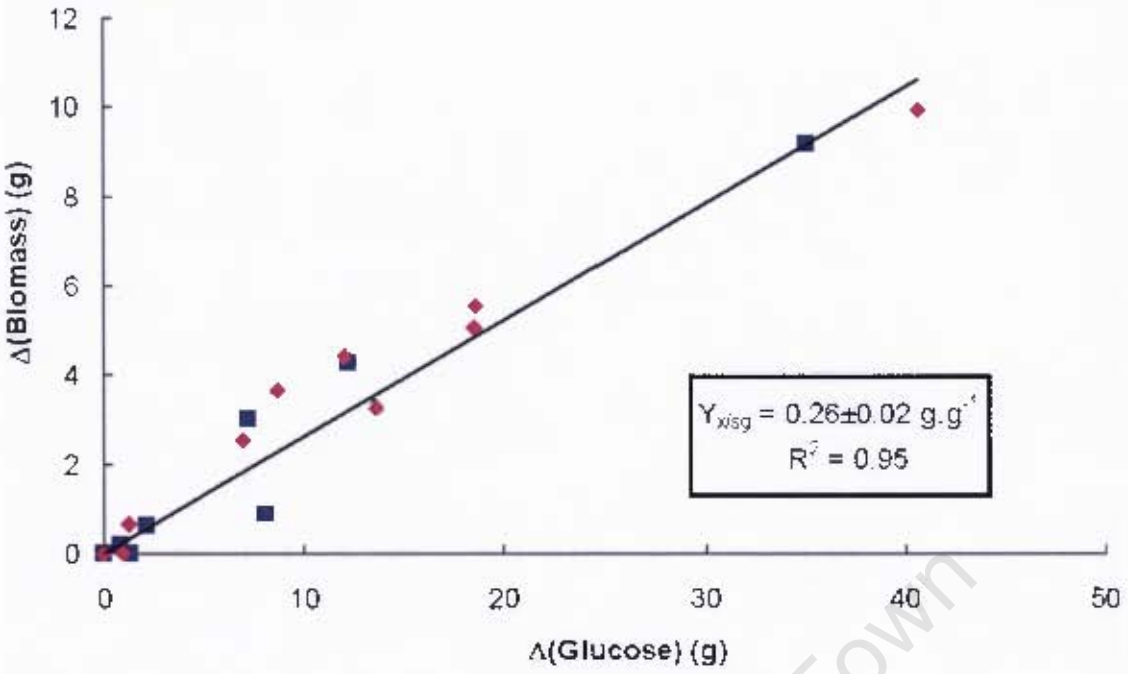

b. Specific Growth Rate

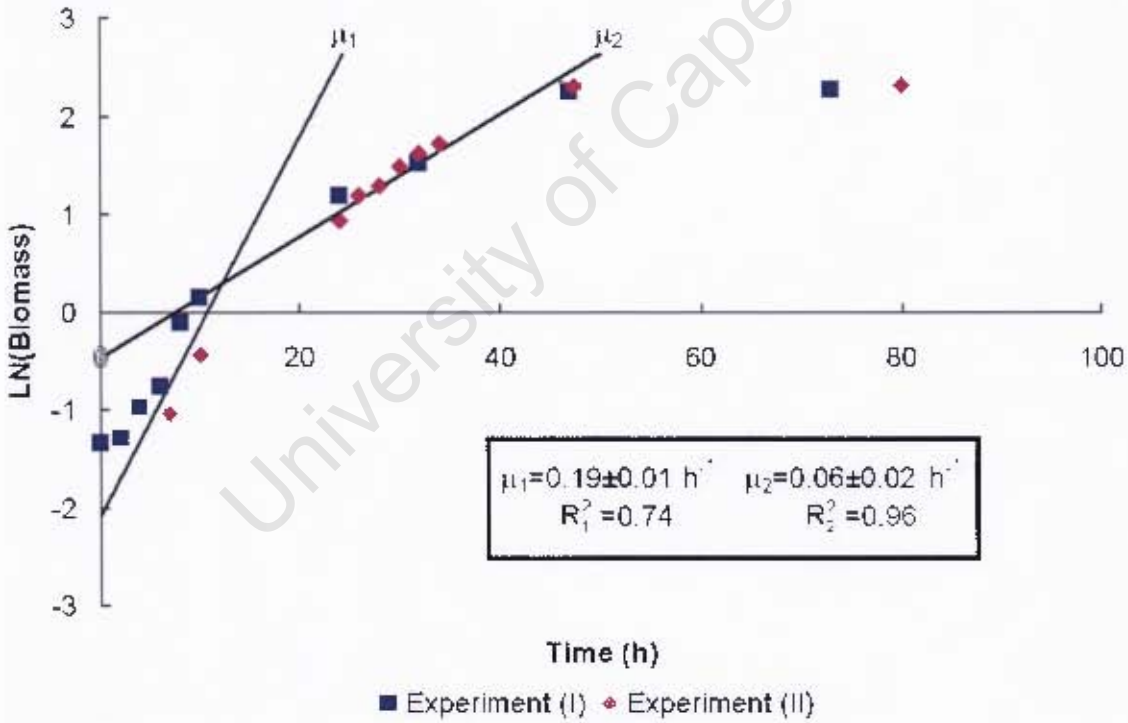

Figure 5.7: Graphical estimation of (a) the average yield coefficient and (b) the average specific growth rates for the base case experiments. Using modified Picataggio medium strain TVN 497 was cultured in the Braun BIOSTAT C bioreactor. The initial glucose concentration, pH, temperature, aeration rate and agitation speed of the medium were set at 40 g.l^{-1}, pH 6.0, 30 °C, 0.8 vvm and 700 rpm, respectively. A 10% (v/v) inoculum was used.

a. Yield Coefficient

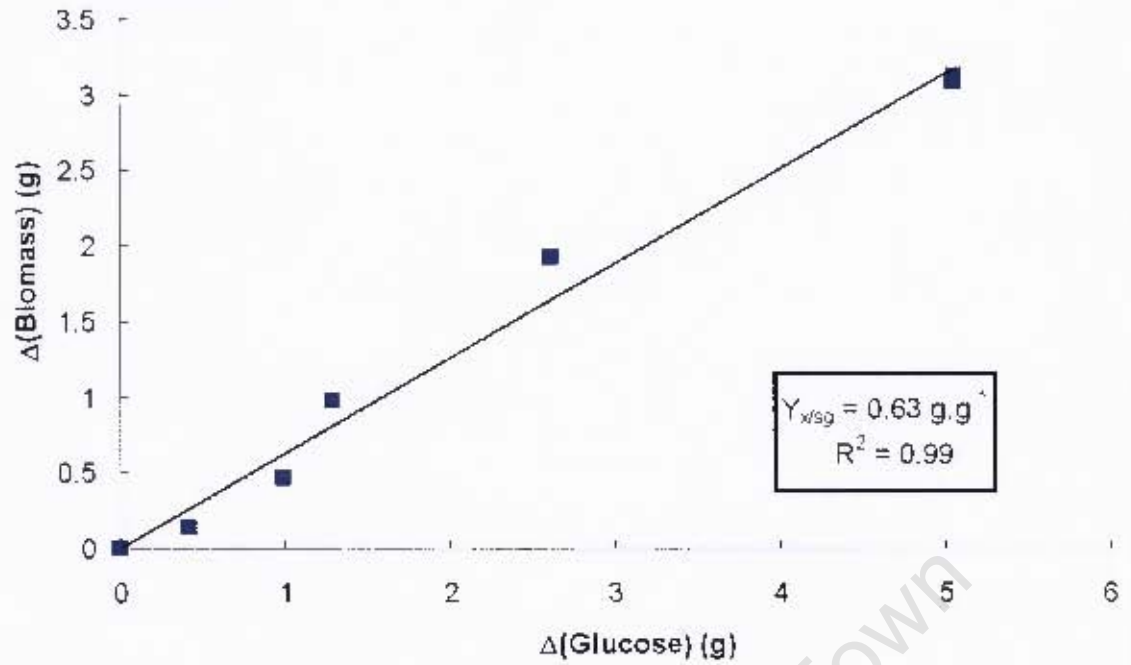

b. Specific Growth Rate

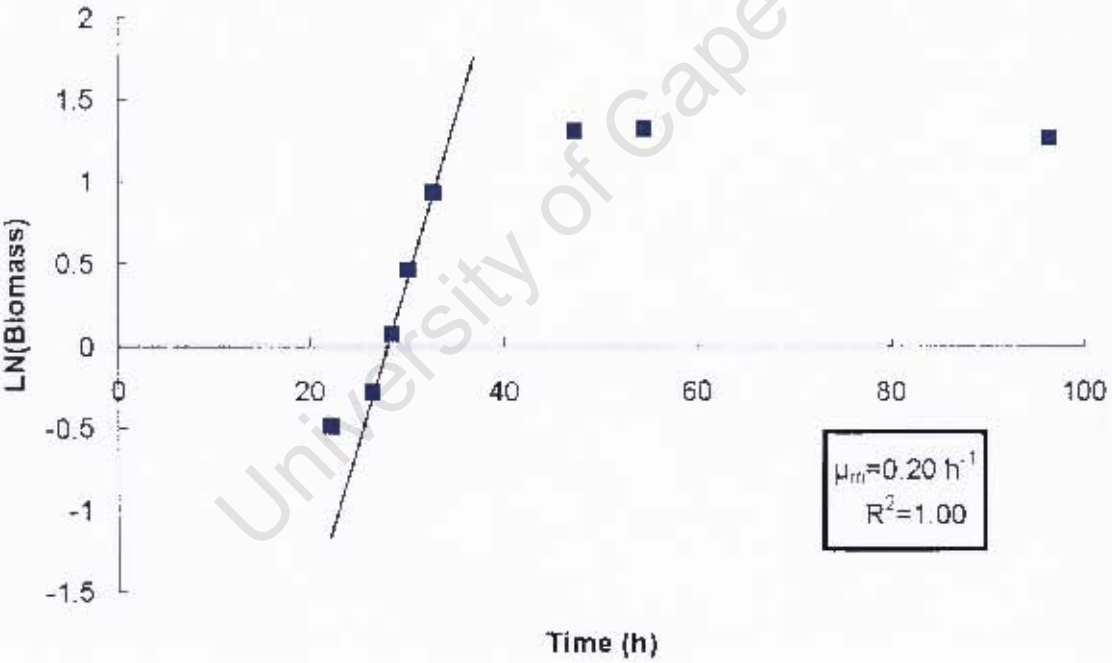

Figure 5.8: Graphical estimation of (a) the yield coefficient and (b) the specific growth rate using Antonucci semi-defined medium at an initial glucose concentration of 5 g.l^{-1}. Strain TVN 497 was cultivated in the Braun BIOSTAT C bioreactor. The pH, temperature, aeration rate and agitation speed of the medium were set at 5 g.l^{-1}, pH 6.0, 30 °C, 0.8 vvm and 700 rpm, respectively. A 10% (v/v) inoculum was used.

substitutable substrate acts as the rate liming substrate (Egli, 1995: Harder and Dijkhuizen, 1982; Kovarova-Kovar and Egli, 1998; Neidhardt and Magasanik, 1957; Daugthton *et al.*, 1979). However, in this study glucose acted as the stoichiometric growth limiting substrate in all the base case experiments and the period of induction of a new catabolic pathway is not obvious. Hence, classic diauxic growth is not present. While the provision of nitrogen was not limiting in the base case experiments, two different nitrogen sources (ammonium ion in ammonium nitrate and complex protein in peptone) were present in the complex medium. The utilisation of the ammonium ion was investigated by conducting a third experiment under the same conditions as the base case experiments. The results of the experiment are presented in Figure 5.9.

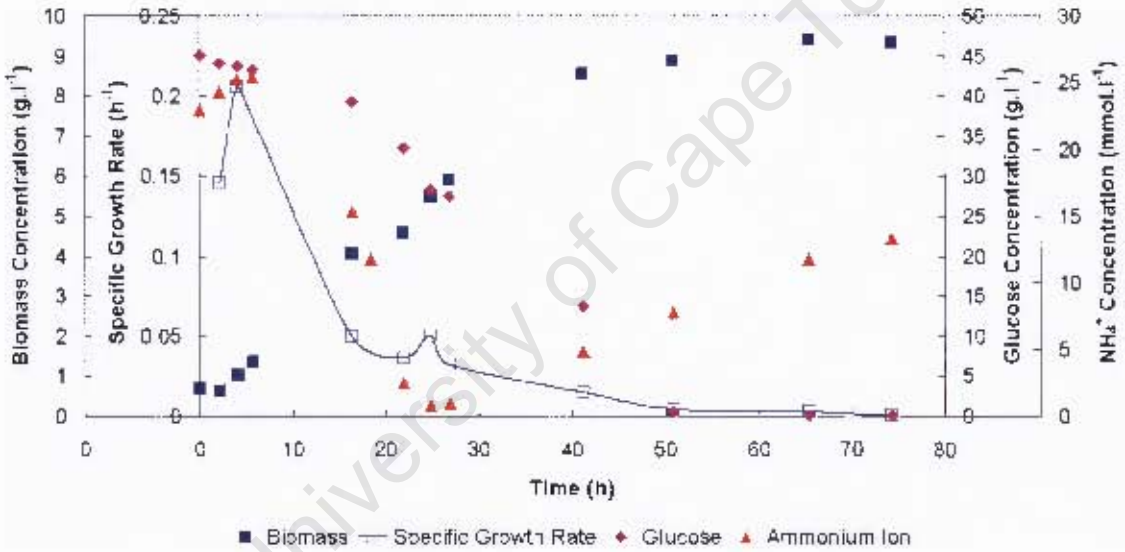

Figure 5.9: Comparison of the instantaneous specific growth rates of strain TVN 497 in the modified Picataggio complex medium relative to available ammonium ion and glucose. The experiment was conducted on the complex medium in the Braun BIOSTAT C bioreactor. The initial glucose concentration, pH, temperature, aeration rate and agitation speed of the medium were set at 40 g.l^{-1}, pH 6.0, 30 °C, 0.8 vvm and 700 rpm, respectively. A 10% (v/v) inoculum was used.

The results in Figure 5.9 show that, following a lag phase, the instantaneous specific growth rate of *Y. lipolytica* TVN 497 is initially high at 0.26 h^{-1}. Thereafter it decreases as the residual ammonium ion concentration decreases to completion approximately 25 h after inoculation, suggesting that

ammonium ion is kinetically limiting thereby affecting the specific growth rate. Biomass production, however, did not cease at the time of ammonium ion depletion but continued to increase at a lower production rate, suggesting that the less preferable nitrogen source (complex protein in peptone) was being utilised. However, since the specific production rate during period continued to decrease in the presence of an excess amount of complex nitrogen, it was proposed that glucose have acted as both the stoichiometric and kinetic limiting substrate.

As sufficient appropriate data were not available to determine the value of K_s by a Lineweaver-Burke plot (Blanch and Clark, 1997), K_s was estimated by plotting (Figure 5.10) the functional relationship between the specific growth rate and the glucose concentration (Section 2.5.2.2). The value of K_s, represents the limiting substrate concentration, in this case glucose, at which the specific growth rate is half of its maximum value (Bailey and Ollis, 1986). From Figure 5.10 it is clear that an unexpected functional relationship exists between the specific growth rate and the glucose concentration of the base case experiments. This phenomenon is related to the ammonium ion concentration which acted as the kinetic limiting substrate at concentration high than 3 $mmol.l^{-1}$ (open symbols). Beyond this concentration the specific growth rate (close symbols) appears to be independent of the ammonium ion concentration and directly related to the glucose concentration.

To be coherent with the assumptions made in developing the kinetic model (Section 4.1), an estimated value of K_s was obtained from the portion of the graph where the ammonium ion concentration was less than 3 $mmol.l^{-1}$. The value of K_s, in accordance with the definition as described above, should then typically range between residual glucose concentrations of 5 $g.l^{-1}$ and 8 $g.l^{-1}$. The experimental data obtained for the semi-defined experiment conducted at an initial glucose concentration of 5 $g.l^{-1}$, was more conclusive since the ammonium ion was added in excess. From Figure 5.10 it is clear that the K_s value of the semi-defined medium experiment should typically range between 2 $g.l^{-1}$ and 2.5 $g.l^{-1}$. It was assumed that, the value of K_s in all semi-defined medium experiments had a similar order of magnitude.

To estimate a single value of K_s, an initial estimate of K_s, based on the data above, was chosen and applied to the computer based iterative process (Section 4.3.2). This value was manually adjusted until the model best fitted the experimental data. During this manual iterative process the initial estimates of μ_m and $Y_{x/sg}$ were held constant. The estimated K_s values for both the base case and semi-defined medium experiments are shown in Table 5.3.

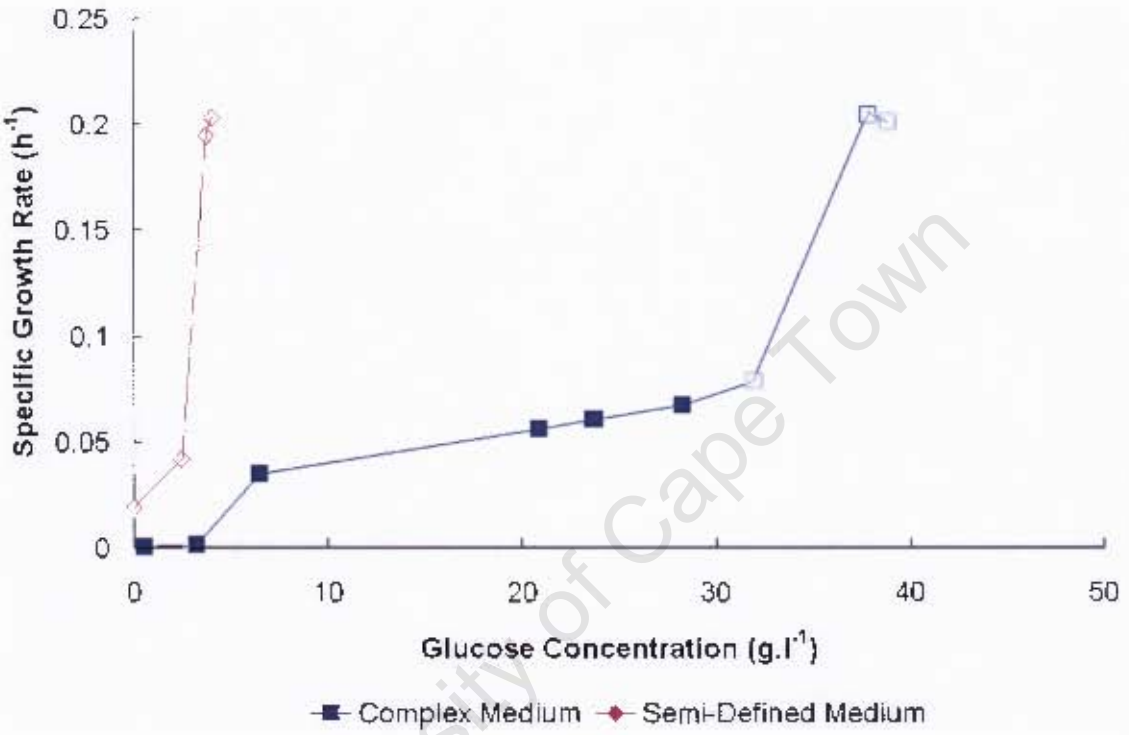

Figure 5.10: Functional relationship between the specific growth rate of *Y. lipolytica* TVN 497 and the residual glucose concentration in complex and semi-defined media. Both experiments were conducted in the Braun BIOSTAT C bioreactor under the conditions stipulated in Section 3.5.2. The figure was used to estimate the value of K_s for both the base case and semi-defined medium experiments. The value of K_s represents the glucose concentration at which the specific growth rate is half its maximum value. The closed and open squares represent specific growth rates obtained below and above an ammonium ion concentration of 3 mmol l^{-1}, respectively.

The value of K_s represents the affinity of *Y. lipolytica* TVN 497 for glucose. Bull and Bushell (1976) and Postma *et al.* (1989a&b) observed typical K_s values for strains of *Saccharomyces cerevisiae* and *Candida utilis* on glucose to lie in the range 10 $\mu g.l^{-1}$ to 110 $mg.l^{-1}$. Little or no information is available for K_s for *Yarrowia lipolytica* under similar conditions. In all cases the K_s values for *Y. lipolytica* appear significantly higher than typical values for conventional

yeast strain. It is note that in the presence of excess ammonium ion as the nitrogen source, the K_s values approach those for conventional yeast (semi-defined).

The basic kinetic parameters of the individual experiments were re-calculated using the computer based iterative process described in Section 4.3.2. Assuming glucose limitation conditions Equations 5.3 and 5.4 were numerically integrated with the aid of the fourth order Runga-kutta method. The integrated values obtained were compared with the experimental data after which, depending on the error, new values were determined for μ_m, $Y_{x/sg}$ and K_s using the Nelder-Mead non-linear least squares method. This process continued until the errors between the experimental and the predicted values were minimised. In Figures 5.11 and 5.12, the predictions of the basic kinetic model against the experimental data obtained during the complex and semi-defined medium experiments, respectively, are compared. The corresponding basic kinetic parameters are tabulated in Table 5.4. It must be noted that optimisation of the model fit for the complex medium requires further modification to account for the kinetic effect of the changing nitrogen source.

Table 5.4: Model-based growth kinetic parameters of both the complex and semi-defined medium experiments

Medium	Initial Glucose Concentration ($g.l^{-1}$)	Model Based Estimations of Kinetic Parameters		
		$Y_{x/sg}$ ($g.g^{-1}$)	μ_m (h^{-1})	K_s ($g.l^{-1}$)
Complex	40	0.27	0.17	19.61
Semi-Defined	5	0.68	0.18	0.37
	13	0.46	0.19	0.50
	42	0.29	0.20	0.10

Table 5.4 depicts a single specific growth rate for both base case complex medium experiments. This corresponds to the use of the ammonium ion as the nitrogen source. Existing literature on the modelling of *Yarrowia lipolytica* are limited to applications which concern citric acid production in which wild-type strains are used under nitrogen limiting conditions. Moresi (1994) and Rane and Sims (1993) did, however, perform a portion of their work under

glucose limiting conditions, for which values of μ_m and $Y_{x/sg}$ were calculated. These values are tabulated in Table 5.5. The maximum specific growth rates, calculated for *Y. lipolytica* TVN 497 in both the complex and the semi-defined medium, agree with the range of maximum specific growth rates published by Moresi (1994). In contrast to this, the maximum specific growth rate published by Rane and Sims (1993) is approximately twice as high as the maximum specific growth rates calculated. In this study the estimated values of the overall yield coefficients correlate well with the work published by both Moresi (1994) and Rane and Sims (1993), depending on glucose excess.

Table 5.5 Preliminary growth kinetic parameters for wild-type strains of *Y. lipolytica* under glucose limiting conditions in a semi-defined medium

Parameters	Moresi (1994)	Rane and Sims (1993)
C_{sg}* ($g.l^{-1}$)	42.8-108	30
μ_m (h^{-1})	0.16-0.3	0.38
$Y_{x/sg}$ ($g.g^{-1}$)	0.36-0.39	0.68
Strain	*Y. lipolytica* ATCC 2046	*C. lipolytica* Y 1095

* Initial glucose concentration

In Figure 5.11, it is seen that the trend of the model for biomass formation and glucose utilisation in the complex medium follows that of the experimental data. This suggests that the form of the model is appropriate. An offset however, exists between the predicted and experimental values. The model underestimated glucose utilisation in the exponential phase by 14% and biomass production in the early exponential phase by 43% and overestimated biomass production in the stationary phase by 9%. It is proposed that these offsets can be minimised or eliminated by extending Equations 5.3 and 5.4 to include for the rate limiting effect of the ammonium ion:

$$\frac{dC_x}{dt} = \left(\mu'_g \cdot \frac{C_{sg}}{K_g + C_{sg}} + \mu'_{NH_4^+} \cdot \frac{C_{sNH_4^+}}{K_{NH_4^+} + C_{sNH_4^+}} \right) C_x \qquad (5.5)$$

$$\frac{dC_{sg}}{dt} = \frac{1}{Y_{x/sg}} \left(\frac{dC_x}{dt} \right) \qquad (5.6)$$

$$\frac{dC_{sNH_4^+}}{dt} = \frac{1}{Y_{x/sNH_4}}\left(\frac{dC_x}{dt}\right) \qquad (5.7)$$

where μ'_g and $\mu'_{NH_4^+}$ represent the maximum specific growth rate with glucose and ammonium ion as the rate limiting substrate (h^{-1}), respectively, K_g and K_{NH_4} the saturation constant of glucose and ammonium ion ($g.l^{-1}$), respectively, $C_{sNH_4^+}$ the intracellular ammonium ion concentration ($g.l^{-1}$) and Y_{x/sNH_4^+} the yield coefficient of biomass from ammonium ion ($g.g^{-1}$). This model extension will form the subject of a later study.

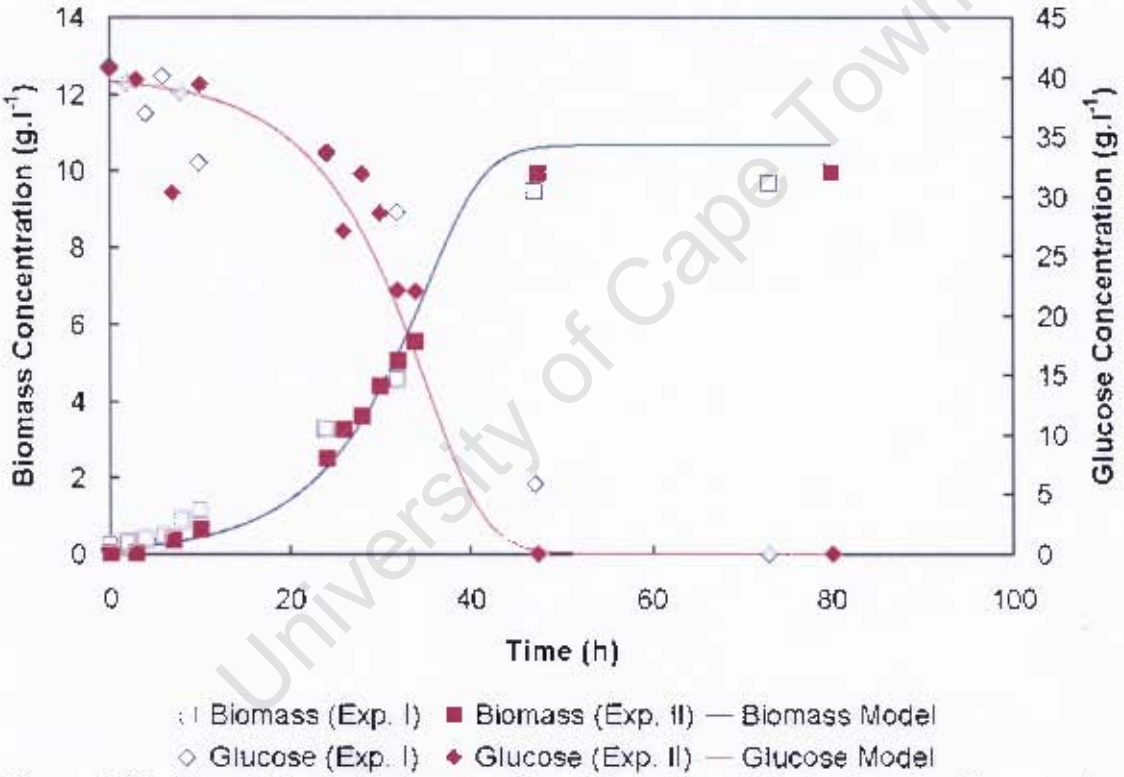

Figure 5.11: Correlation between experimental and predicted values for the complex medium base case experiments. Strain TVN 497 was cultivated in the Braun BIOSTAT C bioreactor on the modified Picataggio medium. The initial glucose concentration, pH, temperature, aeration rate and agitation speed of the medium were set at 40 $g.l^{-1}$, pH 6.0, 30 °C, 0.8 vvm and 700 rpm, respectively. The solid lines represent the predictions of Equations 5.3 and 5.4 using the basic kinetic parameter values in Table 5.4.

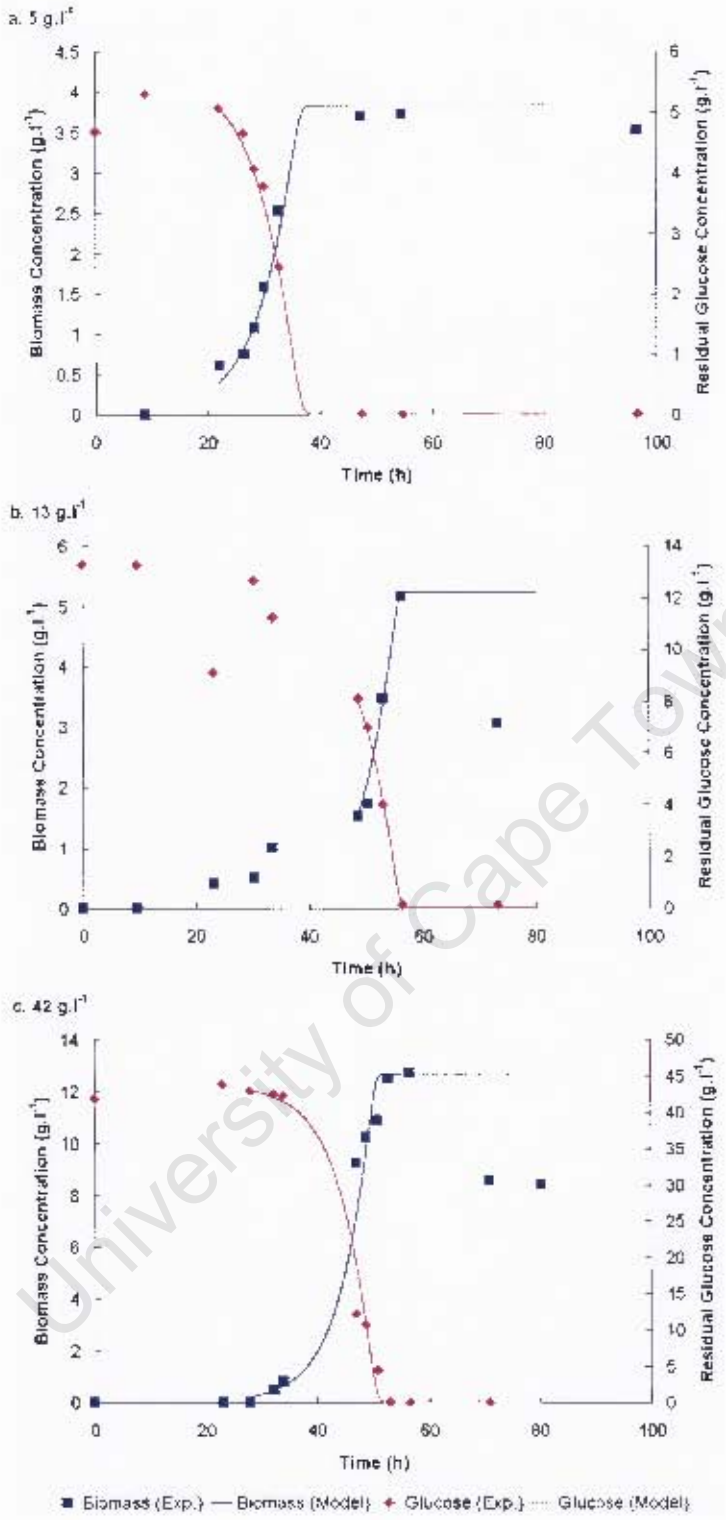

Figure 5.12: Correlation between experimental data and predictive model for biomass production and glucose utilisation in semi-defined medium at an initial glucose concentration of (a) 5 g.l^{-1}, (b) 13 g.l^{-1} and 42 g.l^{-1}. The experiments were carried out with strain TVN 497 in the Braun BIOSTAT C bioreactor using the modified Antonucci medium. The pH, temperature, aeration rate and agitation speed of the medium were set at pH 6.0, 30 °C, 0.8 vvm and 700 rpm, respectively. The solid lines represent the predictions of Equations 5.3 and 5.4 using the basic kinetic parameter values in Table 5.4.

The basic kinetic model did, predicted growth and substrate consumption in the semi-defined medium satisfactory as illustrated in Figure 5.12. This is indicated by the r^2 values which varied between 0.92 and 1.00. The model did not account for the lag phase and cell death.

5.3 Investigating Factors which Influence Biomass Production

5.3.1 The effect of high substrate concentration on specific growth rate

The kinetic model developed in Section 4.1 accounts for substrate limitation but ignores the possibility of substrate inhibition. Lack of knowledge about substrate inhibition can lead to inefficient utilisation of substrates, affecting process economics (Andrews, 1968). The objective of these studies was to determine whether *Y. lipolytica* TVN 497 is affected by substrate (glucose) inhibition. If so, the glucose concentration for optimal specific growth rate and refinement of the Monod equation to incorporate substrate inhibition would be required.

The effect of substrate inhibition was evaluated by performing five shake flask experiments at increasing glucose concentrations. Each experiment was performed in a 500 ml Erlenmeyer flask containing 50 ml of the UFS medium. Initial glucose concentrations ranged from 10 $g.l^{-1}$ to 60 $g.l^{-1}$. The media was buffered to a pH of 6.0 and inoculated with 5 ml of pre-culture, prepared as described in Section 3.5.4. After inoculation, the strains were cultivated at 29 °C on a rotary shaker at 180 rpm. Biomass and glucose concentrations were measured at regular intervals throughout the growth phase. Due to the small bioreactor-volume, turbidity measurements were used as the preferred method to determine the optical density.

The specific growth rate for each experiment was determined using the graphical approach. To eliminate the potential for oxygen limitation at high biomass concentrations and to investigate the specific glucose concentration range, the application of the graphical approach was limited to the first 10 h

after inoculation. The specific growth rate is given as a function of the initial glucose concentration in Figures 5.13.

Substrate inhibition is characterised by an initial increase in specific growth rate with an increase in glucose concentration. After reaching a maximum the specific growth rate decreases as the initial glucose concentration continues to increase (Marrot *et al.*, 2006). Figure 5.13 clearly attributes this character to strain TVN 497, thereby confirming glucose inhibition. The maximum specific growth for strain TVN 497 of 0.34 h^{-1} was found at an initial glucose concentration of 20 $g.l^{-1}$.

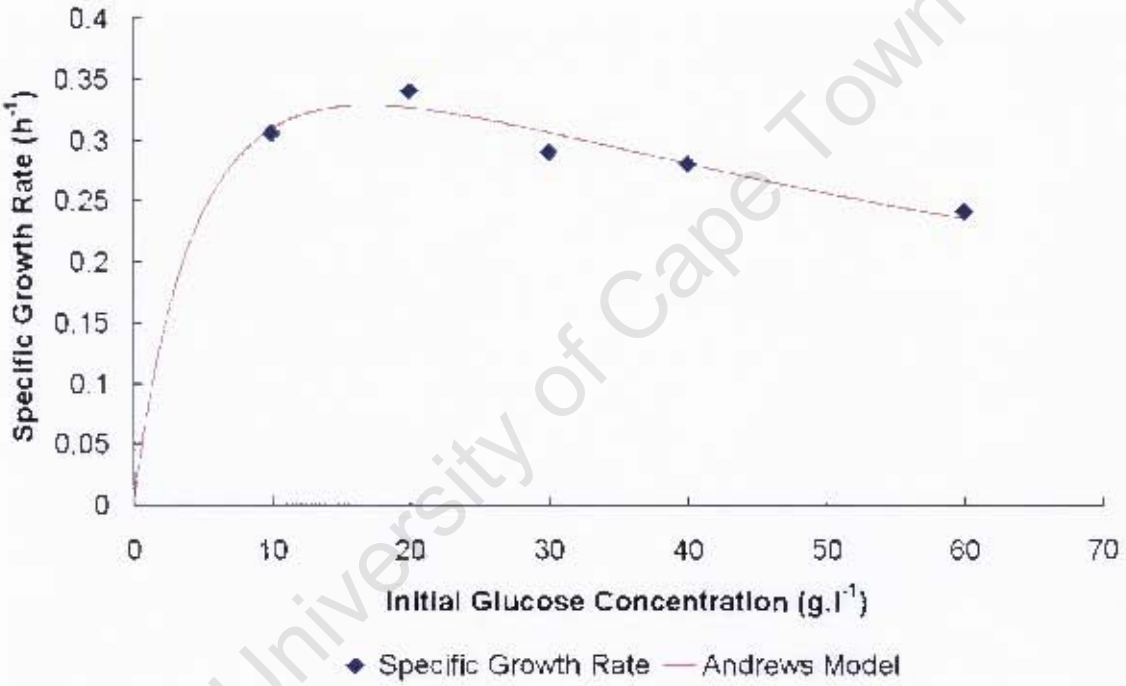

Figure 5.13: Correlation between the Andrews model predictions for specific growth rate and the experimental values obtained at different initial glucose concentrations, by applying the estimated basic kinetic parameters in table 4.6. Strain TVN 497 was cultured in shake flasks using the UFS media buffered to pH 6 at 29°C on a rotary shaker at 180 rpm. The initial glucose concentrations were chosen as 10, 20, 30, 40 and 60 $g.l^{-1}$, respectively.

Analysis of the data of Moresi (1994) indicates a similar trend for a wild type strain of *Yarrowia lipolytica*. From Moresi's data, the maximum specific growth rate of 0.34 h^{-1} was obtained at a glucose concentration of 61.7 $g.l^{-1}$ i.e. the optimal glucose concentration was significantly higher than that for strain TVN 497 while the maximum specific growth rate was similar.

The Andrews model (Andrews, 1968) describes substrate inhibition as follows:

$$\mu = \mu_m \frac{1}{K_s + C_{sg} + C_{sg}^2/K_i} \tag{5.8}$$

where K_i is a inhibition constant, numerically equals the highest substrate concentration at which the specific growth rate is equal to one-half the maximum specific growth rate in the absence of inhibition ($g.l^{-1}$). The computer based iterative process discussed in Section 4.3.2 was used to predict the kinetic parameters μ_m, K_s and K_i. In the presence of the following boundary conditions: (1) μ_m>0.34 h^{-1}, since it represents the theoretical maximum specific growth rate that could have been achieved, had there been no substrate inhibition (Gokulakrishnan, 2006) (2) K_s<K_i, since the values of K_s and K_i represent the lowest and highest concentration of substrate, respectively, at which the specific growth rate is equal to one-half of the maximum specific growth rate in the absence of inhibition. The estimated kinetic parameters are tabulated in Table 5.6.

Table 5.6: Basic kinetic parameters determined for the Andrews model

Basic Kinetic Parameters	Value	Unit
μ_m	0.56	h^{-1}
K_s	6.1	$g.l^{-1}$
K_i	47.6	$g.l^{-1}$

Figure 5.13 shows clearly that the Andrews model predicts the specific growth rates at the different initial glucose concentrations. The value of the saturation constant, K_s, (Table 5.6) of strain TVN 497 is, again, high compared to the value of K_s proposed by literature (Bull and Bushell, 1976 and Postma *et al.* 1989a&b). The value of K_i could not be validated since no inhibition studies on *Y. lipolytica* are reported. K_i values calculated by Phisalaphong *et al.* (2006) and Ghaly and El-Taweel (1997) for *Saccharomyces cerevisiae* and *Candida pseudotropicalis*, respectively, ranged between 100 $g.l^{-1}$ and 1600 $g.l^{-1}$, suggesting that *Y. lipolytica* TVN 497 is more sensitive to glucose.

5.3.2 The effect of alkane concentration on growing cells

Green *et al.* (2000) and Mimura *et al.* (1973) observed that mutant cells of *C. cloacae* and *C. petrophilum*, respectively, achieve lower yields of biomass when cultured in media containing hydrocarbons. It was proposed that the affinity of the yeast to adsorb onto hydrocarbon droplets were related to this phenomenon. To investigate the effect of alkane on growing cells of *Y. lipolytica* TVN 497, four experiments were conducted during which different concentrations of alkane were added to each culture medium 18 h after inoculation. To prevent intracellular accumulation of α,ω-dicarboxylic acids, the pH of two experiments was changed from pH 6.0 to pH 7.8 at the time of alkane addition. Since growth is also affected by pH, two control experiments were conducted during which the medium was maintained at pH 6.0. The experimental conditions are tabulated in Table 5.7.

Table 5.7: Experiments investigating the effect of alkane and medium pH on growing cells of *Y. lipolytica* TVN 497

Experiments	Volume Alkane	Medium pH Before Alkane Addition	Medium pH After Alkane Addition	Time of Alkane Addition
	l	pH	pH	h
I	0.00	6	6.0	-
II	0.10	6	7.8	18
III	0.15	6	6.0	18
IV	0.30	6	7.8	18

The experiments were conducted in the Braun BIOSTAT C bioreactor in the modified Picataggio medium at an initial glucose concentration of 40 $g.l^{-1}$. The cultures were grown aerobically at pH, temperature, aeration rate and agitation rate of pH 6.0, 30.0 °C, 0.8 vvm and 700 rpm, respectively. To evaluate the immediate effect of alkane on growing cells of *Y. lipolytica* TVN 497, the instantaneous specific growth rates of each experiment was calculated using Equation 2.10. The instantaneous specific growth rate, at the time of alkane addition (Figure 5.14), was calculated using the biomass concentration data at the time of alkane addition and approximately 1 h thereafter. The supportive growth data are included in Appendix F1.

The instantaneous specific growth rate in Experiments I, II, III and IV initially increased to a maximum value of 0.17 ± 0.01 h^{-1}, approximately 4 h to 7 h after inoculation. Hereafter the instantaneous specific growth rate in Experiments II, III and IV decreased to reach pseudo minimum values of 0.015 h^{-1}, 0.000 h^{-1} and 0.022 h^{-1}, immediately after alkane addition. In contrast, the instantaneous specific growth rate in Experiment I, where no alkane was added to culture medium, displayed no disturbance. After reaching a pseudo minimum, the instantaneous specific growth rates in Experiments II, III and IV again increased whereafter they decreased until growth ceased, approximately 48 h after inoculation.

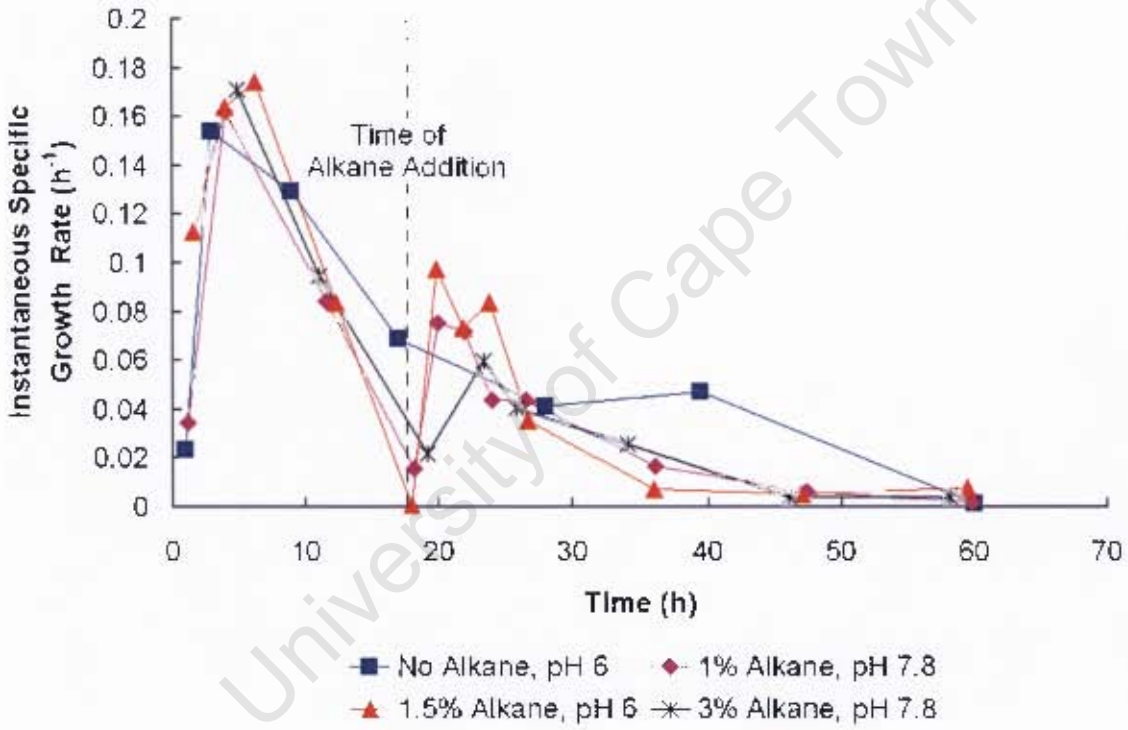

Figure 5.14: The effect of alkane and medium pH on the instantaneous specific growth rate of *Y. lipolytica* TVN 497. The experiments were performed with *Y. lipolytica* TVN 497 under the conditions stipulated in Section 4.1.1. Four different alkane concentrations 0.00%, 0.10%, 0.15%l and 0.30% (v/v) were added to the culture media 18 h after inoculation. The instantaneous specific growth rate, at the time of alkane addition, was calculated using the biomass concentration data at the time alkane addition and 1 h thereafter. The instantaneous specific growth rate in each case was calculated using Equation 2.10.

Hug *et al.* (1974) have made a similar observation with a wild-type strain of *C. tropicalis* in a continuous process. It was observed that when the carbon substrate was changed from glucose to hexadecane, microbial growth ceased

for approximately 2 h. It was suggested that since hydrocarbon growing cells contain twice as much lipid as cells which grow on glucose, the production of biomass are briefly arrested until such time that the cells have adapted themselves to their new lipophilic environment. It was also suggested that this may be related to the diversion of energy to synthesise the P450s required for alkane oxidation (Dunlap and Perry, 1967; Mizuno and Anraku, 1967; Johnson, 1967).

To evaluate the overall effect of alkanes on the growth of *Y. lipolytica* TVN 497, the graphical approach (Section 4.3.1) was applied to estimate the specific growth rate of each experiment after alkane addition (18 h after inoculation). These results and the final biomass concentrations of the experiments are tabulated in Table 5.8. By conducting a one-sided hypothesis test on the specific growth rate obtained for Experiment III, it was concluded with a 0.05 level of significance that the specific growth rate estimated exceeded the specific growth rates estimated in Experiments I, II and IV. The statistical analysis is shown in Appendix F2. It was therefore concluded that alkane in the culture medium improved growth of *Y. lipolytica* TVN 497 when the pH of the medium was maintained at pH 6.

Table 5.8: Specific growth rates of strain TVN 497 after alkane addition

Experiment	Specific Growth Rate After Alkane Addition*	Final Biomass Yield
	h^{-1}	$g.l^{-1}$
I	0.0561	9.66
II	0.0563	10.87
III	0.0835	10.50
IV	0.0529	9.34

* The graphical approach (Section 4.3.1) was applied to growth data obtained after alkane addition

The biomass yields alternatively, were not affected by the presence of alkane in the medium, since it was concluded that with a 0.05 level of significance, the mean yield of biomass calculated for Experiments II, III and IV did not exceed the biomass yield obtained in Experiment I. The statistical analysis is shown in Appendix F3. This finding contradicts the observations made by

Green *et al.* (2000) and Mimura *et al.* (1973) that alkane negatively affects the final biomass concentration of strains cultivating in its presence. It is speculated that since alkane was not added to the culture media at the time of inoculation, as was the case for Green *et al.* (2000) and Mimura *et al.* (1973), growth of *Y. lipolytica* TVN 497 was less affected.

5.4 Conclusions

In this chapter the growth of *Y. lipolytica* TVN 497 was evaluated in both the modified Picataggio complex medium and the Antonucci semi-defined medium. The experimental results obtained, indicated that in the complex medium, the strain utilises more than one nitrogen source for growth. It was also concluded that the strain utilises ammonium nitrogen preferentially to complex protein sources. These conclusions were drawn from the observation that growth continued after the depletion of the ammonium ion nitrogen source and ceased only when the carbon source (glucose) was depleted. For the experiments conducted in the semi-defined medium, glucose acted as the growth limiting substrate at initial glucose concentrations 5 $g.l^{-1}$, 13 $g.l^{-1}$ and 42 $g.l^{-1}$. At an initial glucose concentration of 50 $g.l^{-1}$ however, the experimental results indicated that growth may have become nitrogen limited.

Closing of the oxygen balance over the Braun BIOSTAT C bioreactor indicated negligible oxygen error for both the complex and semi-defined media. The error in closing the carbon balance for the complex and semi-defined media was less than 6% and 8%, respectively. Considering the degree of experimental error associated with biomass and glucose assays, the above errors are considered insignificant, confirming the assumptions made in the development of the basic unstructured kinetic model.

For the semi-defined medium, biomass production and glucose utilisation was predicted satisfactorily by the simplified kinetic model based on the Monod equation. While reasonable prediction of growth in the complex medium was found, the value of the saturation constant (K_s) was higher than the values

proposed by literature. This is expected to contribute to the model's reduced prediction accuracy. This reduced accuracy was further accentuated by the observation that whilst glucose acted as the limiting substrate, it may not have acted as the rate-limiting substrate as the instantaneous specific production rate decreased with a corresponding decrease in residual ammonium ion concentration.

The specific growth rate of *Y. lipolytica* TVN 497 was negatively affected by high glucose concentrations. The maximum specific growth rate of 0.34 h^{-1} was found at an initial glucose concentration of 20 $g.l^{-1}$. On increasing the initial glucose concentration, the specific growth rate decreased. This phenomenon was adequately described by the Andrews model.

The presence of alkane in the culture medium also affected growth. This conclusion was confirmed by the brief arrest (2 h) of biomass production which occurred when alkane was added to culture medium 18 h after inoculation. This was attributed to the time required by the strain to adapt to the new lipophilic environment.

Chapter 6

Results and Discussion II

Biotransformation of Alkanes into α,ω-Dicarboxylic Acids using *Yarrowia lipolytica* TVN 497 as Biocatalyst

6.1 Microbial Oxidation of Alkanes into α,ω-Dicarboxylic Acids

During the second phase of the research, factors affecting the conversion of alkane into α,ω-dicarboxylic acids and factors which are affected by α,ω-dicarboxylic acid accumulation were evaluated. The objectives of this chapter were:

- to evaluate the effect of the initial alkane concentration on α,ω-dicarboxylic acid production,
- to evaluate the effect of medium pH on α,ω-dicarboxylic acid production,
- to evaluate the effect of the growth medium (complex versus semi-defined) on α, ω-dicarboxylic acid production,
- to evaluate the effect of α,ω-dicarboxylic acid production on the carbon dioxide production rate and the oxygen utilisation rate, and
- to evaluate the effect of the presence of alkane on the solubility of oxygen in the medium.

All experiments were conducted in the Braun BIOSTAT C bioreactor with an initial glucose concentration of 40 $g.l^{-1}$. A 10% (v/v) inoculum was used. For the complex medium the pH, temperature, aeration rate and agitation speed were set at pH 6.0, 30°C, 0.8 vvm and 700 rpm, respectively. For the semi-defined medium, these were pH 5.0, 30°C, 0.6 vvm and 900 rpm, respectively.

6.1.1 Characterisation of alkane bioconversion and the effect of the initial alkane concentration

To evaluate the effect of the initial alkane concentration on α,ω-dicarboxylic acid production, an alkane concentration of 1% and 3% (v/v) were added to Experiments I and II, respectively. Both experiments were conducted in the modified Picataggio complex medium. To prevent possible product inhibition, the media pH of the production phase was increased to pH 7.8. In each case, the alkane was added to the culture media 18 h after inoculation.

Results in Figure 6.1 show that product formation was initiated at the time of alkane addition, regardless of the alkane concentration used. After alkane addition the dodecanedioic acid concentration in Experiments I and II increased at an equal rate until final concentrations of 1.40 $g.l^{-1}$ and 1.29 $g.l^{-1}$, respectively, were reached approximately 165 h after inoculation. By constructing a parity plot (Figure 6.2) with the corresponding dodecanedioic acid concentrations obtained in Experiments I and II, an r^2 value of 0.93 was calculated, suggesting that the production rate of dodecanedioic acid was unaffected by the initial alkane concentration.

Unexpectedly the equivalent parity was not found with respect to tridecanedioic acid production (Figure 6.2). Final tridecanedioic acid concentrations of 1.44 $g.l^{-1}$ and 0.9 $g.l^{-1}$ resulted when initial alkane concentrations of 1% and 3% (v/v) were used. Toxicity of linear alkanes is typically reported to decrease with an increase in carbon number owing to decreasing solubility. The cause of the reduced productivity has not being established.

Alkane utilisation in each case followed an inverse relationship to α,ω-dicarboxylic acid production. During the biotransformation period the residual dodecane concentration in Experiments I and II decreased from 3.5 $g.l^{-1}$ to 0.0 $g.l^{-1}$ and from 9.0 $g.l^{-1}$ to 5.2 $g.l^{-1}$, resulting in average dodecane to dodecanedioic acid molar-ratios of 5.6 and 4.8, respectively. Similarly, the

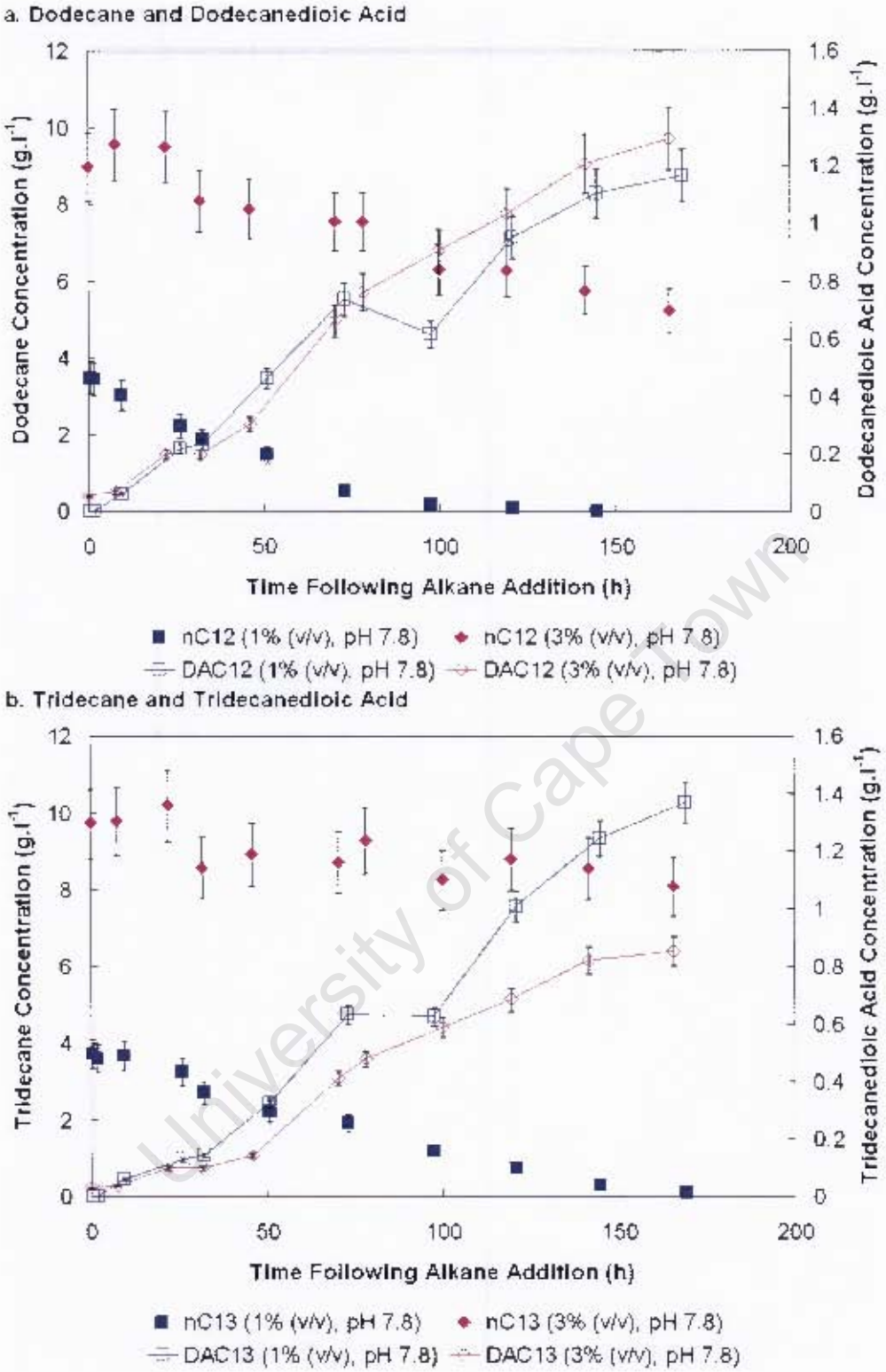

Figure 6.1: (a) The effect of alkane concentration on dodecane utilisation and dodecanedioic acid production. (b) The effect of alkane concentration on tridecane utilisation and tridecanedioic acid production. Both experiments were performed with *Y. lipolytica* TVN 497 under the conditions stipulated in Section 4.1.1. An initial alkane concentration of 1% and 3% (v/v) were added to the culture media 18 h after inoculation. The pH of the production phase was set at pH 7.8. The error bars represent the analytical error.

a. Dodecanedioic Acid

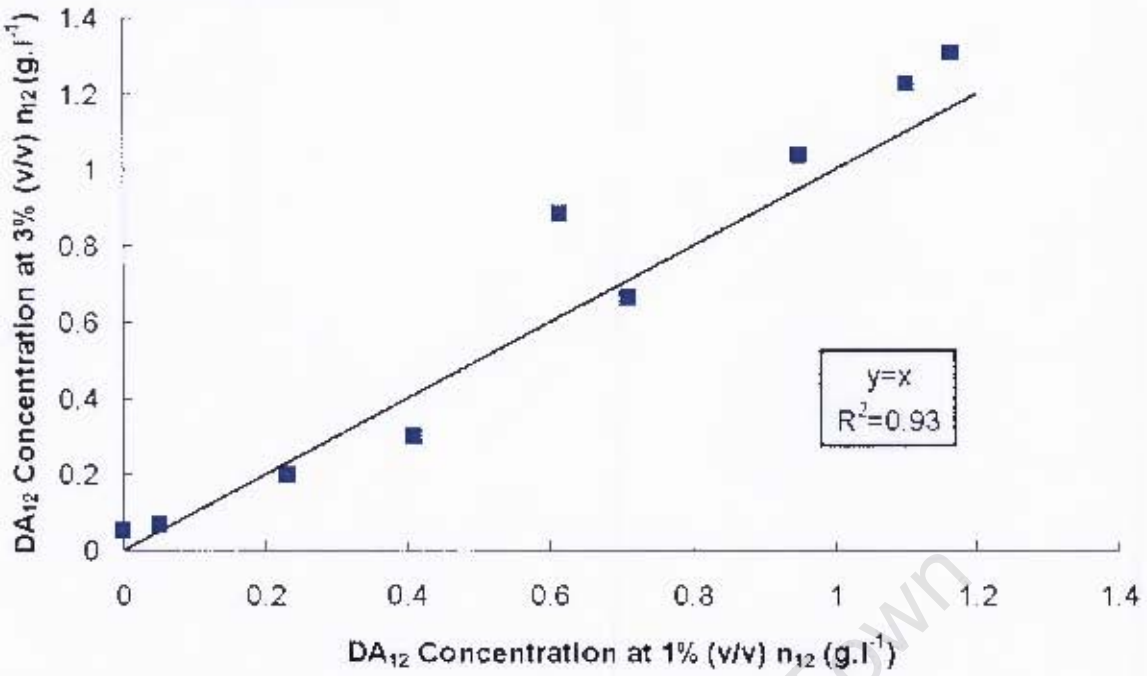

b. Tridecanedioic Acid

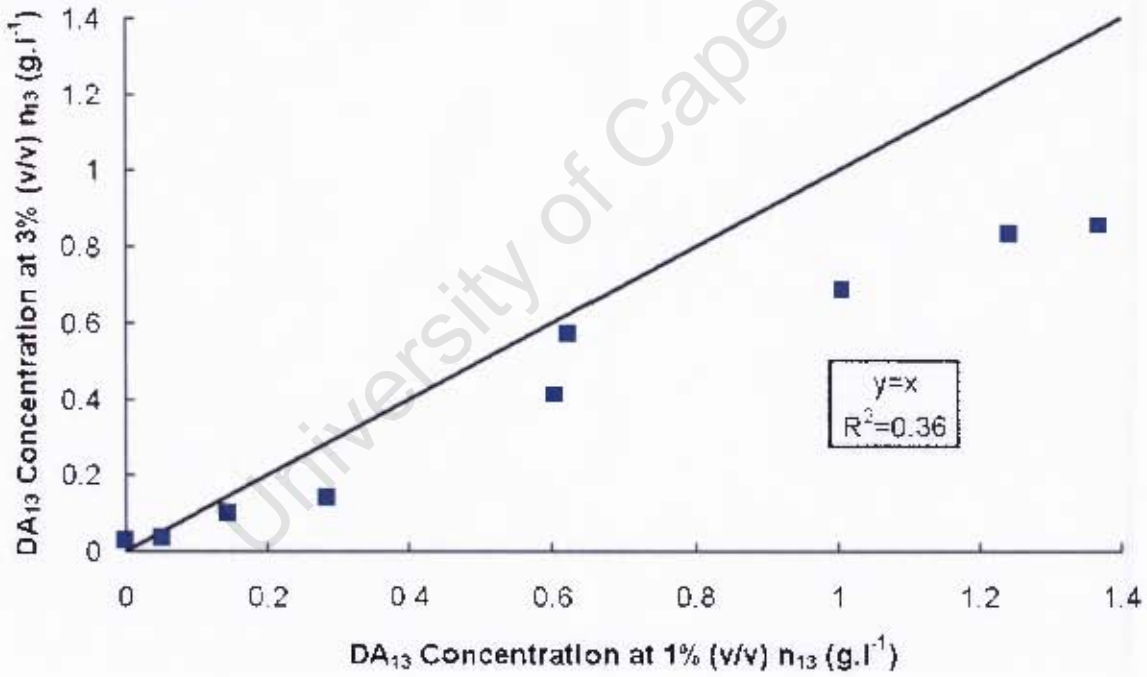

Figure 6.2: Parity plots of the corresponding (a) dodecanedioic acid and (b) tridecanedioic acid concentrations achieved with experiments conducted at initial alkane concentrations of 1% and 3% (v/v). Both experiments were performed with *Y. lipolytica* TVN 497 under the conditions stipulated in Section 4.1.1. An initial alkane concentration of 1% and 3% (v/v) were added to the culture media 18 h after inoculation. In each case the pH of the production phase was set at pH 7.8.

residual tridecane concentration decreased from 3.7 $g.l^{-1}$ to 0.0 $g.l^{-1}$ and from 9.7 $g.l^{-1}$ to 8.1 $g.l^{-1}$, resulting in average tridecane to tridecanedioic acid molar-ratios of 4.0 and 3.1, respectively. Except for the tridecane to tridecanedioic acid ratio in Experiment II, the ratios remained constant throughout the experiment. The latter was confirmed by the r^2 values in Figure 6.7 and Appendix H2. The theoretical molar ratio of alkane into α,ω-dicarboxylic acid is however,1.0, suggesting that the β-oxidation pathway of the strains were not completely blocked, evaporation of alkanes took place or the intracellular storage of alkanes in the form of lipids.

6.1.2 The effect of medium pH on alkane bioconversion

A preliminary experiment was conducted to evaluate the effect of medium pH on α,ω-dicarboxylic acid production. In addition to Experiments I and II, Experiment III was conducted during which the pH of the production phase was maintained at pH 6.0. The production phase was initiated 18 h after inoculation by adding 1.5% (v/v) alkane to the culture medium. The combined alkane and α,ω-dicarboxylic acid concentration of Experiments I, II and III are shown in Figure 6.3.

The results in Figure 6.3 show that product formation was initiated at the time of alkane addition, regardless of the pH. Hereafter, the α,ω-dicarboxylic acid concentration in Experiments I, II and III increased at similar rates. However, after reaching an α,ω-dicarboxylic acid concentration of 1.58 $g.l^{-1}$, approximately 100 h after alkane addition, product formation in Experiment III ceased, suggesting product inhibition. This phenomenon was previously reported by Chan *et al.* (1997) when *Pseudomonas aeruginosa* was unable to produce more than 0.85 $g.l^{-1}$ hexadecanedioic acid in a batch bioreactor. It is therefore suggested that an elevated medium pH is required to facilitate product formation at high α,ω-dicarboxylic acid concentrations.

The alkane concentration in each case followed an inverse relationship to α,ω-dicarboxylic acid production. The alkane concentration in Experiment III

however, continued to decrease although the α,ω-dicarboxylic acid concentration remained approximately constant. It appears therefore that *Y. lipolytica* TVN 497 metabolise linear alkane through an alternative pathway.

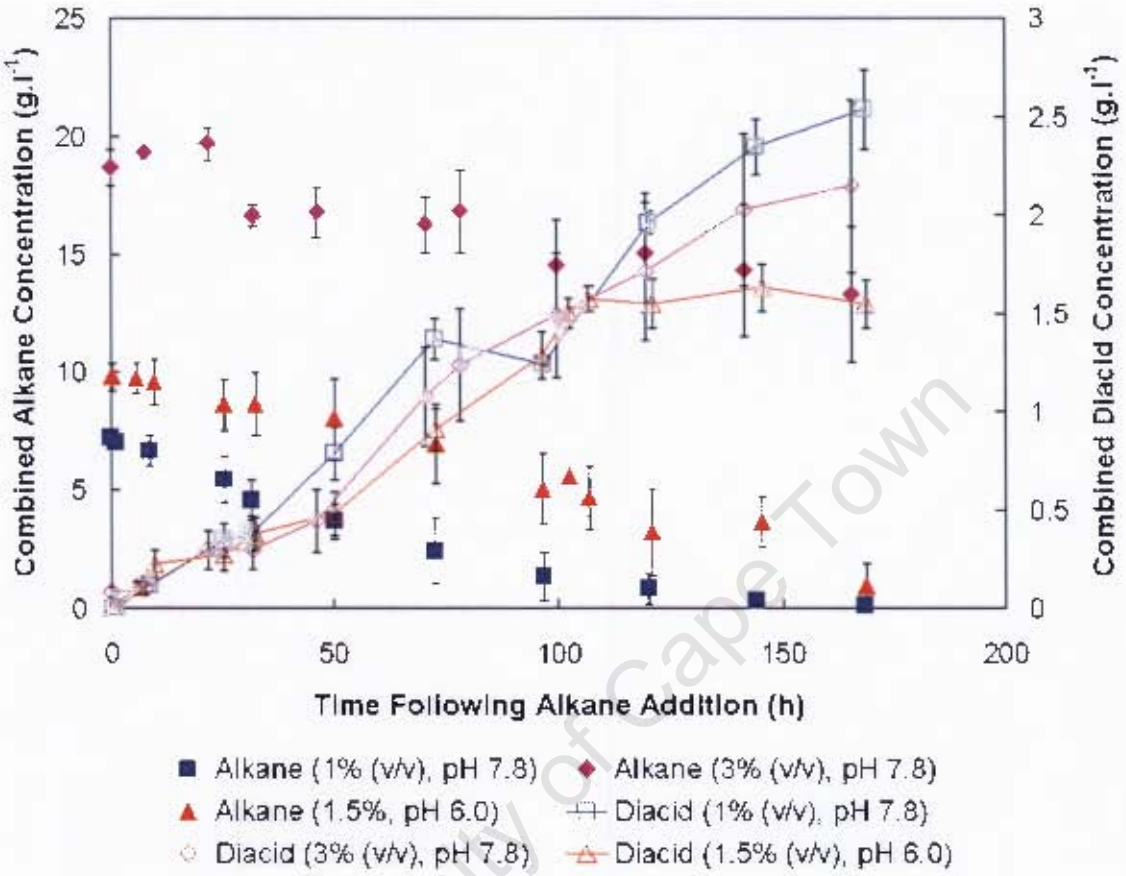

Figure 6.3: The effect of medium pH on alkane utilisation and α,ω-dicarboxylic acid production. The experiments were performed with *Y. lipolytica* TVN 497 under the conditions stipulated in Section 4.1.1. An initial alkane concentration of 1%, 1.5% and 3% (v/v) were added to the culture media 18 h after inoculation. In the case of 1% and 3% (v/v) alkane, the pH of the production phase was set at pH 7.8 whereas for 1.5% (v/v) alkane, the pH of the medium remained at pH 6. The error bars represent either the difference between the two alkane or α,ω-dicarboxylic acid concentrations obtained for the same experiment.

6.1.3 The effect of medium composition on alkane bioconversion

To evaluate the effect of different media on α,ω-dicarboxylic acid production, experiments were conducted using modified Picataggio complex medium (Section 5.1.1) and Antonucci semi-defined medium (Section 5.1.2). Using a dodecane-tridecane cut, 3% (v/v) alkane was added 18 h after inoculation,

resulting in 10.5 $g.l^{-1}$ dodecane and 11.4 $g.l^{-1}$ tridecane. The resulting dodecanedioic acid and tridecanedioic acid and residual dodecane and tridecane concentrations are shown as a function of time in Figure 6.4.

From Figure 6.4 it is clear that the production of α,ω-dicarboxylic acids was significantly affected by the type of medium used. In the case of the complex medium, the concentrations of both dodecanedioic acid and tridecanedioic acid increased from zero, over a period of 100 h, to final values of 0.9 $g.l^{-1}$ and 0.6 $g.l^{-1}$, respectively. During the same period the corresponding substrate (dodecane and tridecane) concentration decreased from 10.5 $g.l^{-1}$ to 6.3 $g.l^{-1}$ and from 11.4 $g.l^{-1}$ to 8.2 $g.l^{-1}$, respectively, corresponding to a ratio of alkane used to α,ω-dicarboxylic acids formed of 2.3 to 3.3 on a molar basis. This non-proportionality between product formation and substrate utilisation may again be attributed to the β-oxidation pathway not being completely blocked, evaporation of alkanes taking place or the intracellular storage of alkanes by the strains in the form of lipids.

In the case of the semi-defined medium experiment the dodecanedioic acid and tridecanedioic acid concentration did not exceed 0.09 $g.l^{-1}$ (10% of the above). Product formation ceased 47 h after alkane addition. During the same period the dodecane and tridecane concentration decreased from 11.4 $g.l^{-1}$ to 7.5 $g.l^{-1}$ and from 12.0 $g.l^{-1}$ to 10.4 $g.l^{-1}$, respectively. The ratio of alkane utilised to α,ω-dicarboxylic acids produced ranged from 27 to 59, clearly indicating preferred metabolism by an alternative pathway or loss of alkane from the system.

Shiio and Uchio (1971) observed a similar difference between the α,ω-dicarboxylic acid yields obtained with the semi-defined medium and those obtained with the complex medium and attribute this to the presence of NH_4NO_3 in the Antonucci medium (Section 2.3). Shiio and Uchio (1971) observed that NH_4NO_3 is not desirable for α,ω-dicarboxylic acid production although it well suited as a nitrogen source for biomass production.

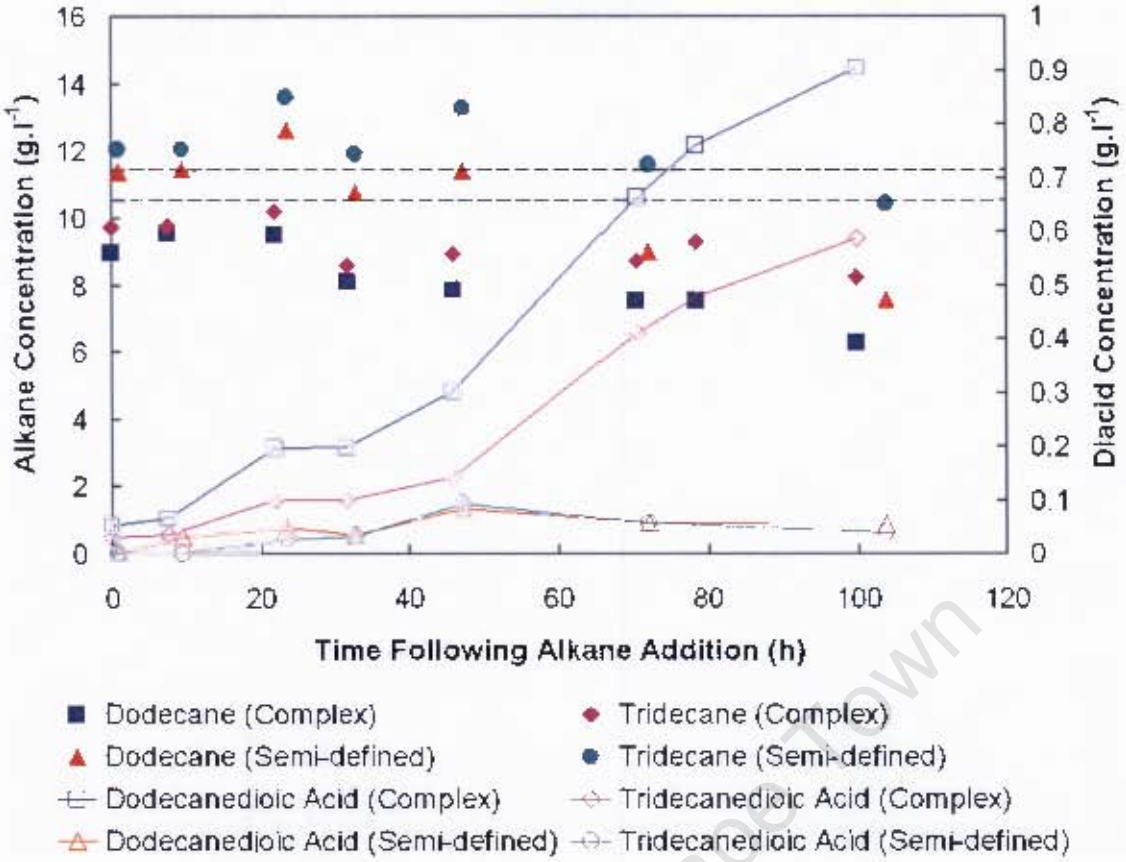

Figure 6.4: The effect of different growth media on the production of α,ω-dicarboxylic acid. α,ω-Dicarboxylic acid production was evaluated in the modified Picataggio complex medium and the Antonucci semi-defined medium using *Y. lipolytica* TVN 497 cultured in the Braun BIOSTAT C bioreactor at initial glucose and alkane concentrations of 40 $g.l^{-1}$ and 3%(v/v), respectively. The theoretical initial tridecane and dodecane concentration in the medium are presented by the upper and lower dotted line, respectively.

6.1.4 The effect of α,ω-dicarboxylic acids production on carbon dioxide production and the oxygen utilisation

To evaluate the effect of α,ω-dicarboxylic acids production on the carbon dioxide production rate and the oxygen utilisation rate, an experiment was conducted with the modified Picataggio complex medium at an initial alkane concentration of 1% (v/v). Figure 6.5 shows that, whilst the carbon dioxide production rate and the oxygen utilisation rate decreased from 26.3 $mmol.h^{-1}$ to 4.6 $mmol.h^{-1}$ and from 33.6 $mmol.h^{-1}$ to 9.6 $mmol.h^{-1}$, respectively, the dodecanedioic acid and tridecanedioic acid concentrations increased from 0.5 $g.l^{-1}$ to 1.2 $g.l^{-1}$ and from 0.3 $g.l^{-1}$ to 1.3 $g.l^{-1}$, respectively. The stoichiometric equations:

$$C_6H_{12}O_6 + 6O_2 \rightarrow 6H_2O + 6CO_2 \quad (6.1)$$

$$H_3C\text{-}(CH_2)_n\text{-}CH_3 + 3O_2 \rightarrow HO_2C\text{-}(CH_2)_n\text{-}CO_2H + 2H_2O \quad (6.2)$$

$$H_3C\text{-}(CH_2)_n\text{-}CH_3 + (1.5n + 3.5)\cdot O_2 \rightarrow (n+3)\cdot H_2O + (n+2)\cdot CO_2 \quad (6.3)$$

Equation 6.1 represents cell maintenance from glucose, Equation 6.2 the production of α,ω-dicarboxylic acids from linear alkanes and Equation 6.3 cell maintenance from alkanes. During the stationary phase, the activity of the cell is maintained by energy which is released when reserved glucose is oxidised into water and carbon dioxide. During this process equimolar oxygen and carbon dioxide are utilised and produced (Equation 6.1). However, when α,ω-dicarboxylic acids are produced as non-growth associated products, additional oxygen is required (Equation 6.2). If a portion of the alkane is processed through β-oxidation to assist in energy provision, Equation 6.3 may be expected to describe the stoichiometry of relative oxygen utilisation and carbon dioxide production.

In Figure 6.5, a decrease in both the rates of oxygen utilisation and carbon dioxide production is observed across the biotransformation period from 33.6 mmol.h^{-1} to 4.8 mmol.h^{-1} and from 26.3 mmol.h^{-1} to 2.9 mmol.h^{-1}, respectively. This is attributed to a decline in cell activity through the stationary phase period. The lower production rate of carbon dioxide compared to the utilisation rate of oxygen can be attributed to the production of α,ω-dicarboxylic acids, which requires additional oxygen without concomitant carbon dioxide production. Further, possible conversion of alkanes through β-oxidation to assist in energy provision also favours oxygen consumption.

From Equation 6.2, an additional 0.35 gmol oxygen was required to produce the 2.78 g α,ω-dicarboxylic acids detected. If it is assumed that the remaining alkanes were metabolised as energy source, Equation 6.3 can be applied to calculate that additional 1.96 gmol oxygen would be required. An excess of

2.32 gmol oxygen over the carbon dioxide produced was therefore expected during the biotransformation phase. The actual excess oxygen used was calculated from the area between the carbon dioxide production rate and oxygen utilisation rate data in Figure 6.5. The total actual excess oxygen was calculated as 1.33 gmol. Since an error of more that 25% existed between the two estimated values, it was suggested that only a fraction of the remaining alkanes underwent complete oxidation to CO_2 through β-oxidation. The remaining difference in residual alkane concentration may have resulted either from their partial conversion to high energy products or their loss from the system as a result of evaporation.

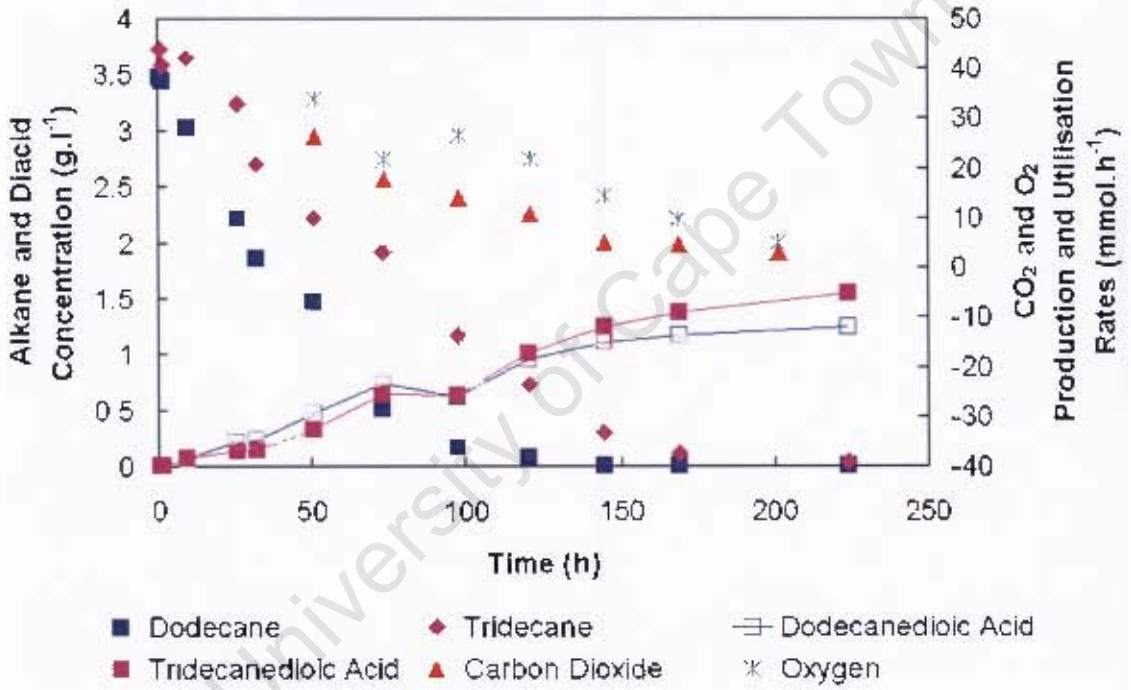

Figure 6.5: The effect α,ω-dicarboxylic acid production has on the carbon dioxide production rate and the oxygen utilisation rate. The experiment was conducted in the modified Picataggio medium with the Braun BIOSTAT C bioreactor. The initial glucose concentration, pH, temperature, aeration rate and agitation speed were set at 40 $g.l^{-1}$, pH 6.0, 30 °C, 0.8 vvm and 700 rpm, respectively. Eighteen hours after inoculation a 1% (v/v) alkane cut was added to the medium whereafter the medium pH was increased to 7.8.

6.1.5 The effect of alkane on oxygen solubility, and thereby transfer rate

To evaluate the effect of alkane on the oxygen solubility in the complex medium, an experiment was conducted during which 0.1 l alkane was added

to the culture medium, 18 h after inoculation. At this point growth was in the early exponential phase. The instantaneous specific growth rate, oxygen utilisation rate, total residual alkane concentration (dodecane and tridecane) and the oxygen concentration in the medium are shown as a function of time in Figure 6.6.

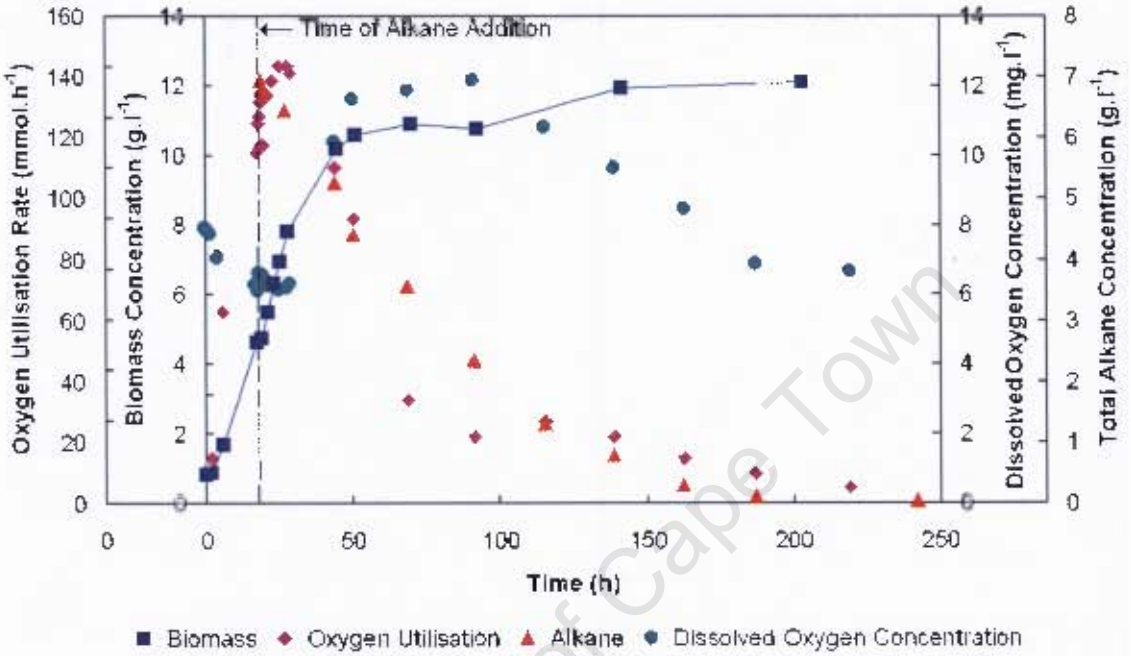

Figure 6.6: The effect of alkane on the solubility of oxygen in the medium. The experiment was conducted in the modified Picataggio medium with the Braun BIOSTAT C bioreactor. The initial glucose concentration, pH, temperature, aeration rate and agitation speed were set at 40 g.l^{-1}, pH 6.0, 30 °C, 0.8 vvm and 700 rpm, respectively. Eighteen hours after inoculation a 1% (v/v) alkane cut was added to the medium whereafter the medium pH was elevated to 7.8.

During the first 18 h before alkane addition, the biomass concentration and oxygen utilisation rate (OUR) increased from 0.8 g.l^{-1} to 4.6 g.l^{-1} and from 9.6 mmol.h^{-1} to 124.3 mmol.h^{-1}, respectively. The enhanced OUR is attributed to both the growth rate and the increase in biomass concentration in this period. Concurrently, the oxygen concentration in the medium decreased concomitantly from 7.9 mg.l^{-1} to 6.1 mg.l^{-1}. After alkane addition, the OUR continued to increase for a further 10 h to a maximum utilisation rate of 134.3 mmol.h^{-1}. The biomass concentration increased from 4.6 g.l^{-1} to 7.8 g.l^{-1} whereas the oxygen concentration in the medium remained constant at a value of 6.4 ± 0.2 mg.l^{-1}. It is therefore apparent that the oxygen transfer rate

(OTR) into the system increased without affecting the oxygen concentration in the medium.

Since the oxygen transfer rate (OTR) equals the oxygen utilisation rate in a balanced system, either the overall mass transfer coefficient (K_La) or the saturation oxygen concentration (C*) or both were affected by alkane in the medium (Section 2.4.1), according to Equation 6.4:

$$OTR = K_La(C^* - C) \quad (6.4)$$

where C represents the actual oxygen concentration in the medium. According to Clarke *et al.* (2006), the K_La value calculated in a 7.5-liter baffled New Brunswick bioreactor at an aeration rate of 1.25 vvm and agitation rate of 800 rpm, did not change by more than 10% when the alkane concentration was varied between 0% (v/v) and 5% (v/v). Conversely a 20% increase in oxygen saturation concentration was observed over the same increase in alkane concentration in an alkane-water system. This is an indication that alkane acts as an oxygen vector since it increases the saturation oxygen concentration of the medium to which it is added. This is mediated by the increased solubility of some 6 fold of oxygen in the dodecane-tridecane fraction (Ju and Ho 1989). This increased oxygen solubility is clearly illustrated in Figure 6.6.

When biomass production ceased with an associated decrease in OUR, approximately 50 h after inoculation, a maximum dissolved oxygen concentration of 11.8 ± 0.8 $mg.l^{-1}$ was obtained and maintained until the combined alkane concentration reduced to 2.4 $g.l^{-1}$, approximately 90 h after inoculation. It is therefore evident that alkane has acted as an oxygen vector. The oxygen concentration was however, 1.2 times larger than the oxygen concentration reported by Clarke *et al.* (2006). This discrepancy may be attributed to the fact that the experiment was conducted under a positive air pressure.

6.2 Quantification of the Kinetic Parameters for α,ω-Dicarboxylic Acid Production and Alkane Oxidation

The kinetic analyses for α,ω-dicarboxylic acid production and alkane oxidation is presented for data collected using the complex medium only. While it is recognised that rigorous kinetic studies are better conducted with a semi-defined medium (Shuler and Kargi, 2002), Shiio and Uchio (1971) observed that NH_4NO_3, present in the semi-defined Antonucci medium, is not desirable for α,ω-dicarboxylic acid production as was shown in Section 6.1. The very low α,ω-dicarboxylic acid production observed in semi-defined medium was not subjected to kinetic analysis.

Kinetic analysis of α,ω-dicarboxylic acid formation was performed on three experiments during which *Y. lipolytica* TVN 497 was cultivated in the Braun BIOSTAT C bioreactor. The initial glucose concentration for all three experiments was set at 40 $g.l^{-1}$. The culture was grown aerobically at pH 6.0 and 30 °C, with agitation at 700 rpm and an aeration rate of 0.8 vvm. An alkane cut, comprising of equal volumes of dodecane and tridecane was added to the culture media, 18 h after inoculation to provide initial alkane concentrations of 1%, 1.5% and 3% (v/v).

Luedeking-Piret kinetics was applied to predict the ability of *Y. lipolytica* TVN 497 to convert alkanes into α,ω-dicarboxylic acids (Section 4.2). It was assumed that the utilisation and production rate of alkanes into α,ω-dicarboxylic acids was proportional to the biomass concentration as follow:

$$-\frac{dC_{sdd}}{dt} = \left(\frac{1}{Y_{dda/dd}}\right)\cdot(\beta_{dda}C_x) \tag{6.5}$$

$$\frac{dC_{dda}}{dt} = \beta_{dda}C_x \tag{6.6}$$

$$-\frac{dC_{std}}{dt} = \left(\frac{1}{Y_{tda/td}}\right) \cdot (\beta_{tda} C_x) \quad (6.7)$$

$$\frac{dC_{tda}}{dt} = \beta_{tda} C_x \quad (6.8)$$

where C_{sdd} and C_{std} represent the dodecane and tridecane concentrations ($g.l^{-1}$), respectively, C_{dda} and C_{tda} the dodecanedioic acid and tridecanedioic acid concentrations ($g.l^{-1}$), respectively, β_{dda} and β_{tda} the specific production rates of dodecanedioic acid and tridecanedioic acid (h^{-1}), respectively and C_x the biomass concentration ($g.l^{-1}$).

By applying the graphical approach developed in Section 4.3.1, initial estimates were provided for kinetic parameters β_{dda}, $Y_{dda/dd}$, β_{dda} and $Y_{dda/dd}$. The graphical approach of the experiment conducted at an initial alkane concentration of 1% (v/v) is shown in Figures 6.7 and 6.8. Analysis of the remainder is included in Appendix H1 and summarised in Tables and 6.1 and 6.2.

The kinetic parameters were refined using the computer-based iterative process described in Section 4.3.2. Equations 6.5, 6.6, 6.7 and 6.8 were numerically integrated with the aid of the fourth order Runga-kutta method. The integrated values were compared with the experimental data. Where necessary, based on the error, new values were estimated for β_{dda}, $Y_{dda/dd}$, β_{tda} and $Y_{tda/td}$ using the Nelder-Mead non-linear least squares method. This process was repeated to minimise the errors between the experimental and the predicted values. The resultant values of the kinetic parameters are tabulated in Tables 6.3 and 6.4.

a. Overall Yield Coefficient (dodecane into dodecanedioic acid)

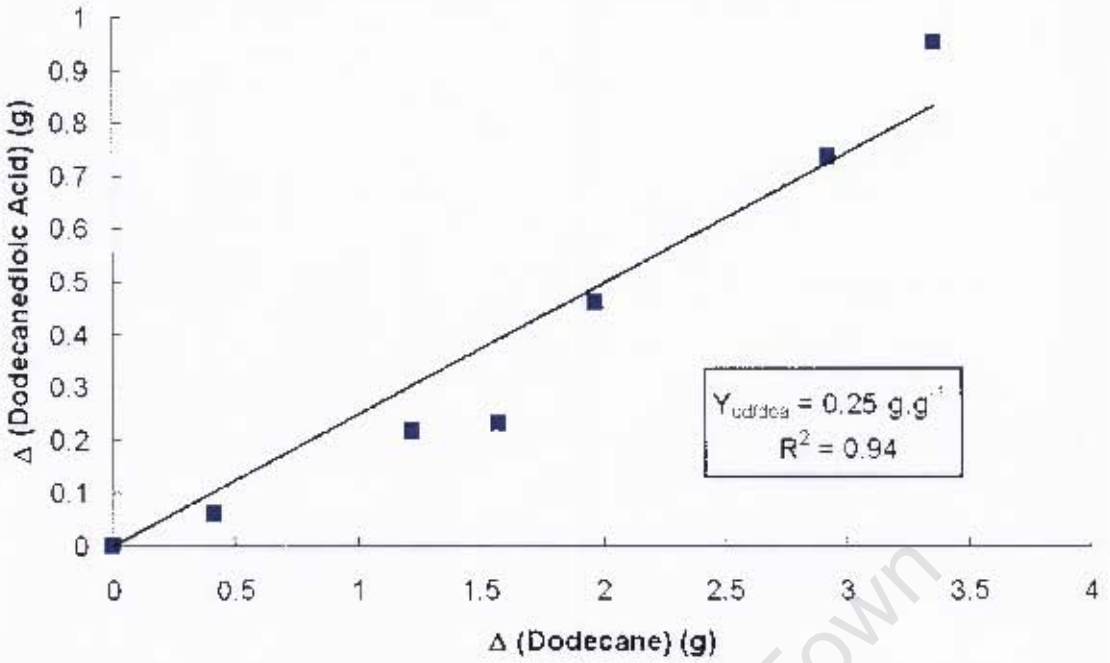

b. Overall Yield Coefficient (tridecane into tridecanedioic acid)

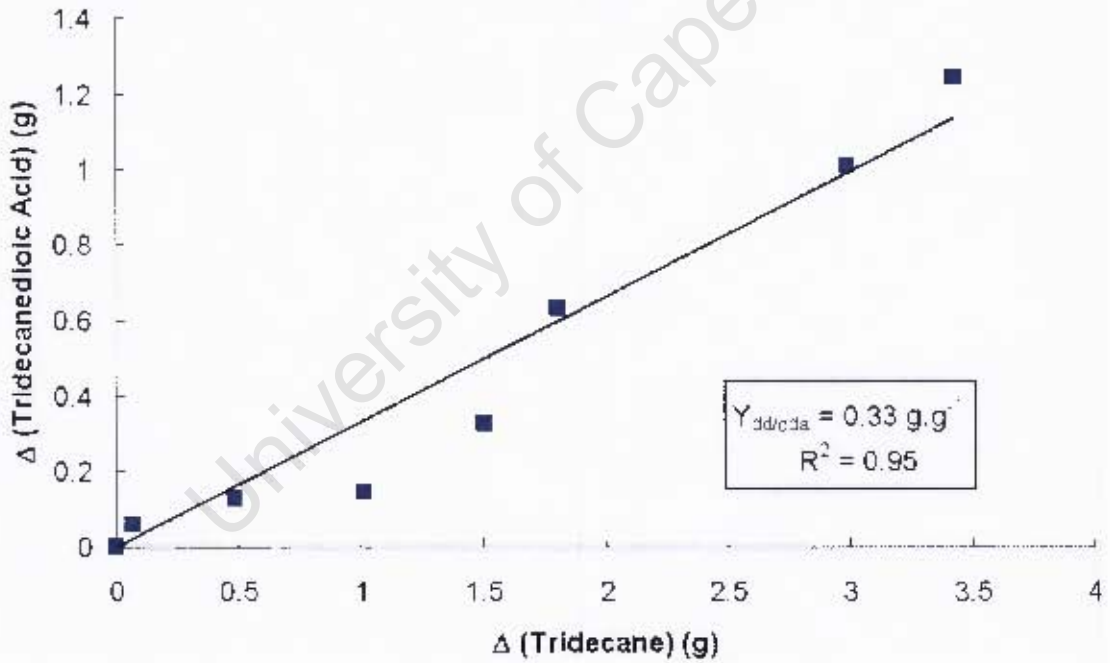

Figure 6.7: Graphical estimation of the overall product yield coefficient at an initial alkane concentration of 1% (v/v). a) Conversion of dodecane into dodecanedioic acid; b) Conversion of tridecane into tridecanedioic acid. Experiments were carried out with strain TVN 497 in the Braun BIOSTAT C bioreactor using the modified Picataggio complex medium. The initial glucose concentration, pH, temperature, aeration rate and agitation speed of the medium were set at 40 g.l^{-1}, pH 6.0, 30 °C, 0.8 vvm and 700 rpm, respectively. Alkane addition occurred 18 h after inoculation.

a. Constant of Proportionality (dodecane into dodecanedioic acid)

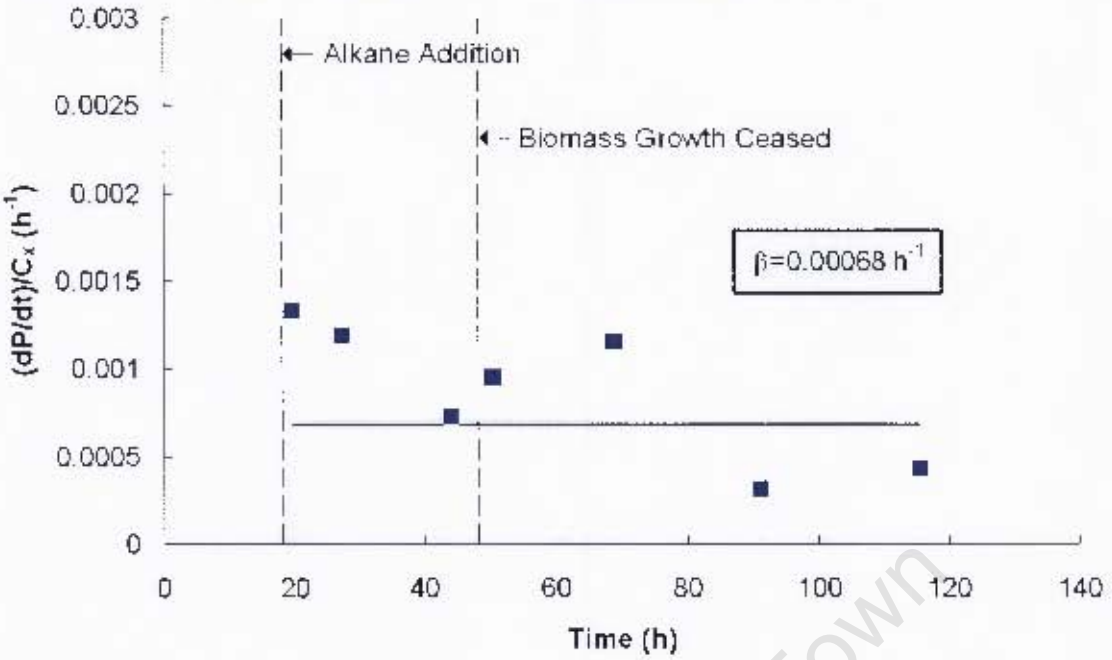

b. Constant of Proportionality (tridecane into tridecanedioic acid)

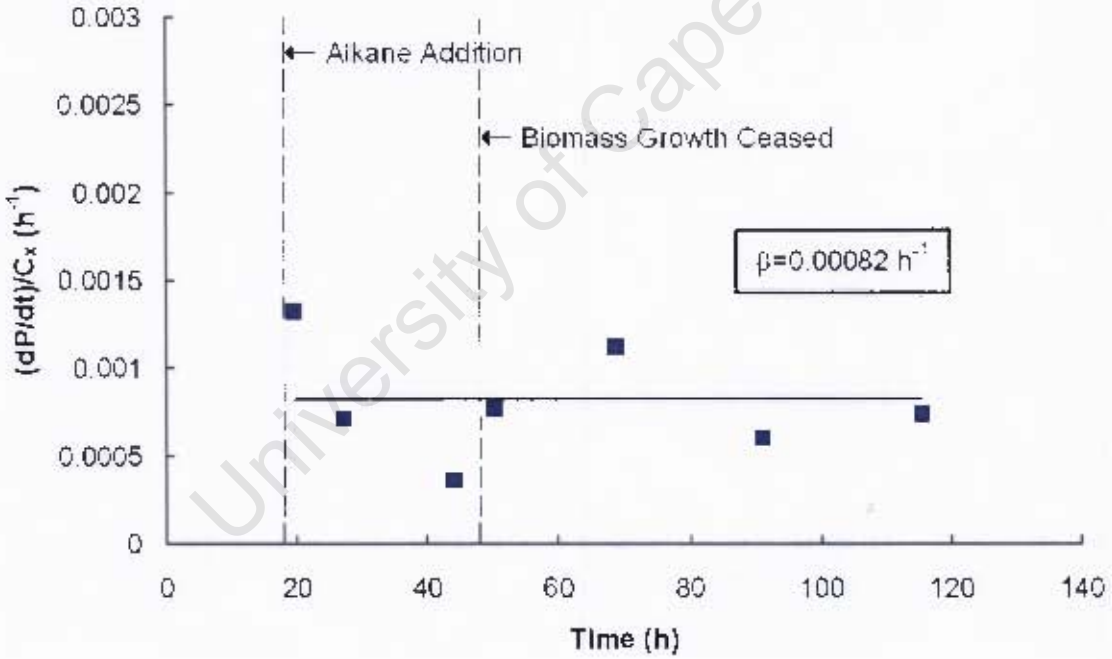

Figure 6.8: Graphical estimation of the proportionality constant at an initial alkane concentration of 1% (v/v). (a) Conversion of dodecane into dodecanedioic acid; (b) Conversion of tridecane into tridecanedioic acid. Experiments were carried out with strain TVN 497 in the Braun BIOSTAT C bioreactor using the modified Picataggio medium. The initial glucose concentration, pH, temperature, aeration rate and agitation speed of the complex medium were set at 40 $g.l^{-1}$, pH 6.0, 30 °C, 0.8 vvm and 700 rpm, respectively. Alkane addition occurred 18 h after inoculation.

Table 6.1: Initial estimates of product yield coefficient as a function of initial alkane concentration (graphical approach)

Initial Alkane Concentration (v/v)	Product Yield Coefficient			
	$Y_{dda/dd}$		$Y_{tda/td}$	
	($g.g^{-1}$)	($gmol.gmol^{-1}$)	($g.g^{-1}$)	($gmol.gmol^{-1}$)
1.0%[a]	0.25	0.18	0.33	0.25
1.5%[b]	0.22	0.16	0.25	0.19
3.0%[a]	0.28	0.21	0.43	0.32

[a] Conducted at pH 7.8

[b] Conducted at pH 6

Table 6.2: Initial estimates of the specific production formation rate as a function of initial alkane concentration (graphical approach)

Initial Alkane Concentration (v/v)	Specific Product Formation Rate	
	$\beta_{dda}x10^{-4}$ (h^{-1})	$\beta_{tda}x10^{-4}$ (h^{-1})
1.0%[a]	6.8	8.2
1.5%[b]	9.4	7.9
3.0%[a]	8.8	6.1

[a] Conducted at pH 7.8

[b] Conducted at pH 6

The theoretical values of $Y_{dda/dd}$ and $Y_{tda/td}$ are 1.35 $g.g^{-1}$ and 1.33 $g.g^{-1}$, respectively. It is therefore suggested that the β-oxidation pathway was not completely blocked, alkanes evaporated or products of alkane conversion accumulated intracellularly or a combination of these. At a confidence level of 95%, dodecane and tridecane demonstrated similar yield coefficients (Table 6.3). The average specific production rate of dodecanedioic acid was however, significantly higher than the specific production rate of tridecanedioic acid, suggesting substrate inhibition (Section 6.1.1). The statistical analysis is shown in Appendixes H3 and H4. From Table 6.4, it is also clear that the specific production rate of α,ω-dicarboxylic acid was negatively (10%-24%) affected by a low medium pH, suggesting product inhibition (Section 6.1.2).

Table 6.3: Refined product yield coefficients as a function of initial alkane concentration

Initial Alkane Concentration (v/v)	Yield Coefficient			
	$Y_{dda/dd}$		$Y_{tda/td}$	
	($g.g^{-1}$)	($gmol.gmol^{-1}$)	($g.g^{-1}$)	($gmol.gmol^{-1}$)
1.0%[a]	0.22	0.16	0.26	0.20
1.5%[b]	0.24	0.18	0.34	0.26
3.0%[a]	0.24	0.18	0.39	0.29

[a] Conducted at pH 7.8

[b] Conducted at pH 6

Table 6.4: Refined specific production formation rate as a function of initial alkane concentration

Initial Alkane Concentration (v/v)	Proportionality Constant	
	$\beta_{dda} x10^{-4}$ (h^{-1})	$\beta_{tda} x10^{-4}$ (h^{-1})
1.0%[a]	8.4	6.2
1.5%[b]	6.8	5.3
3.0%[a]	9.0	5.9

[a] Conducted at pH 7.8

[b] Conducted at pH 6

The model was fitted to the experimental data using the kinetic parameters in Tables 6.3 and 6.4. The model developed provided a suitable approximation of the experimental data. This is demonstrated by the parity plots (Figure 6.11) for which average r^2 values of 0.98 and 0.94 were calculated for alkane utilisation and product formation, respectively. A shortcoming of the model however, is its inability to predict substrate utilisation and product formation at low substrate concentrations as the model continues to predict product formation even in the absence of substrate. The model can therefore only be applied to the linear phase, where the production rate is directly proportional to the biomass concentration. Equations 6.5, 6.6, 6.7 and 6.8 were modified to include the rate limiting effect of alkanes on the production rate α,ω-dicarboxylic acid as follows:

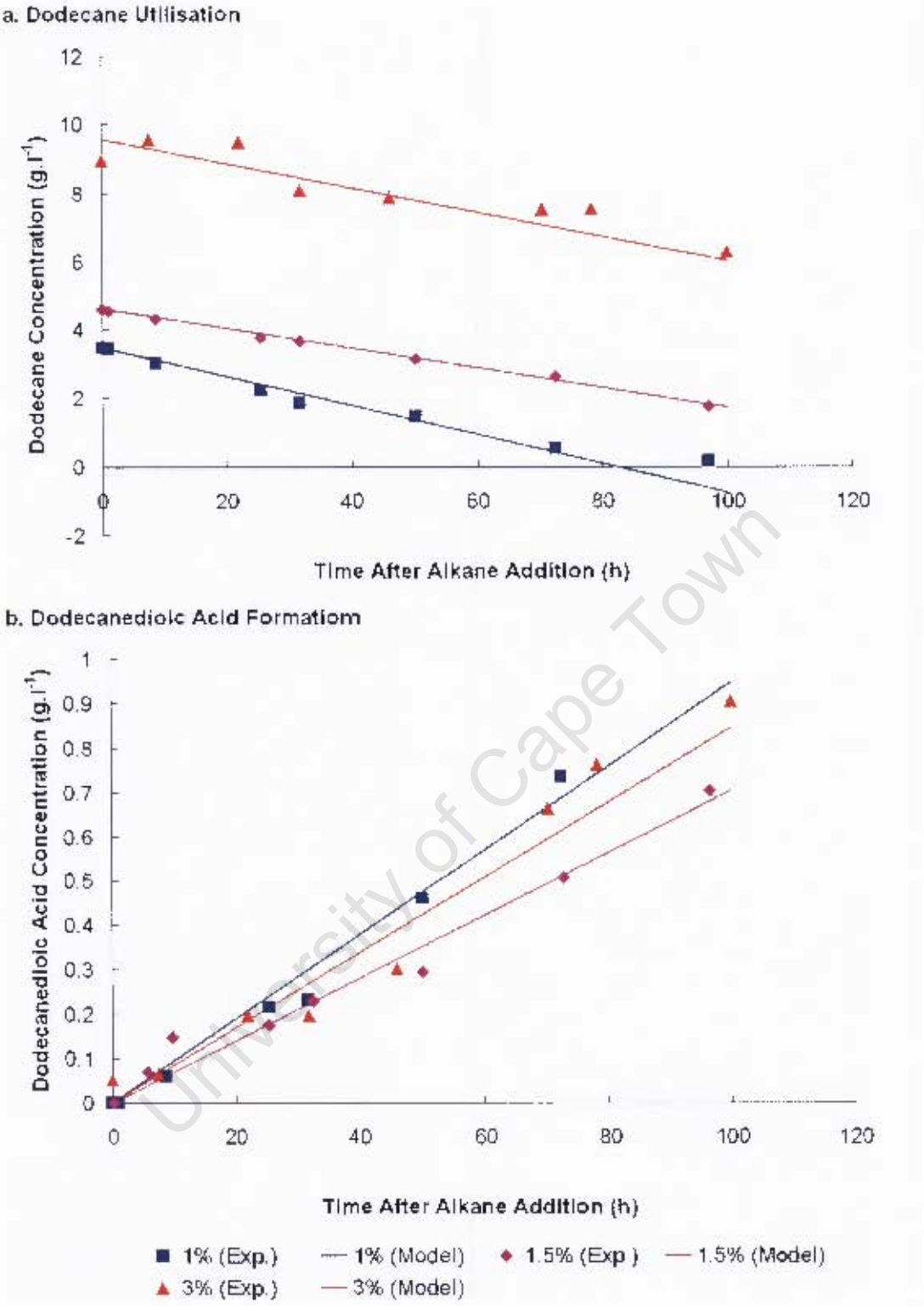

Figure 6.9: Correlation between experimental data and the predictive model for (a) dodecane utilisation; (b) dodecanedioic acid formation. The experiments were carried out with strain TVN 497 in the Braun BIOSTAT C bioreactor using the modified Picataggio medium. The initial glucose concentration, pH, temperature, aeration rate and agitation speed of the medium were set at 40 $g.l^{-1}$, pH 6.0, 30 °C, 0.8 vvm and 700 rpm, respectively. The solid lines represent the predictions of Equations 6.5, 6.6, 6.7 and 6.8 using the basic kinetic parameter values in Tables 6.3 and 6.4.

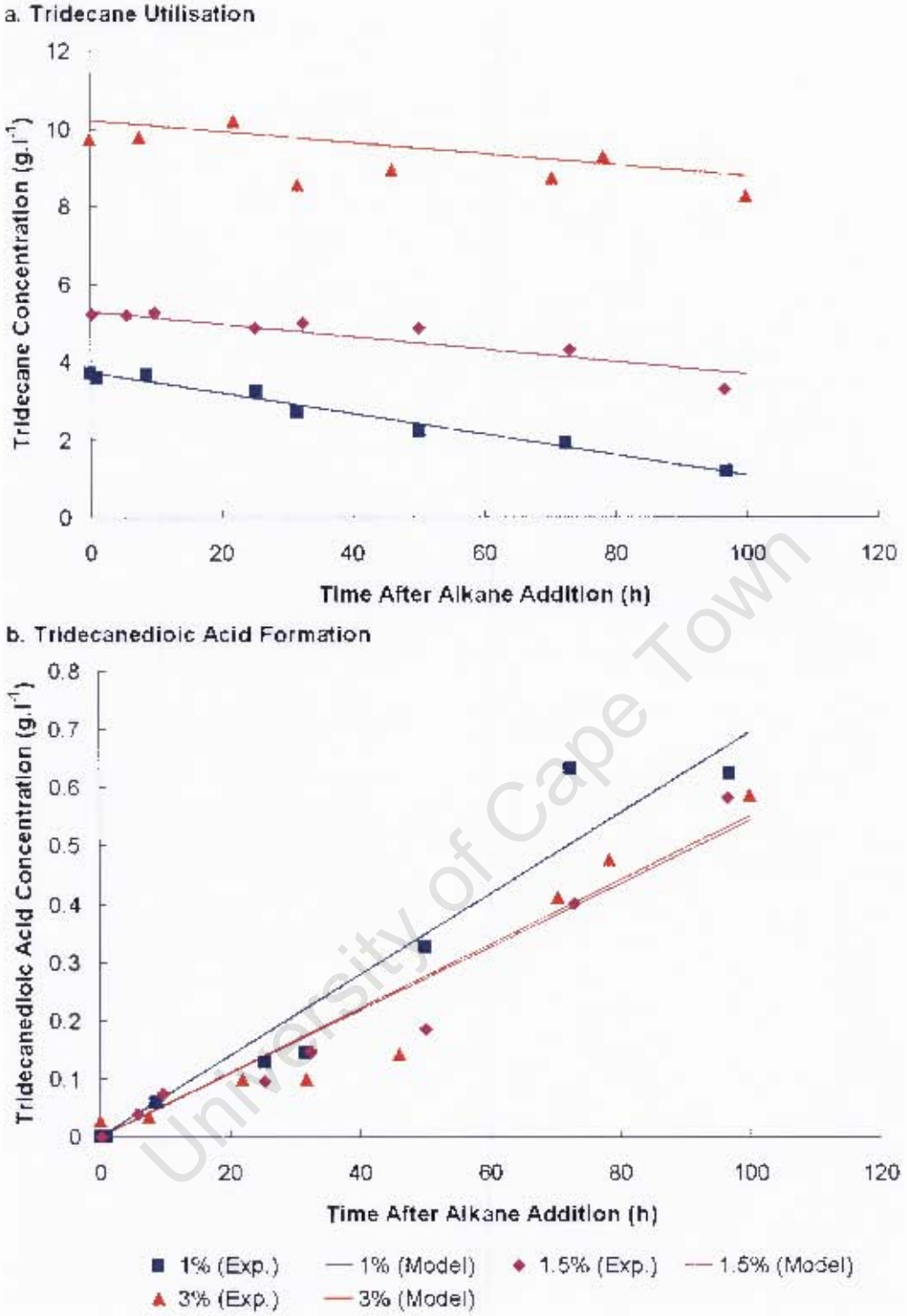

Figure 6.10: (a) Correlation between experimental data and predictive model for (a) tridecane utilisation; (b) tridecanedioic acid formation. The experiments were carried out with strain TVN 497 in the Braun BIOSTAT C bioreactor using the modified Picataggio medium. The initial glucose concentration pH, temperature aeration rate and agitation speed of the medium were set at **40** $g.l^{-1}$, pH 6.0, 30 °C, 0.8 vvm and 700 rpm, respectively. The solid lines represent the predictions of Equations 6.5 6.6, 6.7 and 6.8 using the basic kinetic parameter values in Tables 6.3 and 6.4.

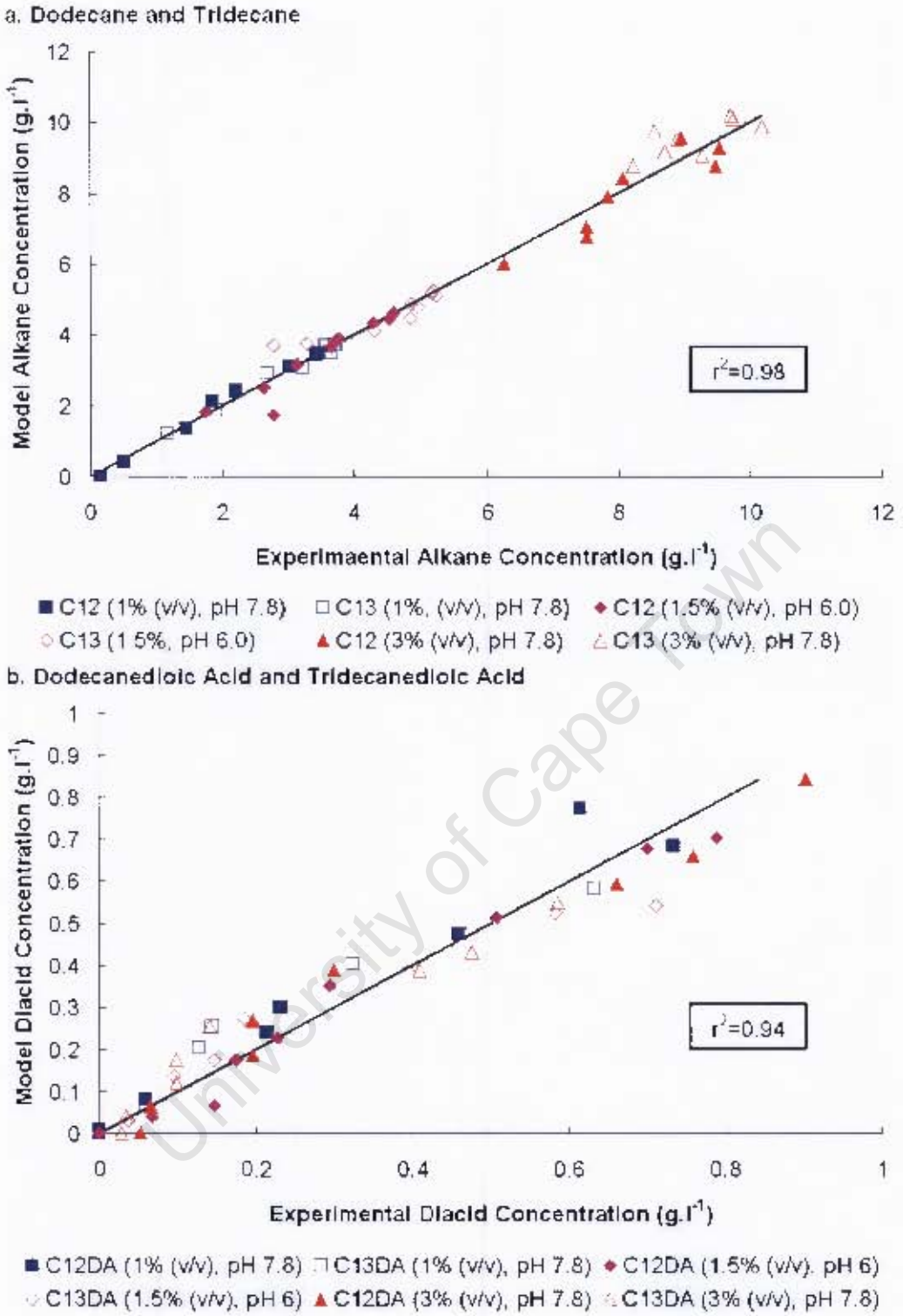

Figure 6.11: Parity plot illustrating goodness of fit between predicted values obtained with basic biotransformation model and experimental data. (a) Predicted and experimental (a) dodecane and tridecane concentrations; (b) dodecanedioic acid and tridecanedioic acid concentrations. The experiments were performed with *Y. lipolytica* TVN 497 under the conditions stipulated in Section 4.1.1. An initial alkane concentration of 1%, 1.5% and 3% (v/v) were added to the culture media 18 h after inoculation. In the case of 1% and 3% (v/v) alkane, the pH of the production phase was set at pH 7.8 whereas for 1.5% (v/v) alkane, the pH of the medium remained at pH 6.

$$-\frac{dC_{sdd}}{dt} = \left(\frac{1}{Y_{dda/dd}}\right) \cdot \beta'_{dda} \cdot \left(\frac{C_{sdd}}{K_{dd} + C_{sdd}}\right) \cdot C_x \quad (6.9)$$

$$\frac{P_{dda}}{dt} = \beta'_{dda} \cdot \left(\frac{C_{sdd}}{K_{dd} + C_{sdd}}\right) \cdot C_x \quad (6.10)$$

$$-\frac{dC_{std}}{dt} = \left(\frac{1}{Y_{tda/dd}}\right) \cdot \beta'_{tda} \cdot \left(\frac{C_{std}}{K_{td} + C_{std}}\right) \cdot C_x \quad (6.11)$$

$$\frac{P_{tda}}{dt} = \beta'_{tda} \cdot \left(\frac{C_{tdd}}{K_{td} + C_{std}}\right) \cdot C_x \quad (6.12)$$

where β'_{dda} and β'_{tda} represent the maximum specific production rate of dodecanedioic acid and tridecanedioic acid (h^{-1}), respectively and K_{dd} and K_{td} the saturation constants of dodecane and tridecane ($g.l^{-1}$), respectively.

The new model was applied to experimental data collected at an initial alkane concentration of 1% (v/v) as the residual alkane was depleted. To obtain initial estimates of K_{dd} and K_{td} the functional relationship between the specific production rate of both α,ω-dicarboxylic acids and the corresponding alkane concentration was used as was done for K_s in Section 5.2. From Figure 6.12 it is estimated that the specific production rate of dodecanedioic acid was half its maximum value at a residual dodecane concentration between 0.5 $g.l^{-1}$ and 1 $g.l^{-1}$ whilst for tridecanedioic acid production, K_{td} ranged between 0.2 $g.l^{-1}$ and 0.4 $g.l^{-1}$. The initial estimates were applied to the modified equations and manually adjusted until the model best fitted the experimental data while corresponding values of β_{dda}, $Y_{dda/dds}$, β_{tda} and $Y_{tda/td}$ (Tables 6.3 and 6.4) were held constant. The estimated values of K_{dd} and K_{td} are shown in Table 6.5.

a. Specific Production Rate of Dodecanedioic Acid

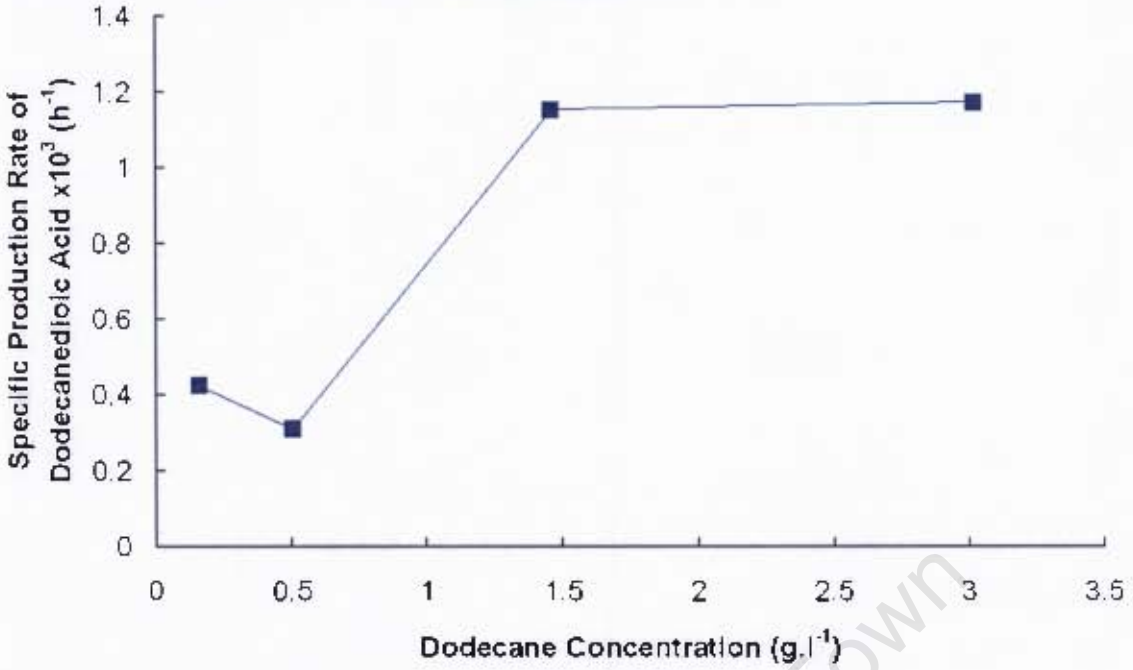

b. Specific Production Rate of Tridecanedioic Acid

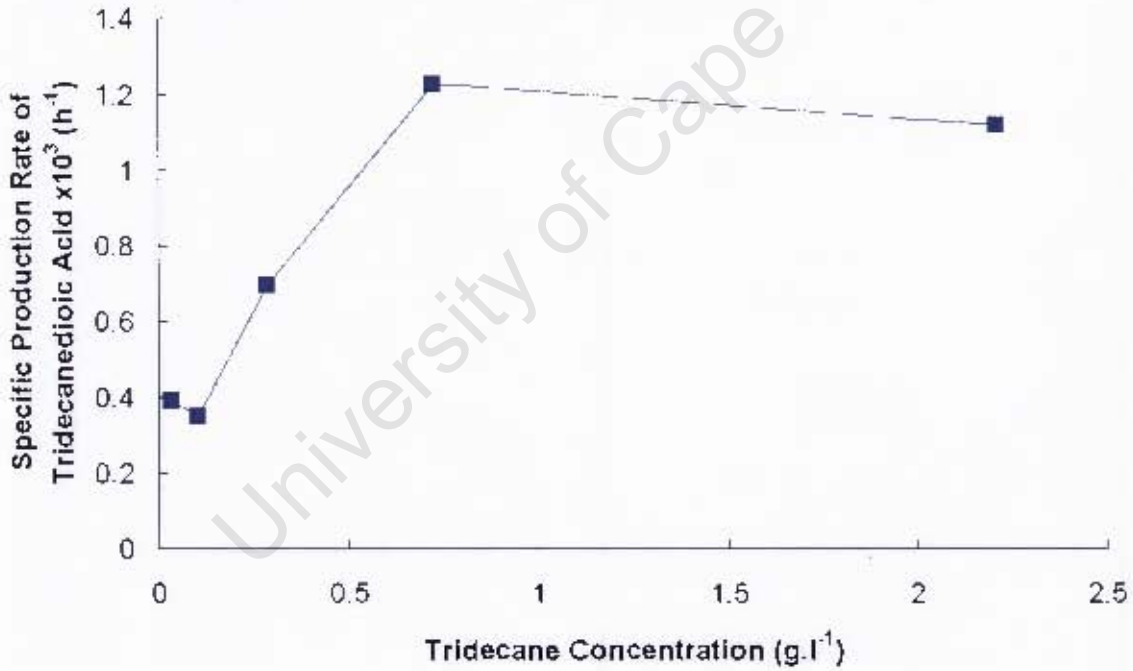

Figure 6.12: Functional relationship between the specific product formation rate of (a) dodecanedioic acid and (b) tridecanedioic acid as a function of the corresponding alkane concentration. The experiment was performed with *Y. lipolytica* TVN 497 under the conditions stipulated in Section 4.1.1. An initial alkane concentration of 1% (v/v) was added to the culture media, 18 h after inoculation. The medium pH of the production phase was set at pH 7.8. Figures a and b were used to estimate the values of saturation constants K_{dc} and K_{td}. The values of K_{dc} and K_{td} represent the alkane concentration at which the specific product formation rate is half its maximum value.

Table 6.5: Estimated values of the saturation constants for dodecane and tridecane, determined at an initial alkane concentration of 1% (v/v)

Initial Kinetic Parameters	
K_{dd} ($g.l^{-1}$)	K_{td} ($g.l^{-1}$)
0.80	0.30

To obtain the kinetic parameters of the modified model the estimates of K_{dd} and K_{td} and the calculated kinetic parameters in Tables 6.3 and 6.4, were applied to the computer based iterative process and solved as before. The resultant kinetic parameters are tabulated in Tables 6.6 and 6.7.

Table 6.6: Product yield coefficients calculated at an initial alkane concentration of 1% (v/v) using the modified model

Initial Alkane Concentration (v/v)	Yield Coefficients			
	$Y_{dda/dd}$		$Y_{tda/td}$	
	($g.g^{-1}$)	($gmol.gmol^{-1}$)	($g.g^{-1}$)	($gmol.gmol^{-1}$)
1%	0.25	0.18	0.35	0.26

Table 6.7: Specific product formation rates and saturation constants calculated at an initial alkane concentration of 1% (v/v) using the modified model

Initial Alkane Concentration (v/v)	Proportionality Constants (h^{-1})		Saturation Constants ($g.l^{-1}$)	
	$\beta_{dda}x10^{-3}$	$\beta_{tda}x10^{-4}$	K_{dd}	K_{td}
1%	1.42	8.95	1.00	0.26

The predictive model, using the kinetic parameters in Tables 6.6 and 6.7, is compared with experimental data in Figure 6.13. This modified model suitably predicted the experimental data with r^2 values ranging between 0.93 and 0.97. The model was unable to predict product formation after alkane depletion, resulting in underprediction. To further improve the model requires that the model account for the intracellular storage of alkanes by *Y. lipolytica* TVN 497.

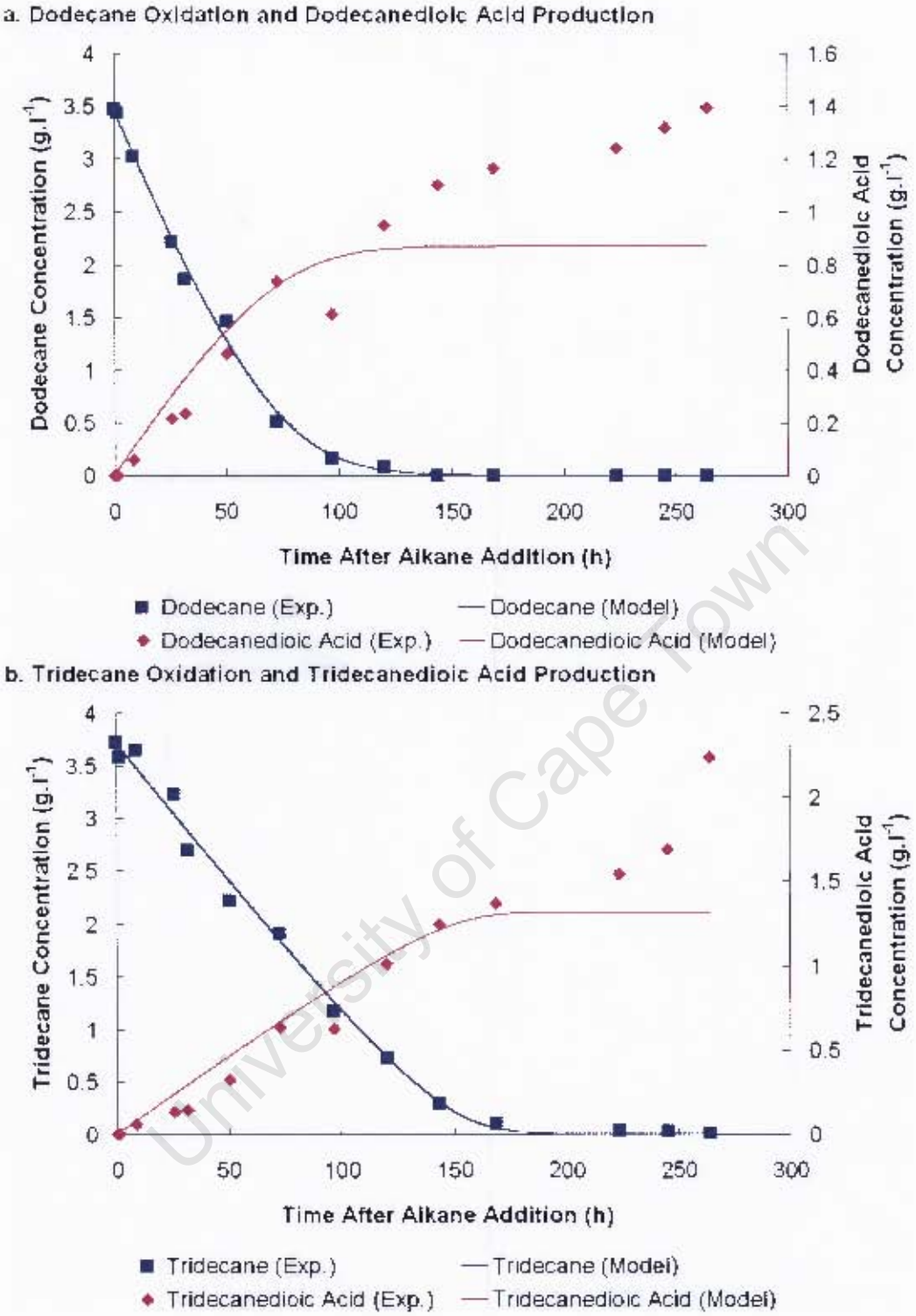

Figure 6.13: (a) Correlation between the experimental data and modified predictive model for alkane oxidation and α,ω-dicarboxylic acid production, at an initial alkane concentration of 1% (v/v). (a) C_{12} compounds; (b) C_{13} compounds. Strain TVN 497 was grown in the Braun BIOSTAT C bioreactor using the modified Picataggio complex medium and an initial glucose concentration, pH, temperature, aeration rate and agitation speed of the medium of 40 $g.l^{-1}$, pH 6.0, 30 °C, 0.8 vvm and 700 rpm, respectively. The solid lines represent the predictions of Equations 6.9, 6.10, 6.11 and 6.12 using the basic kinetic parameter values in Tables 6.6 and 6.7.

6.3 The Effect of Glucose on α,ω-Dicarboxylic Acids Production

It is reported that glucose catabolically represses the induction of cytochrome P450 in *C. tropicalis and C. guilliermondii*, both in the presence and absence of alkane (Mauersberger *et al.* 1980; Gallo *et al.* 1973; Sanglard *et al.* 1984; Gilewicz *et al.*, 1978). Since cytochrome P450 catalyses the first rate limiting step of α,ω-dicarboxylic acid production (conversion of alkane into alcohol), alkanes are typically added to the culture media on glucose depletion (Green *et al.* 2000; Picataggio *et al.* 1992). To investigate the effect of glucose on alkane conversion in *Yarrowia*, Experiments I and II were conducted during which alkane was added 18 h and 48 h after inoculation.

The experiments used modified Picataggio medium with *Y. lipolytica* TVN 497 in the Braun BIOSTAT C bioreactor. The cultures were aerobically grown at an initial glucose concentration of 40 $g.l^{-1}$, pH 6, 30 °C and an aeration rate and agitation speed of 0.8 vvm and 700 rpm, respectively. In each case 0.3 l alkane was added to the culture medium. The pH of the alkane conversion phase was pH 7.8. The α,ω-dicarboxylic acids and residual glucose concentrations are shown as a function of time in Figure 6.14.

On addition of alkane 18 h after inoculation, product formation was initiated at a residual glucose concentration of 38 $g.l^{-1}$. Hence the cytochrome P450s present in *Y. lipolytica* TVN 497 were active in the presence of glucose. Product formation occurred concomitantly with biomass formation, implying that *Y. lipolytica* TVN 497 can produce α,ω-dicarboxylic acids in batch, fed-batch and continuous processes. Since α,ω-dicarboxylic acids are low-value, high-volume products its continuous production may be advantageous. When alkane was added to the culture medium 48 h after inoculation, a higher initial production rate was observed. After reaching a α,ω-dicarboxylic acid concentration of 0.96 $g.l^{-1}$, the acid concentration in Experiments I and II increased at an equal rate until final combined acid concentrations of 1.71 $g.l^{-1}$ and 1.74 $g.l^{-1}$ were obtained approximately 130 h after inoculation, respectively.

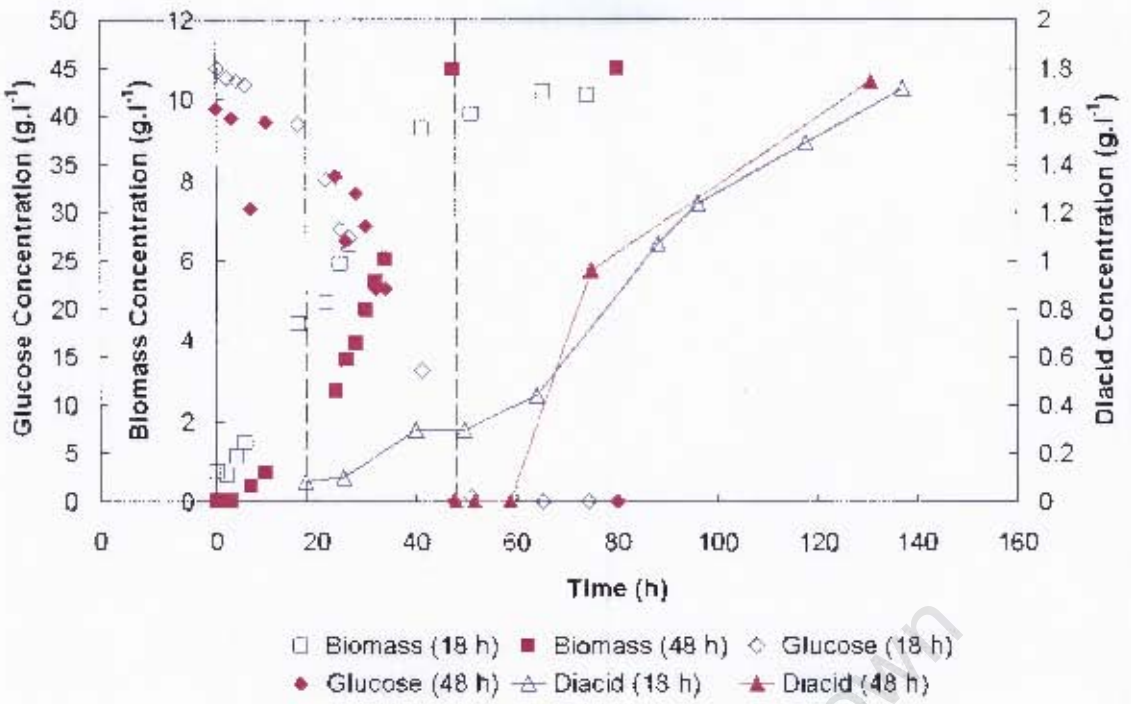

Figure 6.14: The effect of glucose on α,ω-dicarboxylic acids production. Strain TVN 497 was cultivated aerobically on modified Picataggio medium at pH 6.0 in the Braun BIOSTAT C bioreactor. An alkane volume of 0.3 l was added to the culture medium, 18 h and 48 h after inoculation. In each case the pH of the production phase was pH 7.8. The dotted lines represent time of alkane addition (18 h and 48 h).

6.4 Conclusions

In this chapter, the ability of *Y. lipolytica* TVN 497 to activate linear alkanes through the production of α,ω-dicarboxylic acids was evaluated in terms of the type of medium used, alkane concentration and the medium pH of the biotransformation phase. The α,ω-Dicarboxylic acid production was significantly affected by the type of medium used. The complex medium was more suited for product formation. The final α,ω-dicarboxylic acid concentration obtained with the modified Picataggio medium was approximately 10 times greater than the concentration obtained with the Antonucci medium during the same biotransformation period. It was hypothesised that the presence of NH_4NO_3 in the Antonucci medium negatively affected α,ω-dicarboxylic acid production (Shiio and Uchio, 1971).

Dodecanedioic acid production was unaffected by alkane concentration across the range 1 to 3% by volume. The production rate of and the final

tridecanedioic acid concentration however, appeared to decrease with increasing alkane concentration across this range. This is an unexpected finding since the toxicity of linear alkanes is typically reported to decrease with an increase in carbon number owing to decreasing solubility. The cause of this reduced productivity has not been established yet. The medium pH of the production phase played a significant role during biotransformation. Under conditions where the medium pH of the production phase was elevated to pH 7.8, the formation of α,ω-dicarboxylic acid continued until the experiment was terminated. In contrast, when the medium pH of the production phase was maintained at pH 6.0, the production of α,ω-dicarboxylic acids ceased at a final concentration of 1.58 $g.l^{-1}$.

A simplified unstructured kinetic model based on the Luedeking-Piret kinetics adequately predicted α,ω-dicarboxylic acid production and alkane utilisation prior to alkane depletion. Correlation coefficients ranging between 0.94 and 0.98 were calculated for three experiments conducted at initial alkane concentrations of 1%, 1.5% and 3% (v/v). A shortcoming of the model was its inability to predict substrate utilisation and product formation at low substrate concentrations. The extended version of the Luedeking-Piret model, which takes cognisance of substrate inhibition, increased the predictive power of the model. However, the refined model did not predict product formation after alkane depletion, assumed to result from the conversion of intracellular alkane.

The presence of residual glucose in the biotransformation phase did not prevent α,ω-dicarboxylic acid production. Product formation was initiated on alkane addition when the residual glucose concentration was 38 $g.l^{-1}$. This finding for *Y. lipolytica* TVN 497 contradicts the general notion that cytochrome P450s are catabolically repressed by the presence of glucose in the culture medium (Green *et al.* 2000). This characteristic of *Y. lipolytica* TVN 497 enables α,ω-dicarboxylic acid production in continuous culture.

Chapter 7

Results and Discussion III

A Comparison of Four Different Recombinant *Yarrowia lipolytica* Strains

During the final phase of the research, four different recombinant *Y. lipolytica* strains i.e. TVN 497, TVN 499, TVN 501 and TVN 502 were evaluated in terms of their biomass and α,ω-dicarboxylic acid productivity. Their ability to produce α,ω-dicarboxylic acids was also compared to existing literature. These strains may perform differently because the cloning vectors used introduce random mutations into the genome of the parent strain on insertion of the genes encoding the cytochrome P450 monooxygenase (P450ALK) and the accompanying NADPH cytochrome P450 reductase (CPR), at random sites on the genome. The vectors used also allowed the introduction of multiple copies of these genes into the genome (van Rooyen, 2005).

7.1 Evaluating Biomass and α,ω-Dicarboxylic Acid Productivity

The ability of the strains to produce biomass and α,ω-dicarboxylic acids was evaluated in shake flasks. Each experiment was performed in duplicate, using a 500 ml Erlenmeyer flask containing 50 ml of the UFS medium buffered to pH 7.8. A 5 ml inoculum (Section 3.5.4) was used. After inoculation, the strains were cultivated at 29 °C on a rotary shaker at 180 rpm. After 48 h, an alkane cut (3% (v/v)), comprised of equal volumes of dodecane and tridecane, was added to each culture. Growth and biotransformation conditions were identical. Biomass, glucose, alkane and α,ω-dicarboxylic acid concentrations were measured at regular intervals. Due to the small bioreactor-volume, turbidity measurements were used to determine the biomass density.

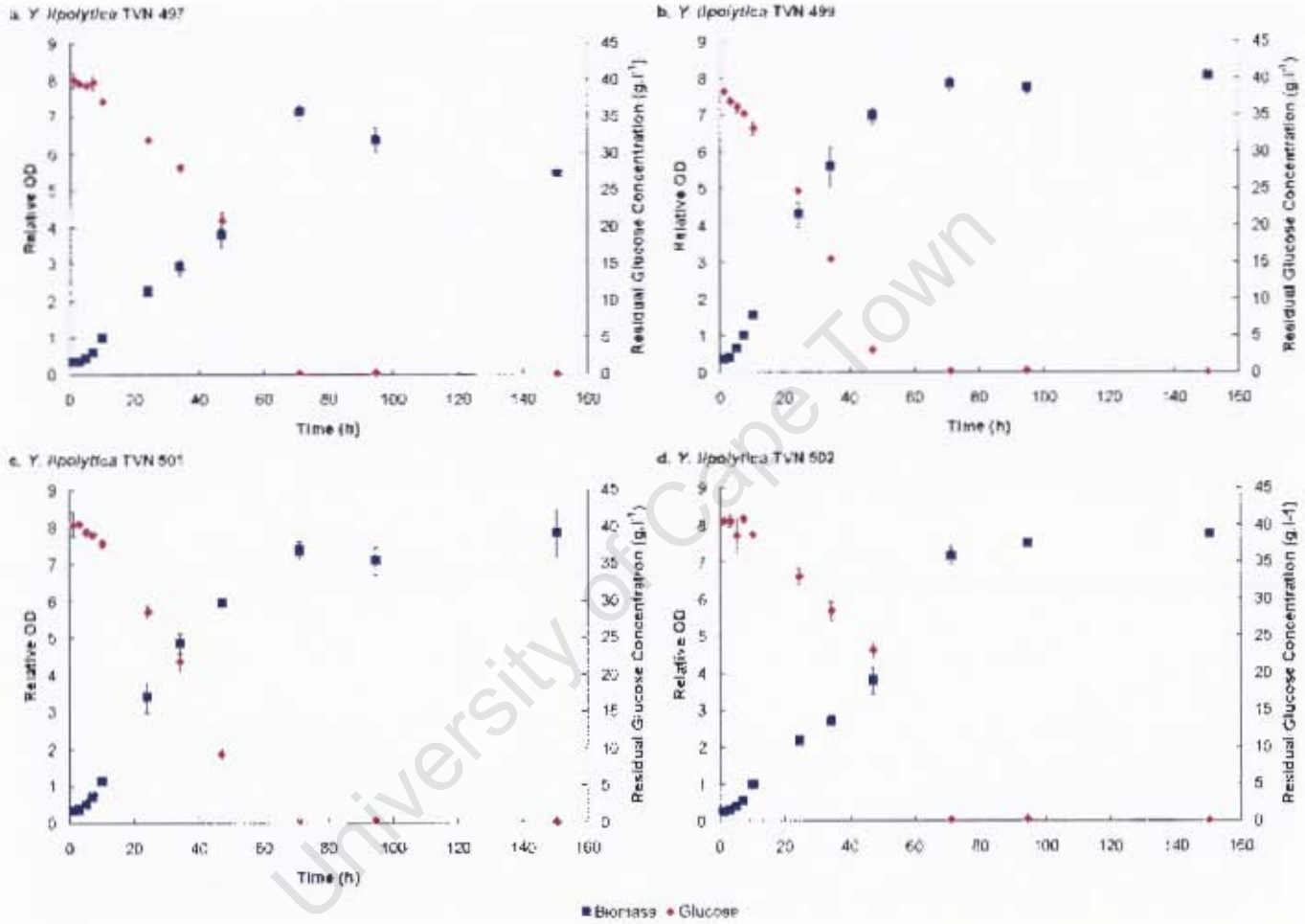

Figure 7.1: Biomass production and associated glucose utilisation of recombinant *Y. lipolytica* strains TVN 497 (a), TVN 499 (b), TVN 501 (c) and TVN 502 (d). The strains were cultivated on a rotary shaker at 180 rpm in shake flasks using the UFS media buffered to pH 7.8 at 29 °C. (The error bars represent the standard deviation of repeated experiments to confirm reproducibility).

Optical density and residual glucose concentration are shown as a function of time in Figure 7.1 for strains TVN 497, TVN 499, TVN 501 and TVN 502. Each experiment commenced at an initial optical biomass density of approximately 0.32 ± 0.04. After inoculation, strains TVN 497, TVN 499, TVN 501 and TVN 502 grew exponentially for approximately 7 h at initial rates of 0.16 ± 0.005 h^{-1}, 0.20 ± 0.004 h^{-1}, 0.17 ± 0.002 h^{-1} and 0.17 ± 0.009 h^{-1}, respectively. Thereafter the specific growth rates of strains TVN 497 and TVN 502 declined at constant rates of 0.024 ± 0.00028 h^{-1} and 0.026 ± 0.00059 h^{-1}, respectively. It is therefore apparent that more than one substrate acted as rate limiting substrate. In contrast, the specific growth rates of strains TVN 499 and TVN 501, continued to decline towards zero at an apparent constant rate of decline, in tandem with the depletion in the glucose concentration.

Glucose utilisation in all cases followed an inverse relationship to biomass production. When the residual glucose was depleted, approximately 71 h after inoculation, strains TVN 497, TVN 499, TVN 501 and TVN 502 reached final optical densities of 7.11 ± 0.21, 8.04 ± 0.02, 7.88 ± 0.52 and 7.74 ± 0.11, respectively. It is therefore apparent that in all cases glucose acted as the growth limiting substrate. It is further concluded that at a confidence level of 95%, strain TVN 497 produced less biomass than strains TVN 499, TVN 501 and TVN 502. The statistical analysis is shown in Appendix J4.

The residual dodecane, tridecane, dodecanedioic acid and tridecanedioic acid concentrations of the experiments conducted with strains TVN 497, TVN 499, TVN 501 and TVN 502 are given as a function of time in Figure 7.2. Except for the experiment conducted with *Y. lipolytica* TVN 497, α,ω-dicarboxylic acid production was delayed for at least an hour. Hereafter, the concentrations of both acids increased simultaneously with dodecanedioic acid at an apparent higher production rate, provided that its concentration in most cases was higher than that of tridecanedioic acid. After a biotransformation period of 104 h strains TVN 497, TVN 499, TVN 501 and TVN 502 reached final combined acid concentrations of 1.31 ± 0.15 $g.l^{-1}$, 2.58 ± 0.13 $g.l^{-1}$,

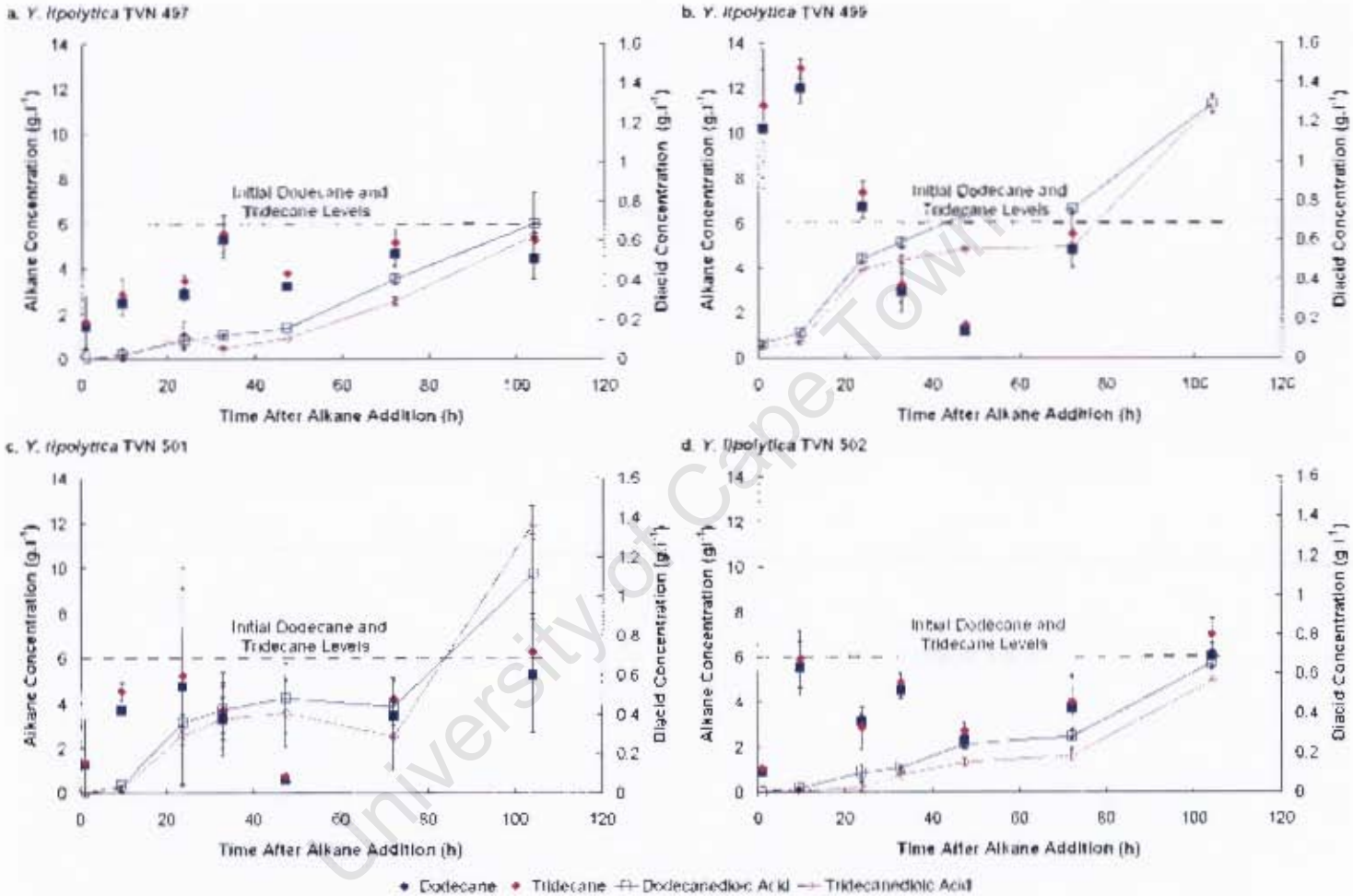

Figure 7.2: Alkane utilisation and α,ω-dicarboxylic acid production by recombinant *Y. lipolytica* strains TVN 497 (a), TVN 499 (b), TVN 501 (c) and TVN 502 (d). The strains were cultivated on a rotary shaker at 180 rpm in shake flasks using the UFS media buffered to pH 7.8 at 29 °C. Alkanes were added to each culture media, 48hrs after inoculation. (The error bars represent the standard deviation of repeated experiments to confirm reproducibility)

2.49 ± 0.29 $g.l^{-1}$ and 1.21 ± 0.01 $g.l^{-1}$, respectively. At a confidence level of 95%, strains TVN 499 and TVN 501 produced a higher combined α,ω-dicarboxylic acid concentration than strains TVN 497 and TVN 502. The statistical analysis is shown in Appendix J5.

The alkane concentration varied erratically and followed no expected trend. In some instances the alkane concentration exceeded the maximum level of alkane added. The inaccuracy may have resulted from non representative sampling of dispersed alkane droplets. It is also suggested that since hydrocarbon utilising strains excrete biological surfactants, pseudo-soluble alkanes were also analysed. Many authors have reported such phenomena (Suzuki *et al.* 1969, Rapp and Wagner, 1976; Itoh *et al.* 1971).

7.2 A Comparison between *Y. lipolytica* and *C. tropicalis*

Although the results confirmed product formation, the α,ω-dicarboxylic acid concentrations obtained during this research are roughly 150 times lower than the acid yields obtained by Liu *et al.* (2004), Jiao *et al.* (2001) and Picataggio *et al.* (1992) with recombinant strains of *Candida tropicalis* under similar conditions (Table 7.1). This disparity between the ability of *Y. lipolytica* and *C. tropicalis* to produce α,ω-dicarboxylic acids may be attributed to a number of factors. According to Scheller *et al.* (1998), the activity of the cytochrome P450s, cloned from *C. maltosa*, is inhibited by hexadecanedioic acid which competes with hexadecane for the same active site. Since it appears as if *Y. lipolytica* is only able to produce only small quantities of α,ω-dicarboxylic acid in comparison to *C. tropicalis*, it is possible that the CYP450s in *Y. lipolytica* are inhibited at lower α,ω-dicarboxylic acid concentrations.

A second factor which may have contributed to this disparity is the absence of fatty-alcohol oxidase genes in *Y. lipolytica* (Fickers *et al.* 2005). These genes express the enzyme responsible for catalysing the oxidation of alcohols in both the monoterminal and diterminal pathways in *C. tropicalis* (Cheng *et al.* 2005). In *C. tropicalis* alcohols are ultimately produced from alkanes via a

reaction which is catalysed by a cytochrome P450 monooxygenase and the accompanying NADPH cytochrome P450 reductase. A terminal carboxylic function is ultimately formed from two additional steps, catalysed by a fatty alcohol oxidase and a $NAD(P)^+$- dependent fatty-aldehyde dehydrogenase. Fatty acids produced via this pathway can be oxidised via the same pathway to the corresponding α,ω-dicarboxylic acids (Craft *et al.* 2003).

Table 7.1: Comparison of *Yarrowia lipolytica* with *Candida tropicalis* in term of its ability to produce α,ω-dicarboxylic acids.

Author	Strain	Type of Substrate	Final Concentration $g.l^{-1}$	Productivity $g.l^{-1}.h^{-1}$
Picataggio *et al.* 1992	*C. tropicalis* H5343	C_{13}	120	1.30
Jiao *et al.* 2001	*C. tropicalis* CT1-12	C_{13}	154	1.18
Liu *et al.* 2004	*C. tropicalis* CGMCC 356	C_{12},C_{13} & C_{14}	166, 153 & 138	1.38, 1.28 & 1.15
Smit *et al.* (2005)	*Y. lipolytica* MTLY 37	C_{12} & C_{14}	8 & 0.7	0.05 & 0.005
Current Research	*Y. lipolytica* TVN 499	C_{12} & C_{13}	1.4 & 2.3	0.005 & 0.008

It has been shown that CYP450s belonging to the CYP52 family can ultimately convert a methyl carbon to a carboxylic acid (Scheller et al., 1998). The formation of the acid in this case is dependent on NADPH and is assumed to proceed *via* two further hydroxylations (each consuming NADPH) of the hydroxyl bearing carbon to form an *ortho*-acid intermediate that is subsequently dehydrated. Since *Y. lipolytica* apparently has no fatty alcohol oxidase gene, it appears as if the cytochrome P450 hydroxylase complex is responsible for the complete oxidation of alkanes to α,ω-dicarboxylic acids. It is therefore proposed that the α,ω-dicarboxylic acids productivity of *Y. lipolytica* is lower than that of *C. tropicalis*, since the complete oxidation by the cytochrome P450 hydroxylase complex requires more energy in the form of NADPH.

Regardless of the above shortcomings, *Y. lipolytica* is still considered a potential biocatalyst for α,ω-dicarboxylic acid production. *Y. lipolytica* is regarded as one of the most extensively studied "non-conventional" yeast strains, with a completely sequenced genome; hence new metabolic engineering techniques can be applied to improve the productivity of the strain. A novel technique, yet to be performed on *Y. lipolytica*, is to disrupt the gene encoding the acetyl-CoA transport system thereby preventing α,ω-dicarboxylic acids form entering the mitochondrion (Cao *et al.* 2006). This technique may improve the α,ω-dicarboxylic acid productivity of *Y. lipolytica* to reach benchmark production levels since additional energy is obtained through an intact β-oxidation pathway.

7.3 Conclusions

In this chapter the ability of recombinant *Y. lipolytica* strains TVN 499, TVN 501, TVN 497 and TVN 502 to produce biomass and α,ω-dicarboxylic acid was evaluated and compared with *C. tropicalis*. The ability to produce biomass for all strains was similar. Strains TVN 499 and TVN 501 were however, superior to strains TVN 497 and TVN 501 in their ability to produce α,ω-dicarboxylic acid. When comparing strains TVN 499 and TVN 501 with *C. tropicalis*, it was found that their α,ω-dicarboxylic acid productivity was approximately 150 fold lower than that of *C. tropicalis* under the conditions of this study. It was postulated that that the CYP450s in *Y. lipolytica* are inhibited at lower α,ω-dicarboxylic acid concentrations than *C. tropicalis* or that complete oxidation of alkane occurs in these *Y. lipolytica* strains owing to incomplete blocking of β-oxidation or both requires more energy than *C. tropicalis* in the form of NADPH.

Chapter 8

Conclusions and Recommendations

Current literature focuses mainly on the use of *Candida* sp. as a suitable biocatalyst for α,ω-dicarboxylic acid production. As a result little information is available regarding α,ω-dicarboxylic acid production using *Y. lipolytica* as biocatalyst. *Y lipolytica* strains TVN 497, TVN 499, TVN 501 and TVN 502 have been constructed through metabolic engineering to transform linear alkanes selectively into α,ω-dicarboxylic acids. In order to characterise the above metabolically engineered strains of *Y. lipolytica* in terms of growth and biotransformation and to refine operating conditions, limitations of the studies reported to date have been identified. These led to the development of the objectives of this study and the research questions presented in Section 2.6. In this chapter, the conclusions that can be drawn from the study conducted are presented. Thereafter, the proposed direction recommended for further study is proposed.

8.1 Conclusions

Comparison of Performance of Recombinant *Y. lipolytica* Strains

The four recombinant *Y. lipolytica* strains TVN 497, TVN 499, TVN 501 and TVN 502 developed by the collaborating research group at the University of the Free State all prove to be able to produce α,ω-dicarboxylic acid. Strains TVN 499 and TVN 501 were superior to strains TVN 499 and TVN 501 in their ability to produce α,ω-dicarboxylic acid. When comparing dicarboxylic acid production using strains TVN 499 and TVN 501 with that achieved by *C. tropicalis* however, it was found that their α,ω-dicarboxylic acid productivity was approximately 150 times lower than that of *C. tropicalis*. It was postulated that the CYP450s in *Y. lipolytica* are inhibited at lower α,ω-dicarboxylic acid concentrations than *C. tropicalis* or that complete oxidation of alkane by *Y. lipolytica* requires more energy than *C. tropicalis* in the form of NADPH or both. This low productivity makes the current recombinant strains of *Yarrowia*

lipolytica inadequate for industrial applications and indicates that further genetic modification and media and process optimisation will be required prior to *Yarrowia lipolytica* being identified as a potential vehicle for the commercial production of dicarboxylic acids or activation of linear alkanes.

Growth and Product Formation Kinetics for *Y. lipolytica* and the Kinetic Model

Currently, little literature exists which describe the quantitative relationship between the environmental parameters and the kinetics of *Y. lipolytica* growth and alkane oxidation, under glucose and alkane limiting conditions. Since such a model for *Y. lipolytica* TVN 497 may serve as a mathematical tool to isolate important parameters and to reduce the number of experiments required to design and optimise the process conditions, an unstructured basic kinetic model, based on the Monod and Luedeking-Piret relationships, was developed for growth and biotransformation, respectively.

The simplified kinetic growth model, based on the Monod equation adequately predicted biomass production and glucose utilisation in the semi-defined medium. The model at times however, under or over predicted both biomass production and glucose utilisation in the complex medium. The saturation constant (K_s) calculated for the complex medium was also significantly higher than the values proposed by literature. It is expected that the poor estimation of K_S in complex media may have contributed to the model's reduced prediction accuracy. This reduced accuracy was further accentuated by the observation that whilst glucose acted as the limiting substrate, it may not necessarily have acted as the rate-limiting substrate.

The simplified kinetic model for product formation, based on the Luedeking-Piret kinetics, adequately predicted α,ω-dicarboxylic acid production and alkane utilisation up to the point of alkane depletion. This was confirmed by an r^2 values ranging between 0.94 and 0.98 calculated for three experiments conducted at initial alkane concentrations of 1%, 1.5% and 3% (v/v). A shortcoming of the model was its inability to predict substrate utilisation and product formation at low substrate concentrations. The extended Luedeking-

Piret model, which takes cognisance of substrate limitation, increased the predictive power of the model. A shortcoming of the model was its inability to predict product formation after depletion of the extracellular alkane.

The modified and extended model developed during this research together with important factors which affect growth and biotransformation establishes a foundation of understanding that can assist in process development and process optimisation. The model provides a basis for future refinement into a more complex kinetic model able to verify the economic viability of *Y. lipolytica* TVN 497 in a hydrocarbon-based process.

Effect of Glucose Concentration on Alkane Oxidation

According to Picataggio *et al.* (1992) and Jiao *et al.* (2001) alkane should be added to the culture medium once microbial growth has reached the stationary phase. As such, the time of alkane addition has become a condition specified in the experimental protocol. Green *et al.* (2000) rationalised this by proposing that glucose suppresses the oxidation of lauric acid, a mono-oxidised derivative of dodecane, into dicarboxylic acid. To evaluate this phenomenon on *Y. lipolytica* TVN 497, alkane was added to the culture media in the early exponential phase when the initial glucose concentration was 38 $g.l^{-1}$. The experimental results concluded that the presence of residual glucose in the biotransformation phase does not prevent α,ω-dicarboxylic acid production. This finding for *Y. lipolytica* TVN 497 contradicts the general notion that cytochrome P450s are catabolically repressed by the presence of glucose in the culture medium.

Effect of Glucose Concentration on Specific Growth Rate

To evaluate the effect of substrate inhibition on *Y. lipolytica* TVN 497, shake flask experiments were conducted at different initial glucose concentrations ranging between 10 and 60 $g.l^{-1}$. The results of these experiments indicated that the specific growth rate of *Y. lipolytica* TVN 497 was negatively affected by glucose concentrations exceeding 20 $g.l^{-1}$. This conclusion was drawn from the observation that after reaching a maximum specific growth rate of 0.34 h^{-1}, at 20 $g.l^{-1}$ glucose, the specific growth rate decreased with a further increase

in glucose concentration. Moresi (1994) obtained similar results with a wild-type *Yarrowia lipolytica* strain on a semi-defined medium when evaluating citric acid production at different glucose concentrations. In this study the strain reached a maximum specific growth rate of 0.36 h^{-1} at a significantly higher initial glucose concentration (61.7 $g.l^{-1}$) when compared to *Y. lipolytica* TVN 497. Hereafter the specific growth rate decreased with a further increase in initial glucose concentration. Although this is a clear indication of substrate inhibition it was not identified as such by the author

Effect of Alkane Concentration and medium pH on the Specific Production Rate of α,ω -Dicarboxylic Acids

To evaluate the effect of alkane concentration, two experiments were conducted during which 0.1 l and 0.3 l alkane, comprising equal volumes dodecane and tridecane, were added to the culture media, 18 h after inoculation. The pH of the production phase in both experiments was increased to pH 7.8 at the time of alkane addition. The production rate of dodecanedioic acid was unaffected by alkane concentration whereas the production rate and final tridecanedioic acid concentration appeared to have decreased with an increase in alkane concentration. This was an unexpected finding since the toxicity of linear alkanes is typically reported to decrease with an increase in carbon number owing to decreasing solubility. The cause of this reduced productivity has not yet been established.

The effect of medium pH was evaluated by conducting a third experiment during which the pH of the production phase was maintained at pH 6.0. The production rate of the combined acids was similar to the production rates obtained with the experiments where the pH of the production phase was set at pH 7.8. However, after reaching an α,ω-dicarboxylic acid concentration of 1.58 $g.l^{-1}$, approximately 100 h after alkane addition, product formation suddenly ceased, suggesting product inhibition. This phenomenon was previously reported by Chan *et al.* (1997) when *Pseudomonas aeruginosa* was unable to produce more than 0.85 $g.l^{-1}$ hexadecanedioic acid in a batch bioreactor. It is therefore suggested that an elevated medium pH is required to facilitate product formation at high α,ω-dicarboxylic acid concentrations.

8.2 Recommendations

Based on the findings of this research, the following recommendations are made:

- In order to improve the estimate of the saturation constant for biomass production, K_s, it is recommended that kinetic data be collected chemostat culture.
- Further to account for dependence on the second rate limiting substrate, it is necessary to first predict the intracellular ammonium ion concentration. To validate the model with respect to dependence on glucose, addition of excess ammonium nitrate is recommended such that glucose is the only rate limiting substrate.
- To predict product formation after depletion of extracellular alkane, it is recommended that the extended model be further extended to incorporate the phenomenon of intracellular storage of alkane or α,ω-dicarboxylic acid or both by the strain. This requires extension of the model towards a structured approach.
- In view of the fact that growing cells of *Y. lipolytica* TVN 497 are able to produce α,ω-dicarboxylic acid, it is recommended that both the continuous and fed-batch configurations be considered for α,ω-dicarboxylic acid production.
- To enhance the predictive ability of the model, it should be extended to include the effect of cell maintenance and cell death.
- *Y. lipolytica* is one of the most extensive studied "non-conventional" yeasts with a completely sequenced genome, hence it is recommended that further studies should be conducted to provide understanding of the limitations of the current genetic modifications expressed in strains TVN497, 499, 501 and 502. Further, new metabolic engineering approaches should be used to increase the productivity of *Y. lipolytica* for use as a biocatalyst for the production of α,ω-dicarboxylic acids.

References

1. Akabori, SA, Shiio, I and Uchio, R (1974). "Method of Producing Long-Chain Alpha-Hydroxyalkanoic Acids", US Patent No. 3 843 466.
2. Allsop, PJ, Chisti, Y, Young, MM and Sullivan, GR (1993). "Dynamics of Phenol Degradation by *Pseudomonas putida*", *Biochemistry and Biotechnology*, **41**, 572-580.
3. Anastassiadis, S and Aivasidis, WC (2002). "Citric Acid Production by *Candida* Strains Under Intracellular Nitrogen Limitation", *Applied Biochemistry and Biotechnology*, **60**, 81-87.
4. Andrade, J, Koehler, K and Prescher, G (1988). "Process for the Production of 1,12-Dodecanoic Diacid", US Patent No. 4 733 007.
5. Andrews, JF (1968). "A Mathematical Model for the Continuous Culture of Microorganisms Utilizing Inhibitory Substrates", *Biotechnology and Bioengineering*, **5** (6), 707-723.
6. Antonucci, S, Bravi, M, Bubbico, R, Michele, AD and Verdone, N (2001). "Selectivity in Citric Acid Production by *Yarrowia lipolytica*", *Enzyme and Microbial Technology*, **28**, 189-195.
7. Atkinson, B and Mavituna, F (1991). "Biochemical Engineering and Biotechnology Handbook", Sockton Press, New York.
8. Atomi, H, Yu, C and Hara, A (1994). "Characterization of Dicarboxylic Acid-Producing Mutants of the Yeast *Candida tropicalis*", *Journal of Fermentation and Bioengineering*, **77**, 205-207.
9. Aurich, A, Förster, A, Mauersberger, S, Barth, G and Stootmeister, U (2002). "Citric Acid Production from Renewable Resources by *Yarrowia lipolytica*", Third *Yarrowia lipolytica* International Meeting, Dresden.
10. Ayala, M and Torres, E (2004). "Enzymatic Activation of Alkanes: Constraints and Prospective", *Applied Catalysis A: General*, **272**, 1-13.
11. Bailey, JE and Ollis, DF (1986). "Biochemical Engineering Fundamentals", 2nd ed., McGraw-Hill, New York.
12. Baranyi, J and Pin, C (1999). "Estimating Bacterial Growth Parameters by Means of Detection Times", *Applied and Environmental Microbiology*", **65** (2), 732-736.

13. Bati, N, Hammond, EG and Glatz, BA (1984). "Biomodification of Fats and Oils: Trials with *Candida lipolytica*", *Journal of the American Oil Chemists' Society*, **61**, 1743-1746.
14. Bell, GH (1973). "Solubilities of Normal Aliphatic Acids, Alcohols and Alkanes in Water", *Chemistry and Physics of Lipids*, **10**, 1–10.
15. Birol, G, Űndey, C and Çinar, A (2002). "A modular Simulation Package for Fed-Batch Fermentation: Penicillin Production", *Computer and Chemical Engineering*, **26**, 1553-1565.
16. Blanch, HW and Clark, DS (1997). "Biochemical Engineering", John Wiley and Sons Inc., New York.
17. Blanch, HW and Einsele, A (1973). "The Kinetics of Yeast Growth on Pure Hydrocarbons", *Biotechnology and Bioengineering*, **15** (5), 861-877.
18. Borchert, H, Dingerdissen, R and Roesky, R (2001). "Process and Catalyst for Preparing Acetic Acid by Catalytic Oxidation of Ethane", US Patent No. 6 274 765.
19. Boswell, C (1999). "The Technology Frontier", In: *Chemical Market Reporter of Alkane Activation*, New York, (Dic. 20).
20. Briffaud, J and Engasser, J (1979). "Citric Acid Production from Glucose. I. Growth and Excretion Kinetics in a Stirred Fermentor", *Biotechnology and Bioengineering*, **21**, 2083-2092.
21. Broadway, NM, Dickinson, M and Ratledge, C (1993). "Long-Chain Acyl-CoA Ester Intermediates of β-Oxidation of Mono- and Di-Carboxylic Fatty Acids by Extracts of *Corynebacterium* sp Strain 7E1C", *Biochemical Journal*, **285**, 117-122.
22. Bull, AT and Bushell, ME (1976). "Environmental Control of Fungal Growth", In: Smith, JE and Berry, DR (eds.), *The Filamentous Fungi*, 2nd, John Wiley and Sons, New York.
23. Cameotra, SS and Singh, HD (1990). "Uptake of Volatile *n*-Alkanes by *Pseudomonas* PG-1", *Journal of Bioscience*, **15**, 313.322.
24. Cameotra, SS, Singh, HD, Hazarika, AK and Baruah, JN (1983). "Mode of uptake of insoluble solid substrates by microorganisms II: Uptake of Solid n-Alkanes by Yeast and Bacterial Species", *Biotechnology and Bioengineering*, **25**, 2945–2956.

25. Cao, Z, Gao, H, Liu, M and Jiao, P (2006) "Engineering the Acetyl-CoA Transportation System of *Candida tropicalis* the Production of Dicarboxylic Acid", *Biotechnology Journal*, **1**, 68-74.

26. Casey, GP and Ingledew, WM (1986). "Ethanol Tolerance in Yeast", *Critical Reviews in Microbiology*, **13**, 219-280.

27. Caswell, P (2006). "Market Prices of α,ω-Dicarboxylic Acids", *Personal conversation with Sales Manager*, Cathay Biotech Limited.

28. Chan, E-C and Kuo, J (1997). "Biotransformation of Dicarboxylic Acid by Immobilized *Cryptococcus* Cells", *Enzyme and Microbial Technology*, **20** (8), 585-589.

29. Chan, EC, Kuo, J, Lin, HP and Mou, DG (1991). "Stimulation of n-Alkane Conversion to Dicarboxylic Acid by Organic-Solvent- and Detergent-Treated Microbes", *Applied Microbiology and Biotechnology*, **34**, 772-777.

30. Clarke, KG, Williams, PC, Smit, MS and Harrison, STL (2006). "Enhancement and Repression of the Volumetric Oxygen Transfer Coefficient through Hydrocarbon Addition and its Influence on Oxygen Transfer Rate in Stirred Tank Bioreactors", *Biochemical Engineering Journal*, **28** (3), 237-242.

31. Coty, VF, Gorring, RL, Heilweil, IJ, Leavitt, RI and Srinivasan, S (1971). "Growth of Microbes in an Oil-Continuous Environment", *Biotechnology and Bioengineering*, **13**, 825-1971.

32. Cowles, PB (1938). "The Germicidal Power of some Alcohols for *Bacterium typhosum* and *Staphylococcus aureus*, and its Relation to Surface Tension", *Yale Journal of Biology and Medicine*, **2**, 127-135.

33. Craft, DL, Madduri, KM, Eshoo, M and Wilson, CR (2003). "Identification and Characterization of the *CYP52* Family of *Candida tropicalis* ATCC 20336, Important for the Conversion of Fatty Acids and Alkanes to α,ω-Dicarboxylic", *Applied and Environmental Microbiology*, **59**, 5983-5991.

34. Daughton, CG, Cook, AM and Alexander, M (1979). "Phosphate and Soil Binding: Factors Limiting Bacterial Degradation of Ion

Phosphorous-Containing Pesticide Metabolites", *Applied and Environmental Microbiology*, **37**, 507-609.

35. Deindoerfer, FH (1960)., *Fermentation Kinetics and Model Processes*, **2**, 321-335.
36. Dufek, EJ, Parker, WE and Koos, RE (1974)., *Journal of the American Oil Chemists' Society*, **51**, 351.
37. Dunlap, KR and Perry, JJ (1967). "Effect of Substrate on the Fatty Acid Composition of Hydrocarbon-utilizing Microorganisms", *Journal of Bacteriology*, **94** (6), 1919-1923.
38. Egli, T (1995). "The Ecological and Physiological Significance of the Growth Heterotrophic Microorganisms with Mixture of Substrate", *Advances in Microbial Ecology*, **14**, 305-386.
39. Erickson, LE, Fan, LT, Shah, PS and Chen, MSK (1970). "Growth Models of Cultures with Two Liquid Phases. IV. Cell Adsorption, Drop Size, and Batch Growth", *Biotechnology and Bioengineering*, **12**, 713-746.
40. Eschenfeldt, WH, Zhang, Y, Samaha, H, Stols, L, Eirich, LD, Wilson, CR and Donnelly, MI (2003). "Transformation of Fatty Acids Catalyzed by Cytochrome P450 Monooxygenase Enzymes of *Candida tropicalis*", *Applied and Environmental Microbiology*, **69**, 5992-5999.
41. Fickers, P, Benetti, PH, Waché, Y, Marty, A, Mauersberger, S, Smit, MS and Nicaud, JM (2005). "Hydrophobic Substrate Utilisation by the Yeast *Yarrowia lipolytica*, and its Potential Applications", *FEMS Yeast Research*, **5**, 527-543.
42. Fickers, P, Nicaud, JM, Gaillardin, C, Destain, J and Thonard, P (2004). "Carbon and Nitrogen Sources Modulated Lipase Production in the Yeast *Yarrowia lipolytica*", *Journal of Applied Microbiology*, **96**, 742-749.
43. Foster, JW (1962). "The Oxygenases", In: Hayaishi (ed.), Academic Press, New York.
44. Fredrickson, AG, Megee, RD and Tsuchiya HM (1970). "Mathematical Models for Fermentation Processes", *Advances in Applied Microbiology*, **24**, 419-465.

45. Fukui, S and Tanaka, A (1980). "Production of Useful Compounds from Alkanes Medium in Japan", *Advances in Biochemical Engineering*, **17**, 1-35.

46. Gallo, M, Bertrand, JC, Roche, B and Azoulay, E (1973). "Alkane Oxidation in *Candida tropicalis*", *Biochimica et Biophysica Acta*, **296**, 624-638.

47. Ghaly, AE and El-Taweel, AA (1997). "Kinetic Modelling of Continuous Production of Ethanol from Chees Whey", *Biomass and Bioenergy*, **12** (6), 461-472.

48. Gilewicz, M, Zacek, M, Bertrand, JC and Azoulay, E (1978). "Hydroxylase Regulation in *Candida tropicalis* Grown on Alkanes", *Canadian Journal of Microbiology*, **25** (2), 201-206.

49. Gill, CO and Ratledge, C (1972). "Toxicity of *n*-Alkanes, *n*-Alk-1-Enes, *n*-Alkan-1-ols and *n*-Alkyl-1-Bromides towards Yeast", *Journal of General Microbiology*, **72**, 165-172.

50. Gmünder, FK, Käppeli, O and Fiechter, A (1981). "Chemostat Studies on the Assimilation of Hexadecane by the Yeast *Candida tropicalis*", *European Journal of Applied Microbiology and Biotechnology*, **12**, 129-134.

51. Gokulakrishnan, S and Gummadi, SN (2006). "Kinetics of Cell Growth and Caffeine Utilization by *Pseudomonas* sp GSC 1182" *Process Biochemistry*, **41**, Issue 6, 1417-1421.

52. Goma, G, Pareilleux, A and Durand, G (1973). "Specific Hydrocarbon Solubilization during Growth of *Candida lipolytica*", *Journal of Fermentation Technology*, **51**, 616-618.

53. Goswami, P and Singh, HD (1991). "Different Modes of Hydrocarbon Uptake by Two *Pseudomonas* Specie", *Biotechnology and Bioengineering*, **37** (1), 1-11.

54. Green, KD, Turner, MK and Woodley, JM (2000). "*Candida cloacae* Oxidation of Long-Chain Fatty Acids to Dioic Acids", *Enzyme and Microbial Technology*, **27**, 205-211.

55. Gutierrez, JR and Erickson, LE (1977). "Hydrocarbon Uptake in Hydrocarbon Fermentations", *Biotechnology and Bioengineering*, **19** (9), 1331–1349.

56. Hao, OJ, Kim, MH, Seagren, EA and Kim, H (2002). "Kinetics of Phenol and Chlorophenol Utilisation by *Acinetobacter* species", *Chemosphere*, **46**, 797-807.

57. Hara, A, Udea, M and Matsui, T (2001). " Repression of Fatty-Acyl-CoA Oxidase-Encoding Gene Expression is not Necessarily a Determined of High-Level Production of Dicarboxylic Acids in Industrial Dicarboxylic Acid-Producing *Candida tropicalis*", *Applied Microbiology and Biotechnology*, **56**, 478-485.

58. Harder, W and Dijkhuizen, L (1982). "Strategies of Mixed Substrate Utilisation in Microorganisms", *Philosophical Transactions of the Royal Society B: Biological Sciences*, **297**, 459-480.

59. Hill, FF, Venn, I and Lukas, KL (1986). "Studies on the Formation of Long-Chain Dicarboxylic Acids from Pure *n*-alkanes by a Mutant of *Candida tropicalis*", *Applied Microbiology and Biotechnology*, **24**, 168-174.

60. Himmelblau, DM (1996). "Basic Priciples and Calculations in Chemical Engineering", 6th ed., Prentice-Hall, New Jersey.

61. Hisatsuka, K, Nakahara, T, Minoda, Y and Yamada, K (1977). "Formation of Protein-Like Activator for *n*-Alkane Oxidation and its Properties", *Agricultural and Biological Chemistry*, **41**, 445-450.

62. Holcberg, IB and Margalith, P (1981). "Alcoholic Fermentation by Immobilized Yeast at High Sugar Concentrations", *European Journal of Applied Microbiology and Biotechnology*, **13**, 133-140.

63. Hug, H, Blanch, HW and Fiechter, A (1974). "The Functional Role of Lipids in Hydrocarbon Assimilation", *Biotechnology and Bioengineering*, **16**, 965-985.

64. Itoh, S, Honda, H, Tomita, F and Suzuki, T (1971). "Rhamnolipid Produced by *Pseudomonas aeruginosa* Grown on *n*-Paraffin", *Journal of Antibiotics*, **24**, 855-859.

65. Jane, AR (1944). "The Colorimetric Estimation of Small amounts of Ammonium by the Phenol-Hypochlorite Reaction", *Journal of Biological Chemistry*, **156**, 457-462.

66. Jiao, P, Huan, Y, Li, S, Hua, Y and Cao, Z (2001). "Effect and Mechanism of H_2O_2 on Production of Dicarboxylic Acid", *Biotechnology and Bioengineering*, **75** (3), 456-462.

67. Johnson, MJ (1964). "Utilization of Hydrocarbons by Microorganisms", *Chemistry and Industry*, **36**, 1532-1537.

68. Johnson, MJ (1967). "Growth of Microbial Cells on Hydrocarbons", *Science*, **24**, 1515-1519.

69. Kamzolova, S, Morgunov, I, Aurich, A, Perevoznikova, S, Shiskanova, N, Stottmeister, U and Finogenova, T (2005). "Lipase Secretion and Citric Acid Production in *Yarrowia lipolytica* Yeast Grown on Animal and Vegetable Fat", *Food Technology and Biotechnology*, **43** (2), 113-122.

70. Kamzolova, SV, Chistyakova, TI, Dedyuhina, EG, Shishkanova, NV and Finogenova, TV (1996). "Effect of Temperature, pH, and Ethanol Concentration on the Maximal Specific Growth Rate and Biomass Composition of *Yarrowia lipolytica*, Mutant Strain no. 1", *Microbiology*, **65**, 176-180.

71. Kamzolova, SV, Shiskanova, NV, Morgunov, I and Finogenova, TV (2003). "Oxygen Requirements for Growth and Citric Acid Production of *Yarrowia lipolytica*", *FEMS Yeast Research*, **3**, 217-222.

72. Kato, K and Uemura, N (1982). "Process for the Preparation of Long-Chain Dicarboxylic Acids by Fermentation", US Patent No. 4 339 536.

73. Katy, JH (1989). "Process for the Production of Pimelic Acid", US Patent No. 4 888 443.

74. Klasson, TK, Clausen, EC and Gaddy, JL (1989). "Continuous Fermentation for the Production of Citric Acid from Glucose", *Applied Biochemistry and Biotechnology*, **20**, 491-509.

75. Kompala, DS, Ramkrishna, D and Tsao, GT (1984). "Cybernetic Modeling of Microbial Growth on Multiple Substrates", *Biotechnology and Bioengineering*, **26** (11), 1272-1281.

76. Kovarova-Kovar, K and Egli, T (1998) "Growth Kinetics of Suspended Microbial Cells: From Single-Substrate-Controlled Growth to Mixed-Substrate Kinetics" *Microbiology and Molecular Biology Reviews*, **62**, 646-666.

77. Labinger, JA (2004). "Selective Alkane Oxidation: Hot and Cold Approaches to a Hot Problem", *Journal of Molecular Catalyses A: Chemical*, **220**, 27-35.

78. Labinger, JA and Bercaw, JE (2002). "Understanding and Exploiting C-H Bond Activation", *Nature*, **417**, 507-514.

79. Leung, R, Poncelet, DR and Neufeld, J (1997). "Enhancement of Oxygen Transfer Rate using Microencapsulated Silicone Oils as Oxygen Carriers", *Chemical Technology and Biotechnology*, **68**, 37-46.

80. Levi, JD, Shennan, JL and Ebbon, GP (1979). "Microbial Biomass", In: Rose, AH (ed.), *Economic Microbiology*: *Biomass from liquid n-alkanes*, Volume 4, Academic Press, London, 361-419.

81. Lin, R, Cao, Z and Zhang, Z (2000). "Secretion in Long-Chain Dicarboxylic Acid Fermentation", *Bioprocess Engineering*, **22**, 391-396.

82. Liu, S, Li, C, Fang, X and Cao, Z (2004). "Optimal pH Control Strategy for High-Level Production of Long-Chain α,ω-Dicarboxylic Acid by *Candida tropicalis* ", *Enzyme and Microbial Technology*, **34** (1), 73-77.

83. Lowery, CE Jr, Foster, JW and Jurtshuk, P (1968). "The Growth of Various Filamentous Fungi and Yeasts on *n*-Alkanes and Ketones", *Archives of Microbiology*, **60**, 246-254.

84. Luedeking, R and Piret, EL (1959). "A Kinetic Study of the Lactic Acid Fermentation: Batch Process at Controlled pH", *Journal of Biochemical and Microbiological Technology and Engineering*, **1** (4), 393-431.

85. Maiorella, B (1985). "Ethanol", In: Moo-Young, M (ed.), *Comprehensive Biotechnology*, Pergamon, Oxford.

86. Marrot, B, Barrios-Martinez, A, Moulin, P and Roche, N (2006). "Biodegradation of High Phenol Concentration by Activated Sludge in an Immersed Membrane Bioreactor", *Biochemical Engineering Journal*, **30** (2), 174-183.

87. Mauersberger, S, Matyashova, RN, Müller, HG and Losinov, AB (1980). "Influence of the Growth Substrate and the Oxygen Concentration in the Medium on the Cytochrome P-450 Content in *Candida guilliermondii*", *Applied Microbiology and Biotechnology*, **9**, 285-294.

88. Mauersberger, S, Ohkuma, M, Schunck, W-H and Takagi, M (1996). "*Candida maltosa*", In: Wolf, K (ed.), *Non-conventional Yeast in Biotechnology*, Springer, p 411-580.

89. Miller, GL (1959). "Use of Dinitrosalicylic Acid Reagent for Determination of Reducing Sugar", *Analytical Chemistry*, **31**, 426-428.

90. Mimura, A, Sugeno, M, Ooka, T and Takeda, I (1971a). "Biochemical Engineering Analysis of Hydrocarbon Fermentation", *Journal of Fermentation Technology*, **49**, 245-254.

91. Mimura, A, Takeda, I and Wakasa, R (1973). "Some Characteristic Phenomena of Oxygen Transfer in Hydrocarbon Fermentation", *Biotechnology and Bioengineering Symposium*, **4**, 467-484.

92. Mimura, A, Watanabe, S and Takeda, I (1971b). "Biochemical Engineering Analysis of Hydrocarbon Fermentation. III. Analysis of Emulsification Phenomena", *Journal of Fermentation Technology*, **49**, 255-271.

93. Miranda, JCS (2006). "Kinetic, Intracellular ATP Growth and Maintenance Studies, and Modeling of Metabolically Engineered *Zymomonas mobilis* Fermenting Glucose and Xylose Mixture", *PhD Thesis*, University of Puerto Rico, United States of America.

94. Mizuno, D and Anraku, Y (1967). "The Turnover of Ribonucleic Acid. Their Degradation by Characteristic Enzymic Pathway in *Escherichia coli*", *Journal of Medical Science and Biology*, **20**, 127-149.

95. Monod, J (1947). "The Phenomenon of Enzymatic Adaptation and its Bearings on Problems of Genetics and Cellular Differentiation", *Growth*, **11**, 223-289.

96. Moo-Young, M and Shimizu, T (1971). "Hydrocarbon Fermentations using *Candida lipolytica*. II. A Model for Cell Growth Kinetics", *Biotechnology and Bioengineering*, **13** (6), 761–778.

97. Moresi, M (1994). "Effect of Glucose Concentration on Citric Acid Production by *Yarrowia lipolytica*", *Journal of Chemical Technology and Biotechnology*, **60** (4), 387-395.

98. Moresi, M, Cimarelli, D, Gasparrini, G, Liuzzo, G and Marinelli, R (1980). "Kinetic of Citric Acid Fermentation from *n*-Paraffins by Yeast", *Journal of Chemical Technology and Biotechnology,* **30**, 266-277.

99. Morgan, P (1979). "Dicarboxylic Acids", In: Kirk-Othmer (ed.), *Encyclopaedia of Chemical Technology*, **3** (7), 614-618, John Wiley and Sons, New York.

100. Moser, A (1985). "Kinetics of Batch Fermentations", In: Rehm, HJ and Reed, G (eds.), *Biotechnology: Verlagsgesellschaft mbH*, VCH, Weinheim. 243-283

101. Murib, JH and Katy JH (1989). "Process for the Production of Pimelic Acid", US Patent No. 4 888 443.

102. Nakahara, T, Erickson, LE and Gutierrez JR (1977). "Characteristics of Hydrocarbon Uptake in Cultures with Two Liquid Phases", *Biotechnology and Bioengineering*, **19** (1), 9–25.

103. Nakazawa, K, Fujitani K and Manomi, H (1986). "Process for Preparing Carboxylic Acid", US Patent No. 4 606 863.

104. Nakazawa, K, Fujitani, K and Manomi, H (1986). "Isolation of Carboxylic Acids from Fermentation Broth", US Patent No. 4 606 863.

105. Neidhardt, FC and Magasanik B (1957). "Reversal of the Glucose Inhibition of Histidase Biosynthesis in *Aerobacter aerogenes*", *Journal of Bacteriology*, **73** (2), 253-259.

106. Nielsen, J and Villadsen, J (1994). "Bioreaction Engineering Principles", New York, Plenum Press, p. 61

107. Papanikolaou, S and Aggelis, G (2002). "Lipid Production by *Yarrowia lipolytica* Growing on Industrial Glycerol in a Single-Stage Continuous Culture", *Bio-resource Technology*, **82** (1), 43-49.

108. Papanikolaou, S, Muniglia, L, Chevalot, I, Aggelis, G and Marc, I (2002). "*Yarrowia lipolytica* as a Potential Producer of Citric Acid from Raw Glycerol", *Journal of Applied Microbiology*, **92**, 737-744.

109. Periana, RA, Bhalla, G, Tenn, WJ III, Young, KJH, Liu, XY, Mironov, O, Jones, CJ and Ziatdinov, VR (2004). "Perspectives on some Challenges and Approaches for Developing the next Generation of Selective, Low Temperature, Oxidation Catalysts for Alkane Hydroxylation Based on the CH Activation Reaction", *Journal of Molecular Catalysis A: Chemical*, **220** (1), 7-25.

110. Phisalaphong, M, Srirattana, N and Tanthapanichakoon, W (2006). "Mathematical Modeling to Investigate Temperature effect on Kinetic

Parameters of Ethanol Fermentation", *Biochemical Engineering Journal*, **28** (1), 36-43.

111. Picataggio, S, Deanda, K and Mielenz, J (1991). "Determination of *Candida tropicalis* Acyl Coenzyme A Oxidase Isozyme Function by Sequential Gene Disruption", *Molecular and Cellular Biology*, **11** (9), 4333-4339.
112. Picataggio, S, Rohrer, T, Deanda, K, Lanning, D, Reynolds, R, Mielenz, J and Eirich, LD (1992). "Metabolic Engineering of *Candida tropicalis* for the Production of Long-Chain Dicarboxylic Acids", *Bio-Technology*, **10**, 894-898.
113. Postma, E, Kuiper, A, Tomasouw, WF, Scheffers, WA and van Dijken, JP (1989). "Competition for Glucose between the Yeasts *Saccharomyces cerevisiae* and *Candida utilis*", *Applied and Environmental Microbiology*, **55**, 3214-3220.
114. Postma, E, Verduyn, C, Kuiper, A, Scheffers, WA and van Dijken, JP (1990). "Substrate-Accelerated Death of *Saccharomyces cerevisiae* CBSb8066 under Maltose Stress", *Yeast*, **6**, 149-158.
115. Preusting, H, van Houten, R, Hoefs, A, van Langenberghe, EK, Favre-Bulle, O and Witholt, B (1993). "High Cell Density Cultivation of *Pseudomonas oleovorans*: Growth and Production of Poly (3-Hydroxyalkanoates) in Two-Liquid Phase Batch and Fed-Batch Systems", *Biotechnology and Bioengineering*, **41** (5), 550-556.
116. Rane, K and Sims, K (1993). "Production of Citric Acid by *Candida lipolytica* Y 1095: Effect of Glucose Concentration on Yield and Productivity", *Enzyme and Microbial Technology*, **15**, 646-651.
117. Rane, K and Sims, K (1995). "Citric acid Production by *Candida lipolytica* Y 1O95 in Cell Recycle and Fed-Batch Fermentors", *Biochemistry and Biotechnology*, **46**, 325-332.
118. Rapp, P and Wagner, F (1976). "Formation of Trehaloselipid by *Nocardia rhodochrous* sp. grown on n-alkane" International Fermentation Symposium, Verlag, Berlin, p 133.
119. Reynders, MB, Rawlings, DE and Harrison, STL (1996). "Studies on the Growth, Modelling and Pigment Production by the Yeast *Phaffia*

rhodozyma during Fed-Batch Cultivation" *Biotechnology Letters*, **18** (6), 649-654.

120. Russell, JA (1944). "The Colorimetric Estimation of Small Amounts of Ammonium by the Phenol-Hypochlorite Reaction" *The Journal of Biological Chemistry*, **156**, 457-462.
121. Sanglard, D, Käppeli, O and Fiechter, A (1984). "Metabolic Conditions Determining the Composition and Catalytic Activity of Cytochrome P-450 Monooxygenase in *Candida tropicalis*", *Journal of Bacteriology*, **157** (1), 297-302.
122. Scheller, U, Zimmer, T, Becher, D, Schauer, F and Schunck, W-H (1998). "Oxygenation Cascade in Conversion of *n*-Alkanes to α,ω-Dioic Acids Catalyzed by Cytochrome P450 52A3", *The Journal of Biological Chemistry*, **273** (49), 32528-32534.
123. Schmid, A, Sonnleitner, B and Witholt, B (1998). "Medium Chain Length Alkane Solvent-Cell Transfer Rates in Two-Liquid Phase, *Pseudomonas oleovorans* Cultures", *Biotechnology and Bioengineering*, **60** (1), 10-23.
124. Shu, CH and Yang, ST (1990). "Effect of Temperature on Cell Growth and Xannthan Production in Batch Cultures of *Xanthomonas campestris*", *Biotechnology and Bioengineering*, **35**, 454-468.
125. Shuler, ML and Kargi, F (2002). "Bioprocess Engineering: Basic Concepts", 2nd ed., Prentice-Hall, New Jersey.
126. Sinegani, AAS and Emtiaz, G (2006). "The Relative Effects of some Elements on the DNS Method in Cellulase Assay", *Journal of Applied Sciences and Environmental Management*, **10**, 93- 96.
127. Smit, MS, Mokgoro, MM, Setati, E and Nicaud, J-M (2005). "α,ω-Dicarboxylic Acid Accumulation by Acyl-CoA Oxidase Deficient Mutants of *Yarrowia lipolytica*", *Biotechnology Letters*, **27**, 859-864.
128. Sriram, G, Rao, MY, Suresh, AK and Sureshkumar, GK (1998). "Oxygen Supply without Gas-Liquid Film Resistance to *Xanthomonas campestris* Cultivation", *Biotechnology and Bioengineering*, **59**, 714-723.
129. Stetter, H and Forest, W (1963). "Newer Methods of Preparative Organic Chemistry", Volume 2, Academic Press, New York, 79.

130. Stewart, GG, Panchal, CJ, Russell, I and Sills, AM (1984). "Biology of Ethanol Production Microorganisms", *Critical Reviews in Biotechnology*, **1** (3), 161-188.

131. Stewart, J (1999). "Calculus" 4th ed., Brook/Cole, California.

132. Suh, IS, Herbst, H, Schumpe, A and Deckwer, WD (1990). "The Molecular Weight of Xanthan Polysaccharide Produced Under Oxygen Limitation", *Biotechnology Letters*, **12**, 201-206.

133. Suzuki, T, Tanaka, K, Matsubara, I and Kinoshita, S (1969). "Trehalose Lipid and α-branched β-Hydroxy Fatty Acid Formed by Bacteria Grown on *n*-alkanes", *Agricultural and Biological Chemistry*, **33**, 1619-1627.

134. Uchio, R and Shiio, I (1971). "Microbial Production of Long-Chain Dicarboxylic Acids from *n*-alkanes Part I. Screen and Properties of Microorganisms Production Dicarboxylic Acids", *Agricultural and Biological Chemistry*, **35** (13), 2033-2042.

135. Uchio, R and Shiio, I (1972a). "Microbial Production of Long-Chain Dicarboxylic Acids from *n*-alkanes Part II. Production by *Candida cloacae* Mutant unable to assimilate Dicarboxylic Acids", *Agricultural and Biological Chemistry*, **36** (3), 426-433.

136. Uchio, R and Shiio, I (1972b). "Production of Dicarboxylic Acids by *Candida cloacae* Mutant unable to assimilate *n*-Alkane", *Agricultural and Biological Chemistry*, **36** (7), 1169-1175.

137. Uchio, R and Shiio, I (1972c). "Tetradecane 1,14-Dicarboxylic Acid Production from *n*-Hexadecane by *Candida cloacae*", *Agricultural and Biological Chemistry*, **36** (8), 1389-1397.

138. Uemura, N, Taoka, A and Takagi, M (1988). "Production of Dicarboxylic Acids by Fermentation", In: *Proceeding of the World Conference on Biotechnology for the Fats and Oils Industry*, American Oil Chemists Society USA, Campaign, 148-152.

139. van Beilen, JB, Li, Z, Duetz, WA, Smits, THM and Witholt, B (2003). "Diversity of Alkane Hydroxylase Systems in the Environment", *Oil and Science and Technology*, **58** (4), 427-440.

140. van Eyk, J and Bartels, TJ (1968). "Paraffin Oxidation in *Pseudomonas aeruginosa* I. Induction of Paraffin Oxidation", *Journal of Bacteriology*, **96**, 706-712.

141. van Rooyen, N (2005). "Biotransformation of Alkylbenzenes and their Derivatives by Genetically Engineered *Yarrowia lipolytica* strains", *MSc Thesis*, University of the Free State, South Africa.

142. Vasileva-Tonkova, E, Balasheva, DM and Galabova D (1996). "Influence of Growth Temperature on the Acid Phosphatase Activity in the Yeast *Yarrowia lipolytica*", *FEMS Microbiology Letters*, **145** (2), 267-271.

143. Volesky, B and Votruba, J (1992). "Modeling of Fermentation Processes. Process Simulation and Modeling, 1: Modeling and Optimization of Fermentation Processes", Elsevier, New York.

144. Wang, DIC and Ochoa, A (1972). "Measurements on the Interfacial Areas of Hydrocarbon in Yeast Fermentations and Relationships of Specific Growth Rates", *Biotechnology and Bioengineering*, **14**, 345–360.

145. Wayman, M and Tseng, MC (1976). "Inhibition-Threshold Substrate Concentrations", *Biotechnology and Bioengineering*, **18** (3), 383-387.

146. Weatherburn, MW (1956). "Phenol-Hypochlorite Reaction for the Determination of Ammonia", *Analytical Chemistry*, **28**, 971-974.

147. Williams, PC (2005). "Biological Conversion of Alkanes to Dicarboxylic Acids", *MSc Thesis*, University of Cape Town, South Africa.

148. Yi, ZH and Rehm, HJ (1982). "Metabolic Formation of Dodecanedioic Acid from *n*-Dodecane by a Mutant of *Candida tropicalis*", *European Journal of Applied Microbiology and Biotechnology*, **14**, 254-258.

149. Zajic, JE, Guignard, H and Gerson, DF (1977). "Emulsifying and Surface Active Agents from *Corynebacterium hydrocarboclastus*", *Biotechnology and Bioengineering*, **19** (9), 1285–1301.

Appendix

Appendix A: Developing of Calibration Curves

Appendix A1: Reducing sugars

Preparation Method

- Place 1 g of glucose in a 2 l volumetric flask.
- Fill the volumetric flask with distilled water to the 2 litre mark.
- Use a magnetic bar to stir the solution for 5 minutes.
- From the volumetric flask take 750 µl, 1500 µl, 2250 µl, and 3000 µl samples and place in 4 different 10 ml test tubes.
- Full each test tube to 3 ml with distilled water.
- To each test tube add 3 ml of DNS reagent (Section 3.6.3).
- Lightly cap the test tubes and place in a 90°C water-bath for 10 minutes.
- After heating add 1 ml of potassium sodium tartrate solution (40% (w/v)) to each test tube.
- Cool to room temperature.
- Analyse each the samples by adding 200 µl of each sample into a Labsystem iEMS microtitre plate reader MF (Thermo BioAnylysis Company, Helsinki Finland).
- Record absorbance readings at 575 nm.
- Develop calibration curve by plotting the absorbance to the corresponding glucose concentration.

The straight line in Figure A1 was obtained by linear regression and can be applied to calculate the unknown glucose concentration in the medium. The reproducibility of the assay is shown in Table A1.

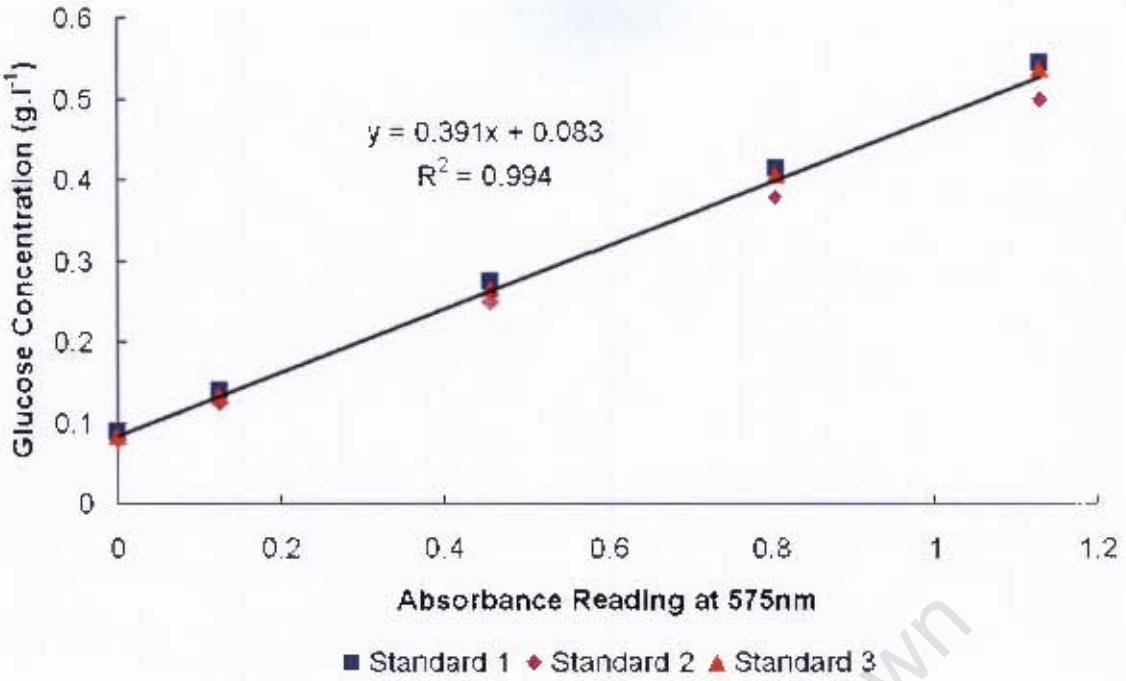

Figure A1: Calibration curve for estimating glucose concentration at a wave length of 575nm

Table A1: Reproducibility of the reducing sugar assay

	Standard 1	Standard 2	Standard 3	Average	
Absorbance	glucose	glucose	glucose	Glucose	Error
@ 575 nm	$g.l^{-1}$	$g.l^{-1}$	$g.l^{-1}$	$g.l^{-1}$	
0.00	0.09	0.08	0.08	0.08	0.01
0.13	0.14	0.13	0.13	0.13	0.01
0.46	0.27	0.25	0.27	0.26	0.01
0.81	0.41	0.38	0.41	0.40	0.02
1.13	0.54	0.50	0.54	0.53	0.02

Appendix A2: Ammonium ion

Preparation Method

- Place 1 g of ammonium nitrate in a 2 l volumetric flask.
- Fill the volumetric flask, with distilled water, to the 2 litre mark.
- Use a magnetic bar to stir the solution for 5 minutes.
- From the volumetric flask take a 150 µl sample and place in a 2 ml Eppendorf tube.
- Add to the Eppendorf tube, 1350 µl of distilled water.

- Vortex for 5 minutes.
- From the Eppendorf tube take 100 µl, 200 µl, 300 µl, 400 µl and 500 µl samples and place in 5 different 1.5 ml Eppendorf tubes.
- Full eppendorfs to 500ml with distilled water.
- Vortex for 5 minutes.
- From the second set of Eppendorf tubes take 100 µl samples and place in 5 different 1.5 ml Eppendorfs.
- To each Eppendorf tube add 550 µl of reagent A and B, respectively (Section 3.6.4).
- Wait 30 minutes.
- Analyse each the samples by adding 200 µl of each sample into a Labsystem iEMS microtitre plate reader MF (Thermo BioAnylysis Company, Helsinki Finland).
- Record absorbance readings at 625 nm.
- Develop calibration curve by plotting the absorbance to the corresponding ammonium ion concentration.

The straight line in Figure A2 was obtained by linear regression and can be applied to calculate the unknown ammonium ion concentration in the medium. The reproducibility of the assay is shown in Table A2.

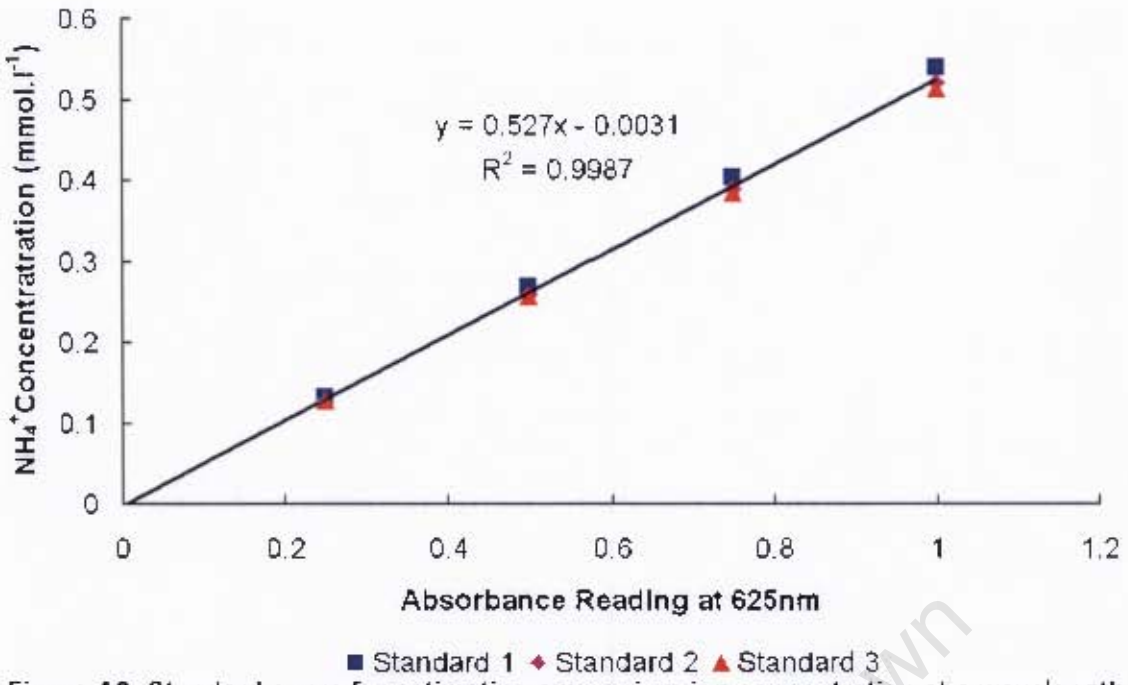

Figure A2: Standard curve for estimating ammonium ion concentration at a wavelength of 625nm.

Table A2: Reproducibility of the ammonium ion assay

	Standard 1	Standard 2	Standard 3	Average	
Absorbance	glucose	glucose	glucose	Glucose	Error
@ 575 nm	g.l^{-1}	g.l^{-1}	g.l^{-1}	g.l^{-1}	
0.00	0.00	0.00	0.00	0.00	0.00
0.25	0.13	0.13	0.13	0.13	0.00
0.50	0.27	0.26	0.26	0.26	0.01
0.75	0.40	0.39	0.38	0.39	0.01
1.00	0.54	0.52	0.51	0.52	0.01

Appendix A3: Dodecane and tridecane

Preparation Method

- Place 300 µl of either dodecane or tridecane in a 2 ml Ependorf tube.
- Add to it a solution of tertiary butyl methyl ether (1200 µl).
- The solution should contain suberic acid (0.2% (w/v)) as internal standard.
- Vortex the ether-alkane mixture for 5 minutes.
- From the mixture taken 300 µl and place in a second 2 ml Eppendorf tube.

- Add to it a solution of tertiary butyl methyl ether (1200 µl).
- Vortex for another 5 minutes.
- From the second Eppendorf tube take 100 µl, 200 µl, 300 µl, 400 µl and 500 µl samples and place in 5 different 1.5 ml Eppendorf tubes.
- Full eppendorf tubes to 500ml with tertiary butyl methyl ether solution.
- Vortex for 5 minutes.
- From each Eppendorf tube take a 50 µl sample and mix with 50 µl of trimethylsulphonium hydroxide in 1.5 ml Eppendorfs.
- Vortex for 5 minutes.
- From each Eppendorf tube inject a 1 µl sample into GC.
- Develop standard curve by plotting the ratios of the alkane-internal standard peak area to the different known alkane concentrations.

The straight lines in Figures A3 and A4, which were obtained by linear regression, can be applied to calculate the unknown alkane concentration in the medium. The reproducibility of the GC method (dodecane and tridecane) is shown in Tables A3 and A4, respectively.

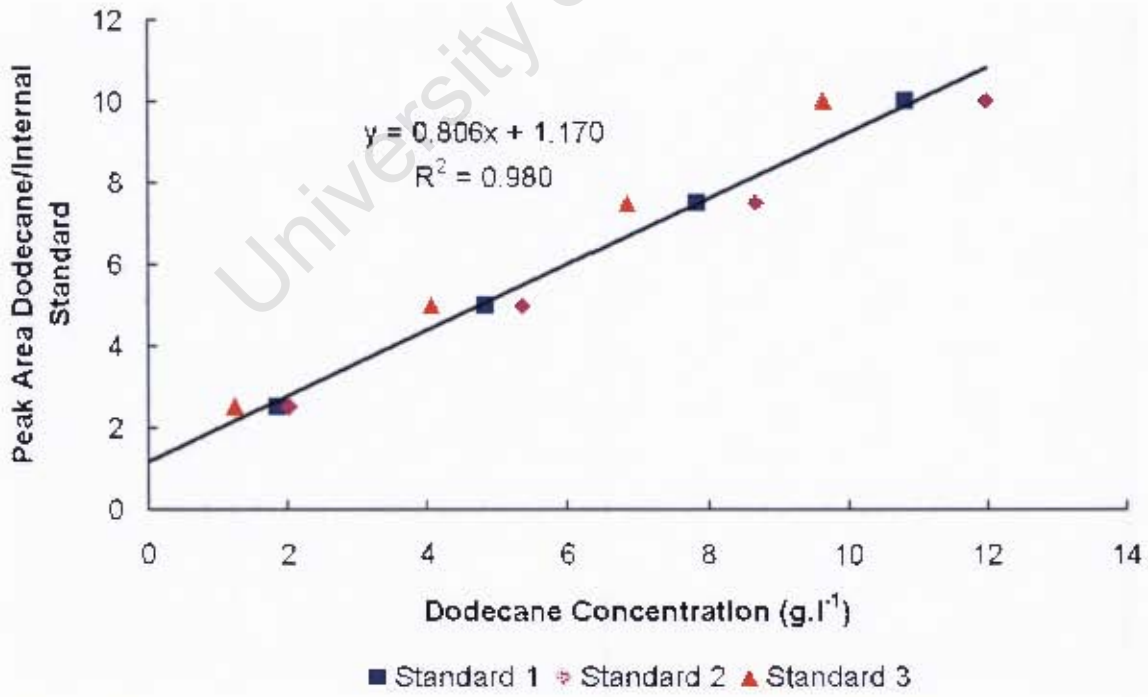

Figure A3: Calibration curve relating dodecane concentration to the peak area ratio of dodecane and suberic acid.

Table A3: Reproducibility of GC (dodecane)

	Standard 1	Standard 2	Standard 3	Average	
Ratio	nC_{12}	nC_{12}	nC_{12}	nC_{12}	Error
mVolts/mVolts	$g.l^{-1}$	$g.l^{-1}$	$g.l^{-1}$	$g.l^{-1}$	
0.00	-	-	-	-	-
2.50	1.86	2.02	1.25	1.71	0.41
5.00	4.85	5.35	4.05	4.75	0.66
7.50	7.84	8.68	6.85	7.79	0.92
10.00	10.83	12.00	9.66	10.83	1.17

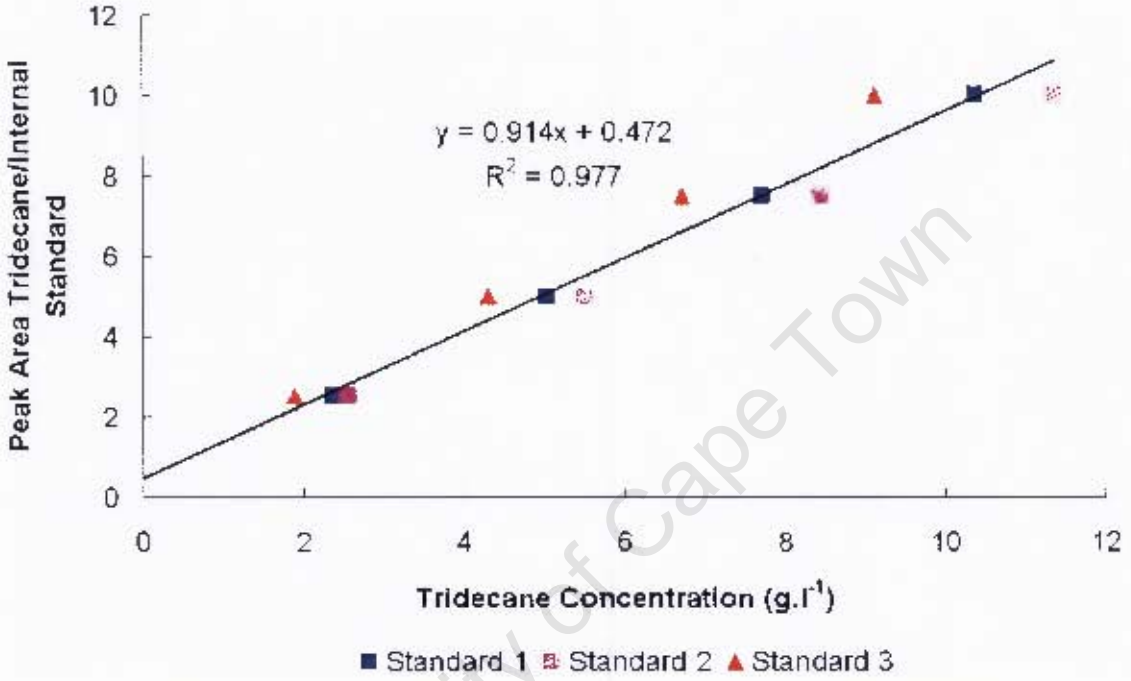

Figure A4: Calibration curve relating dodecane concentration to the peak area ratio of dodecane and suberic acid.

Table A4: Reproducibility of GC (tridecane)

	Standard 1	Standard 2	Standard 3	Average	
Ratio	nC_{13}	nC_{13}	nC_{13}	nC_{13}	Error
mVolts/mVolts	$g.l^{-1}$	$g.l^{-1}$	$g.l^{-1}$	$g.l^{-1}$	
0.00	-	-	-	-	-
2.50	2.37	2.57	1.90	2.28	0.34
5.00	5.05	5.51	4.31	4.95	0.60
7.50	7.72	8.44	6.72	7.63	0.86
10.00	10.39	11.38	9.14	10.30	1.12

Appendix A4: Dodecanedioic acid and tridecanedioic acid

Preparation Method

- Place 10 mg of either dodecanedioic acid or tridecanedioic acid in a 2 ml Ependorf tube.
- Add to it a solution of tertiary butyl methyl ether (1500 µl).
- The solution should contain suberic acid (0.2% (w/v)) as internal standard.
- Vortex the ether-alkane mixture for 5 minutes.
- From the mixture taken 300 µl and place in a second 2 ml Eppendorf tube.
- Add to it a solution of tertiary butyl methyl ether (1200 µl).
- Vortex for another 5 minutes.
- From the second Eppendorf tube take 100 µl, 200 µl, 300 µl, 400 µl and 500 µl samples and place in 5 different 1.5 ml Eppendorf tubes.
- Full eppendorfs to 500ml with tertiary butyl methyl ether solution.
- Vortex for 5 minutes.
- From each Eppendorf tube take a 50 µl sample and mix with 50 µl of trimethylsulphonium hydroxide in 1.5 ml Eppendorfs.
- Vortex for 5 minutes.
- From each Eppendorf tube inject a 1 µl sample into GC.
- Develop calibration curve by plotting the ratios of the α,ω-dicarboxylic acid-internal standard peak area to the different known α,ω-dicarboxylic acid concentrations.

The straight lines in Figures A5 and A6, were obtained by linear regression, and can be applied to calculate the unknown α,ω-dicarboxylic acid concentration in the medium. The reproducibility of the GC method (dodecanedioic acid and tridecanedioic acid) is shown in Tables A5 and A6, respectively.

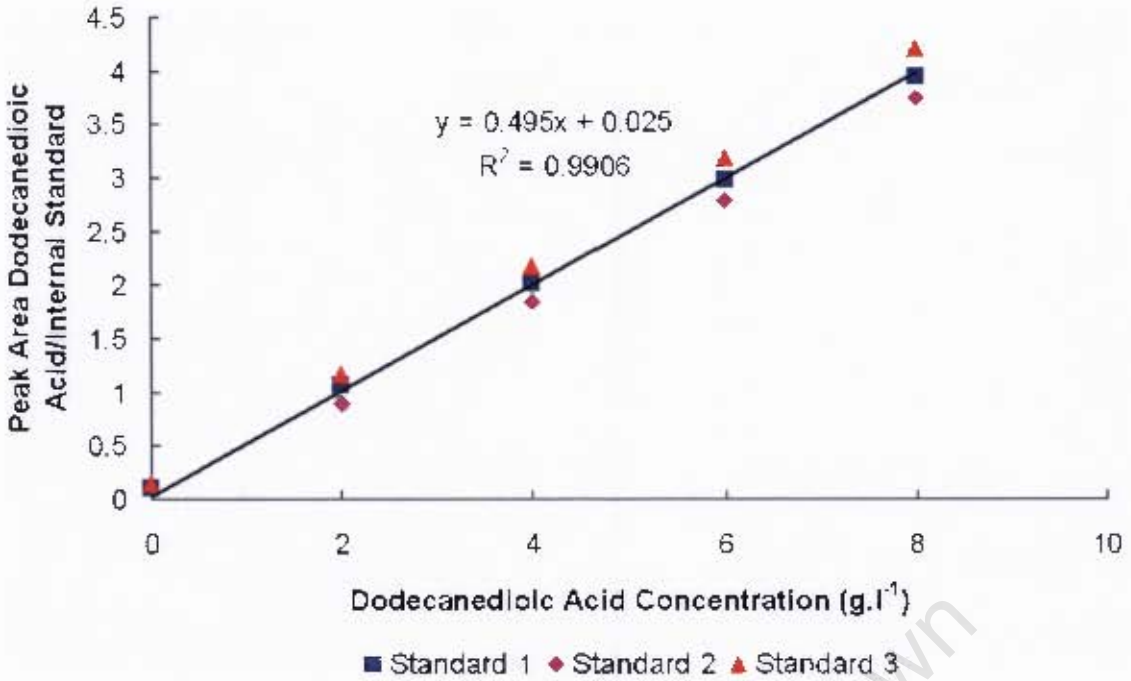

Figure A5: Calibration curve relating dodecanedioic acid concentration to the peak area ratio of dodecanedioic acid and suberic acid.

Table A5: Reproducibility of GC (dodecanedioic acid)

	Standard 1	Standard 2	Standard 3	Average	
Ratio	$C_{12}DC$	$C_{12}DC$	$C_{12}DC$	$C_{12}DC$	Error
mVolts/mVolts	$g.l^{-1}$	$g.l^{-1}$	$g.l^{-1}$	$g.l^{-1}$	
0.00	-	-	-	-	-
1.00	1.95	2.20	1.81	1.98	0.20
2.00	3.94	4.32	3.72	3.99	0.30
3.00	5.93	6.44	5.64	6.00	0.41
4.00	7.92	8.56	7.55	8.01	0.51

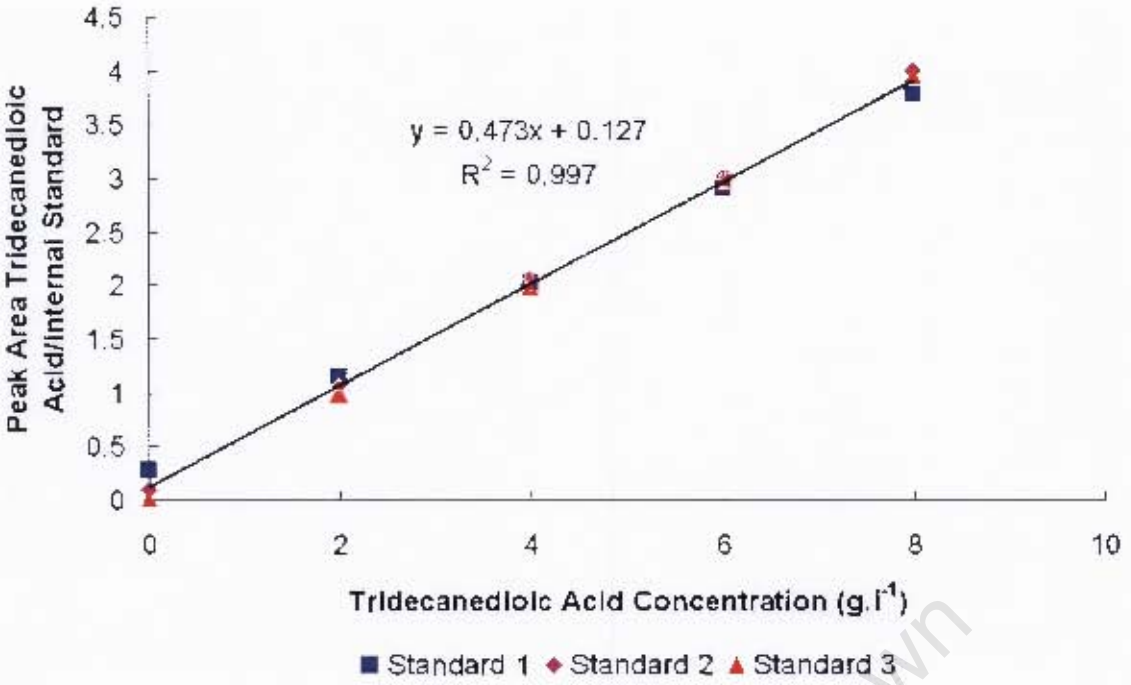

Figure A6: Calibration urve relating tridecanedioic acid concentration to the peak area ratio of tridecanedioic acid and suberic acid.

Table A6: Reproducibility of GC (tridecanedioic acid)

	Standard 1	Standard 2	Standard 3	Average	
Ratio	$C_{13}DC$	$C_{13}DC$	$C_{13}DC$	$C_{13}DC$	Error
mVolts/mVolts	$g.l^{-1}$	$g.l^{-1}$	$g.l^{-1}$	$g.l^{-1}$	
0.00	-	-	-	-	-
1.00	1.79	1.87	2.02	1.89	0.12
2.00	3.90	3.90	4.04	3.95	0.08
3.00	6.02	5.94	6.07	6.01	0.07
4.00	8.14	7.97	8.09	8.07	0.09

Appendix A5: Biomass

Table A7: Reproducibility of the biomass assay

Standard 1	Standard 2	Standard 3	Average	
Biomass	Biomass	Biomass	Biomass	Error
$g.l^{-1}$	$g.l^{-1}$	$g.l^{-1}$	$g.l^{-1}$	
0.90	0.73	0.80	0.81	0.09
4.75	4.55	4.50	4.60	0.13
6.38	6.25	6.25	6.29	0.07
11.00	10.43	10.23	10.56	0.40
11.70	12.30	12.25	12.08	0.33

Appendix B: Experimental Data of Section 5.1 (base case experiments)

Appendix B1: Cell growth data

Table B1: Biomass and glucose concentrations of base case experiments

	Experiment I		Experiment II		Average			
Time	Biomass	Glucose	Biomass	Glucose	Biomass	Error	Glucose	Error
h	$g.l^{-1}$	$g.l^{-1}$	$g.l^{-1}$	$g.l^{-1}$	$g.l^{-1}$		$g.l^{-1}$	
0	0.26	41.15	0.00	40.66	0.13	0.19	40.90	0.34
3	0.33	38.50	0.00	39.72	0.16	0.23	39.11	0.86
7	0.68	39.63	0.35	30.32	0.51	0.23	34.97	6.58
10	1.15	33.04	0.64	39.39	0.89	0.36	36.22	4.49
24	3.28	33.87	2.52	33.70	2.90	0.53	33.79	0.12
32	4.55	28.88	5.05	22.14	4.80	0.35	25.51	4.76
47	9.44	11.35	9.94	0.00	9.69	0.35	5.67	8.03
73	9.66	0.00	9.95	0.00	9.81	0.20	0.00	0.00

Table B2: Biomass, glucose and ammonium ion concentrations of experiment III (base case experiment)

Time	Biomass	Glucose	Ammonium Ion
h	$g.l^{-1}$	$g.l^{-1}$	$mmol.l^{-1}$
0.13	0.66	44.95	22.87
2.22	0.60	43.98	24.25
4.15	1.01	43.56	25.15
5.77	1.34	43.18	25.37
16.42	4.06	39.12	15.28
21.92	4.58	33.43	11.67
24.88	5.46	28.25	2.42
26.78	5.90	27.38	0.72
41.23	8.55	13.61	0.87
50.87	8.89	0.43	4.77
65.42	9.40	0.00	7.73
74.28	9.34	0.00	11.67
89.28	9.21	0.00	13.26
97.65	9.32	0.00	13.80
123.78	9.44	0.00	14.45
215.03	9.63	0.00	15.86

Appendix B2: Carbon and oxygen balance

Table B3: Flow-rate constants

Entity	Value	Unit
Air Pressure	101.33	Kpa
Temperature	303.05	K
Air Flow-rate In	24121.28	$mmol.h^{-1}$
Nitrogen Flow Rate In	18948.59	$mmol.h^{-1}$
Oxygen Flow-Rate In	4937.19	$mmol.h^{-1}$
Argon Flow-Rate	225.29	$mmol.h^{-1}$
Carbon Dioxide Flow-Rate In	10.20	$mmol.h^{-1}$

Table B4: Carbon dioxide production rates and oxygen utilisation rates

		Carbon Dioxide		$O_2:N_2$	Oxygen	
	Time	Production Rate	Accumulated Values		Utilisation Rate	Accumulated Values
	h	$mmol.hr^{-1}$	Mmol		$mmol.hr^{-1}$	mmol
Growth Phase	0.00	0.00		20.67	0.00	
	1.20	8.10	4.86	20.64	9.03	5.42
	1.90	11.34	6.80	20.63	12.04	7.37
	3.40	15.15	19.86	20.61	18.05	22.57
	4.20	19.51	13.86	20.59	24.06	16.85
	5.77	35.14	42.82	20.54	39.08	49.46
	7.42	50.53	70.68	20.49	54.07	76.85
	7.85	42.96	20.26	20.51	48.08	22.13
	7.93	41.97	3.54	20.51	48.08	4.01
	8.10	39.99	6.83	20.52	45.08	7.76
	8.63	36.11	20.29	20.53	42.08	23.24
	9.75	32.66	38.40	20.54	39.08	45.31
	10.17	32.08	13.49	20.54	39.08	16.28
	10.58	34.13	13.79	20.53	42.08	16.91
	24.08	91.83	850.24	20.30	110.89	1032.52
	25.68	99.74	153.26	20.26	122.81	186.96
	28.42	113.95	292.04	20.22	134.73	351.97
	30.38	138.53	248.27	20.17	149.60	279.59
	32.33	160.21	291.27	20.11	167.43	309.11
	34.42	182.14	356.62	20.06	182.27	364.27
	48.05	166.49	2376.46	20.00	200.04	2606.07
		Total	**4843.66**		**Total**	**5444.67**
Stationary Phase	48.30	185.64	44.02	19.96	211.88	51.49
	48.63	173.36	59.83	19.96	211.88	70.63
	48.83	172.71	34.61	19.97	208.92	42.08
	49.18	169.36	59.86	19.98	205.96	72.60
	49.47	37.48	29.30	20.23	131.75	47.84
	51.47	72.07	109.56	20.39	84.01	215.76
	59.20	41.97	440.98	20.51	48.08	510.74
	75.38	21.01	509.62	20.58	27.07	608.05
	95.67	27.81	495.13	20.58	27.07	549.02
	107.22	35.46	365.38	20.56	33.07	347.32
	107.38	39.51	6.25	20.55	36.08	5.76
	120.00	21.01	381.78	20.67	0.00	
		Total	**2536.32**		**Total**	**2521.31**

Table B3 were used to calculate the values in Table B4 by applying the steady state mass balance approach described in Section 3.7.

Appendix C: Experimental Data of Section 5.1.2 (semi-defined medium experiments)

Appendix C1: Cell growth data

Table C1: Biomass, glucose and ammonium ion concentrations

5 g.l^{-1}			
Time	Biomass	Glucose	Ammonium Ion
h	g.l^{-1}	g.l^{-1}	mmol.l^{-1}
0.00	0.00	4.67	49.47
8.85	8.85	5.28	53.21
22.18	22.18	5.06	47.22
26.50	26.50	4.64	45.35
28.42	28.42	4.06	47.41
30.17	30.17	3.77	45.48
32.80	32.80	2.44	44.58
47.43	47.43	0.01	40.84
54.58	54.58	0.00	36.91
96.50	96.50	0.01	37.68

13 g.l^{-1}			
Time	Biomass	Glucose	Ammonium Ion
H	g.l^{-1}	g.l^{-1}	mmol.l^{-1}
0.00	0.00	13.27	48.93
9.60	0.00	13.25	52.05
23.17	0.40	9.08	50.63
30.17	0.50	12.64	52.05
33.50	1.01	11.21	47.18
48.58	1.52	8.07	43.92
50.50	1.73	6.96	39.05
53.02	3.46	4.02	32.86
56.25	5.17	0.13	24.15
73.25	3.06	0.10	31.74

42 g.l^{-1}			
Time	Biomass	Glucose	Ammonium Ion
h	g.l^{-1}	g.l^{-1}	mmol.l^{-1}
0.00	0.00	41.82	45.00
23.00	0.00	43.73	51.82
28.00	0.00	42.84	42.56
32.17	0.48	42.44	39.80
34.00	0.80	42.22	39.31
47.00	9.24	12.18	1.30
48.83	10.23	10.62	1.14
50.83	10.89	4.43	0.81
53.00	12.48	0.00	0.97
56.50	12.68	0.00	0.32
70.83	8.55	0.00	4.39
120.33	8.40	0.00	14.46

51 g.$^{-1}$			
Time	Biomass	Glucose	Ammonium Ion
H	g.l^{-1}	g.l^{-1}	mmol.l^{-1}
0.00	0.00	51.25	54.90
21.75	0.75	49.08	47.49
32.00	3.68	51.16	39.64
45.42	7.18	41.80	24.12
48.08	8.88	37.26	15.52
50.00	10.73	38.21	11.18
53.25	13.40	32.91	2.20
55.25	14.68	31.68	0.06
69.38	19.95	7.77	0.00
80.00	18.55	0.00	0.25
117.75	13.38	0.00	12.44

Appendix C2: Carbon and oxygen balance

Table C2: Flow-rate constants

Entity	Value	Unit
Air Pressure	101.33	Kpa
Temperature	303.05	K
Air Flow-rate In	19297.02	$mmol.hr^{-1}$
Nitrogen Flow Rate In	15143.91	$mmol.hr^{-1}$
Oxygen Flow-Rate In	3965.12	$mmol.hr^{-1}$
Argon Flow-Rate	180.23	$mmol.hr^{-1}$
Carbon Dioxide Flow-Rate In	7.76	$mmol.hr^{-1}$

Table C3: Carbon dioxide production rates and oxygen utilisation rates calculated for the semi-defined medium experiment conducted with an initial glucose concentration of 5 $g.l^{-1}$

		Carbon Dioxide		$O_2:N_2$	Oxygen	
	Time	Production Rate	Accumulated Values		Utilisation Rate	Accumulated Values
	h	$mmol.hr^{-1}$	Mmol		$mmol.hr^{-1}$	mmol
Growth Phase	0.43	0.98		20.74	2.41	
	3.87	1.27	3.88	20.74	2.41	8.28
	7.05	2.05	5.28	20.74	2.41	7.67
	9.03	3.11	5.11	20.74	2.41	4.78
	22.50	8.68	79.39	20.72	7.23	64.92
	26.38	17.08	50.02	20.68	16.86	46.78
	27.30	20.53	17.24	20.67	19.27	16.56
	28.67	29.04	33.88	20.63	28.89	32.91
	30.00	41.68	47.15	20.57	43.30	48.13
	31.45	54.30	69.59	20.53	52.90	69.75
		Total	**889.43**		**Total**	**794.14**
Stationary Phase	33.05	72.06	101.09	20.46	69.67	98.06
	47.60	10.03	597.20	20.69	14.46	612.03
	49.20	9.28	15.45	20.66	21.68	28.91
	55.30	4.46	41.91	20.71	9.64	95.52
	73.35	0.41	43.89	20.72	7.23	152.26
	82.32	0.12	2.34	20.74	2.41	43.23
		Total	**1159.04**		**Total**	**1502.36**

Table C4: Carbon dioxide production rates and oxygen utilisation rates calculated for the semi-defined medium experiment conducted with an initial glucose concentration of 13 g.l^{-1}

		Carbon Dioxide		O_2:N_2	Oxygen	
	Time	Production Rate	Accumulated Values		Utilisation Rate	Accumulated Values
	h	mmol.hr^{-1}	Mmol		mmol.hr^{-1}	mmol
Growth Phase	0.00	0.74	0.19	20.73	1.81	
	0.45	0.12	0.38	20.73	1.81	0.81
	2.20	0.32	0.93	20.73	1.81	3.16
	3.93	0.75	2.33	20.73	1.81	3.13
	6.53	1.04	4.62	20.74	0.00	2.35
	9.50	2.07	41.71	20.74	0.00	0.00
	23.00	4.11	7.36	20.73	1.81	12.20
	24.65	4.80	7.14	20.72	3.62	4.47
	26.15	4.72	5.86	20.73	1.81	4.07
	27.37	4.92	5.62	20.73	1.81	2.20
	28.48	5.15	16.12	20.74	0.00	1.01
	31.43	5.77	14.98	20.73	1.81	2.67
	33.97	6.05	442.84	20.74	0.00	2.29
	48.60	54.48	25.22	20.43	55.84	408.53
	49.05	57.63	39.92	20.41	59.42	25.93
	49.72	62.12	69.51	20.38	64.80	41.41
	50.77	70.28	204.70	20.34	71.96	71.80
	53.28	92.39	207.64	20.22	93.41	208.10
		Total	**2536.32**		**Total**	**2521.31**
Stationary Phase	56.20	49.99	464.43	20.44	54.04	215.04
	73.18	4.70	6.57	20.68	10.84	550.95
	73.85	15.01	2.06	20.61	23.47	11.44
	73.98	15.96	5.42	20.60	25.27	3.25
	74.32	16.59	5.80	20.60	25.27	8.42
	74.82	6.60	13.36	20.61	23.47	12.18
		Total	**2536.32**		**Total**	**2521.31**

Table C5: Carbon dioxide production rates and oxygen utilisation rates calculated for the semi-defined medium experiment conducted with an initial glucose concentration of 42 g.l^{-1}

		Carbon Dioxide		O_2:N_2	Oxygen	
	Time	Production Rate	Accumulated Values		Utilisation Rate	Accumulated Values
	h	mmol.hr^{-1}	Mmol		mmol.hr^{-1}	mmol
Growth Phase	0.00	0.38			0.00	
	0.47	0.43	0.19	20.67	0.00	0.00
	1.87	0.68	0.78	20.67	1.81	1.26
	3.52	1.01	1.40	20.66	1.81	2.98
	5.73	1.68	2.98	20.66	1.81	4.00
	6.77	2.13	1.97	20.66	0.00	0.93
	8.80	4.07	6.30	20.67	1.81	1.84
	22.60	7.41	79.19	20.66	7.22	62.30
	24.37	8.37	13.93	20.63	9.03	14.35
	25.48	9.51	9.98	20.62	19.84	16.12
	25.82	9.68	3.20	20.56	25.25	7.52
	26.98	11.29	12.23	20.53	45.02	40.99
	27.97	12.98	11.93	20.42	52.20	47.80
	28.87	15.30	12.73	20.38	55.79	48.59
	32.10	31.96	76.39	20.36	34.24	145.55
	33.52	42.23	52.55	20.48	41.43	53.60
	34.37	48.53	38.57	20.44	46.82	37.51
	46.48	263.03	1887.51	20.41	264.22	1884.35
		Total	**2211.83**		**Total**	**2369.70**
stationary Phase	46.97	253.72	124.88	19.18	257.25	126.02
	48.00	252.07	261.33	19.22	258.99	266.73
	48.57	249.45	142.10	19.21	260.74	147.26
	49.58	245.13	251.41	19.20	257.25	263.31
	50.03	243.45	109.93	19.22	257.25	115.76
	50.67	241.85	153.68	19.22	255.51	162.37
	51.92	236.38	298.90	19.23	253.77	318.30
	52.73	232.85	191.60	19.24	252.02	206.53
	53.67	203.91	203.82	19.25	208.30	214.82
	55.22	98.59	234.43	19.50	100.46	239.29
	55.33	95.12	11.30	20.11	96.90	11.51
	56.77	64.40	114.32	20.13	64.74	115.84
	57.08	61.78	19.98	20.31	61.16	19.93
	70.62	26.85	599.74	20.33	28.85	609.06
	73.17	11.56	48.97	20.51	14.44	55.19
	76.95	4.94	31.21	20.59	5.42	37.56
	79.97	3.82	13.21	20.64	3.61	13.62
	97.38	4.54	72.85	20.65	3.61	62.91
	107.25	6.30	53.48	20.65	3.61	35.64
	120.32	9.93	106.00	20.65	7.22	70.79
	144.20	11.17	251.98	20.63	10.83	215.59
		Total	**3295.12**		**Total**	**3308.04**

Table C6: Carbon dioxide production rates and oxygen utilisation rates calculated for the semi-defined medium experiment conducted with an initial glucose concentration of 51 g.l^{-1}

		Carbon Dioxide		O_2:N_2	Oxygen	
	Time	Production Rate	Accumulated Values		Utilisation Rate	Accumulated Values
	h	mmol.hr^{-1}	Mmol		mmol.hr^{-1}	mmol
Growth Phase	0.00	1.92		20.70	1.81	
	4.53	7.25	20.80	20.67	7.23	20.48
	9.75	10.12	45.30	20.64	12.64	51.82
	21.28	13.92	138.62	20.60	19.85	187.39
	22.22	14.56	13.29	20.60	19.85	18.53
	24.83	15.09	38.80	20.59	21.66	54.31
	24.93	15.12	1.51	20.59	21.66	2.17
	25.70	16.08	11.96	20.59	21.66	16.60
	31.95	20.83	115.32	20.57	25.26	146.61
	45.40	86.76	723.51	20.19	93.37	797.81
	45.90	90.55	44.33	20.17	96.94	47.58
	48.00	106.83	207.25	20.06	116.53	224.14
	49.95	120.99	222.12	19.98	130.74	241.08
	51.07	126.90	138.41	19.94	137.83	149.95
	53.20	138.61	283.22	19.86	152.00	309.16
	53.70	140.31	69.73	19.85	153.77	76.44
	54.75	124.92	139.24	19.93	139.61	154.02
	55.18	122.51	53.61	19.93	139.61	60.50
	69.30	124.17	1741.11	19.83	157.31	2095.71
	69.95	124.21	80.72	19.82	159.08	102.82
		Total	**4088.84**		**Total**	**4757.12**
Stationary Phase	71.95	123.24	247.46	19.82	159.08	318.15
	74.05	120.87	256.32	19.83	157.31	332.20
	78.42	95.11	471.55	20.13	104.07	570.67
	79.90	41.36	101.22	20.48	41.45	107.93
	93.52	13.21	371.56	20.66	9.03	343.70
	99.17	14.44	78.13	20.65	10.84	56.13
	103.82	13.69	65.41	20.65	10.84	50.39
	117.42	13.05	181.86	20.65	10.84	147.37
		Total	**1773.50**		**Total**	**1926**.54

Table C2 were used to calculate the values in Tables C3, C4, C5 and C6 by applying the steady state mass balance approach described in Section 3.7.

Appendix D: Experimental data of Section 5.2 (calculating growth kinetics)

Appendix D1: Graphical approach

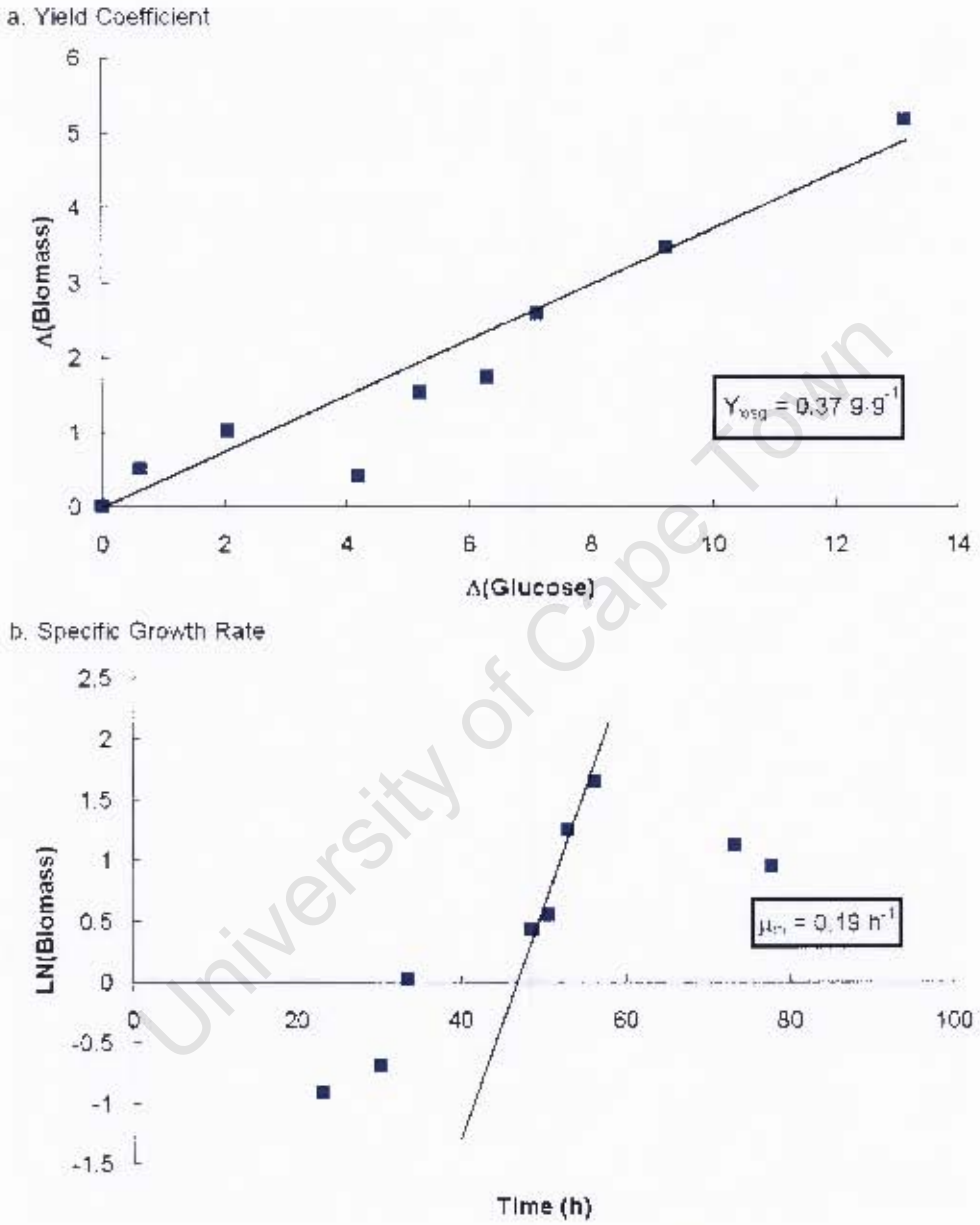

Figure D1: (a) Graphical estimation of (a) the yield coefficient and (b) the specific growth rate at an initial glucose concentration of 13 g.l^{-1}. The experiment was carried out with strain TVN 497 in the Braun BIOSTAT C bioreactor using the Antonucci semi-defined medium. The pH, temperature, aeration rate and agitation speed of the medium were set at 5 g.l^{-1}, pH 6.0, 30 °C, 0.8 vvm and 700 rpm, respectively. A 10% (v/v) inoculum was used.

a. Yield Coefficient

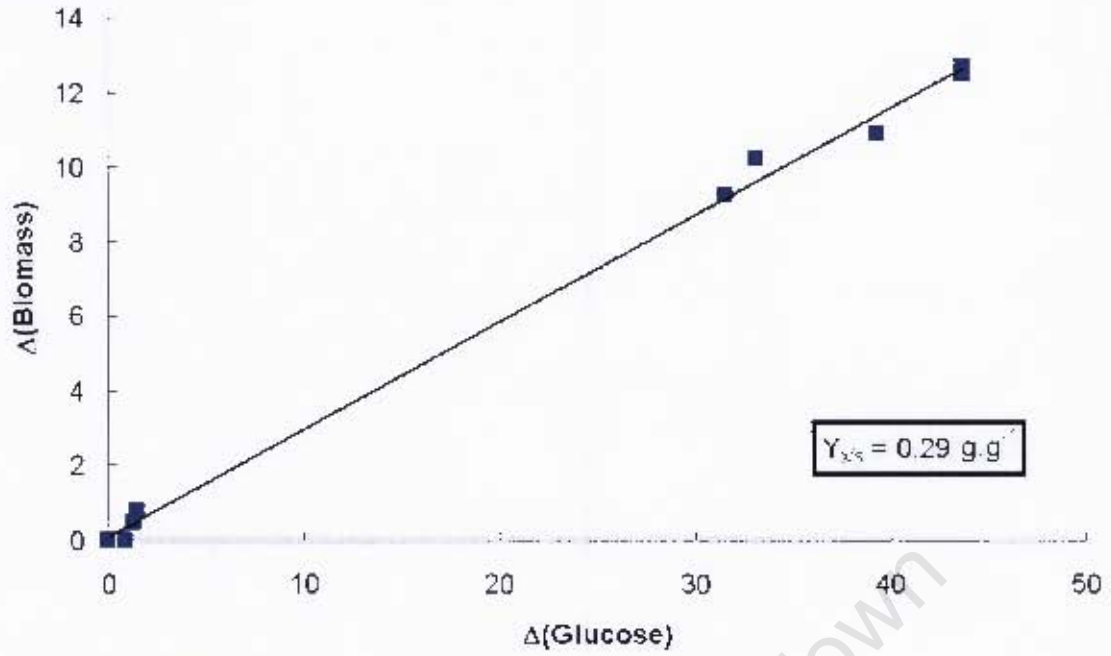

b. Specific Growth Rate

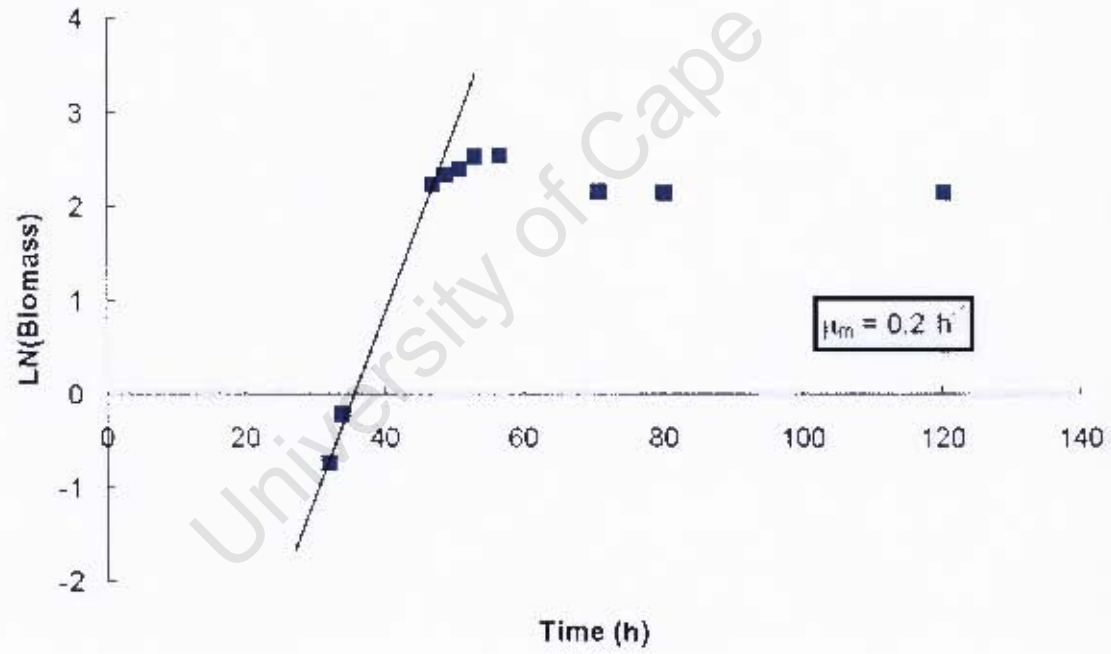

Figure D2: (a) Graphical estimation of (a) the yield coefficient and (b) the specific growth rate at an initial glucose concentration of 42 g.l^{-1}. The experiment was carried out with strain TVN 497 in the Braun BIOSTAT C bioreactor using the Antonucci semi-defined medium. The pH, temperature, aeration rate and agitation speed of the medium were set at 5 g.l^{-1}, pH 6.0, 30 °C, 0.8 vvm and 700 rpm, respectively. A 10% (v/v) inoculum was used.

Appendix D2: Modeling growth using the basic kinetic model (Computer program)

The following algorithm was used to calculate the values of kinetic parameters μ_m, K_s and $Y_{x/s}$.

Main (Initial estimates of the kinetic parameters)

```
close all;clear all;clc
po=[Ks  μm  Yx/s];
p = fminsearch('LSI2',log(p0));
I = LSI2(p)
p = exp(p)
```

LSI2b (Description of the differential equations that needs to be solved)

```
function dCdt = bioodes(t,C)
global p1
% 1 - biomass
% 2 - substrate
% 3 - product
Ks  = p1(1);
μm  = p1(2);
Yx/s  = p1(3);
μ= μm*C(2)/(Ks+C(2));
dCdt(1,1) = μ*C(1);
dCdt(2,1) = -dCdt(1,1)/Yx/s;
```

Xbiodes (Solving of the differential equations using the least squared method)

```
global p1;
p1 = exp(p);
t_exp  =[to.....tn];
```

```
Cx      =[Cxo.....Cxn];
Csg     =[Csgo.....Csg];
Co = [Cx(1) Csg(1)];
[t,C] = ode23s('xbioodes',[t_exp(1) t_exp(end)],Co);
Cxm = interp1(t,C(:,1),t_exp);
Csgm = interp1(t,C(:,2),t_exp);
I = sum(((Cxm-Cx)./Cx).^2 + ((Csgm-Csg)./Csg).^2);
plot(t_exp,[Cx Csg],'x', t,C,'-')
legend('data','model')
drawnow
```

Appendix D3: Growth and growth predictions

Table D1: Growth and growth predictions of the complex medium base case experiments

		Experiment 1		Experiment 2		Model			
	Time	Biomass	Glucose	Biomass	Glucose	Biomass	r^2	Glucose	r^2
	h	$g.l^{-1}$	$g.l^{-1}$	$g.l^{-1}$	$g.l^{-1}$	$g.l^{-1}$		$g.l^{-1}$	
Early Exponential Phase	0.00	0.26	40.89	0.00	0.00	0.13	0.66	39.58	0.17
	2.00	0.28	39.58	-	-	0.17		39.45	
	3.00	-	-	0.00	39.72	0.21		39.37	
	4.00	0.38	36.89	-	-	0.19		39.28	
	6.00	0.46	40.03	-	-	0.27		39.07	
	7.00	-	-	0.35	30.32	0.30		38.94	
	8.00	0.89	38.70	-	-	0.34		38.80	
Exponential Phase	10.00	1.15	32.78	`0.64	39.39	0.43	0.94	38.45	0.68
	24.00	3.28	33.61	2.52	33.70	2.23		31.68	
	26.00	-	-	3.26	27.02	2.79		29.59	
	28.00	-	-	3.63	31.93	3.47		27.04	
	30.00	-	-	4.40	28.57	4.28		24.01	
	32.00	4.55	28.62	5.05	22.14	5.21		20.49	
Late Expo-nential Phase	34.00	-	-	5.55	22.03	6.26	0.16	20.49	0.48
	47.00	9.44	5.83	9.94	0.00	10.58		16.54	
	73.00	9.66	0.00	-	-	10.67		0.00	
	80.00	-	-	9.95	0.00	10.67		0.00	

Table D2: Growth and growth predictions of the semi-defined medium experiment conducted with an initial glucose concentration of 5 $g.l^{-1}$

	Experiment		Model			
Time	Biomass	Glucose	Biomass	r^2	Glucose	r^2
h	$g.l^{-1}$	$g.l^{-1}$	$g.l^{-1}$		$g.l^{-1}$	
0.00	0.00	4.67	-		-	
8.85	0.00	5.28	-	-	-	-
22.18	0.61	5.06	-		-	
26.50	0.75	4.64	0.75		4.64	
28.42	1.07	4.06	1.05		4.18	
30.17	1.58	3.77	1.44	0.99	3.60	0.92
32.80	2.53	2.44	2.29		2.30	
47.43	3.69	0.01	3.79		0.00	
54.58	3.73	0.00	3.79		0.00	
96.50	3.53	0.01	-	-	-	-

Table D3: Growth and growth predictions of the semi-defined medium experiment conducted with an initial glucose concentration of 13 $g.l^{-1}$

	Experiment		Model			
Time	Biomass	Glucose	Biomass	r^2	Glucose	r^2
h	$g.l^{-1}$	$g.l^{-1}$	$g.l^{-1}$		$g.l^{-1}$	
0.00	0.00	13.27	-		-	
9.60	0.00	13.25	-		-	
23.17	0.40	9.08	-	-	-	-
30.17	0.50	12.64	-		-	
33.50	1.01	11.21	-		-	
48.58	1.52	8.07	1.52		8.07	
50.50	1.73	6.96	2.15	0.98	6.71	1
53.02	3.46	4.02	3.34		4.11	
56.25	5.17	0.13	5.19		0.10	
73.25	3.06	0.10	-	-	-	-

Table D4: Growth and growth predictions of the semi-defined medium experiment conducted with an initial glucose concentration of 42 $g.l^{-1}$

	Experiment		Model			
Time	Biomass	Glucose	Biomass	r^2	Glucose	r^2
h	$g.l^{-1}$	$g.l^{-1}$	$g.l^{-1}$		$g.l^{-1}$	
0.00	0.00	41.82	-		-	
23.00	0.00	43.73	-	-	-	-
28.00	0.00	42.84	-		-	
32.17	0.48	42.44	0.48		42.44	
34.00	0.80	42.22	0.69		41.70	
47.00	9.24	12.18	9.22		11.88	
48.83	10.23	10.62	12.62	0.97	0.00	0.94
50.83	10.89	4.43	12.62		0.00	
53.00	12.48	0.00	12.62		0.00	
56.50	12.68	0.00	12.62		0.00	
70.83	8.55	0.00	-	-	-	-
120.33	8.40	0.00	-		-	

Appendix E: Experimental data of Section 5.3.1 (substrate inhibition)

Appendix E1: Cell growth data

Table E1: Optical density data for experiment investigating substrate inhibition

	Initial Glucose Concentration				
Time	10 $g.l^{-1}$	20 $g.l^{-1}$	30 $g.l^{-1}$	40 $g.l^{-1}$	60 $g.l^{-1}$
H	Relative OD	Relative OD	Relative OD	Relative OD	Relative OD
1.00	0.25	0.24	0.27	0.28	0.28
3.00	0.55	0.56	0.61	0.51	0.47
5.00	0.86	0.92	0.88	0.87	0.86
7.00	1.37	1.24	1.26	1.07	1.16
10.00	2.07	1.97	1.96	2.19	1.88
22.50	3.96	4.38	4.36	4.26	3.92
36.50	6.32	6.50	6.34	6.52	6.19
59.75	4.62	6.06	7.56	7.02	7.20
72.00	4.38	6.24	7.68	8.46	8.16
96.73	4.38	6.00	7.86	9.24	9.90

Appendix E2: Substrate Inhibition

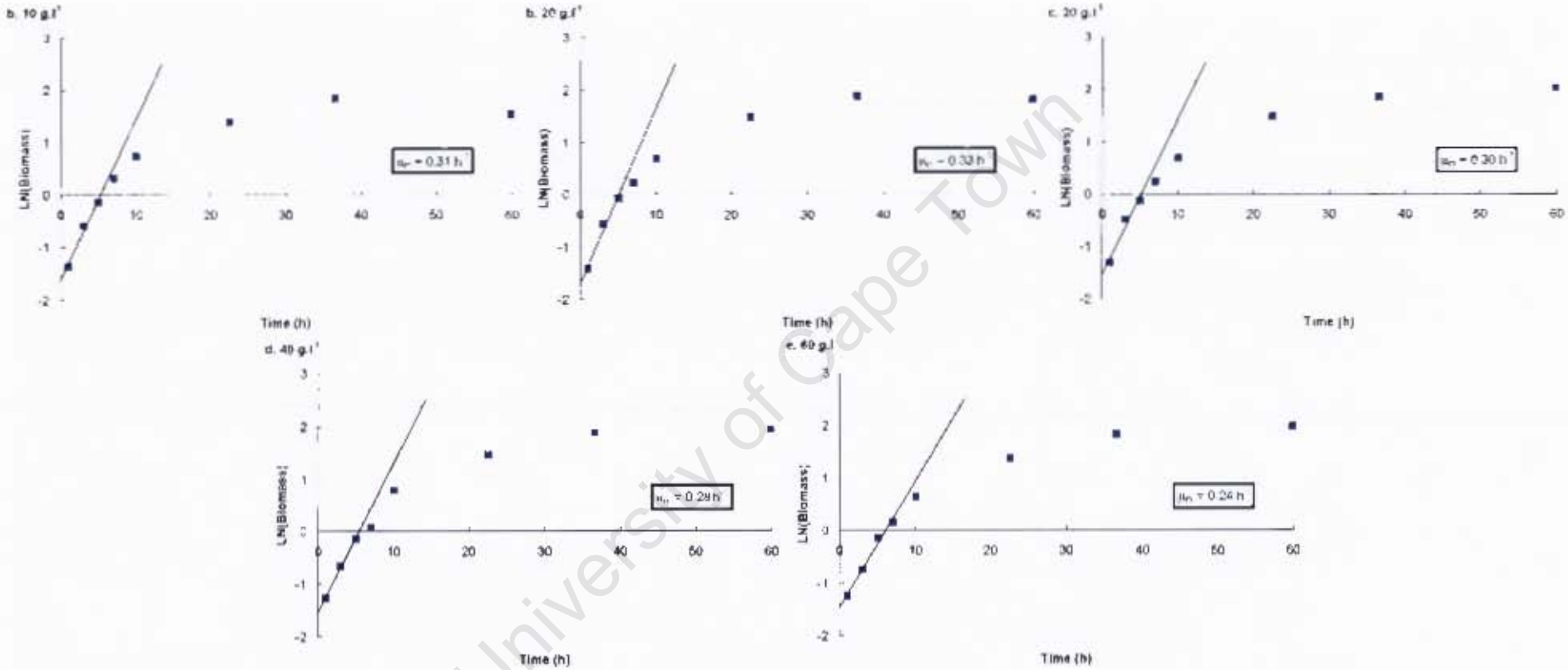

Figure E1: Graphical estimations of the specific growth rates for the experiments investigating substrate inhibition. Strain TVN 497 was cultivated in shake flasks using the UFS media buffered to pH 6 at 29°C on a rotary shaker at 180 rpm. The initial glucose concentrations were chosen as 10, 20, 30, 40 and 60 $g.l^{-1}$, respectively.

Appendix E3: Modeling the inhibition effect of glucose on the specific growth rate of *Y. lipolytica* TVN 497

The following algorithm was used to calculate the values of kinetic parameters μ_m, K_s and K_i.

Main (Initial estimates of the kinetic parameters)

```
close all; clear all; clc
po=[μm Ks Ki];
p= fminsearch('LSI2',Log(po))
I = LSI2(p)
p = exp(p)
```

LSI2 (Solving of the differential equations using the least squared method)

```
function I = LSI2(p1)
% 1 - substrate
Ks = p1(1);
μm = p1(2);
Ki = p1(3);
μ= μm*C(1)/(ks+C(1)+ (C(1)^2)/K);
global p1;
p1 = exp(p);
μe      =[μo.....μn];
Csg     =[Cxo.....Cxn];
I = sum(((μm-μe)./μe).^2 + ((Csgm-Csg)./Csg).^2);
plot(Csg,μ)
legend('data','model')
drawnow
```

Appendix F: Experimental data of Section 5.3.2 (complex medium experiments investigating the effect of alkane on biomass production)

Appendix F1: Cell growth data

Table F1: The effect of residual glucose and medium pH on growth of *Y. lipolytica* TVN 497

1st Reference		1% Alkane		3% Alkane		2nd Reference	
Time	Biomass	Time	Biomass	Time	Biomass	Time	Biomass
H	$g.l^{-1}$	h	$g.l^{-1}$	H	$g.l^{-1}$	H	$g.l^{-1}$
0.00	0.00	0.30	0.81	0.13	0.66	0.12	0.63
3.00	0.00	2.07	0.86	2.22	0.60	3.03	0.87
7.00	0.35	6.00	1.66	4.15	1.01	5.03	1.21
10.00	0.64	17.25	4.60	5.77	1.34	7.58	1.90
24.00	2.52	19.03	4.73	16.42	4.06	17.10	4.40
26.00	3.26	21.00	5.48	21.92	4.58	18.88	4.21
28.00	3.63	22.95	6.29	24.88	5.46	20.90	5.13
30.00	4.40	25.18	6.93	26.78	5.90	22.88	5.93
32.00	5.05	27.83	7.78	41.23	8.55	24.88	7.00
34.00	5.55	44.28	10.18	50.87	8.89	28.55	7.96
47.50	9.94	50.60	10.56	65.42	9.40	43.47	8.85
80.00	9.95	69.10	10.87	74.28	9.34	50.67	9.18
		91.40	10.73	89.28	9.21	68.37	10.50
		139.17	11.92	97.65	9.32	91.02	10.43
		266.00	12.08	123.78	9.44	114.87	10.33
				215.03	9.63	138.72	10.43
						187.12	10.08

Appendix F2: Statistical analyses of the specific growth rate

The eight-step procedure of the One-sided *t*-Test was applied as follows:

1. Test the null hypothesis that the average specific growth rate In Experiments I, II and IV is at least 0.0835 h^{-1} at the 5% significance level..
2. H_0: μ equal or larger than 0.0835 h^{-1}
3. H_1: μ smaller than 0.0835 h^{-1}
4. $\alpha = 0.05$
5. The test statistic is:

$$t_0 = \frac{\bar{d} - \mu}{S_d / \sqrt{n}} \quad \text{(F1)}$$

6. Do not reject H_0 if $t_0 > t_{0.05,2} = -2.9199856$.
7. Computation: The sample average and standard deviation of the differences d_j are $\bar{d} = 0.0551\ h^{-1}$ and $S_d = 0.001908\ h^{-1}$, so the test is:

$$t_0 = \frac{-0.0284}{0.001908/\sqrt{3}} = -25.782693 \quad \text{(F2)}$$

Conclusion: Since $t_0 = -25.782693 < -2.9199856$, it was concluded that the specific growth rate obtained with Experiment III was significantly higher than the specific growth rate obtained by with Experiments I, II and IV

.

Appendix F3: Statistical analyses of the final biomass concentration

The eight-step procedure of the One-sided *t*-Test was applied as follows:

1. Test the null hypothesis that the average final biomass concentration in Experiments II, III and IV is at least 9.66 $g.l^{-1}$ at the 5% significance level..
2. H_0: μ equal or larger than 9.66 $g.l^{-1}$
3. H_1: μ smaller than 9.66 $g.l^{-1}$
4. $\alpha = 0.05$
5. The test statistic is:

$$t_0 = \frac{\bar{d} - \mu}{S_d / \sqrt{n}} \quad \text{(F3)}$$

6. Do not reject H_0 if $t_0 > t_{0.05,2} = -2.9199856$.
7. Computation: The sample average and standard deviation of the differences d_j are $\bar{d} = 10.23667\ g.l^{-1}$ and $S_d = 0.798269\ g.l^{-1}$, so the test is:

$$t_0 = \frac{0.576667}{0.798269/\sqrt{3}} = 1.2512274 \qquad \text{(F4)}$$

Conclusion: Since t_0 = 1.2512274 > -2.9199856, it is concluded that the final biomass concentration obtained with Experiment I was not significantly different from the final biomass concentrations obtained with Experiments II, III and IV

Appendix G: Experimental data of Section 6.1 (biotransformation in both a complex and semi-defined medium)

Appendix G1: Biotransformation data in a Complex and Semi-defined Medium

Table G1: GC Data

Complex Medium					Semi-Defined Medium				
Time	nC_{12}	$C_{12}DA$	nC_{13}	$C_{13}DA$	Time	nC_{12}	$C_{12}DA$	nC_{13}	$C_{13}DA$
H	$g.l^{-1}$	$g.l^{-1}$	$g.l^{-1}$	$g.l^{-1}$	H	$g.l^{-1}$	$g.l^{-1}$	$g.l^{-1}$	$g.l^{-1}$
18.00	8.96	0.05	9.71	0.03	79.00	11.36	0.00	12.04	0.00
25.57	9.54	0.07	9.76	0.03	87.50	11.43	0.03	12.04	0.00
39.98	9.47	0.20	10.19	0.10	101.67	12.61	0.05	13.58	0.02
49.73	8.08	0.20	8.55	0.10	110.83	10.75	0.03	11.89	0.03
64.07	7.85	0.30	8.91	0.14	125.25	11.40	0.08	13.26	0.09
88.40	7.52	0.66	8.71	0.41	150.00	8.98	0.06	11.57	0.06
96.35	7.53	0.76	9.28	0.48	182.00	7.55	0.05	10.44	0.04
117.98	6.27	0.90	8.24	0.59					
137.23	6.26	1.03	8.79	0.68					
159.52	5.75	1.21	8.54	0.82					
183.48	5.22	0.05	8.08	0.85					

Appendix G2: The effect of biotransformation on the carbon dioxide production rate and the oxygen utilisation rate

Table G2: GC data and carbon dioxide production rates and oxygen utilisation rates

Time	$C_{12}DA$	$C_{13}DA$	Carbon Dioxide	Oxygen
h	$g.l^{-1}$	$g.l^{-1}$	$mmol.hr^{-1}$	$mmol.hr^{-1}$
18.67	0.00	0.00	113.89	131.44
19.75	0.00	0.00	79.02	117.19
27.33	0.06	0.06	134.56	143.30
44.08	0.22	0.13	88.61	110.06
50.33	0.23	0.14	73.06	110.06
68.83	0.46	0.33	26.30	93.39
91.17	0.73	0.63	17.71	33.63
115.58	0.61	0.62	13.82	21.63
138.83	0.95	1.01	10.67	26.43
162.67	1.10	1.24	4.88	21.63
187.18	1.16	1.37	4.63	14.43
242.23	1.24	1.54	2.93	9.62

Appendix G3: The effect of alkane on the oxygen solubility in the medium

Table G3: GC data and oxygen solubility data

Time	Biomass	Time	nC_{12}	nC_{13}	Oxygen Solubility
H	$g.l^{-1}$	h	$g.l^{-1}$	$g.l^{-1}$	$mg.l^{-1}$
0.30	0.81	0.03	-	-	7.896
2.07	0.86	0.65	-	-	7.832
6.00	1.66	1.00	-	-	7.8
17.25	4.60	1.87	-	-	7.736
19.03	4.73	4.00	-	-	7.048
21.00	5.48	17.05	-	-	6.272
22.95	6.29	18.07	-	-	6.104
25.18	6.93	18.35	-	-	6.616
27.83	7.78	18.55	3.47	3.71	6.568
44.28	10.18	18.82	-	-	6.496
50.60	10.56	18.98	-	-	6.552
69.10	10.87	19.60	3.44	3.58	6.568
91.40	10.73	20.93	-	-	6.384
139.17	11.92	21.90	-	-	6.248
266.00	12.08	25.13	-	-	6.128
		27.77	3.02	3.65	6.192
		28.75	-	-	6.312
		44.22	2.21	3.23	10.376
		50.50	1.86	2.70	11.592
		69.03	1.46	2.21	11.864
		91.17	0.51	1.91	12.144
		115.73	0.17	1.17	10.8
		139.07	0.08	0.73	9.632
		162.93	0.00	0.29	8.448
		187.18	0.00	0.10	6.864
		219.50	-	-	6.64
		242.23	0.00	0.03	-
		283.00	0.00	0.01	-

Appendix G4: The effect of alkane on the oxygen solubility in the medium

Table G4: GC Data

1% (v/v)				
Time	nC_{12}	$C_{12}DA$	nC_{13}	$C_{13}DA$
h	$g.l^{-1}$	$g.l^{-1}$	$g.l^{-1}$	$g.l^{-1}$
18.67	3.47	0.00	3.71	0.00
19.75	3.44	0.00	3.58	0.00
27.33	3.02	0.06	3.65	0.06
44.08	2.21	0.22	3.23	0.13
50.33	1.86	0.23	2.70	0.14
68.83	1.46	0.46	2.21	0.33
91.17	0.51	0.73	1.91	0.63
115.58	0.17	0.61	1.17	0.62
138.83	0.08	0.95	0.73	1.01
162.67	0.00	1.10	0.29	1.24
187.18	0.00	1.16	0.10	1.37
242.23	0.00	1.24	0.03	1.54
263.95	0.00	1.32	0.02	1.69
283.00	0.00	1.40	0.01	2.23

1.5% (v/v)				
Time	nC_{12}	$C_{12}DA$	nC_{13}	$C_{13}DA$
H	$g.l^{-1}$	$g.l^{-1}$	$g.l^{-1}$	$g.l^{-1}$
18.25	4.60	0.00	5.20	0.00
23.67	4.54	0.07	5.19	0.04
27.75	4.30	0.15	5.26	0.07
43.25	3.76	0.17	4.86	0.09
50.50	3.66	0.23	4.98	0.15
68.20	3.14	0.30	4.87	0.19
91.00	2.63	0.51	4.32	0.40
114.67	1.75	0.70	3.28	0.58
120.50	2.78	0.79	2.78	0.71
125.00	1.66	0.82	2.98	0.75
139.00	0.68	0.84	2.54	0.71
163.38	1.27	0.88	2.36	0.75
186.75	0.00	0.83	0.93	0.71
197.00	0.00	0.88	1.01	0.75

3% (v/v)				
Time	nC_{12}	$C_{12}DA$	nC_{13}	$C_{13}DA$
h	$g.l^{-1}$	$g.l^{-1}$	$g.l^{-1}$	$g.l^{-1}$
18.00	8.96	0.05	9.71	0.03
25.57	9.54	0.07	9.76	0.03
39.98	9.47	0.20	10.19	0.10
49.73	8.08	0.20	8.55	0.10
64.07	7.85	0.30	8.91	0.14
88.40	7.52	0.66	8.71	0.41
96.35	7.53	0.76	9.28	0.48
117.98	6.27	0.90	8.24	0.59
137.23	6.26	1.03	8.79	0.68
159.52	5.75	1.21	8.54	0.82
183.48	5.22	1.29	8.08	0.85

Appendix H: Experimental Data of Section 6.2 (calculating biotransformation kinetics)

Appendix H1: Graphical approach

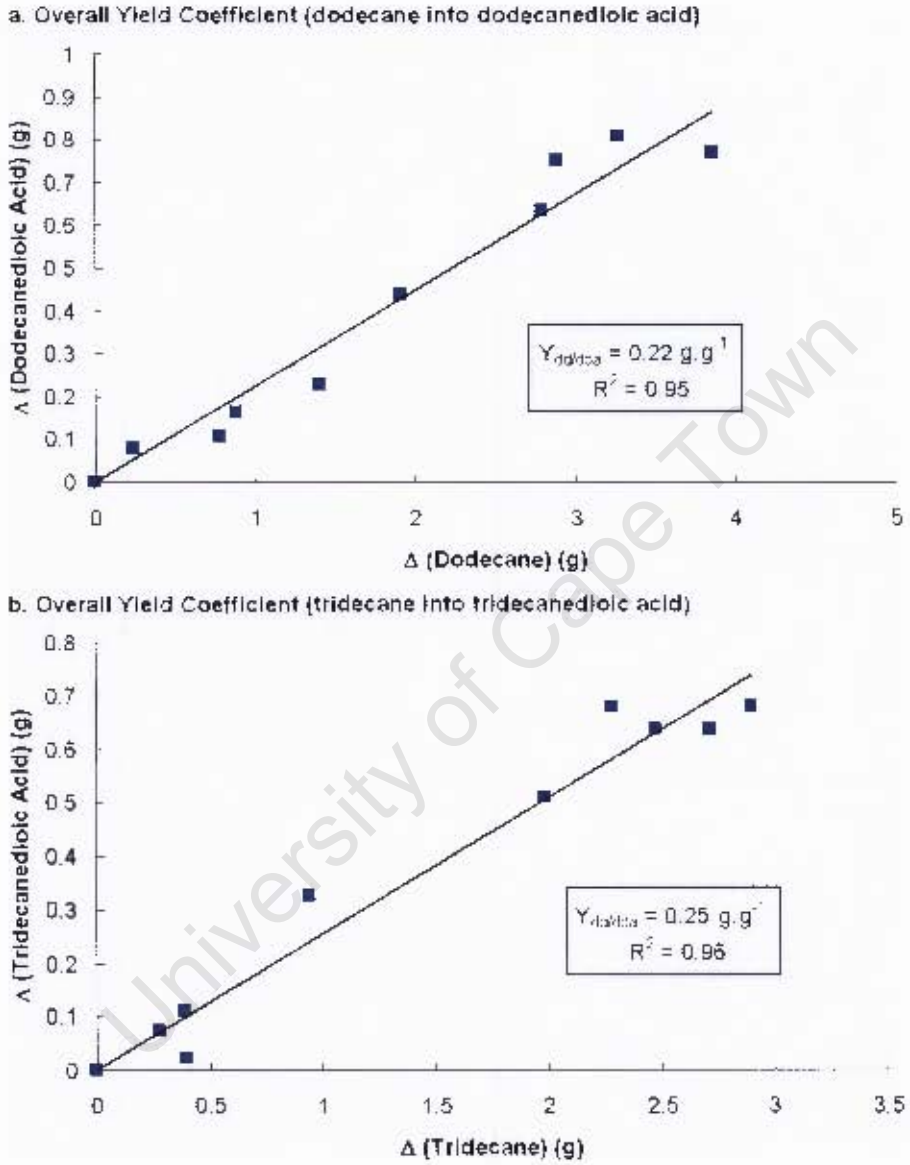

Figure H1: Graphical estimation of the overall product yield coefficient at an initial alkane concentration of 1.5% (v/v). (a) conversion of dodecane into dodecanedioic acid (b) conversion of tridecane into tridecanedioic acid. Experiments were carried out with strain TVN 497 in the Braun BIOSTAT C bioreactor using the modified Picataggio medium. The initial glucose concentration, pH, temperature, aeration rate and agitation speed of the complex medium were set at 40 g.l^{-1}, pH 6.0, 30 °C, 0.8 vvm and 700 rpm, respectively. Alkane addition occurred 18 h after inoculation.

a. Overall Yield Coefficient (dodecane into dodecanedioic acid)

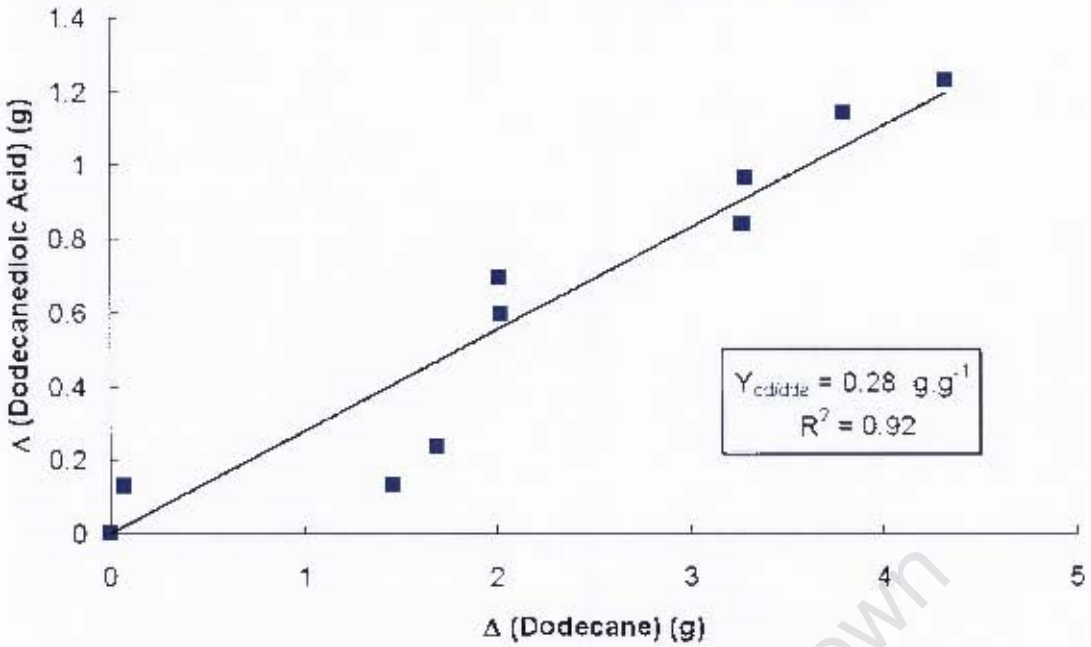

b. Overall Yield Coefficient (tridecane into tridecanedioic acid)

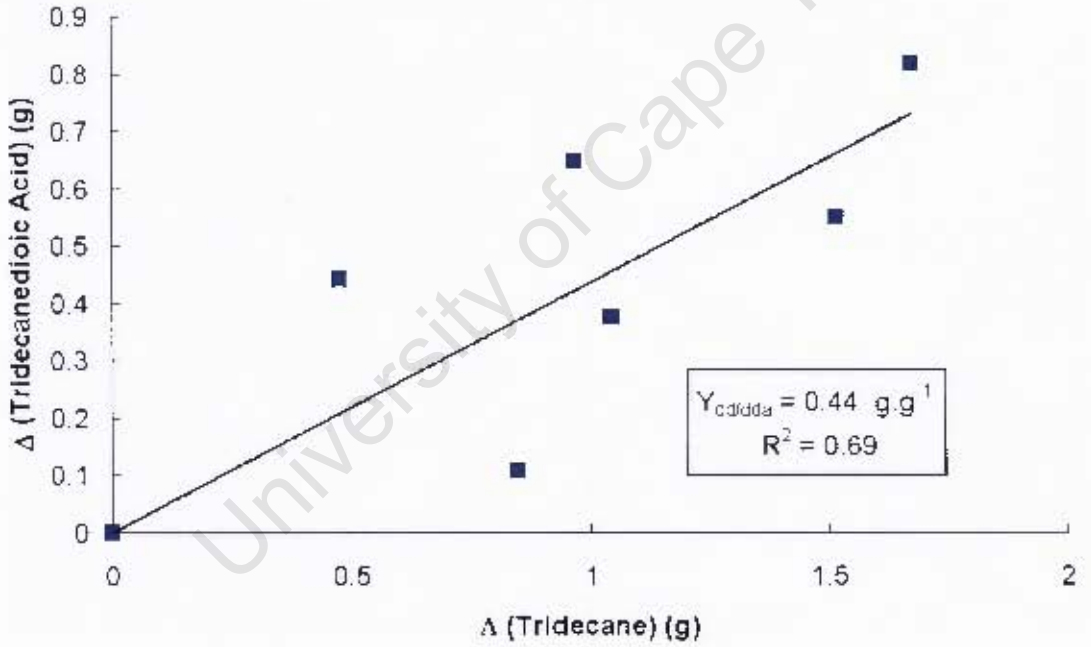

Figure H2: Graphical estimation of the overall product yield coefficient at an initial alkane concentration of 3 (v/v). (a) conversion of dodecane into dodecanedioic acid (b) conversion of tridecane into tridecanedioic acid. Experiments were carried out with strain TVN 497 in the Braun BIOSTAT C bioreactor using the modified Picataggio medium. The initial glucose concentration, pH, temperature, aeration rate and agitation speed of the complex medium were set at 40 g.l^{-1}, pH 6.0, 30 °C, 0.8 vvm and 700 rpm, respectively. Alkane addition occurred 18 h after inoculation.

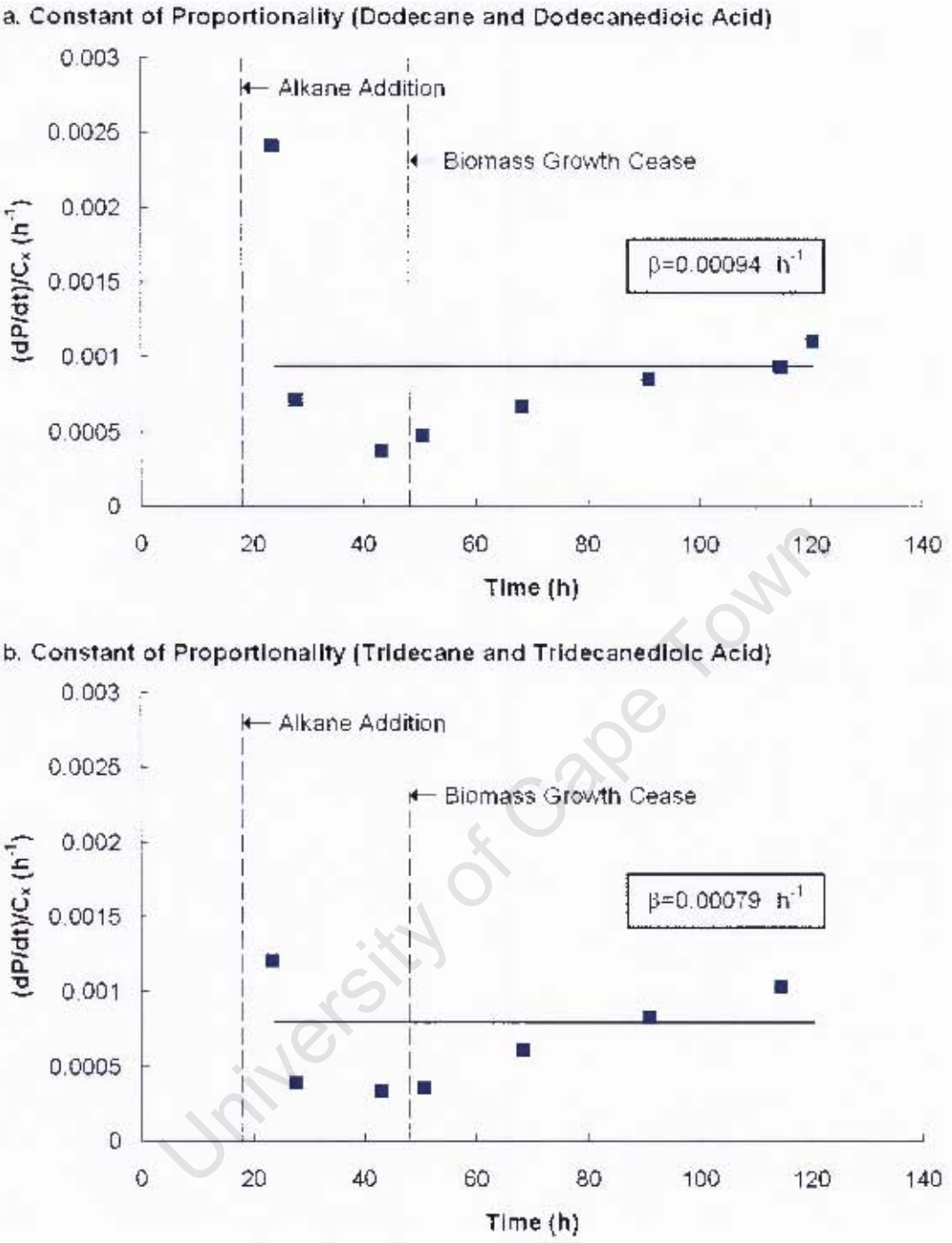

Figure H3: Graphical estimation of the proportionality constant at an initial alkane concentration of 1.5% (v/v). (a) conversion of dodecane into dodecanedioic acid (b) conversion of tridecane into tridecanedioic acid in the complex medium experiment conducted with an initial alkane concentration of 1.5% (v/v). Experiments were carried out with strain TVN 497 in the Braun BIOSTAT C bioreactor using the modified Picataggio complex medium. The initial glucose concentration, pH, temperature, aeration rate and agitation speed of the medium were set at 40 $g.l^{-1}$, pH 6.0, 30 °C, 0.8 vvm and 700 rpm, respectively. Alkane addition occurred 18 h after inoculation.

a. Constant of Proportionality (Dodecane and Dodecanedioic Acid)

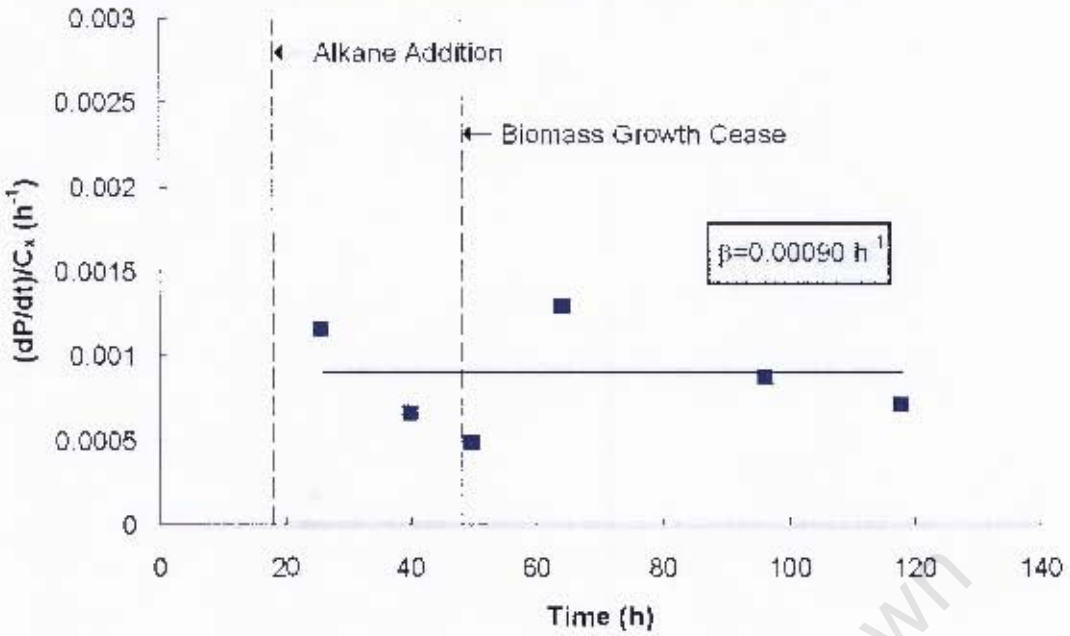

b. Constant of Proportionality (Tridecane and Tridecanedioic Acid)

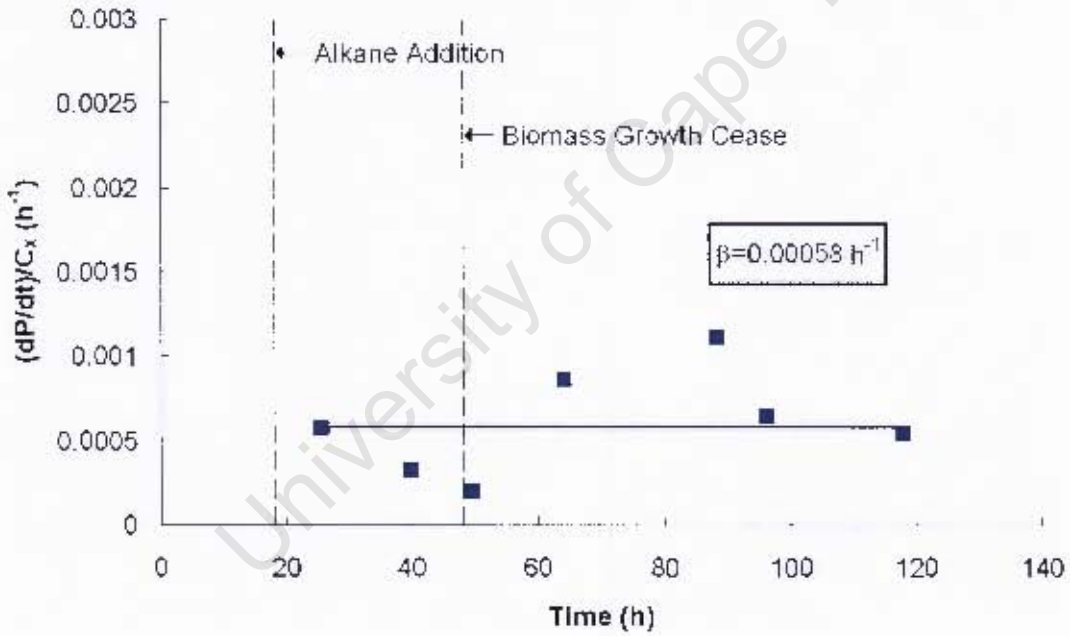

Figure H4: Graphical estimation of the proportionality constant at an initial alkane concentration of 3% (v/v). (a) conversion of dodecane into dodecanedioic acid (b) conversion of tridecane into tridecanedioic acid in the complex medium experiment conducted with an initial alkane concentration of 1.5% (v/v). Experiments were carried out with strain TVN 497 in the Braun BIOSTAT C bioreactor using the modified Picataggio complex medium. The initial glucose concentration, pH, temperature, aeration rate and agitation speed of the medium were set at 40 $g.l^{-1}$, pH 6.0, 30 °C, 0.8 vvm and 700 rpm, respectively. Alkane addition occurred 18 h after inoculation.

Appendix H2: Modeling biotransformation using the basic kinetic model (computer program)

The following algorithm was used to calculate the values of kinetic parameters β_{dda}, $Y_{dda/dd}$, β_{tda} and $Y_{tda/td}$.

Main (Initial estimates of the kinetic parameters)

```
close all;clear all;clc
po=[βgen  Ygen];
p = fminsearch('LSI2',log(p0));
I = LSI2(p)
p = exp(p)
```

LSI2 (Description of the differential equations that needs to be solved)

```
function dCdt = bioodes(t,C)
global p1
% 1 – α,ω-dicarboxylic acid
% 2 –  alkane
βgen    = p1(1);
Ygen    = p1(2);
dCdt(1,1) = βgen*Cxf;
dCdt(2,1) = -dCdt(1,1)/Ygen;
```

Xbiodes (Solving the differential equations using the least squared method)

```
global p1;
p1 = exp(p);
t_exp  =[to.....tn];
Cda    =[Cxo.....Cxn];
Csa    =[Csgo.....Csg];
Co = [Cda(1) Csa(1)];
```

[t,C] = ode23s('xbioodes',[t_exp(1) t_exp(end)],C_o);

C_{dam} = interp1(t,C(:,1),t_exp);

C_{sam} = interp1(t,C(:,2),t_exp);

I = sum(((C_{dam}-C_{da})./C_{da}).^2 + ((C_{sam}-C_{sa})./C_{sa}).^2);

plot(t_exp,[C_{da} C_{sa}],'x', t,C,'-')

legend('data','model')

drawnow

Appendix H3: Statistical analysis of the yield coefficients

The eight-step procedure of the Paired *t*-Test was applied as follows:

8. The parameters of interest are the difference in mean yield coefficient obtained with dodecane and tridecane, $\mu_D = \mu_1 - \mu_2 = 0$.
9. H_0: $\mu_D = 0$
10. H_1: $\mu_D \neq 0$
11. $\alpha = 0.05$
12. The test statistic is:

$$t_0 = \frac{\bar{d}}{S_d/\sqrt{n}} \qquad \text{(H1)}$$

13. Reject H_0 if $t_0 > t_{0.025,2} = 4.303$ or if $t_0 < -t_{0.025,2} = -4.303$.
14. Computation: The sample average and standard deviation of the differences d_j are $\bar{d} = 0.096667\ g.g^{-1}$ and S_d = 0.055076 $g.g^{-1}$, so the test is:

$$t_0 = \frac{0.096667}{0.055076/\sqrt{3}} = 3.040 \qquad \text{(H2)}$$

15. Conclusion: Since $t_0 = 3.040 < 4.303$, it is concluded that the dodecane and tridecane yield similar yield coefficients.

Appendix H4: Statistical analysis of the specific production rates

The eight-step procedure of the Paired *t*-Test was applied as follows:

1. The parameters of interest are the difference in mean yield coefficient obtained with dodecane and tridecane, $\mu_D = \mu_1 - \mu_2 = 0$.
2. H_0: $\mu_D = 0$
3. H_1: $\mu_D \neq 0$
4. $\alpha = 0.05$
5. The test statistic is:

$$t_0 = \frac{\bar{d}}{S_d/\sqrt{n}} \qquad \text{(H3)}$$

6. Reject H_0 if $t_0 > t_{0.025,2} = 4.303$ or if $t_0 < -t_{0.025,2} = -4.303$.
7. Computation: The sample average and standard deviation of the differences d_j are $\bar{d} = 2.266667\ g.g^{-1}$ and $S_d = 0.802081\ g.g^{-1}$, so the test is:

$$t_0 = \frac{2.266667}{0.802081/\sqrt{3}} = 4.895 \qquad \text{(H4)}$$

8. Conclusion: Since $t_0 = 4.895 > 4.303$, it is concluded that the production rate of dodecanedioic acid is larger than the production rate of tridecanedioic acid.

Appendix H5: Modeling biotransformation using the refined basic kinetic Model

The following algorithm was used to calculate the values of kinetic parameters β_{dda}, $Y_{dda/dd}$, K_{dd}, β_{tda}, $Y_{tda/td}$ and K_{td}.

Main (Initial estimates of the kinetic parameters)

close all;clear all;clc

p_o=[β_{gen} Y_{gen} K_{gen}];

```
p = fminsearch('LSI2',log(p0));
I = LSI2(p)
p = exp(p)
```

LSI2 (Description of differential equations that needs to be solved)

```
function dCdt = bioodes(t,C)
global p1
% 1 – α,ω-dicarboxylic acid
% 2 – alkane
βgen  = p1(1);
Ygen  = p1(2);
Kgen  = p1(3);
dCdt(1,1) = βgen*Cxf*(C(2)/(Kgen+C(2));
dCdt(2,1) = -dCdt(1,1)/Ygen;
```

Xbiodes (Solving differential equations using the least squared method)

```
global p1;
p1 = exp(p);
t_exp  =[to.....tn];
Cda    =[Cxo.....Cxn];
Csa    =[Csgo.....Csg];
Co = [Cda(1) Csa(1)];
[t,C] = ode23s('xbioodes',[t_exp(1) t_exp(end)],Co);
Cdam = interp1(t,C(:,1),t_exp);
Csam = interp1(t,C(:,2),t_exp);
I = sum(((Cdam-Cda)./Cda).^2 + ((Csam-Csa)./Csa).^2);
plot(t_exp,[Cda Csa],'x', t,C,'-')
legend('data','model')
drawnow
```

Appendix I: Experimental Data of Section 6.3 (effect of glucose on biotransformation)

Appendix I1: The effect of residual glucose on α,ω-dicarboxylic acid production

Table I1: GC and glucose concentration data

Experiment 1			
Time	Glucose	Time	Total DC
H	$g.l^{-1}$	h	$g.l^{-1}$
0.00	40.66	48.00	0.00
3.00	39.72	51.67	0.00
7.00	30.32	58.83	0.00
10.00	39.39	74.83	0.96
24.00	33.70	130.83	1.74
26.00	27.02	143.83	4.10
28.00	31.93		
30.00	28.57		
32.00	22.14		
34.00	22.03		
47.50	0.00		

Experiment 2			
Time	Glucose	Time	Total DC
h	$g.l^{-1}$	h	$g.l^{-1}$
0.30	40.84	18.67	0.00
2.07	39.13	19.75	0.00
6.00	40.39	27.33	0.12
17.25	35.37	44.08	0.34
19.03	32.57	50.33	0.38
21.00	29.97	68.83	0.79
22.95	26.75	91.17	1.37
25.18	23.61	115.58	1.24
27.83	21.07	138.83	1.96
44.28	1.75	162.67	2.35
50.60	0.87	187.18	2.53
69.10	0.00	242.23	2.78
91.40	0.00	263.95	3.01
139.17	0.00	283.00	3.63

Experiment 3			
Time	Glucose	Time	Total DC
H	$g.l^{-1}$	h	$g.l^{-1}$
0.12	44.58	18.25	0.00
3.15	45.45	23.67	0.10
5.15	41.86	27.75	0.22
7.70	42.47	43.25	0.27
17.22	37.06	50.50	0.37
19.00	35.94	68.20	0.48
21.02	34.02	91.00	0.91
23.00	29.79	114.67	1.28
25.00	26.97	120.50	1.50
28.67	23.03	125.00	1.57
43.58	10.96	139.00	1.55
50.78	2.27	163.38	1.63
68.48	0.00	186.75	1.55
91.13	0.00	197.00	1.64
114.98	0.00		

Experiment 4			
Time	Glucose	Time	Total DC
h	$g.l^{-1}$	h	$g.l^{-1}$
0.13	44.95	18.00	0.08
2.22	43.98	25.57	0.10
4.15	43.56	39.98	0.29
5.77	43.18	49.73	0.30
16.42	39.12	64.07	0.44
21.92	33.43	88.40	1.07
24.88	28.25	96.35	1.24
26.78	27.38	117.98	1.49
41.23	13.61	137.23	1.71
50.87	0.43	159.52	2.02
65.42	0.00	183.48	2.14
74.28	0.00		
89.28	0.00		
97.65	0.00		
111.53	0.00		

Appendix J: Experimental Data of Section 7.1 (comparison between different recombinant *Y. lipolytica* strains)

Appendix J1: Evaluating growth of different recombinant *Y. lipolytica* Strains

Table J1: Growth data for experiments conducted in duplicate with *Y. lipolytica* TVN 497

	Experiment 1		Experiment 2		Average			
Time	Biomass	Glucose	Biomass	Glucose	Biomass	Error	Glucose	Error
H	OD	$g.l^{-1}$	OD	$g.l^{-1}$	OD		$g.l^{-1}$	
1.00	0.31	37.89	0.36	40.63	0.34	0.04	39.26	1.94
3.00	0.31	38.64	0.34	39.75	0.33	0.02	39.19	0.78
5.00	0.39	39.08	0.44	39.31	0.42	0.04	39.19	0.16
7.00	0.55	37.67	0.61	40.32	0.58	0.04	39.00	1.88
10.00	0.96	37.71	1.00	36.74	0.98	0.03	37.23	0.69
24.00	2.31	31.30	2.19	31.92	2.25	0.08	31.61	0.44
34.00	3.06	26.93	2.78	28.38	2.92	0.20	27.66	1.03
47.00	4.05	18.61	3.54	21.66	3.80	0.36	20.14	2.16
71.00	7.26	0.09	6.96	0.18	7.11	0.21	0.13	0.06
94.42	6.11	0.22	6.59	0.13	6.35	0.34	0.18	0.06
150.33	5.43	0.00	5.43	0.00	5.43	0.00	0.00	0.00

Table J2: Growth data for experiments conducted in duplicate with *Y. lipolytica* TVN 499

	Experiment 1		Experiment 2		Average			
Time	Biomass	Glucose	Biomass	Glucose	Biomass	Error	Glucose	Error
H	OD	$g.l^{-1}$	OD	$g.l^{-1}$	OD		$g.l^{-1}$	
1.00	0.36	38.16	0.37	38.24	0.36	0.01	38.20	0.06
3.00	0.38	36.48	0.40	37.27	0.39	0.01	36.87	0.56
5.00	0.65	35.50	0.66	36.56	0.65	0.01	36.03	0.75
7.00	1.02	35.41	0.98	34.93	1.00	0.03	35.17	0.34
10.00	1.54	33.78	1.56	32.63	1.55	0.01	33.20	0.81
24.00	4.07	24.89	4.55	24.49	4.31	0.34	24.69	0.28
34.00	5.21	15.43	5.97	15.39	5.59	0.54	15.41	0.03
47.00	6.83	3.05	7.11	3.05	6.97	0.20	3.05	0.00
71.00	7.68	0.27	7.97	0.18	7.82	0.20	0.22	0.06
94.42	7.62	0.18	7.83	0.13	7.73	0.15	0.15	0.03
150.33	8.03	0.00	8.06	0.00	8.04	0.02	0.00	0.00

Table J3: Growth data for experiments conducted in duplicate with *Y. lipolytica* TVN 501

	Experiment 1		Experiment 2		Average			
Time	Biomass	Glucose	Biomass	Glucose	Biomass	Error	Glucose	Error
H	OD	$g.l^{-1}$	OD	$g.l^{-1}$	OD		$g.l^{-1}$	
1.00	0.32	39.17	0.31	41.38	0.31	0.01	40.28	1.56
3.00	0.35	39.97	0.33	40.63	0.34	0.02	40.30	0.47
5.00	0.49	38.95	0.49	39.53	0.49	0.00	39.24	0.41
7.00	0.69	38.95	0.71	38.73	0.70	0.01	38.84	0.16
10.00	1.14	37.27	1.10	38.07	1.12	0.03	37.67	0.56
24.00	3.11	29.14	3.68	27.90	3.39	0.40	28.52	0.88
34.00	4.68	22.59	5.04	21.05	4.86	0.25	21.82	1.09
47.00	5.97	9.37	5.88	9.20	5.93	0.06	9.28	0.13
71.00	7.52	0.22	7.19	0.22	7.35	0.23	0.22	0.00
94.42	6.80	0.27	7.32	0.22	7.06	0.37	0.24	0.03
150.33	7.34	0.00	8.25	0.00	7.79	0.65	0.00	0.00

Table J4: Growth data for experiments conducted in duplicate with *Y. lipolytica* TVN 502

	Experiment 1		Experiment 2		Average			
Time	Biomass	Glucose	Biomass	Glucose	Biomass	Error	Glucose	Error
H	OD	$g.l^{-1}$	OD	$g.l^{-1}$	OD		$g.l^{-1}$	
1.00	0.26	40.50	0.27	40.50	0.26	0.00	40.50	0.00
3.00	0.27	41.07	0.30	39.97	0.29	0.03	40.52	0.78
5.00	0.40	36.92	0.40	40.23	0.40	0.00	38.58	2.34
7.00	0.53	40.45	0.56	41.29	0.55	0.03	40.87	0.59
10.00	0.96	38.64	0.98	38.77	0.97	0.01	38.71	0.09
24.00	2.13	32.36	2.19	33.82	2.16	0.04	33.09	1.03
34.00	2.69	27.59	2.70	29.22	2.69	0.01	28.41	1.16
47.00	3.56	23.79	4.05	22.37	3.80	0.35	23.08	1.00
71.00	6.99	0.27	7.32	0.13	7.16	0.23	0.20	0.09
94.42	7.40	0.13	7.56	0.22	7.48	0.12	0.18	0.06
150.33	7.82	0.00	7.67	0.00	7.74	0.11	0.00	0.00

Appendix J2: Graphical approach

a. Specific Growth Rate (*Y. lipolytica* TVN 497)

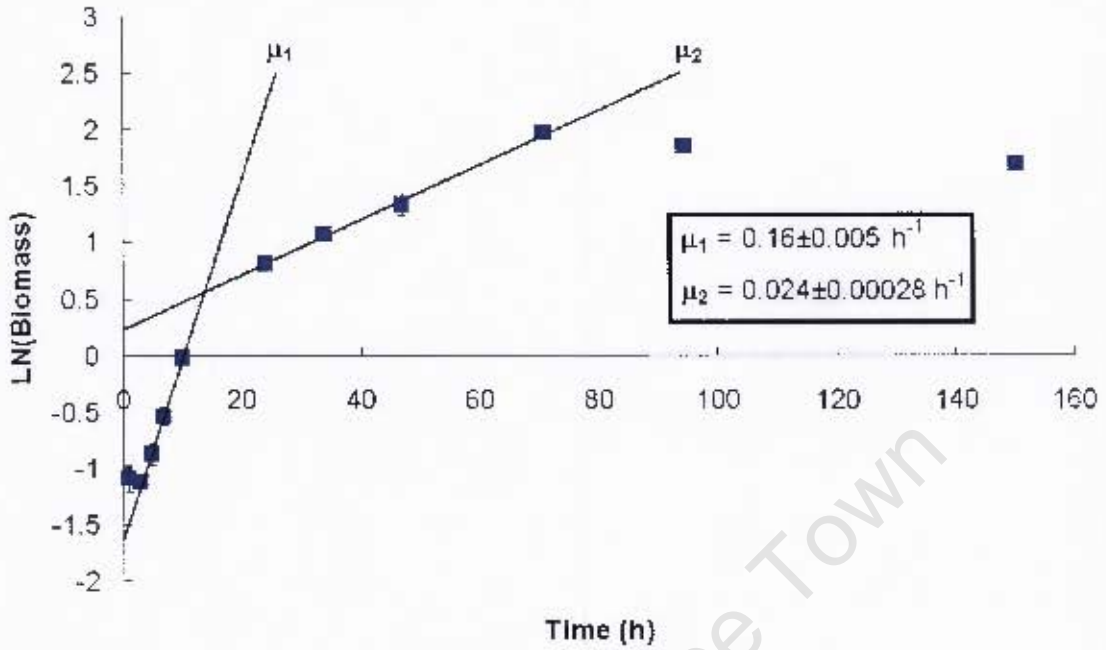

b. Specific Growth Rate (*Y. lipolytica* TVN 499)

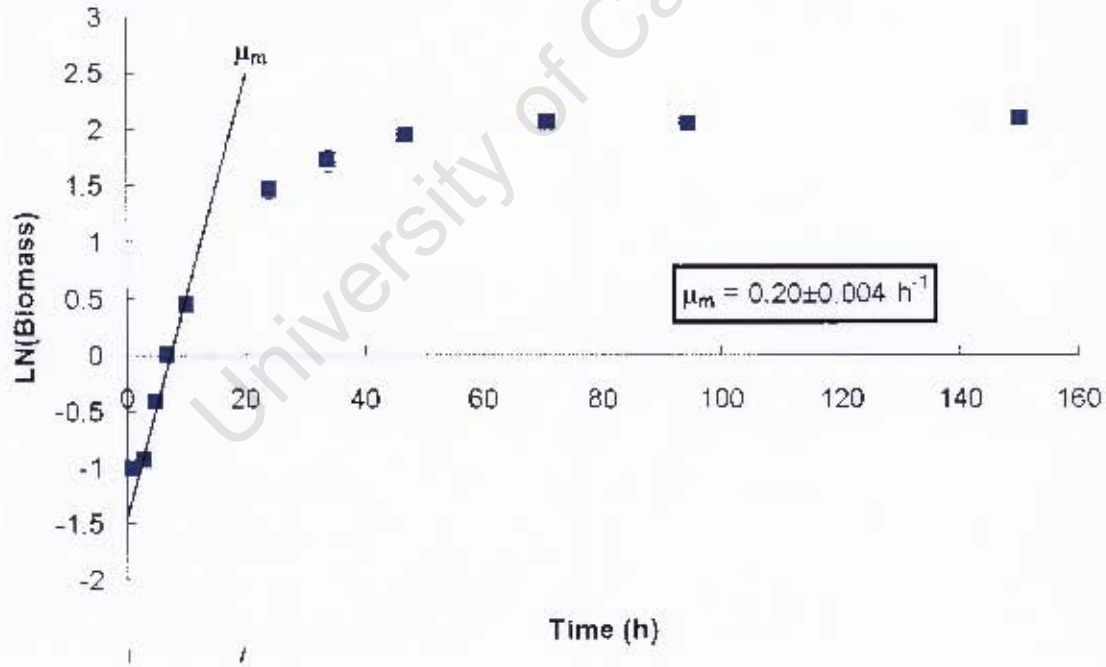

Figure J1: Graphical estimation of the specific growth rates of strains *Y. lipolytica* TVN (a) TVN 497 and (b) TVN 499. The strains were cultivated on a rotary shaker at 180 rpm in shake flasks using the UFS media buffered to pH 7.8 at 29°C. (The error bars represent the standard deviation of repeated experiments to confirm reproducibility).

a. Specific Growth Rate (*Y. lipolytica* TVN 501)

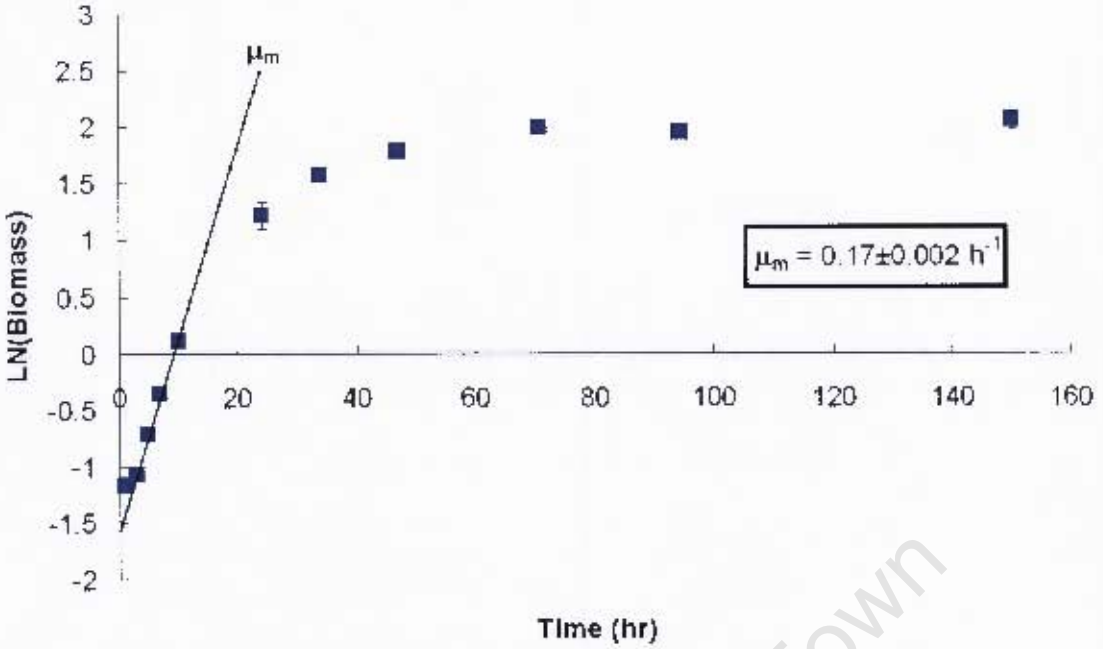

b. Specific Growth Rate (*Y. lipolytica* TVN 502)

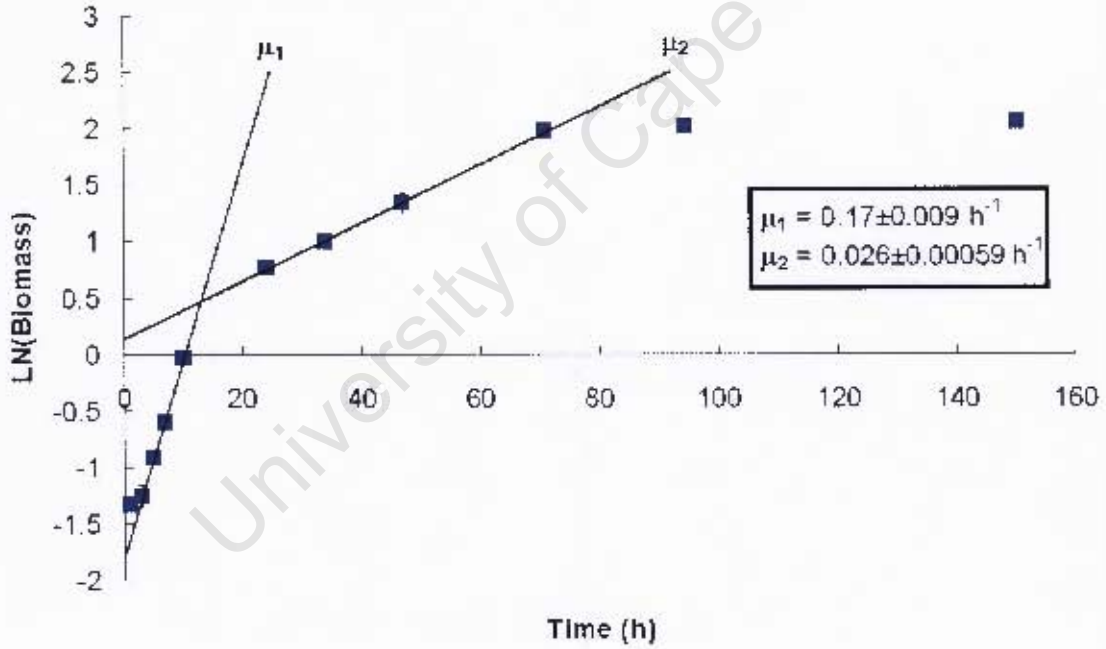

Figure J2: Graphical estimation of the specific growth rates of strains *Y. lipolytica* TVN (a) TVN 501 and (b) TVN 502. The strains were cultivated on a rotary shaker at 180 rpm in shake flasks using the UFS media buffered to pH 7.8 at 29°C. (The error bars represent the standard deviation of repeated experiments to confirm reproducibility).

Appendix J3: Evaluating biotransformation of different recombinant *Y. lipolytica* Strains

Table J5: Biotransformation data for experiments conducted in duplicate with *Y. lipolytica* TVN 497

	Experiment 1				Experiment 2				Average							
	Alkanes		Diacids		Alkanes		Diacids		Alkanes				Diacids			
Time	C_{12}	C_{13}	C_{12}	C_{13}	C_{12}	C_{13}	C_{12}	C_{13}	C_{12}	Error	C_{13}	Error	C_{12}	Error	C_{13}	Error
h	$g.l^{-1}$	$g.l^{-1}$	$g.l^{-1}$	$g.l^{-1}$	$g.l^{-1}$	$g.l^{-1}$	$g.l^{-1}$	$g.l^{-1}$	$g.l^{-1}$		$g.l^{-1}$		$g.l^{-1}$		$g.l^{-1}$	
49.00	2.12	2.45	0.00	0.00	0.71	0.83	0.00	0.00	1.42	0.99	1.64	1.14	0.00	0.00	0.00	0.00
57.50	2.81	3.34	0.00	0.00	2.09	2.36	0.05	0.01	2.45	0.51	2.85	0.69	0.02	0.03	0.01	0.01
71.67	2.68	3.24	0.11	0.17	3.03	3.64	0.07	0.07	2.85	0.25	3.44	0.28	0.09	0.03	0.12	0.07
80.83	4.74	5.01	0.11	0.06	5.81	6.15	0.12	0.05	5.28	0.75	5.58	0.81	0.12	0.01	0.05	0.01
95.25	3.20	3.80	0.15	0.10	3.20	3.80	0.15	0.10	3.20	0.00	3.80	0.00	0.15	0.00	0.10	0.00
120.00	4.29	4.71	0.42	0.31	4.99	5.54	0.38	0.28	4.64	0.49	5.13	0.59	0.40	0.03	0.29	0.02
152.00	3.82	4.79	0.80	0.62	5.03	5.77	0.57	0.63	4.43	0.86	5.28	0.70	0.68	0.16	0.63	0.01

Table J6: Biotransformation data for experiments conducted in duplicate with *Y. lipolytica* TVN 499

	Experiment 1				Experiment 2				Average							
	Alkanes		Diacids		Alkanes		Diacids		Alkanes				Diacids			
Time	C_{12}	C_{13}	C_{12}	C_{13}	C_{12}	C_{13}	C_{12}	C_{13}	C_{12}	Error	C_{13}	Error	C_{12}	Error	C_{13}	Error
h	$g.l^{-1}$	$g.l^{-1}$	$g.l^{-1}$	$g.l^{-1}$	$g.l^{-1}$	$g.l^{-1}$	$g.l^{-1}$	$g.l^{-1}$	$g.l^{-1}$		$g.l^{-1}$		$g.l^{-1}$		$g.l^{-1}$	
49.00	7.51	8.70	12.81	13.75	0.06	0.04	0.09	0.05	10.16	1.87	11.23	1.78	0.08	0.02	0.05	0.01
57.50	12.63	13.31	11.31	12.44	0.11	0.08	0.14	0.09	11.97	0.47	12.87	0.31	0.13	0.02	0.08	0.01
71.67	7.17	7.87	6.21	6.83	0.48	0.45	0.52	0.45	6.69	0.34	7.35	0.37	0.50	0.03	0.45	0.00
80.83	3.75	4.02	2.06	2.46	0.56	0.52	0.61	0.48	2.90	0.60	3.24	0.55	0.59	0.03	0.50	0.03
95.25	1.08	1.33	1.32	1.63	0.73	0.56	0.72	0.55	1.20	0.09	1.48	0.11	0.73	0.01	0.55	0.01
120.00	5.49	6.34	4.05	4.62	0.74	0.56	0.76	0.57	4.77	0.51	5.48	0.61	0.75	0.01	0.56	0.01
152.00	24.25	27.80	18.78	21.99	1.33	1.34	1.25	1.24	21.52	1.94	24.89	2.05	1.29	0.06	1.29	0.07

Table J7: Biotransformation data for experiments conducted in duplicate with *Y. lipolytica* TVN 501

	Experiment 1				Experiment 2				Average							
	Alkanes		Diacids		Alkanes		Diacids		Alkanes				Diacids			
Time	C_{12}	C_{13}	C_{12}	C_{13}	C_{12}	C_{13}	C_{12}	C_{13}	C_{12}	Error	C_{13}	Error	C_{12}	Error	C_{13}	Error
h	$g.l^{-1}$	$g.l^{-1}$	$g.l^{-1}$	$g.l^{-1}$	$g.l^{-1}$	$g.l^{-1}$	$g.l^{-1}$	$g.l^{-1}$	$g.l^{-1}$		$g.l^{-1}$		$g.l^{-1}$		$g.l^{-1}$	
49.00	0.00	0.00	2.50	2.70	0.00	0.00	0.00	0.00	1.25	1.77	1.35	1.91	0.00	0.00	0.00	0.00
57.50	3.77	4.79	3.56	4.24	0.04	0.03	0.03	0.01	3.66	0.15	4.51	0.39	0.04	0.00	0.02	0.01
71.67	1.62	1.78	7.83	8.61	0.33	0.26	0.39	0.33	4.72	4.39	5.20	4.83	0.36	0.04	0.29	0.05
80.83	2.10	2.49	4.42	4.87	0.34	0.30	0.51	0.45	3.26	1.64	3.68	1.68	0.42	0.12	0.38	0.10
95.25	0.59	0.70	0.60	0.75	0.36	0.29	0.61	0.53	0.60	0.01	0.72	0.04	0.48	0.18	0.41	0.17
120.00	3.13	3.56	3.73	4.78	0.54	0.41	0.33	0.16	3.43	0.43	4.17	0.86	0.44	0.15	0.29	0.17
152.00	3.45	4.39	7.02	8.16	0.97	1.31	1.26	1.43	5.23	2.52	6.27	2.66	1.12	0.20	1.37	0.09

Table J8: Biotransformation data for experiments conducted in duplicate with *Y. lipolytica* TVN 502

	Experiment 1				Experiment 2				Average							
	Alkanes		Diacids		Alkanes		Diacids		Alkanes				Diacids			
Time	C_{12}	C_{13}	C_{12}	C_{13}	C_{12}	C_{13}	C_{12}	C_{13}	C_{12}	Error	C_{13}	Error	C_{12}	Error	C_{13}	Error
h	$g.l^{-1}$	$g.l^{-1}$	$g.l^{-1}$	$g.l^{-1}$	$g.l^{-1}$	$g.l^{-1}$	$g.l^{-1}$	$g.l^{-1}$	$g.l^{-1}$		$g.l^{-1}$		$g.l^{-1}$		$g.l^{-1}$	
49.00	0.83	0.97	0.95	1.09	0.00	0.00	0.00	0.03	0.89	0.08	1.03	0.08	0.00	0.00	0.01	0.02
57.50	6.35	6.82	4.64	5.01	0.01	0.00	0.02	0.02	5.50	1.21	5.92	1.28	0.02	0.01	0.01	0.01
71.67	2.89	3.50	3.35	2.18	0.07	0.01	0.13	0.05	3.12	0.33	2.84	0.94	0.10	0.04	0.03	0.03
80.83	4.27	4.59	4.72	5.18	0.11	0.09	0.13	0.08	4.50	0.32	4.88	0.42	0.12	0.01	0.09	0.00
95.25	2.04	2.46	2.45	2.95	0.25	0.13	0.23	0.17	2.25	0.29	2.70	0.35	0.24	0.01	0.15	0.02
120.00	4.70	4.83	2.72	3.10	0.28	0.21	0.28	0.15	3.71	1.40	3.96	1.22	0.28	0.00	0.18	0.04
152.00	6.44	7.51	5.61	6.49	0.64	0.57	0.66	0.56	6.02	0.59	7.00	0.72	0.65	0.02	0.56	0.01

Appendix J4: Statistical analysis of the final biomass concentrations

The sample mean is $\bar{x} = 7.886667$ and the sample standard deviation is s = 0.150111. Do the data suggest that the mean final biomass concentration exceeds 7.11. It was assumed that the final biomass concentration has a normal distribution and $\alpha = 0.05$ was used.

The solution using the eight-step procedure for hypothesis testing is follows:

1. The parameter of interest is the mean final biomass density, μ.
2. H_0: $\mu = 7.11$.
3. H_1: $\mu > 7.11$. If the H_0 is rejected the mean final biomass density exceeds 7.11.
4. $\alpha = 0.05$.
5. The test statistic is

$$t_0 = \frac{\bar{x} - \mu_0}{s/\sqrt{n}} \qquad \text{(J1)}$$

6. Reject H_0 if $t_0 > t_{0.025,2} = 4.303$.
7. Computation:

$$t_0 = \frac{7.886667 - 7.11_0}{0.150111/\sqrt{3}} = 8.961538 \qquad \text{(J2)}$$

8. Conclusion: Since $t_0 = 8.961538 > 4.303$, the H_0 is rejected and conclude that at the 0.05 level of significant that the mean final biomass concentration exceeds 7.11.

Appendix J5: Statistical analysis of the final combined α,ω-dicarboxylic acid concentrations

The sample mean is $\bar{x} = 2.535\,g.l^{-1}$ and the sample standard deviation is s = 0.06364 $g.l^{-1}$. Do the data suggest that the mean combined α,ω-dicarboxylic acid concentration exceeds 1.31 $g.l^{-1}$. It was assumed that the final biomass density has a normal distribution and α = 0.05 was used.

The solution using the eight-step procedure for hypothesis testing is follows:

1. The parameter of interest is the mean final combined α,ω-dicarboxylic acid concentration, μ.
2. H_0: μ = 1.31 $g.l^{-1}$.
3. H_1: μ > 1.31 $g.l^{-1}$. If the H_0 is rejected the mean final combined α,ω-dicarboxylic acid concentration exceeds 1.31 $g.l^{-1}$.
4. α = 0.05.
5. The test statistic is

$$t_0 = \frac{\bar{x} - \mu_0}{s/\sqrt{n}} \qquad \text{(J3)}$$

6. Reject H_0 if $t_0 > t_{0.025,2}$ =12.706.
7. Computation:

$$t_0 = \frac{2.535 - 1.31_0}{0.06364/\sqrt{2}} = 27.222222 \qquad \text{(J4)}$$

Conclusion: Since t_0 = 27.222 > 12.706, the H_0 is rejected and conclude that at the 0.05 level of significant that the mean final combined α,ω-dicarboxylic acid concentration exceeds 1.31 $g.l^{-1}$.